

CONTRIBUTION TO BIOABSORBABLE STENT MANUFACTURE WITH ADDITIVE MANUFACTURING TECHNOLOGIES

Antonio Jesús Guerra Sánchez

Per citar o enllaçar aquest document:
Para citar o enlazar este documento:
Use this url to cite or link to this publication:
<http://hdl.handle.net/10803/667867>

ADVERTIMENT. L'accés als continguts d'aquesta tesi doctoral i la seva utilització ha de respectar els drets de la persona autora. Pot ser utilitzada per a consulta o estudi personal, així com en activitats o materials d'investigació i docència en els termes establerts a l'art. 32 del Text Refós de la Llei de Propietat Intel·lectual (RDL 1/1996). Per altres utilitzacions es requereix l'autorització prèvia i expressa de la persona autora. En qualsevol cas, en la utilització dels seus continguts caldrà indicar de forma clara el nom i cognoms de la persona autora i el títol de la tesi doctoral. No s'autoritza la seva reproducció o altres formes d'explotació efectuades amb finalitats de lucre ni la seva comunicació pública des d'un lloc aliè al servei TDX. Tampoc s'autoritza la presentació del seu contingut en una finestra o marc aliè a TDX (framing). Aquesta reserva de drets afecta tant als continguts de la tesi com als seus resums i índexs.

ADVERTENCIA. El acceso a los contenidos de esta tesis doctoral y su utilización debe respetar los derechos de la persona autora. Puede ser utilizada para consulta o estudio personal, así como en actividades o materiales de investigación y docencia en los términos establecidos en el art. 32 del Texto Refundido de la Ley de Propiedad Intelectual (RDL 1/1996). Para otros usos se requiere la autorización previa y expresa de la persona autora. En cualquier caso, en la utilización de sus contenidos se deberá indicar de forma clara el nombre y apellidos de la persona autora y el título de la tesis doctoral. No se autoriza su reproducción u otras formas de explotación efectuadas con fines lucrativos ni su comunicación pública desde un sitio ajeno al servicio TDR. Tampoco se autoriza la presentación de su contenido en una ventana o marco ajeno a TDR (framing). Esta reserva de derechos afecta tanto al contenido de la tesis como a sus resúmenes e índices.

WARNING. Access to the contents of this doctoral thesis and its use must respect the rights of the author. It can be used for reference or private study, as well as research and learning activities or materials in the terms established by the 32nd article of the Spanish Consolidated Copyright Act (RDL 1/1996). Express and previous authorization of the author is required for any other uses. In any case, when using its content, full name of the author and title of the thesis must be clearly indicated. Reproduction or other forms of for profit use or public communication from outside TDX service is not allowed. Presentation of its content in a window or frame external to TDX (framing) is not authorized either. These rights affect both the content of the thesis and its abstracts and indexes.



DOCTORAL THESIS

Contribution to Bioabsorbable Stent Manufacture
With Additive Manufacturing Technologies

Antonio Jesús Guerra Sánchez

2019



DOCTORAL THESIS

**Contribution to Bioabsorbable Stent Manufacture
With Additive Manufacturing Technologies**

Antonio Jesús Guerra Sánchez

2019

Doctoral Programme in Technology

Advised by Joaquim de Ciurana i Gay

THESIS BY COMPENDIUM OF MANUSCRIPTS SUBMITTED IN PARTIAL
FULFILLMENT OF THE REQUIREMENTS FOR THE DEGREE OF DOCTOR OF
PHILOSOPHY



El Dr. Joaquim de Ciurana Gay, catedràtic del Departament d'Enginyeria Mecànica i de la Construcció Industrial de la Universitat de Girona,

DECLARA:

Que el treball titulat "*Contribution to Bioabsorbable Stent Manufacture With Additive Manufacturing Technologies*", que presenta Antonio Jesús Guerra Sánchez per a l'obtenció del títol de doctor, ha estat realitzat sota la meva direcció.

I, perquè així consti i tingui els efectes oportuns, signo aquest document.

Signatura

A handwritten signature in blue ink, appearing to be "J. Ciurana", written over a light blue circular scribble.

Girona, 21 de Gener de 2019

*“Imagination is more important than knowledge.
For knowledge is limited to all we now know,
while imagination embraces the entire world,
stimulating progress, giving birth to evolution.”*

Albert Einstein

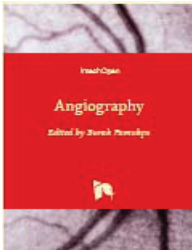
Acknowledgements

I would like to start by thanking the GREP and all its members. Many thanks Quim for choosing me as researcher for your group in 2015 and make me part of this great project. Thank for all the advices both in the profesional as in the personal field and for provide me everything I have needed these years, I have learned many things from you. Many thanks to Jordi Grabalosa, Isabel Bagudanch, Ines Ferrer, and Maria Luisa for your support and friendship these years. Thank you all guys, these years have been one of the best period of my life.

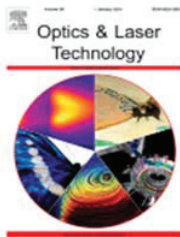
Thanks to the EURECAT team Guillem, Dani, Arcadi for these good coffees and laughing these years, to the guys of SAMART, Francesc, Albert and Oriol for the good times. Thanks to AMADE and its employes Dani, Ivan, and Santi. Many thanks for your help and for open me your facilities for all I have needed. Santi, thanks for your friendship and the good moments that we have had together. Thanks to Teresa Puig and her amazing research group TARGETLAB for helping me and teaching me so much about biology. Marc and Xavi for helping me in everything I have needed. I think that we have created a really great collaboration. Many thanks to The Ohio State University and Dr. David Dean for open me the doors of his lab in Columbus, and allow me to live an amazing experience both in the personal as in the profesional field in U.S.A. Thanks to Jan and Raquel for the fantastic moments we have lived working together. Thanks to Dr. Ciro for help me in everything I needed.

Imposible olvidarme de mi familia. Papa, Mama, Alberto, Vicky, Curro, gracias por estar siempre a mi lado y apoyarme en todo lo que he decidido hacer en la vida. Sin vosotros no hubiera sido posible llegar hasta aquí. Pilar, Alfredo gracias por vuestro apoyo estos años y por haberme ayudado a descubrir el mundo de la investigación en el que disfruto tanto trabajando. Gracias a Ana, Maria, Alvaro, Cris, por vuestro apoyo desde Badajoz, por todos estos años de amistad verdadera y por estar ahí cada vez que lo he necesitado. Paula, Uri, David, Jess, Cris, mi familia Catalana, mil gracias por hacernos parte de vuestro grupo desde el primer día, sois la razón por la que Girona nos enamoró.

Como no he de terminar dandole las gracias a Marta. Gracias por ser el pilar fundamental de mi vida, por tu cariño y apoyo incondicional desde el día que te conocí. Por dejar todo por acompañarme allí donde la tesis me ha llevado. Eres el corazón y alma de este trabajo, mil gracias cariño.



Antonio J. Guerra, Joaquim Ciurana. “Stent Manufacturing Field: Past, Present, and Future Prospects”. *Angiography*. **2018**. Intechopen.



Antonio J. Guerra, Jordi Farjas, Joaquim Ciurana. “Fibre laser cutting of polycaprolactone sheet for stents manufacturing: A feasibility study”. **2017**, 95, 113-123. *Optics and Laser Technology*. [Q2 (31/94) 2017].



Antonio J. Guerra, Joaquim Ciurana. “Effect of fibre laser process on in-vitro degradation rate of a polycaprolactone stent a novel degradation study method”. **2017**, 142, 42-49. *Polymer Degradation & Stability*. [Q1 (16/87) 2017].



Antonio J. Guerra, San, J., Joaquim Ciurana. “Fabrication of PCL/PLA Composite Tube for Stent Manufacturing”. **2017**, 65, 231-235. *Procedia CIRP*.



Antonio J. Guerra, Joaquim Ciurana. “Fibre Laser Cutting of Polymer Tubes for Stents Manufacturing”. **2017**, 13, 190-196. *Procedia Manufacturing*.



Antonio J. Guerra, A. Roca, Joaquim Ciurana. “A Novel 3D Additive Manufacturing Machine To Biodegradable Stents”. **2017**, 13, 718-723. *Procedia Manufacturing*.



Antonio J. Guerra, Joaquim Ciurana. “3D-Printed Bioabsorbable Polycaprolactone Stent: The Effect Of Process Parameters On Its Physical Features”. **2018**, 137, 430–437. *Materials & Design*. [Q1 (53/285) 2017].



Antonio J. Guerra, Joaquim Ciurana. “Three Dimensional Tubular Printing of Bioabsorbable Stents: The Effects Process Parameters Have on In Vitro Degradation”. **2019**, 6 (1), 50-56. *3D Print Addit Manuf*. [Q2 (20/46) 2017].



Antonio J. Guerra, Paula Cano, Marc Rabionet, Teresa Puig, Joaquim Ciurana. “The Effects Of Different Sterilization Processes On The Properties Of A Novel 3D-Printed Polycaprolactone Stent”. **2018**, 0, 1-9. *Polym Advan Technol*. [Q2 (30/87) 2017].



Antonio J. Guerra, P. Cano, M. Rabionet, T. Puig, J. Ciurana. “3D-Printed PCL/PLA Composite Stent: Towards a New Solution for Cardiovascular Problems”. **2018**, 11, 11. *Materials*. [Q2 (111/285) 2017].

International Conferences



Antonio J. Guerra, J. San, J. Ciurana. “Fabrication Of PCL/PLA Composite Tube For Stent Manufacturing”. Oral Communication. 3rd CIRP Conference On Biomanufacturing. Chicago. United States, 2017.



Antonio J. Guerra, A. Roca, J. Ciurana. “A Novel 3D Additive Manufacturing Machine To Biodegradable Stent”. Oral Communication. 7th Manufacturing Engineering Society International Conference. Vigo, Spain, 2017.



Antonio J. Guerra, J. Ciurana. “Fiber Laser Cutting Of Polymer Tubes For Stents Manufacturing”. Poster. 7th Manufacturing Engineering Society International Conference. Vigo, Spain, 2017.

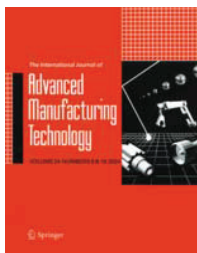


Antonio J. Guerra, J. Ciurana. “Minimum Quantity Lubrication In Fibre Laser Processing For Permanent Stents Manufacturing”. Oral Communication. 8th Manufacturing Engineering Society International Conference. Madrid, Spain, 2019. **Accepted**



Antonio J. Guerra, R. Tejada-Alejandre, Ciro A. Rodríguez, J. Ciurana. “Electrospun Tubular Scaffold for Stenting Application: A Proof of Concept”. Oral Communication. 8th Manufacturing Engineering Society International Conference. Madrid, Spain, 2019. **Accepted**

Thesis Collaborations



Maudes, J., Bustillo, A., **Antonio J. Guerra**, Joaquim Ciurana. “Random Forest Ensemble Prediction Of Stent Dimensions In Microfabrication Processes”. 2017, 91, 879-893. Int J Adv Manuf Tech. [Q2 (23/61) 2017]



Marc Rabionet, **Antonio J. Guerra**, Teresa Puig, Joaquim Ciurana. “3D-Printed Tubular Scaffolds For Vascular Tissue Engineering”. 2018, Procedia CIRP.



Antonio J. Guerra, Luiz Catalan, Matthew Becker, Ciro Rodriguez, Joaquim Ciurana, David Dean. “Photopolymerizable Resins For 3D-Printing Of Tissue Engineered Implants”. **In Press**. Current Drug Targets. [Q2 (88/261) 2017].



M. Rabionet, E. Polonio, **Antonio J. Guerra**, J. Martin, T. Puig, J. Ciurana. “Design Of Scaffold Parameter Selection System With Additive Manufacturing For Biomedical Cell Culture”. 2018, 11, 1427. Materials. [Q2 (111/285) 2017].



E. Polonio-Alcala, M. Rabionet, **Antonio J. Guerra**, M. Yeste, J. Ciurana, T. Puig. “Screening of Additive Manufactured Scaffolds Designs for Triple Negative Breast Cancer 3D Cell Culture and Stem-Like Expansion”. 2018, 19, 3148, IJMS. [Q2 (90/292) 2017].

Thesis Structure

I

Chapter 1 presents the general domain of the thesis, it establishes the conceptual frameworks and exposes the interest, motivation, and objectives reached in this work. The chapter ends with the methodology followed in this thesis.

Chapter 2 presents the framework and review the stents field as well as its manufacture processes. It presents the challenges associated to this device. Finally, the chapter ends with a general state of the art about stent research manufacturing field.

Chapter 3 presents the feasibility of fibre laser to cut Polycaprolactone sheets for stent purpose. This study is motivate by the need of the fiber laser cutting trademarks have to adapt to new stents material market. The effects the fibre laser process have on the cutting precision and material properties is presented and discusses.

Chapter 4 presents the effect of fibre laser process over the in-vitro degradation rate of Polycaprolactone sub-unit flat stent. A novel degradation method is presented relating the laser cutting process and the degradation conditions with the degradation rate of the samples.

Chapter 5 presents the fabrication of polymeric tubes for stent purposes by Dip Coating Process employing Polycaprolactone, Polylactide Acid, and a Composite of them. The effects the Dip Coating process parameters have on their physicochemical features is presented and discussed.

Chapter 6 presents the effect the fibre laser cutting process on the polymeric tubes manufactured in the previous chapter. This study is motivate by the need to know the feasibility of laser cutting process to create real stents and compare the results with the obtained in flat sheets in chapter 3.

Thesis Structure

Chapter 7 presents a novel 3D Tubular Printer based on Fused Filament Fabrication (FFF) technology to manufacture stents with bioabsorbable polymers. This study is motivated by the need to find new manufacturing methods to produce polymeric stents.

Chapter 8 presents the effects the 3D Printing process parameters have on the Polycaprolactone stents. This study is motivated by the need to know if the technology developed is able to manufacture stent with precision. The effects of the process parameters have on printing precision and material properties is presented and discussed.

Chapter 9 presents the effects of 3D printing process parameters over the degradation rate of 3D-Printed Polycaprolactone stents. This study is motivated by the need to know the effect the process parameters have on this important stent's property.

Chapter 10 presents the effects the sterilization processes have on the final properties of 3D-Printed Polycaprolactone stents. This study is motivated by the need of know how the last manufacturing process, the sterilization, modify the stent properties.

Chapter 11 presents a new approach to solve the current problems associated to BRS, the rapid reendothelization and the radial behaviour of polymeric stents. Based on the great results of chapter 6 with PCL/PLA composite stents this chapter present a PCL/PLA composite stent produced with the new 3D Tubular Printer.

Chapter 12 presents the discussion and conclusions of the thesis and an overview of the main results obtained with a serie of future works.

Chapter 13 presents the references employed in the course of this thesis.

List of Figures

- Figure 1.1. Atherosclerosis Disease
- Figure 1.2. PCI Procedure
- Figure 1.3. Methodology Followed
- Figure 2.1. Charles Tomas Stent
- Figure 2.2. Logo of the Stent compound
- Figure 2.3. Sales of Stents 2013 - 2020
- Figure 2.4. Pyramid of Stent Challenges
- Figure 2.5. Coil Stent.
- Figure 2.6. Crossflex Stent.
- Figure 2.7. WallStent.
- Figure 2.8. Palmaz–Schatz stent
- Figure 2.9. Conventional Photolithography Process
- Figure 2.10. Micro – Electro Discharge Process
- Figure 2.11. Electroforming Process
- Figure 2.12. Die – Casting Process
- Figure 2.13. Laser Cutting Process
- Figure 2.14. 3D Printing Processes
- Figure 2.15. Laser Cutting Process of Stents
- Figure 2.16. Thermal Damages and its effects
- Figure 2.17. Stents Post – Processing Techniques
- Figure 2.18. Stents Steps (UP) Descaled; (MID) Crimped (BOT) Expanded.
- Figure 2.19. Component of a typical laser
- Figure 2.20. Laser physics
- Figure 2.21. Laser material interaction
- Figure 2.22. Laser ablation mechanism
- Figure 2.23. Laser wave parameters
- Figure 2.24. Charles Hull
- Figure 2.25. FFF Methodologies (a) Cartesian (b) Cylindrical Proposal
- Figure 2.26. FFF Extruder Method (Energy Balance)
- Figure 2.27. Hospital in the U.S. with centralized 3D printing facilities
- Figure 2.28. Application of 3DP in the Medical Sector
- Figure 2.29. Evolution of Stents Industry
- Figure 12.1. Thesis Contributions

List of Tables

Table 2.1. Coronary Stents Market Key Metrics in the 10MM – 2013 to 2020

Table 2.2. Stent Types in the Market

Table 12.1. Techno-Economical Comparison - Laser and 3D Printing (FFF)

Table 12.2. AM Technologies Comparison

Table 12.3. Initial Evaluation Tests For Consideration (ISO 10993-1)

List of Symbols

I

Δh	Enthalpy Changes
B_T^a	Bed Temperature
C_p	Material Thermal Capacity
$D_{(y)}$	Cutting Depth Profile
E	Laser Energy
$E_{\text{Conduction}}$	Conduction Energy
$E_{\text{Convection}}$	Convection Energy
E_{Laser}	Laser Energy
$E_{\text{Phase change}}$	Phase Change Energy
$E_{T,AM}$	Energy to melt amorphous material
$E_{T,SC}$	Energy to melt semi crystalline material
E_{in}	Energy supplied to the extruder
E_{losses}	Energy lossed in the extruder
E_u	Useful Energy
F	Laser Fluence
h	Convection heat transfer coefficient
h_1	Input enthalpy
h_2	Output Enthalpy
h_f	Enthalpy of Heat Fusion
$I_{(z)}$	Absorption
I_o	Material Absorption
L_H	Layer Height
L_m	Latent Heat of Fusion
L_w	Laser Wavelength
M^2	Beam Quality
M	Mass flow rate
n_{extruder}	Extruder energy efficiency
$N_{F\%}$	Nozzle Flow Rate
N_R	Nozzle Retract
N_T^a	Nozzle Temperature
P	Laser Power
P_1	Initial Pressure
P_2	Final Pressure
P_A	Laser Pulse Amplitude
P_D	Laser Pulse Duration
P_F	Laser Pulse Frequency
P_o	Laser Pulse Overlap
P_s	Printing Speed
P_W	Laser Pulser Wavelength
R	Laser Beam Radiumous
T_1	Initial Temperature

List of Symbols

II

T_2	Final Temperature
T_a	Ambient Temperature
T_1	Media Temperature
T_s	Temperature in the cut off point
V	Laser speed
W_0	Beam Spot Radius
z	Height
α	Absorption Coefficient
φ	Material Density

List of Acronyms

I

10MM	10 Million Market
3D	Three Dimensional
3DP	3D- Printing
AM	Additive Manufacturing
AMI	Acute Myocardial Infarction
APAC	Asian-Pacific Countries
ASP	Average Selling Price
ASTM	American Society Of Testing Materials
BME	Biomedical Engineering
BMS	Bare Metal Stents
BPP	Beam Parameter Product
BRS	Bioresorbable Stents Bioabsorbable Stents Bioabsorbable Stents
CABG	Coronary Artery Bypass Graft
CAD	Coronary Artery Diseases
CAGR	Compound Annual Growth Rate
CLF	Corte Por Laser De Fibra
CTO	Chronic Total Occlusions
CW	Continuous Wavelength
DAPT	Doctors Recommendation On Drug Therapy
DCP	Dip Coating Process
DES	Drug Eluting Stents
DLP	Digital Light Processing
DMLS	Direct Metal Laser Sintering
EDM	Electro Discharge Machining
EPC	Endothelial Progenitor Cells
EU	European Union
FDA	Food And Drug Administration
FDM	Fused Deposition Modeling
FFF	Fused Filament Fabrication
FLC	Fibre Laser Cutting
GREP	Group On Product, Process And Production Engineering
HAZ	Heat Affected Zone
HRSEM	High Resolution Scanning Electron Microscopy
I3D	Impresión 3d
LCD	Liquid Crystal Display
MINECO	Ministry Of Economy And Competitiveness
MIT	Massachusetts Institute Of Technology
MRI	Magnetic Resonance Imaging

List of Acronyms

II

PAD	Peripheral Artery Diseases
PCI	Percutaneous Coronary Intervention
PCL	Polycaprolactone
PF	Pulse Frequency
PLLA	Poly-L-Lactide Acid
PPP	Peak Pulse Power
R&D	Research And Development
SBA	Stents Bioabsorbibles
SCC	Stress Corrosion Cracking
SE	Superelasticity
SL	Stereolithography
SLA	Laser-Based Stereolithography
SLM	Selective Laser Melting
SLS	Selective Laser Sintering
SMA	Shape Memory Alloy
SME	Shape Memory
SVD	Small Vessel Diseases
SW	Short Wavelength
TLF	Tall Laser De Fibra
UDG	University Of Girona
UK	United Kingdom
US	United State
UV	Ultraviolet Light
UW	Ultrashort Wavelength

Content

I

Summary	001
Summary	005
Resumen	005
Resum	005
Chapter 01. Introduction.....	007
1.1 Preface	011
1.2 Interest and Motivation.....	014
1.3 Objectives	015
1.4 Methodology	016
Chapter 02. Background.....	017
2.1 Historical Framework.....	021
2.2 Economical Framework.....	025
2.3 Foundation of Stents	030
2.3.1 Introduction	030
2.3.2 Stent Types.....	031
2.3.3 Stent Mechanical Properties	032
2.3.4 Stent Materials.....	033
2.3.5 Stent Geometries.....	034
2.3.6 Past, Present and Promising Stents Manufacturing	037
2.3.7 Stent Additional Properties.....	040
2.3.8 Current Manufacturing Cycle of Stents.....	042
2.4 Foundation of Laser Technology	046
2.4.1 Introduction	046
2.4.2 The Lasers Physics.....	047
2.4.3 Material Interactions.....	048
2.4.4 Laser Types	051
2.4.5 Laser Processing Parameters	052

Content

II

Chapter 02. Background.....	017
2.5 Foundation of 3D Printing Technologies.....	055
2.5.1 Introduction	055
2.5.2 3D Printing Technologies Types.....	056
2.5.3 Feasibility of Fused Filament Fabrication for BRS	057
2.5.4 Extrusion Melting Physics	058
2.5.5 Fused Filament Fabrication Processing Parameters	060
2.5.6 3D Printing Technologies in the Medical Sector.....	061
2.6 The state of the art	064
Chapter 03. Fibre Laser Cutting of Polymer Sheets.....	069
Chapter 04. Effect of Fibre Laser on Degradation.....	085
Chapter 05. Stents Tubes Fabrication by Dip Coating	097
Chapter 06. Fibre Laser Cutting of Polymer Tubes	107
Chapter 07. Novel 3D Additive Manufacturing Machine	119
Chapter 08. Effect of Printing Process on PCL Stent	129
Chapter 09. 3D Printing Process on Degradation	141
Chapter 10. Effects of Sterilization on 3D-Printed Stent	153
Chapter 11. 3D-Printed Composite BRS.....	167
Chapter 12. Discussion and Conclusions.....	185
12.1 Discussion	189
12.2 Conclusions	202
12.3 Future Works.....	207
12.3.1 Manufacturing	207
12.3.2 Biological.....	207
Chapter 13. References.....	209

Summary Resumen Resum

Abstract

This section presents the summary of the present thesis work in English, Spanish, and Catalan.

Summary

The main motivation of this work was to analyse the feasibility of the current stent's manufacturing process to produce the new bioresorbable stents (BRS) as well as study new manufacturing methods. Fibre Laser Cutting (FLC) has been selected because is the current manufacturing process for stents, and 3D-Printing (3DP) because its capability to process different types of materials for medical applications and their economic aspects. Stents have been selected for being one of the most implanted biomedical device in the world.

The thesis focuses on improve the bioresorbable stent's manufacturing processes, establishing relationships between the process parameters and the key stent aspects, namely, precision, mechanical properties, and other additional properties, and reduce the costs.

Resumen

La principal motivación de este trabajo fue la de analizar la viabilidad del proceso de fabricación actual de los stents para producir los nuevos stents bioabsorbibles (SBA), así como estudiar nuevas formas de fabricación. El Corte por Láser de Fibra (CLF) ha sido seleccionado por ser el proceso de fabricación actual de los stents y la Impresión 3D (I3D) por su capacidad para procesar diferentes tipos de materiales para aplicaciones médicas y por sus aspectos económicos. Los stents han sido seleccionados por ser uno de los dispositivos médicos más implantados en el mundo.

La tesis se centra en mejorar el proceso de fabricación de los stent bioabsorbibles, estableciendo las relaciones entre los parámetros del proceso y los aspectos clave del stent, a saber, precisión, propiedades mecánicas y otras propiedades , y reducir los costos.

Resum

La principal motivació d'aquest treball va ser analitzar la viabilitat del procés de fabricació de stent actual per produir els nous stents bioabsorbibles (SBA), així com estudiar noves maneres de fabricar-los. El tall làser de fibra (TLF) ha estat seleccionat perquè és el procés de fabricació actual per stents i L'impresió 3D (I3D) perquè té la capacitat de processar diferents tipus de materials per a aplicacions mèdiques i els seus aspectes econòmics. Stents ha estat seleccionat per ser un dels dispositius mèdics més implantats del món.

La tesi es centra en la millora dels processos de fabricació de stent, establint relacions entre els paràmetres del procés i els aspectes clau de stent, precisió, propietats mecàniques i altres propietats i reduir els costos.

Chapter 1

Introduction

Abstract

Chapter 1 presents the general domain of the thesis, it establishes the medical framework and exposes the interest, motivation and objectives persecuted in this work. The chapter ends with the methodology followed to accomplish with the objectives presented.

1.1 Preface

In medicine, cardiovascular problems, which results in heart failure, are a life threatening sickness. Cardiovascular diseases includes numerous problems, many of which are related to a process called atherosclerosis. According to The American Heart Association, atherosclerosis, or hardening of the arteries, is a condition that develops when a substance called plaque builds up in the walls of the arteries. Plaque is made of cholesterol, fatty substances, cellular waste products, calcium and fibrin (Figure 1.1).

This plaque may partially or totally block the blood flow through an artery in the heart, brain, pelvis, legs, arms or kidneys. Some of the diseases that may develop as a result of atherosclerosis include coronary heart disease, angina, carotid artery disease, peripheral artery disease (PAD) and chronic kidney disease. Atherosclerosis affects large and medium-sized arteries. The type of artery affected and where the plaque develops varies with each person. It is a slow, and progressive disease that may start in childhood. In some people it appears in their 30s, whereas in others it does in their 50s or 60s.

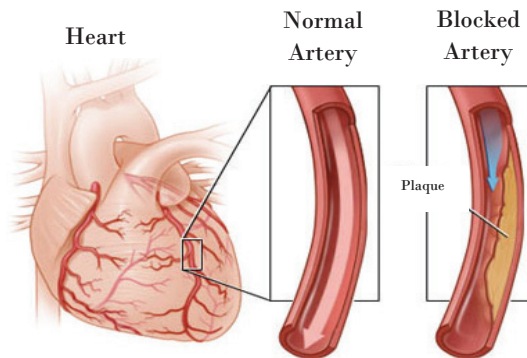


Figure 1.1. Atherosclerosis Disease

It is a complex process to know how atherosclerosis begins or what causes, but some theories have been proposed. Many scientists believe plaque begins to form because the inner lining of the artery, called the endothelium, becomes damaged. Three possible causes of damage to the arterial wall are; (I) Cholesterol, (II) high blood pressure, and (III) smoke.

As example, in the heart case the plaque stimulate the cells of the artery wall to produce other substances, resulting in the accumulation of more cells in the innermost layer of the artery wall where the atherosclerotic lesions form. The arterial wall becomes markedly thickened by these accumulating cells and surrounding material. The artery narrows and blood flow is reduced, thus decreasing the oxygen supply and many cause a heart attack, and death.

Nowadays have certain procedures to help you survive your heart attack and diagnose your condition. In fact, many heart attack patients have undergone thrombolysis, a procedure that involves injecting a clot-dissolving agent to restore blood flow in a coronary artery. This procedure is administered within a few hours of a heart attack. If this treatment is not done immediately after a heart attack, many patients have two options: (I) Angioplasty or (II) Coronary Artery Bypass Graft (CABG) surgery later to improve blood supply.

Angioplasty, also known as Percutaneous Coronary Interventions (PCI), is a procedure where a special tubing, stent, is threaded up to the arteries (Figure 1.2). The stent is a small tubular mesh whose function is to open a narrowed arterial vessel and reduce the chance of a heart attack. Current clinically used stents are made of 316L type stainless steel, titanium and cobalt-chromium alloys, platinum and are implanted on a permanent basis. Depending upon the deployment, these stents can be further classified mainly into; (I) Balloon Expandable, and (II) Self Expandable.

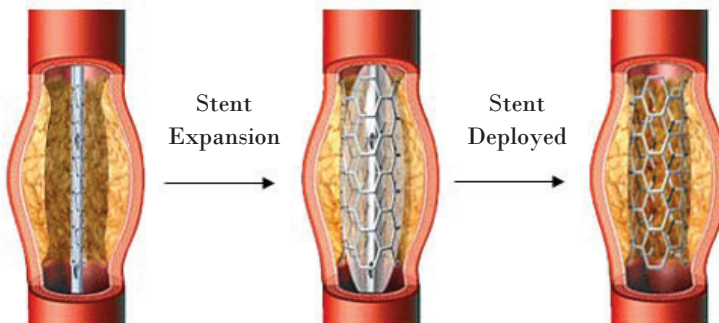


Figure 1.2. PCI Procedure

Nowadays there are two different stents in the market or under investigations. They can be classified into two categories: (I) Permanent, or (II) Degradable. This last one has not well-reach the market yet and it is one of the most medical devices under investigation right now, motivating the present thesis.

Regardless the stent type, they require a deep analysis, in term of thrombogenicity, geometrical aspects, and mechanical performance among many other characteristics. The quality obtained in their manufacture process is crucial to blood compatibility, prevent the activation process of thrombosis and as well as improve the healing efficiency. The forecast atherosclerosis makes necessary a continuous studies on this field, which help to solve the medical and engineering problems of this device.

Today, stents and stenting are the most frequent intervention in vascular surgery, gastrointestinal surgery, radiology, cardiology, neurosurgery, thoracic surgery, and other medical specialities. Since stent appearances it became evident that this device has significant limitations, such as vessel occlusion, and restenosis [1]. To overcome these problems, Bare Metal Stents (BMS) were introduced reducing the vessel occlusion. However BMS presents high rates of restenosis which constitute the major limitation of this stent type for the treatment of complex lesions and patients [2]. To surmount this hurdle, metallic stent coated with anti-proliferative drug were conceived, the Drug Eluting Stents (DES). With the introduction of DES, the anti-proliferative drug over the struts prolonged vessel wall healing, reduced neointima hyperplasia, and consequently decreased the target lesion revascularization. Although metallic stents, BMS and DES, are effective in preventing acute occlusion and reducing late restenosis after coronary angioplasty, many concern still remain.

In most cases, the role of stenting is temporary and is limited to the intervention and shortly thereafter, until healing and re-endothelialization are obtained [3]. Bioresorbable stents (BRS) were introduced to overcome these limitations with important advantages: complete bioresorption, mechanical flexibility, does not produce imaging artefacts in non-invasive imaging modalities, etc. BRS offer the potential to improve long-term patency rates by providing support just long enough for the artery to heal, offering the potential to establish a vibrant market. However, design a bioresorbable structure for an intended period of support is rather difficult. To further illustrate this, note that the concept of BRS dates back to the 1980s, but there are no designs currently well-established on the market yet [4].

Until now, the methods for producing stents include electrical discharge machining, braiding, knitting, welding, photochemical etching and more commonly, laser cutting technology. Nevertheless, the inclusion of BRS concept should make us wonder about the applicability of the current laser cutting manufacturing process for making BRS due to the new materials that have to be used, mostly polymers.

Produce fully BRS with high quality, faster manufacturing process, new materials, lower cost, etc., and, at the same time, accomplish with the strict stent's requirement is still an open challenge. Analyse the feasibility of the current laser cutting process to produce BRS as well as study new manufacturing method to fabricate BRS are the main objectives that have motivated the present thesis work.

1.2 Interest and Motivation

This thesis is carried out in the frame of the Research Group on Product, Process and Production Engineering (GREP). Set up in 1998 by University of Girona faculty members, GREP is currently carrying out research on aspects related to the fields of the product, the process and the production of medical devices, such as:

- Cranial Prosthesis
- Micro Fluidic Devices
- Tissue Engineering Scaffolds
- Prosthesis (Clivus, Jaw, Wrist, Etc.)
- Metallic Stents / Polymeric Stents

The main motivation of this project was to analyse the feasibility of the current stent's manufacturing process to produce the new BRS as well as study new manufacturing methods. Fibre Laser Cutting (FLC) has been selected because is the current stent's manufacturing process, and 3D-Printing (3DP) because its capability to process different types of materials for medical applications and their economic aspects. Stents have been selected for being one of the most implanted device in the world.

Stents can be used for a wide range of indication, including *de novo* lesions, small-vessel disease (SVD), bifurcation lesions, and tortuous and narrows lesions. Stents can improve the clinical outcomes for all of these indications as well as quality of life for patients suffering from this debilitating disease. According Global Data [5], in 2013, sales of DES and BMS in the 10 mayor markets (10MM) were \$ 4.89 billion. It is estimates by 2020, sales of stents, will grow to \$ 5.65 billion, at a Compound Annual Growth Rate (CAGR) of 2.0%.

The thesis focuses on improve the stent's manufacturing processes, and establishing relationships between the process parameters and the key stent aspects, namely, precision, mechanical properties, and other additional properties. The reduction of costs derived by the manufacturing process, employing economic techniques, as well as to know the effect of these manufacturing technologies over the material properties are the main lines of research followed on this thesis work, all of them focus on to develop a fully BRS.

This thesis work has been developed with the financial support from Ministry of Economy and Competitiveness (MINECO, PI2013-45201-P) and University of Girona (UDG, MPCUdG2016/036).

1.3 Objectives

The main objectives of this thesis was to analyse the feasibility of the current stent's manufacturing process to produce the new BRS as well as study new manufacturing methods. More specifically, the objectives of the thesis were:

- Objective A:

Analyse the capability of Fibre Laser Cutting (FLC) to cut Polycaprolactone (PCL) sheets to produce BRS. Study the effects the process parameters have on the main stent's properties (dimensions and material properties).

- Objective B:

Analyse the capability of Fibre Laser Cutting (FLC) to cut Polycaprolactone (PCL) real stent's tubes to produce BRS. Manufacture real stent tubes by Dip Coating Process (DCP) and study the effects the process parameters have on the main stent's properties (dimensions and material properties).

- Objective C:

Analyse new manufacturing ways to produce BRS by 3D Printing and carry out a *Proof of Concept*. Study the effects the process parameters have on the main stent's properties (dimensions and material properties).

- Objective D:

Choose the best manufacturing process for BRS in term of precision and costs. Study the techno-economical aspects of the different technologies employed in this previous objectives.

- Objective E:

Analyse the effects the sterilisation treatments have on the properties of BRS produced with the best manufacturing process. Study the effect of sterilization treatments over the main stent's properties (dimensions and material properties).

- Objective F:

Develop a new BRS that accomplish with all the BRS requirements. Analyse the effects the main stent's properties (dimensions and material) have on the medical aspects (radial behaviour, cell proliferation, toxicity, etc.).

The next section show the methodology followed to achieve the objectives described above. Achieving the objectives established will permit to know the best manufacturing process to BRS from the techno-economical point of view and develop a BRS with the proper medical requirements.

1.4 Methodology

The objectives were separated into two different stage. Published papers from each objective are denoted as *P-N^o of Paper*.

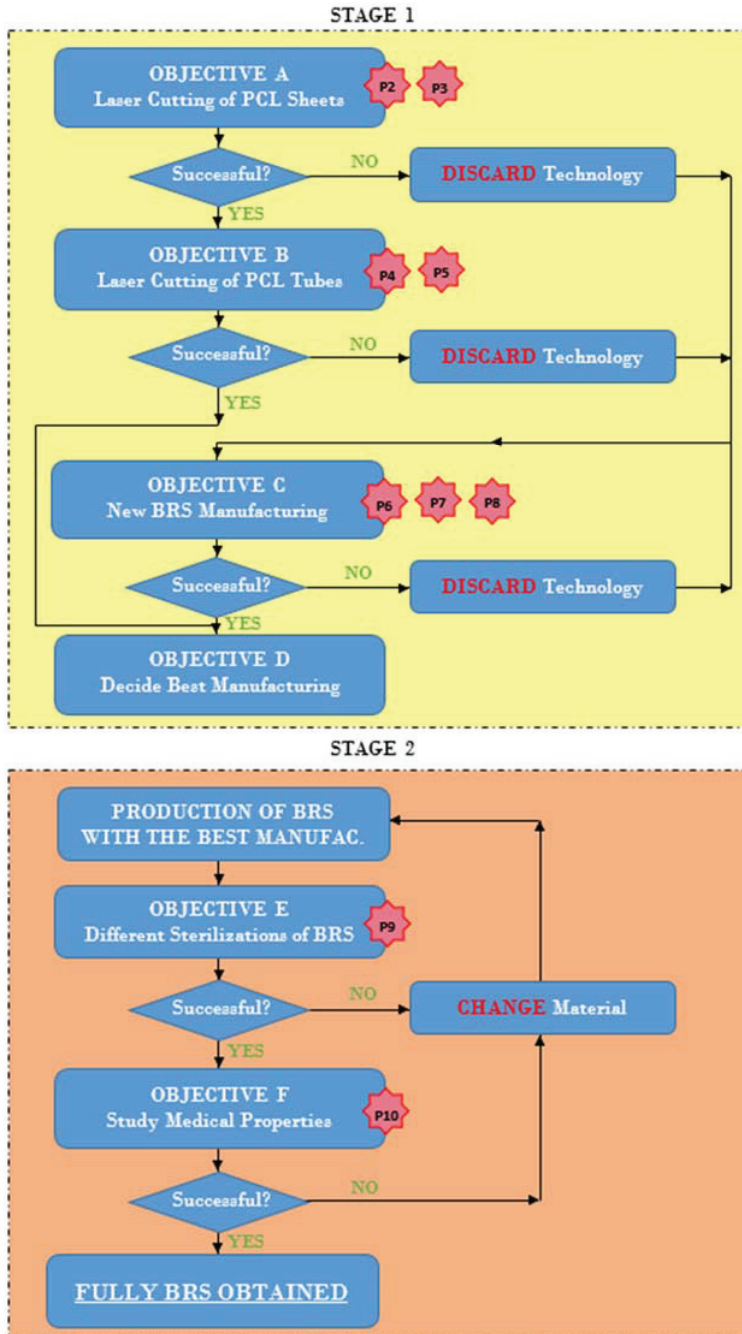


Figure 1.3. Methodology Followed

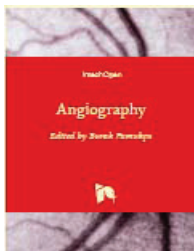
Chapter 2

Background

Abstract

Chapter 2 presents the historical and technical framework of the stents. It also presents the foundation of the two manufacturing techniques employed in the course of this thesis work, Laser Cutting and 3D-Printing technologies. Their material interactions, processing parameters, applications and their associated problems are discussed. Finally the state of the art about stent research field is presented.

Parts of this chapter has been summarized, addapted and published as chapter in the book “Angiography” (Under Publisher Guidelines).



Antonio J. Guerra, Joaquim Ciurana.” Chapter: Stent Manufacturing Field: Past, Present, and Future Prospects”. Angiography. 2018. Intechopen.

2.1 Historical Framework

Biomedical engineering (BME) is the application of engineering principles and design concepts to medicine and biology for healthcare purposes. This field seeks to close the gap between engineering and medicine. It combines the design and problem solving skills of engineering with medical and biological sciences to advance health care treatments [6]. Biomedical engineering has only recently emerged as its own study, compared to many other engineering fields. Such an evolution is common as a new field transitions from being an interdisciplinary specialization among already-established fields, to being considered a field in itself. Much of the work in biomedical engineering consists of research and development, spanning a broad array of subfields like biomechanics, tissue, genetic, neural, pharmaceutical, and medical devices.

This last one is an extremely broad category which essentially covers all health care products that do not achieve their intended results through predominantly chemical or biological means, and do not involve metabolism. Some examples include pacemakers, the heart-lung machine, dialysis machines, artificial organs, implants, artificial limbs, cochlear implants, ocular prosthetics, etc. Between these applications, stand out, the stents.

As it describes Ariel Roguin in his paper “Stent: The Man and Word Behind the Coronary Metal Prosthesis” [7], the current acceptable origin of the word *stent* is that it derives from the name of a dentist. Charles Thomas Stent, notable for his advances in the field of denture-making. He was born in Brighton, England, on October 17, 1807 (Figure 2.1). He was a dentist in London and is most famous for improving and modifying the denture base of the gutta-percha, creating the Stent’s compounding that made it practical as a material for dental impressions.

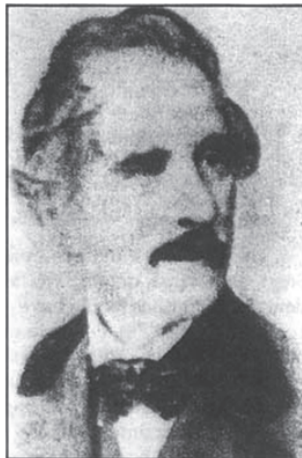


Figure 2.1. Charles Tomas Stent [6]

Gutta-percha is a natural latex produced from tropical trees native to Southeast Asia and northern Australasia. In 1847 it was introduced as a material for making dental impressions. It was used to fill the empty space inside the root of a tooth after it has undergone endodontic therapy.

However, this material was unsatisfactory for several reasons, including its tendency to distort on removal from the patient's mouth and to shrink on cooling. In 1856, Charles Thomas Stent added several other materials to the gutta-percha derived from animal fat that markedly improved the plasticity of the material as well as its stability.

Stent's sons, Charles R. Stent and Arthur H. Stent, became dentists, and together they founded a firm, C. R. and A. Stent, which manufactured the increasingly popular Stent's Compound. The sons continued marketing the compound through the prestigious dental supply company, Claudius Ash and Sons of London. When the last of the Stent brothers died in 1901, Ash's firm purchased all rights to the compound and manufactured it, keeping the Stent name (Figure 2.2). Claudius Ash and Sons became an international company, in 1924 merging with de Trey & Company to form the Amalgamated Dental Company; it is now a division of Plandent Limited.

The transition of the dental impression compound into a surgical tool is attributable to Johannes Fredericus Esser (1887 to 1946), a Dutch plastic surgeon who pioneered innovative methods of reconstructive surgery on soldiers with face wounds during the First World War. This war saw the introduction of trench warfare. Esser was designated Special Surgeon for Plastic Operations and assigned to a hospital in Vienna. He applied sterilized Stent's dental mass to stabilize the skin grafts.



Figure 2.2. Logo of the Stent compound [6]

This he accomplished by means of what he termed the “epidermic inlay technique” which used Stent’s compound to stretch and fix in place grafts to enlarge the conjunctival opening and in ear reconstruction as well as intraoral grafting.

An English army surgeon, H.D. Gillies, cited Esser’s work in his book, *Plastic Surgery of the Face*, when he wrote “The dental composition for this purpose is that put forward by Stent and a mild composed of it is known as a “Stent”. This is probably the first use of Dr. Stent’s name as a noun. The principle of the fixation of skin grafts by “stenting” was quickly adopted and persisted long after Stent’s compound ceased to be the material of choice for this technique.

The application of the word *stent* in the surgical literature was not immediate. Since the beginning of the 20th century, numerous inert tubes and biological tissue to bridge a gap or restore bile duct continuity were tested. Such a device was referred to in various ways: *tube*, *catheter*, *internal splint*, *internal strut*, and *later*, *endoprosthesis*. The first reference to a polyethylene tube “to act as a stent for the anastomosis” in experimental biliary reconstruction in dogs was made in 1954.

In urology, even as genitourinary reconstruction of the ureter and urethra expanded in the first half of the 20th century after First World War, the term used were *tube*, *catheter*, and specifically, *retention catheter*. After Second World War, the terminology remained limited to *ureteral*, *urethral*, and *vassal splinting*. Because the spoken word generally precedes the written word, it is reasonable to suppose that some urologists must have started to use the word *stent* once it was established in the surgical vocabulary.

In urology, stenting first appeared in 1972, when Goodwin wrote a brief commentary titled *Splint, Stent, Stint*, concluding: “Urologists are always talking about putting a tube in a ureter or urethra. When they do this, it is not a splint. It may be a stent. It probably is never a stint. Perhaps the process is most properly described as leaving a tube or stent in an organ.”

By 1980, the urinary tract stent was widely in use in adult and paediatric urologic practice and was also the word used for hypospadias repair, similar to the work described by Esser in 1916.

The first reference in the cardiovascular literature of the word *stent* was by Weldon et al. in 1966, when they described a prosthetic-stented aortic homograft used for mitral valve replacement.

Dotter was the first to use the word in his article in Radiology in April 1983, which was titled “Transluminal Expandable Nitinol Stent Grafting: Preliminary Report.”

The first coronary stent was implanted into a patient by Jacques Puel in Toulouse, France, on March 28, 1986. In their report in French, they used the term *endo-prothèses coronariennes autoexpansives*.

Ulrich Sigwart has been credited with the concept and realization of endoluminal stenting, a procedure that has revolutionized coronary and peripheral arterial revascularization. Sigwart worked at the University Hospital, Lausanne, Switzerland (1979 to 1989), and played a pivotal role in the concept and ultimate application of coronary stenting.

Jacques Puel and Ulrich Sigwart were invited almost simultaneously by the company Medinvent to help with the initial animal and clinical research pertaining to their new product, the Wallstent. Ulrich Sigwart was contacted because he practiced in Lausanne, Switzerland, the headquarters of Medinvent, and the French engineer behind the product contacted his French colleague, Jacques Puel.

Sigwart and Puel were the first to report on the clinical use of stents to prevent sudden occlusion and restenosis after transluminal angioplasty in their landmark work published on March 19, 1987, in the New England Journal of Medicine. The article reported their experience from Lausanne, Switzerland, and Toulouse, France.

Sigwart also observed the shortcoming of stents when, 3 months after one had been implanted in the proximal left anterior descending artery, the patient had recurrent chest pain. Angiography revealed severe restenosis, and he wrote that a combination of mechanical and biological factors would be the *sine qua non* to overcome the problem of recurrence.

Sigwart wrote in a letter to the editor of the American Journal of Cardiology that, “When submitting the first article on human stenting in 1986, the New England Journal of Medicine persuaded me to drop the verb ‘stenting’ and use instead the noun ‘stent.’”

Julio Palmaz, an interventional vascular radiologist, is known for inventing the balloon-expandable stent, for which he received a patent filed in 1985. In October 1987, Palmaz implanted his first peripheral stent in a patient at Freiburg University in Germany. Since then, stents and stenting have evolved establishing a vibrant market.

2.2 Economical Framework

This section present the global analysis and market forecast presented in 2014 by GlobalData [5] as economical motivation of this thesis work. The study is only focus on coronary stents, one of the most used stent in clinical practice, but it serves as an example of the incredible market that stents entail.

Table 2.1 provides the key metrics for coronary stents in the 10MM (US, France, Germany, Italy, Spain, UK, Japan, Brazil, China, and India) during the forecast period from 2013 to 2020.

Table 2.1. Coronary Stents Market Key Metrics in the 10MM – 2013 to 2020 [5]

2013 Coronary Stent Market Sales	
US	\$ 2065.3 m
EU	\$ 573.1 m
APAC	\$ 2123. 3 m
Brazil	\$ 124.0 m
TOTAL	\$ 4885.7 m
2013 Global Market Sales by Type of Stent	
Drug Eluting Stent (DES)	\$ 4335.6 m
Bar Metal Stent (BMS)	\$ 530.1 m
Pipeline Assesment (Stage of Clinical Development)	
Stents in the early development stage	4
Stents in the preclinical stage	13
Stents in the early clinical stage	6
Stent in the late clinical stage	5
Key Events (2015 to 2020)	
2015 - Commercial launch of the CE-Marked DESolve 100, a novolimus-eluting, thin-strut BRS, in the EU.	
2015/2016 - Expected commercial launch of BRS, such as DREAMS by Biotronik and Fantom by REVA Medical, in the EU.	
2016/2017 - Commercial launch of Absorb BVS in the US and APAC, including in Japan and China.	
2019/2020 - Expected commercial launch of BRS, such as DREAMS by Biotronik and Fantom by REVA Medical, in the US.	
2020 Forecast Coronary Stent Market Sales	
US	\$ 1849.9 m
EU	\$ 0555.2 m
APAC	\$ 3023.5 m
Brazil	\$ 0187.8 m
TOTAL	\$ 5616.4 m

Stents can be used for a wide range of indication in Coronary Artery Disease (CAD), including *de novo* lesions, small-vessel disease (SVD), bifurcation lesions, and tortuous lesions. Coronary stents can improve the clinical outcomes for all of these indications as well as quality of life for patients.

Figure 2.3 shows the sales of coronary stents for treating CAD in each of the 10 countries covered in this section during the forecast period. In 2013, sales of DES and BMS in the 10MM were \$ 4.89 bilion. GlobalData estimates by 2020, sales of coronary stents, will grow to \$ 5.65 bilion, at a Compound Annual Growth Rate (CAGR) of 2.0%.

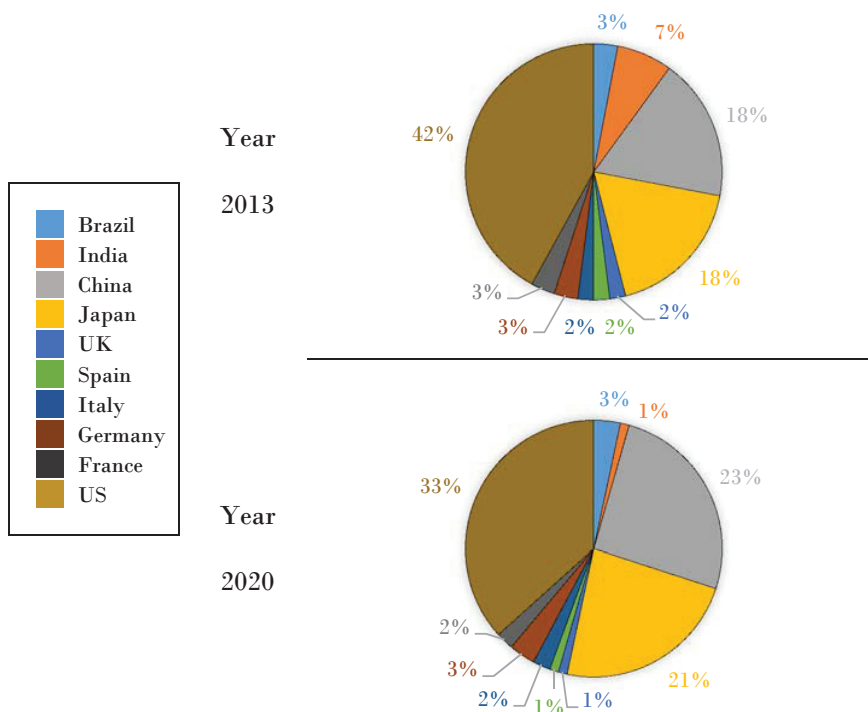


Figure 2.3. Sales of Stents 2013 – 2020 [7]

Of the 10MM covered in the report, the US currently has and will continue to have the largest share in the coronary stents market. Together, the US, the 5EU countries, and Japan will account for 64% of the coronary stents market for BMS and DES in 2020. Collectively, the 5 EU countries are forecast to have only 10% market share in the future. Among the emerging markets, China has captured significant market share, which is expected to increase in the future. The emerging markets, including Brazil, China, and India, are expected to demonstrate the greatest growth in the market.

The key drivers for the coronary stents market during the forecast period are:

- The rising prevalence of CAD in the major markets.
- The need for effective therapies that reduce the risk of complications associated with BMS and DES.
- The cost savings for healthcare payers resulting from the reduced need for repeat revascularization procedures and prolonged dual antiplatelet therapy.
- Reducing the need for stent-in-stent procedures and improving the technical feasibility of future interventions.
- Innovations in stent technology with regard to the platform, material, and coating.
- The increase in patients' disposable income and government insurance coverage in the emerging markets, such as China and India.
- The approval and launch of BRS, such as the Absorb BVS, in the US, Japan, and China

Stenting for coronary applications has been widely adopted in clinical practice and is associated with improved outcomes. BMS and DES are effectively commodities, where the physician has a handful of stents from which to choose.

Within the coronary stents market, DES currently dominate the market and will continue to do so throughout the forecast period, as they are considered the gold standard of treatment. The DES market is a vast and double-digit market, accounting for nearly 90% of the total coronary stent market. In fact, DES sales for coronary applications are nearly eight times those of BMS market sales. Given this large market potential and the rising prevalence of CAD worldwide, device manufacturers have focused primarily on the research and development (R&D) and commercialization of innovative DES systems. The larger market sales of DES can be attributed to physicians' extensive clinical experience and expertise in using these stents, improved outcomes, and the reduced need for repeat intervention. BMS are used in cases where the patient is not a good candidate to receive a DES, such as those planning to undergo other major surgeries in the near future. Non-covered stents are used less often in practice and only in select cases, such as patients with artery perforations.

BRS have only recently entered the market and are not widely adopted in clinical practice, due to the lack of clinical evidence and the high cost of these devices. The gap in their manufacturing process, materials, and mechanical properties is still an open challenge that should be solved by the research community motivating the present thesis work.

Over the years, a plethora of BMS and DES have been developed, featuring innovative materials, designs, structures, coatings, and drug-elution components. The development and optimization of DES has become a primary focus for many stent manufacturers, where they utilize the BMS they have developed as the platform and foundation for their DES. These innovations in technology aim to ensure high radial strength and flexibility, low elastic recoil, optimal vessel coverage, minimal foreshortening, and rapid strut endothelialization.

Although stent technology has evolved over the years, several types of complications remain, such as late thrombosis and restenosis, negative vessel remodeling, delayed endothelialization and healing, lack of homogenous drug distribution, and the need for prolonged dual antiplatelet therapy. Therefore, low-profile drug-delivery systems need to be developed to reduce the risk of restenosis and thrombosis, and improve long-term patency. Effective therapies also need to be developed to treat complex lesions and challenging patient populations, such as chronic total occlusions (CTOs), long lesions, acute myocardial infarction (AMI) (heart attack), and diabetes mellitus. Emerging stent technologies in the coronary stent market, including BRS and the third generation of DES with biodegradable polymer/polymer-free coatings, aim to address these unmet needs. However, these emerging technologies have only recently entered the market and will encounter strong competition from the contemporary stents. The third generation of DES has been developed to eliminate concerns associated with the permanent polymer coating, which is a cause of late and very late stent thrombosis. Drug-eluting BRS represent the fourth generation of DES in the evolution of DES technology. Given that the stent scaffold degrades over a period of time, BRS offer several benefits, including a reduced risk of restenosis, avoiding the implantation of multiple layers of metal inside the vessel, improving the feasibility of future interventions, and enabling for late lumen gain.

The coronary stents market is a vast and dynamic market that is saturated with numerous players worldwide. The competitive landscape consists of large, mid-size, and small companies that have developed different types of coronary stents to target various indications, such as de novo lesions and bifurcation lesions. The coronary stents market is largely dominated by a few key players, including Abbott Vascular, Medtronic, and Boston Scientific, followed by Biosensors International and Terumo Corporation. Companies such as B. Braun, Sahajanand Medical Technologies, MicroPort Scientific Corporation, and Balton are potential competitors to these large corporations, as they develop innovative coronary stent platforms.

As the next generation of DES and BRS enter the market, the current key players will need to retain and acquire market share by improving the clinical performance of their existing products. In addition, they will need to expand into or increase their presence in the emerging markets in order to take revenue away from their competitors in the future.

Each year, millions of individuals worldwide are affected by CAD. Given the high burden of the disease, it is important to develop innovative technologies that can improve outcomes and disease management. Currently, DES are widely adopted in clinical practice, given the clinical evidence, improved outcomes, and physician experience with using these devices. In the US and 5EU, the coronary stents market value is expected to decline slowly in the future, given the decline in the average selling price (ASP) and number of BMS and DES used per procedure. As medical costs continue to rise, healthcare providers are implementing cost-containment policies and “appropriateness criteria” to reduce costs and overstenting.

Unlike in the west, the coronary stents market in the APAC and South American regions is expected to increase and demonstrate steady growth in the future. The APAC countries, including Japan, China, and India, have diverse populations, ethnicities, and clinical practices. Most device manufacturers regard Japan and China as their chief targets, due to their economic growth, pricing structure, and vast populations. In particular, China, with its high proportion of aging individuals and procedure volume, is expected to become a prime market for coronary stents.

Many stent manufacturers have ventured into the R&D of BRS, which is a high-growth market segment. However, BRS technology is in the early stages, where robust, long-term clinical evidence of its therapeutic benefits needs to be shown. Currently, the adoption of BRS in the clinical setting is low, which is attributable to the lack of clinical data and appropriate reimbursement, as well as the high cost of these devices. In real-world practice, the majority of patients with CAD are treated with DES, and this will continue in the future. In addition, the development of the next generation of DES with bioresorbable polymer, polymer-free, and innovative platforms indicates the value of DES in the coronary market, but both BMS as well as DES will be replaced by BRS when these devices are fully developed.

2.3 Foundation of Stents

2.3.1 Introduction

Regardless of the stent choice, BMS, DES, or BRS the challenges associated to this medical device remain similar. Figure 2.4 shows the *Pyramid of Stent Challenges* and it represents the main issues to consider at the time to design and manufacture this medical device.

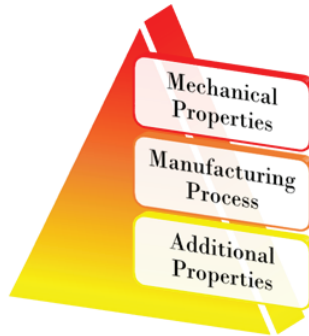


Figure 2.4. *Pyramid of Stent Challenges*

The mechanical properties of the stent govern the decision process. This important property will be in charge of provide the correct longitudinal and radial behaviour. The mechanical properties of the stent mainly depend on the material and its geometry but also on its medical application.

$$(1) \text{ Mechanical Properties} = f(\text{Material, Geometry, Application})$$

Once decided the mechanical properties (material and geometry) according the medical application, we give way to the manufacturing process step. The manufacturing process mainly depends on the materials chose in the previous step and the stent type and geometry.

$$(2) \text{ Manufacturing Process} = f(\text{Material, Type and Geometry})$$

Finally, the additional properties step. Although it is constitute the final layer of the stent pyramid, additional properties cover a range of modifications to stent designs. This last step in directly relate to the stent type and its medical application.

$$(3) \text{ Additional Properties} = f(\text{Stent Type, Application})$$

Next sections present the main issues to consider in the abovementioned decision piramid steps. From desired mechanical properties to the most common additional properties that clinical practice required. Section 2.3 ends with the current steps for the manufacture of the stents.

2.3.2 Stent Types

As mentioned previously, there are currently three type of stents: Bare Metal Stent (BMS), Drug Eluting Stent (DES), and Bioresorbable Stent (BRS). There are briefly present below.

Bare Metal Stents

Bare metal stent are usually stainless steel of nickel alloy and have no special coating. They act as scaffolding to prop open blood vessels after they are widened with angioplasty. As the artery heals, tissue grows around the stent, holding it in place. However, sometimes an overgrowth of scar tissue in the arterial lining increases the risk of restenosis.

Drug Eluting Stents

Drug eluting stents are BMS coated with medication that is released to help prevent the growth of scar tissue in the artery lining. This helps the artery remain smooth and open, ensuring good blood flow and reduces the chances of the artery restenosis. However, it also leads to a higher chance of blood clots.

Due to a relatively slower healing process, patients implanted with DES must strictly follow their doctor's recommendation on drug therapy (DAPT) to help reduce the risk of stent thrombosis.

Within DES category is can be differentiate the Bio-Engineered Stents, also known as antibody-coated stent. This type of stent differs from DES because it does not contain a polymer and does not use a drug. As a result, it helps to speed up the cell lining of the artery (endothelialization), promoting natural healing.

The antibody on the stent's surface attracts circulating Endothelial Progenitor Cells (EPCs) which come from human bone marrow and help speed up the formation of healthy endothelium. This provides rapid coverage over the stent's surface helping to reduce the risk of early and late thrombosis.

Bioresorbable Stent

Bioresorbable Stent is a stent on a dissolvable type of scaffold platform which can be adsorbed by the body over time. Like some of the current available DES, BRS could be coated with a drug released from a polymer that disappears over time to reduce the likelihood of the artery restenosis. The scaffold itself is absorbed overtime.

2.3.3 *Stent Mechanical Properties*

Ideal stents should be corrosion resistant, biocompatible, and visible by X-Ray and/or Magnetic Resonance Imaging (MRI) methodology. Consideration specific to either balloon expandable or self-expandable stents must also be made.

For balloon expandable stents, an infinite elastic modulus prevents recoil. A low yield strength is preferred to allow stent expansion at acceptable balloon pressures and facilitates crimping of the stent on the delivery system. High tensile properties after expansion help to achieve radial strength with a minimal volume of implanted foreign material. Higher tensile properties also permit the use of thinner struts for an overall lower profile, thus improving flexibility, deliverability, and access to smaller vessels. A steep work-hardening rate leads to a desirable rise in strength during expansion. Finally, a high ductility is needed to withstand deformation during expansion.

In self-expandable stents, large recoverable strains are required for both deployment and crush resistance. This is commonly described as superelastic behaviour, with an ideal stress-strain curve showing long and elevated plateaus following an initial elastic loading regime. The device remains within the superelastic range inside the delivery catheter and may gain enter the superelastic range after deployment if sufficient deformation is imparted due to vessel interaction or external forces. Elongation and UTS are of significance during stent manufacturing but are given less attention with respect to the superelastic event itself. To extent that these traditional properties influence fatigue resistance and fracture toughness, elongation and UTS should be regarded as important parameters. Resistance to pulsatile and begging fatigue is of paramount importance, as the stent follows the vessel movements. The biased stiffness of superelastic nitinol that results from the hysteresis between the loading and unloading path is currently debated.

The above properties are interrelated and sometimes contradictory, requiring careful compromise. For example, higher tensile strength materials typically also have higher yield strengths. Although the higher tensile strength is desirable for bolstering radial strength as outline above, the associated higher yields strength promotes the undesired acute recoil upon balloon deflection. The new BRS presents others key factor such as, (I) Biodegradation, (II) Radiopacity, and (III) Electrical conductivity [8]. Research stent's world are trying to solve this answers by finding the best correlation between material and stent geometry.

2.3.4 Stent Materials

Since the introduction of the first stainless steel devices, the materials used for stents have evolved and diversified rapidly. In the drive to obtain a share of what was becoming a vast and growing market, manufacturers invested heavily in research and development to gain continuous. The main materials currently used or which are being investigated are briefly presented below.

Non Bioresorbable Materials

316 Stainless Steels

316 stainless steel, also referred to as marine grade stainless steel, is a chromium, nickel, molybdenum alloy of steel that exhibits relatively good strength and corrosion resistance, and is a common choice for biomedical implants, such as stents.

Nitinol

Nitinol is a metal alloy of nickel and titanium, where the two elements are present in roughly equal atomic percentages. Nitinol alloys exhibit two closely related and unique properties: shape memory (SME), and superelasticity (SE) been perfect to self – expandable stents.

Fully Bioresorbable Materials

Magnesium Alloys

Magnesium is the third most commonly used structural metal. Magnesium is used in super strong, lightweight materials and alloys. Magnesium alloys have been historically used by the magnesium tendency to corrode, creep at high temperature, and combust.

Poly-L-Lactide Acid (PLLA)

PLLA is a biodegradable thermoplastic aliphatic polyester derived from renewable resources, such as corn starch. Degradation is produced by hydrolysis of its ester linkages in physiological conditions.

Polycaprolactone (PCL)

PCL is a biodegradable polyester with a low melting point (60°C) and a glass transition of about -60°C. Degradation is produced by hydrolysis of its ester linkages in physiological conditions and has therefore received a great deal of attention.

2.3.5 Stent Geometries

Following the classification done by Stoeckel et al. in their manuscript “*A survey of stent designs*” [9] stents can be classified into four categories:

Coil

Most common in non-vascular applications, as the coil design allows for retrievability after implantation. These designs are extremely flexible, but their strength is limited and their low expansion ratio results in high profile devices (Figure 2.5).



Figure 2.5. Coil Stent.

Helical Spiral

These designs are generally promoted for their flexibility. With no or minimal internal connection points, they are very flexible, but also lack longitudinal support. As such, they can be subject to elongation or compression during delivery and deployment and, consequently, irregular cell size. With internal connection points, some flexibility is sacrificed in exchange for longitudinal stability and additional control over cell size (Figure 2.6).

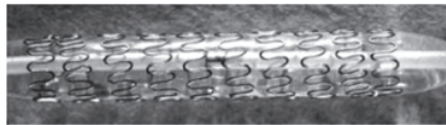


Figure 2.6. Crossflex Stent.

Woven

This category includes a variety of designs constructed from one or more strands of wire. Woven designs are often used for self-expanding structures. While these designs offer excellent coverage, they typically shorten substantially during expansion. The radial strength of such a woven structure is also highly dependent on axial fixation of its ends (Figure 2.7).

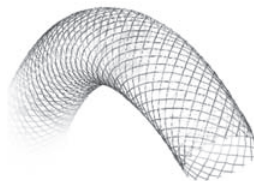


Figure 2.7. WallStent.

Sequential Rings

Sequential rings stents are structures joined by connecting elements known as “bridges”, “hinges”, or “nodes”. This type of stent are the most common stent in the market (70%) (Figure 2.8). This category can be refined according two categories:

1. By their structural elements such as:

Regular Connection

This subcategory includes stents in which their “bridges” are connected to every inflection point around the circumference of a structural member.

Periodic Connection

This subcategory includes stents in which their “bridges” are connected to a subser of the inflection points around the circumference of a structural member. Connected points alternate with unconnected points following a pattern.

Peak-Peak Connection

This subcategory includes stents in which their “bridges” are connected to adjacent structural members.

2. By the nature of the final cells such as:

Closed Cell

This subcategory includes stents wherein all internal inflection points of the structural members are connected by “bridges”. Such a condition this geometry only allow Peak-Peak Connections.

Open Cell

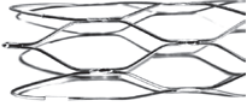
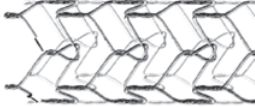
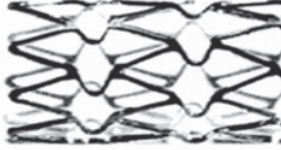



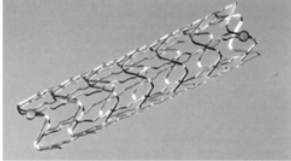
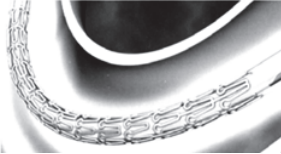
This subcategory includes stents wherein some inflection points of the structural members are connected by “bridges”.



Figure 2.8. Palmaz–Schatz stent

Other examples of stent in the market are (Table 2.2).

Table 2.2. Stent Types in the Market

NAME	FIGURE	DESCRIPTION
Symphony		Nitinol wire welded to form a closed-cell stent
Cook ZA		Nitinol wire knitted to form a closed-cell stent
NR		Closed-Cell Stent with "V" flex-hinges
SMART		Self-Expandable Open-Cell Sequential Ring
AVE S7		Open-Cell Sequential Ring Stent
Navius ZR1		StainlessSteel Ratcheting Stent
BeStent		Open-Cell Sequential Ring Stent
ACS Multilink		Open-Cell Sequential Ring Stent

2.3.6 Past, Present and Promising Stents Manufacturing Techniques

Historically, has been five techniques to produce stents: Etching, Micro–Electro Discharge Machining, Electroforming, Die–Casting, and more commonly, Laser Cutting [10]. These are briefly discusses in this section. Also, Additive Manufacturing (AM) techniques are presented as promising manufacturing technique for stents.

Etching

The etching method is based upon the photolithography process (Figure 2.9). In this process, the desired mask pattern is first projected on the plain sheet coated with photoresist, which after exposure can be developed and etched for the desired pattern. This is then deformed so as to cause the two opposing sides to meet and joined at certain points, resulting in the formation of tubular stent.

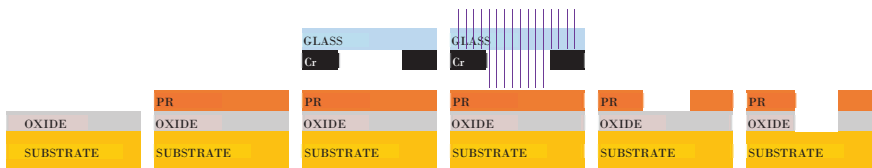


Figure 2.9. Conventional Photolithography Process

Micro – Electro Discharge Machine (EDM)

Micro – EDM technique (Figure 2.10) is able to cut burr–free micro holes with high precision in a conducting material. In this process the material removal takes place by electro – erosion due to electric discharge generated between closely spaced electrodes in presence of dielectric medium. The shape of the machined feature is the mirror image of electrode. The stent is produced either by folding the plane patterned sheet and welding at certain point or directly generating the desired pattern in a cylindrical tube.

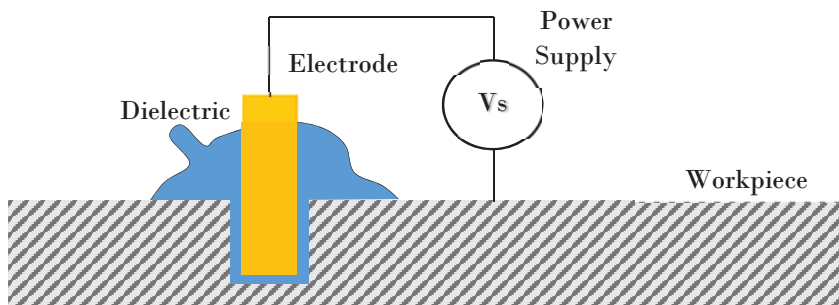


Figure 2.10. Micro – Electro Discharge Process

Electroforming

In this process electroplating is performed on a mandrel in a given pattern. When the desired thickness has been reached, the mandrel is etched away from the electroformed stent, leaving a free standing structure, a fully functional stent. This technique is especially useful for manufacturing stent from the precious metal such as gold (Figure 2.11).

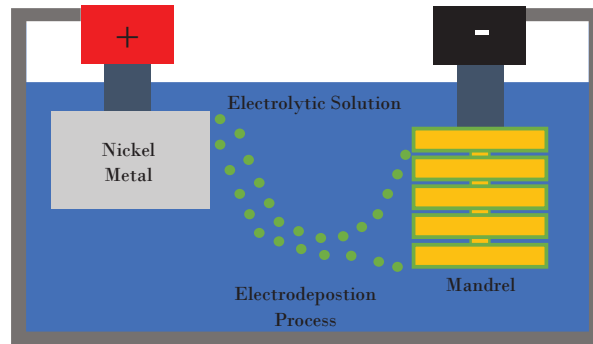


Figure 2.11 Electroforming Process

Die – Casting

This is another technique in which the stent can also be formed by subjecting one or more (Figure 2.12). The metal may be cast directly in a stent like form or cast into sheet or tubes from which the inventive stents are produced by using any of the method mentioned here.

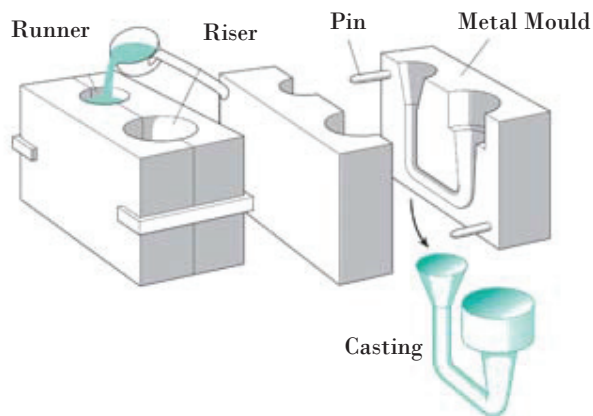


Figure 2.12 Die – Casting Process

Laser Cutting

In this technology the material is removed by energy absorption. When a high energy density laser beam is focused on workpiece surface, the thermal energy is absorbed which heats and transforms the workpiece volume into a molten, vaporized or chemically changed state that can easily be removed by flow of high pressure assist gas jet (Figure 2.13). This manufacturing technique is one of the techniques used in the present thesis work and it is fully explained in the section 2.4 Foundation of Laser Technology.

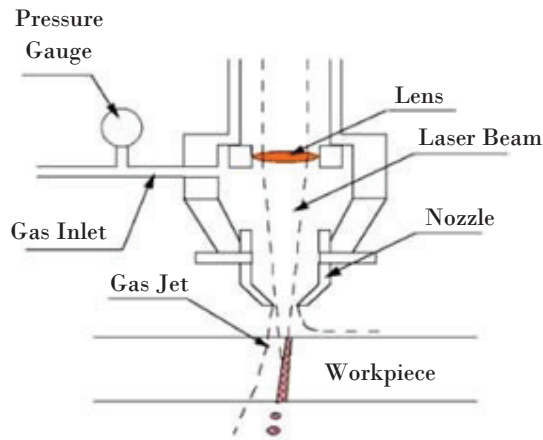


Figure 2.13 Laser Cutting Process

Additive Manufacturing

Additive Manufacturing, also known as 3D Printing, refers to processes used to create a three-dimensional object (3D) in which layers of material are formed under computer control. Mainly, there are four different 3D Printing technologies (Figure 2.14), Inkjet, Stereolithography (SL), Selective Laser Sintering (SLS), and Fused Filament Fabrication (FFF). This last one could be a promising solution to BRS production and it is fully explained in the section 3.5. Foundation of 3D Printing.

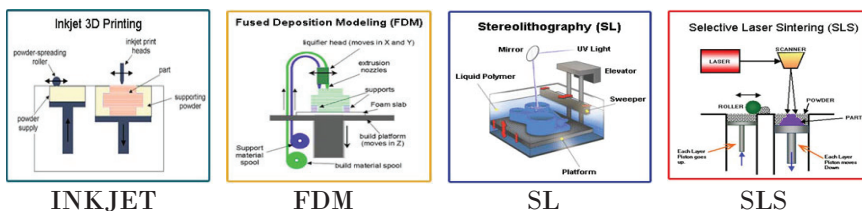


Figure 2.14 3D Printing Processes

2.3.7 Stent Additional Properties

This section briefly presents the most common additional properties that are add to the stents.

Radiopacity

Stents made from stainless steel, nitinol or polymers are sometimes hard to see fluoroscopically. To improve X-Ray visibility, markers are often attached to the stents.

Drug Release

It is the main additional property usually add to stents for the clinical practice to create DES. There are a variety of coating techniques to incorporate drugs to the stent such as:

Dip Coating

Coating by submerging the stent in a solution of drug and/or polymer in a solvent. The stent is then left to dry, allowing for evaporation, in the air/oven.

Electrotreated Coating

The drug/polymer particles are suspended in a liquid medium migrate under the influence of an electric field and are deposited onto an electrode (stent).

Plasma – Treated Coating

Plasma coating (Plasma Activation) is a method of surface modification which improves surface adhesion properties. Plasma produce a reduction of metal oxides, surface cleaning from organic contaminants, and modification of the topography.

Spray Coating

These techniques use apparatuses that spray polymer and drug solutions (using various solvents) onto a stent, enabling consistent deposit of a uniform drug release layer(s) onto the stent surface.

Multiple variables can be adjusted to optimize drug release for cardiovascular stent applications, including biocompatible polymers and antirestenotic drugs. While the presence of a polymer coating on a DES is not required, the process to choose one can be difficult because it has been previously shown that most polymers listed as biocompatible and used in medicine can cause vascular inflammation.

2.3.8 Current Manufacturing Cycle of Stents [11]

From Bulk Material to Tube

The medical grade alloys for permanent stents (BMS and DES), i.e. SS316L and Co-Cr alloys, are commonly made by vacuum melting process to obtain ultra high purity materials. They are then thermo-mechanically treated and delivered as a bulk under annealed condition in the form of billet or rod. The bulk is then cold drawn to form minitubes, the preform for laser cutting, and furnished under cold-worked condition to provide dimensional accuracy, ease of handling and to avoid bending during laser cutting.

Commonly, the desired metallurgical condition of SS316L minitubes will be under $\frac{3}{4}$ hardness, having grain size of ASTM 7-8 (24-34 μm) with 8-10 grains across the wall. Hence, there are two different states of materials with different properties: the ductile bulk material and the hard minitube material.

In this stage, similar process is also employed for biodegradable metals where most of them are produced through melting and thermomechanical treatment. Extrusion was then employed to produce minitubes in the case of the experimental magnesium-based alloys stents.

From Tube to Stent

As mentioned previously, the most common method of making stents is by laser cutting where the minitubes are cut out following a determined pattern. Figure 2.15 shows a typical laser cutting process for making stents in which a stationary laser cuts the moving (translating and rotating) long and continuous minitube.



Figure 2.15. Laser Cutting Process of Stents

However, laser cutting technology, is a thermal process which result in thermal damage (Figure 2.16) such Heat-Affected-Zone (HAZ), recast layer, microcracks, and dross.

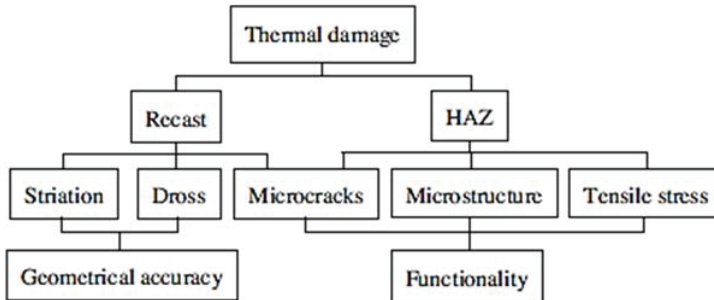


Figure 2.16 Thermal Damages and its effects

Recast

Recast is formed due to the re-deposition of the molten materials on the cut edges. This layer is usually harder than the parent materials, and also is highly stressed which may lead to crack formation.

Dross

Dross is a molten material and witnessed as a solidified drops clinging to the bottom edges of the cut materials. Surface tension and viscosity of the molten material influence significantly the formation of the dross. High surface tension and viscosity resist the molten metal from flowing smoothly out of the cutting zone and it develops the dross formation.

Striations

Striations are defined as periodic lines with a slight inclination from the beam axis appearing on the cut edge after the laser cutting process. Striations occurrence deteriorates the cut edges and cause uneven surface roughness.

Heat Affected Zone (HAZ)

The HAZ is an acknowledgement of the laser cutting process being a thermal phenomenon where a huge amount of energy is absorbed and conducted into the workpiece. HAZ is found in the vicinity of the laser cut area that experience excessive heat but it does not reach the melting point. This region is heat distorted compared to the parent material and usually microcracks are observed in this zone, affecting the tensile stress.

To overcome these thermal damages, basically the following post processing techniques are applied (Figure 2.17): Pickling Techniques, Soft Etching, Annealing and Electropolishing [10]. These are briefly discusses below.

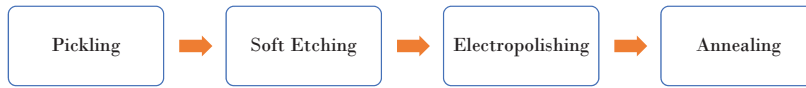


Figure 2.17 Stents Post – Processing Techniques

Pickling

Pickling is a type of cleaning process whereby the underside dross or surface oxide layer is removed by chemical attack. Its mechanism relies on the acid penetration to the steel/surface oxide layer interface and then progressing along the interface. The acid penetration, on the other hand relies on the size and number of cracks in the oxide layer that extend to the steel surface. Pickling is achieved by immersing laser processed part in a thermoplastic tank containing dilute HCL acid. The result should be a dross or oxide free product.

Soft Etching

In this method, basically, all the hydrogen containing etching products i.e. HCL, H₂SO₄ and HNO₃ must be avoided, because of hydrogen brittleness with the test materials. As the hydrogen diffuses along the grain boundaries and combines with the carbon, thus initiating cracks. Therefore, the best results are obtained by electrochemical etching with a weak acid that does not contain hydrogen (FeCl₃).

Electropolishing

It is an electro–chemical polishing process in which a metallic surface is brightened as well as smoothed by polarizing it anodically in an adequate electrolyte solution. Usually it is done in an aqueous solution.

Annealing

Annealing is usually done to make the stent implantable, i.e. sufficiently soft (ductile). By annealing the pickled stent in a vacuum furnace at 1100 °C and then slowly cooling, soften the stent. The typical heating and cooling rates are 3°C/min and 4°C/min respectively. After annealing it is cleaned in distilled water agitated with the ultrasonic bath for about 15 min and then finally dried up in the air.

From Production Line to Implantation Site

Out of production line, stents are normally delivered under crimped (compressed) onto a balloon catheter for practical purpose. During stent implantation procedure, this crimped stent is inserted into the artery through a small incision in arm or groin, delivered through a tortuous passage to reach the targeting site and then expanded under a contact with blood. The whole procedure may take 1.5 to 2.5 hours, but the time frame for a stent, starting from insertion until deployment may take about 15 to 30 minutes. As illustrated in Figure 2.18, a typical external diameter of SS316L stent for large artery is produced at 1.8 mm, crimped to 1.0 mm and expanded to 3.0 mm.

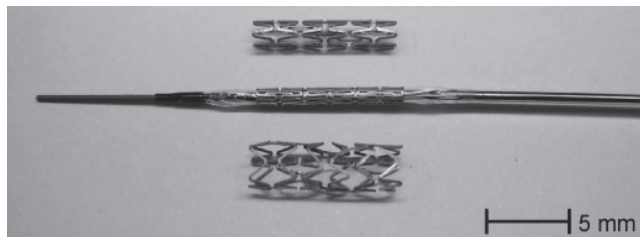


Figure 2.18. Stents Steps (UP) Descaled; (MID) Crimped (BOT) Expanded [11].

During the implantation period, these conditions are favourable for environmentally induced corrosion: corrosive environment (blood and its ions content), degradable metal (the stent), static mechanical stress generated onto the stent during crimping and expansion, and dynamic loading from heart beating. These conditions may lead to localized corrosion under stress, namely stress corrosion cracking (SCC) and corrosion fatigue. SCC was observed on Fe35Mn alloy tested under flowing Modified Hank's solution at 37°C, under applied stress and strain of 483 MPa and 9%, respectively, after 2 weeks of degradation test. Therefore, electrochemical or immersion tests cannot be used alone for the in vitro validation of degradation behaviour of proposed alloys for biodegradable stents in real environment. A more comprehensive in vitro degradation test method accommodating flow condition, stress condition (crimping and expansion), short-term (insertion to expansion) and long-term (expansion to complete degradation) periods should be developed.

As it can appreciate the stents manufacturing process involve many steps, making difficulties to lower its price. Reduce the steps involve in the process in another motivation of the present thesis work.

2.4 Foundation of Laser Technology

2.4.1 Introduction

Since the first laser cutting system, more attention has been put into laser cutting process due to its wide range of applications and its remarkable cutting capability. Nowadays laser technology has been widely applied. Different types of lasers used in material processing include CO_2 lasers, $Nd:YAG$ lasers, fibre lasers, excimer lasers, and ultra-short pulse lasers. This section go in depth of the lasers foundation.

The term “laser” originated as an acronym for “Light Amplification by Stimulated Emission of Radiation” is a device that emits light through a process of optical amplification based on the stimulated emission of electromagnetic radiation. A laser differs from other sources of light in that it emits spatial and temporal light coherently. Spatial coherence allows a laser to be focused to a tight spot, enabling applications such as laser cutting. Temporal coherence can be used to produce pulses of light as short as a femtosecond.

The laser consists of a gain medium, a mechanism to energize it, and something to provide optical feedback (Figure 2.19). The gain medium is a material with properties that allow it to amplify light by way of stimulated emission. Light of a specific wavelength that passes through the gain medium is amplified. To amplify light, it needs to be supplied with energy in a process called pumping. The energy is typically supplied as an electric current or as light at a different wavelength. Electrons and how they interact with electromagnetic fields are important in our understanding of chemistry and physics of the laser technology.

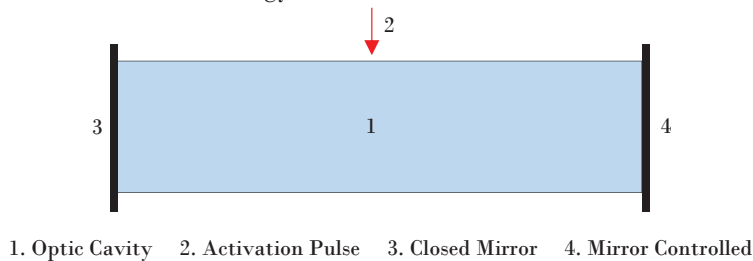


Figure 2.19 Component of a typical laser

This section presents the physics of laser technology, laser processing parameters, the material interactions mechanics, and their mathematical model based on heat transfer equations.

2.4.2 The Lasers Physics

In the classical view, the energy of an electron orbiting an atomic nucleus is larger for orbits further from the nucleus of an atom. However, quantum mechanical effects force electrons to take on discrete positions in orbitals. Thus, electrons are found in specific energy levels of an atom.

When an electron absorbs energy either from light (photons) or heat (phonons), it receives that incident quantum of energy. Transitions are only allowed between discrete energy levels such as the two shown in Figure 2.20. This leads to emission lines and absorption.

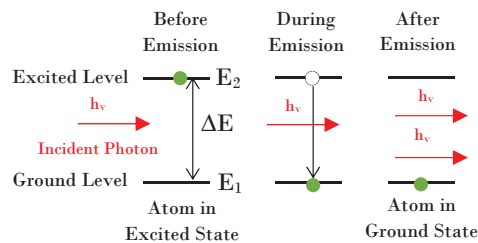


Figure 2.20 Laser physics

An electron in an excited state may decay to a lower energy state which is not occupied, according to a particular time constant characterizing that transition. When such electron decay without external influence, emitting a photon that is called “spontaneous emission”. The phase associated with the photon that is emitted is random. A material with many atoms in such an excited state may thus result in radiation which is very spectrally limited (centred on one wavelength or light), but individual photons would have no common phase relationship and would emanate in random directions.

An external electromagnetic field at a frequency associated with a transition can affect the quantum mechanical state of the atom. As the electron in the atom makes a transition between two stationary states, it enters a transition state which does have a dipole field, and which acts like a small electric dipole, and this dipole oscillates at a characteristic frequency.

In response to the external electric field at this frequency, the probability of the atom entering this transition state is greatly increased. Thus, the rate of transitions between two stationary states is enhanced beyond that due to spontaneous emission. Such a transition to the higher state is called absorption, and it destroys an incident photon. A transition from higher to a lower energy state, however, produces an additional photon; this is the process of stimulated emission.

2.4.3 Material Interactions

Laser radiation is essentially electromagnetic waves. When the electromagnetic radiation is incident on the surface of a material, various phenomena that occur include reflection, refraction, absorption, scattering, and transmission. The most important phenomena in the laser processing of materials is the absorption of the radiation.

Absorption of light can be explained as the interaction of the electromagnetic radiation with the electrons of the material and it depends on both the wavelength of the material and the spectral absorptivity characteristics of the material. The absorption of laser radiation in the material is generally expressed by the Beer – Lambert law:

$$(4) \quad I(z) = I_0^{-\alpha z}$$

Thus, once inside the material, absorption causes the intensity of the light to decay with depth at a rate determined by the material's absorption coefficient α . In general, absorption is a function of wavelength and temperature, but for constant α , intensity decays exponentially with depth.

Laser ablation is the removal of material from a substrate by direct absorption of laser energy. The absorbed laser energy gets converted into thermal energy in the material. The subsequent temperature rise at the surface may facilitate the material removal due to generation of thermal stresses. The onset of ablation occurs above a threshold fluences, which will depend on the absorption mechanism, particular material properties, microstructure, morphology, the presence of defects, and on laser parameters such as wavelength and pulse duration. The laser energy absorbed by the material during laser – material interaction is converted into heat by degradation of the ordered and localized primary excitation energy. The conversion of light energy into heat and its subsequent conduction into the material establishes the temperature distributions in the material.

Depending on the magnitude of the temperature rise, various physical effects in the material include:

- Heating
- Melting
- Vaporization

Furthermore, the ionization of vapour during laser irradiation may lead to generation of plasma. These effects of laser material interactions are schematically presented in Figure 2.21.

When the excitation time is shorter than the thermalization time in the material, non – thermal, photochemical ablation mechanisms can occur. In photochemical ablation, the energy of the incident photon causes the direct bond breaking of the molecular chains in the organic materials resulting in material removal by molecular fragmentation without significant thermal damage. The photon energy must be greater than the bond energy.

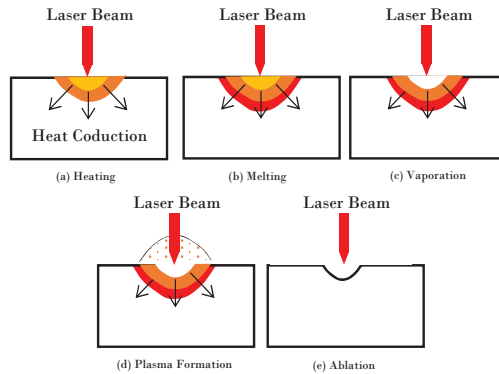


Figure 2.21 Laser material interaction

The laser's temporal pulse length can have a significant effect on the dynamics of the ablation process. In general, as the pulse length is shortened, energy is more rapidly deposited into the material leading to a more rapid material ejection.

The volume of material that is directly excited by the laser has less time to transfer energy to the surrounding material before being ejected. Therefore, the ablated volume becomes more precisely defined by the laser's spatial profile and optical penetration depth, and the remaining material has less residual energy, which reduces the HAZ.

The need for understanding heat transfer concepts can be seen by examining the interactions which take place during laser process (Figure 2.22).

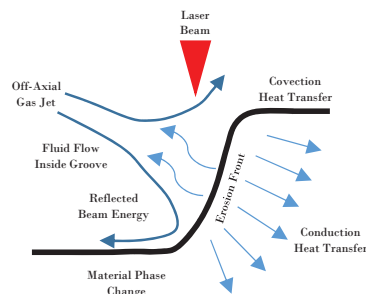


Figure 2.22 Laser ablation mechanism

The equation that govern the laser ablation process are presented in this section following similar approach to [12]:

$$(5) \quad E_{laser}dxdy - E_{conduction}dA - E_{convection}dA = E_{phase\ change}dxdy$$

Where, E_{laser} is the energy density input produced by the beam, $E_{convection}$ is the energy loss by convection, $E_{conduction}$ is the energy conducted across material, and $E_{phase\ changes}$ is the energy necessary to achieve the phase change. Considering the laser as a Gaussian distributed pulse moving in the positive x direction with uniform velocity v , the laser input energy density is given by:

$$(6) \quad E_{laser}dA = \int_{-\infty}^{\infty} I(x, y, z) \frac{dx}{v} dA = \frac{\alpha P}{vR\sqrt{\pi}} e^{-y^2/R^2} dxdy$$

Where, α is the absorption coefficient of the material at laser wavelength and R is the laser beam radius. The energy lost by conduction into the surface is given by:

$$(7) \quad E_{conduction}dA = \left[\int_{-\infty}^{\infty} K \left(\frac{dt}{dn} \right) \frac{dx}{v} \right] dA = \rho C_p (T_s - T_a) D(y) dxdy$$

Where, ρ is the material density, C_p is the thermal capacity of the material, T_s is the temperature in the cut-off point, T_a is the ambient temperature, and $D(y)$ is the cutting depth. The energy loss by convection is given by:

$$(8) \quad E_{convection}dA = \left[\int_{-\infty}^{\infty} h dt \frac{dx}{v} \right] dA = \frac{h}{v} (T_s - T_l) D(y) dxdy$$

Where, h is the convective heat transfer coefficient of the surrounded media, which depends on the type of media (gas or liquid), the flow velocity, viscosity, etc. T_l is the media temperature. The energy needed to achieve the phase change is given by:

$$(9) \quad E_{phase\ change}dA = \rho L_m D(y) dxdy$$

Where ρ is the material density, and L_m is the latent heat of fusion. In conventional laser ablation process (gas assisted) conduction and convection losses are usually negligible, the laser cutting process can be depicted as the following:

$$(10) \quad \frac{\alpha P}{vR\sqrt{\pi}} e^{-y^2/R^2} dxdy = \rho L_m D(y) dxdy$$

To achieve a complete penetration of the material ($D(y) \geq d$), where d is the workpiece thickness, the laser power must be:

$$(11) \quad P \geq \frac{\rho L_m d v R \sqrt{\pi}}{\alpha}$$

2.4.4 Laser Types

There are different types of lasers used in material processing including carbon dioxide (CO₂) lasers, neodymium-doped yttrium aluminium garnet (Nd:YAG) lasers, ytterbium-doped fibre lasers, excimer (KrF, ArF, XeCl) lasers and Ti:Sapphire lasers. In laser cutting and micromachining CO₂, Nd:YAG, fibre and ultra-short pulse lasers (Ti:Sapphire) are the most common lasers applied. These lasers are summarised below.

CO₂ Lasers

CO₂ lasers are one of the molecular gas lasers, which are one of the earliest lasers introduced in the industrial application. This laser emits at a wavelength of 10.6 μm (infrared spectrum). CO₂ lasers contain a mixture of CO₂ (laser active molecules), N₂ and He. The role of N₂ molecules in the mixture is to transfer their energy to CO₂ molecules by collision with electrons in the discharge. The presence of He as an internal heat sink (absorb heat) facilitates CO₂ molecules to get back to the ground level where CO₂ and N₂ repeatedly interact for an ongoing lasing process.

Nd: YAG Lasers

Nd:YAG lasers are a solid state laser with a wavelength of 1.06 μm (near infrared). The lasing material is an yttrium-aluminium garnet (YAG, chemical formula is Y₃Al₅O₁₂) doped with neodymium (Nd³⁺ ion).

Fibre Lasers

A fibre laser in the realm of laser material processing is regarded as the new development for solid state laser technology and it is extensively used in many industrial applications. It was first invented by Elias Snitzer in 1963 with a power milliwatt range.

The configuration of a fibre laser is as follows: the lasing medium is a silica fibre doped with a rare earth element (Ytterbium, Erbium or Thulium) which is optically pumped by a diode laser at the ends and through the cladded shell surface. The wavelength generated by a fibre laser is within the range from 1060 to 1085 nm. A fibre laser consists of a long fibre laser cavity in which the pump energy is deployed along the full length.

Fibre lasers have various advantages over other solid state lasers. Among them is its superior beam quality which gives an excellent focal performance.

2.4.5 Laser Processing Parameters

The material interaction during laser process is affected by the characteristics of the laser beam and the workpiece but is mainly determined by the way that both interact.

The process parameters which can be controlled and modified in order to obtain optimal machining results are the selection of the pulse duration, frequency, scanning speed, and the pulse amplitude which in turn significantly affects the quality of the process. This section describe the main laser processing parameters (Figure 2.23).

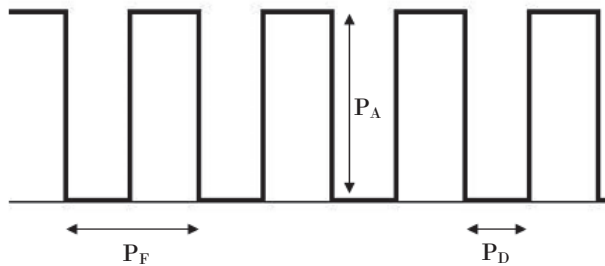


Figure 2.23 Laser wave parameters

Pulse Duration (P_D)

A laser can be classified as operating in continuous wave (CW), short wave (SW), and ultrashort wave (UW) depend on its P_D .

CW lasers emit laser radiation with a laser power that continuously depends on the pump power. CW lasers are used for applications which require a thermal impact, e.g. welding or melt cutting.

SW lasers reduce the thermal impact on the material. Material removal requires an energy density above the ablation threshold. A short laser pulse with an energy density above the ablation threshold is absorbed by the material and a part of this material is transformed into an expanding plasma plume within several picoseconds.

UW lasers are defined as pulses with pulse duration below 10 ps. In contradiction to short laser pulses, the energy is deposited in a time period shorter than the relaxation time between the electron system and the lattice. The vaporization and plasma formation take place much faster than the heat conduction occurs. This leads to a decrease in thermal impact and allows material processing without thermally affecting the surrounding material when processing at moderate fluences.

Pulse amplitude (P_A)

The controlled of pulse amplitude or pulse power could enable processing advantages where different functional properties of the exposed base material are realized by more consequence of the irradiation conditions.

With the advent of the all solid state laser and with particular care in the design of thermal management, it is now possible for lasers to vary the laser power without incurring much loss in pulse-to-pulse stability. In fact, the current generation of pulse have the capability to create any pulse amplitude profile and controllably alter it on a pulse to pulse level. Depending on the application the laser power can be represented in terms of fluence (J/m^2), pulse energy (J), or peak pulse power (J/s):

Fluence

It is the most important parameter affecting the ablation result. The fluence is defined as the energy density on the workpiece. It is calculated dividing the pulse energy by the spot size. The fluence determine the ablation diameter and depth as well as the thermal impact.

$$(12) \quad F = \frac{E}{\phi} \text{ (J/m}^2\text{)}$$

The pulse energy

It is simply the total optical energy content of a pulse, i.e. the integral of its optical power over time. For regular pulse trains, the pulse energy is often calculated by dividing the average power by the pulse frequency.

$$(13) \quad E = \frac{P}{PF} \text{ (J)}$$

Peak pulse power

Is the maximum occurring power. The peak power is calculated by dividing the pulse energy by the pulse duration.

$$(14) \quad PPP = \frac{E}{PW} \text{ (J/s)}$$

Some authors focused their research on the effects of the pulse power on the cutting quality. E.g. Yung et al. [13] performed a qualitative theoretical analysis and experimental investigations of the process parameters on the kerf profile and cutting quality. The result showed that the cutting quality are significantly influenced by the process parameters, with the single pulse energy and pass number having the most significant effects.

Pulse frequency (P_F)

Pulse frequency defines the number of pulses per second used for machining. When the energy is sufficient, every pulse makes an effect on the workpiece.

The thermal impact is caused by two different factors. The first is heat accumulation. Increasing the pulse frequency leads to a reduction of time for heat diffusion into the workpiece. The second cause of thermal impact is particle shielding. Due to the short interval between two pulses, ablated airborne particles are located in the region of the laser radiation.

Pulse overlap (P_O)

The pulse overlap describes the spatial overlap between two subsequent laser pulses. It is not a parameter of the laser system itself, but depends on parameters of the process:

$$(15) \quad O = 1 - \frac{v_{rel}}{\emptyset PF}$$

Where v_{rel} is the scanning speed, PF is the pulse frequency and \emptyset is the focal diameter.

Laser wavelength (L_W)

The wavelength is the characteristic spatial length associated with one cycle of vibration for a photon in the laser beam. The optical resonator of the laser must be properly designed to produce the correct wavelength; the length of the resonator must be such that the laser beam traverses an integral number of half wavelengths of the desired frequency.

The absorptivity of materials can be highly dependent on the wavelength of incident light and thus certain lasers will be more suitable for the processing of different classes of materials.

Beam quality (M^2)

The beam quality M^2 can be expressed as:

$$(16) \quad M^2 = BPP \frac{\pi}{\gamma}$$

$$(17) \quad BPP = \alpha \omega_o$$

Where BPP is the beam parameter product, γ is the laser wavelength, α is the beam divergence, and ω_o is the beam spot radius.

2.5 Foundation of 3D Printing Technologies

2.5.1 Introduction

3D Printing (3DP), also known as Additive Manufacturing (AM) are technologies where a three dimensional (3D) object is created by laying down successive layers of material. It is also known as rapid prototyping, is a mechanized method whereby 3D objects are quickly made on a reasonably sized machine connected to a computer containing blueprints for the object.

The 3D Printing concept of custom manufacturing is exciting to nearly everyone. This revolutionary method for creating 3D models with the use of inkjet technology saves time and cost.

The technology for printing physical 3D objects from digital data was first developed by Charles Hull in 1984 (Figure 2.24). He named the technique as Stereolithography and obtained a patent for the technique in 1986.



Figure 2.24. Charles Hull

While Stereolithography had become popular by the end of 1980s, other similar technologies such as Fused Filament Fabrication (FFF) and Selective Laser Sintering (SLS) were introduced.

In 1993, Massachusetts Institute of Technology (MIT) patented another technology, named “Three Dimensional Printing Techniques”, which is similar to the inkjet technology used in 2D Printers.

In 1996, three major products, “Genisys” from Stratasys, “Actua 2100” from 3D Systems and “Z402” from Z Corporation, were introduced.

In 2005, Z Corp. launched a breakthrough product, named Spectrum Z510, which was the first high definition color 3D Printer in the market.

Another breakthrough in 3D Printing occurred in 2006 with the initiation of an open source project, named Reprap, which was aimed at developing a self-replicating 3D printer.

2.5.2 3D Printing Technologies Types

Inkjet

In this technique an inkjet print head moves across a bed of powder, selectively depositing a liquid binding material. A thin layer of powder is spread across the completed section and the process is repeated with each layer adhering to the last. When the model is complete, unbound powder is automatically and/or manually removed.

Stereolithography (SL)

Stereolithography (SL) works by focusing an ultraviolet (UV) light or Visible Light onto a vat of photopolymerizable resin. It can be differentiate three types of SL Technologies, Laser-Based Stereolithography (SLA) in which a UV laser moves across the print area, and Digital Light Processing (DLP) in which a UV image is projected on the photopolymer, and Liquid Crystal Display (LCD) in which a LCD panel takes responsibility to generate the layer pattern onto the curing area.

Selective laser sintering (SLS)

Selective Laser Sintering (SLS) uses a laser as the power source to sinter powdered material (metals, polymers, etc.), aiming the laser automatically at points in space defined by a 3D model, binding the material together to create a solid structure. It is similar to direct metal laser sintering (DMLS); the two are instantiations of the same concept but differ in technical details. Selective laser melting (SLM) uses a comparable concept, but in SLM the material is fully melted rather than sintered, allowing different properties (crystal structure, porosity, and so on). SLS is a relatively new technology that so far has mainly been used for rapid prototyping and for low-volume production of component parts.

Fused Filament Fabrication (FFF)

Also know Fused Deposition Modelling (FDM), here a hot thermoplastic is extruded from a temperature-controlled print head to produce fairly robust objects to a high degree of accuracy. The filament is melted into the extruder, which deposited the material onto a computer-controlled platform. FFF is the most common 3D Printing technology and based on its economical aspects is the technology selected to be study for BRS production in the present thesis work. Next sections presents everything related to this technology.

2.5.3 Feasibility of Fused Filament Fabrication (FFF) for BRS Production

Due to the most promise materials to manufacture BRS are thermoplastics and 3DP are receiving a great deal of attention in the last years, we hardly believe that 3DP could be a really interesting technique to produce BRS stents based on polymeric materials. Between the different 3DP technologies described previously, stand out the Fused Filament Fabrication (FFF). Besides its lower dimensional precision, compare with Stereolithography or Selective Laser Sintering, FFF presents a series of advantages ✓ and disadvantages ✗:

- ✓ FFF is the most cost-effective way to produce custom thermoplastic object.
- ✓ FFF lead times are short due to the high availability of the technology.
- ✓ FFF allows the production of multi-material objects.
- ✓ FFF allows wide range of thermoplastic materials.
- ✗ FFF has the lowest resolution compared to other 3DP technologies.
- ✗ FFF leaves visible layer lines requiring post-processing to soften surfaces.
- ✗ FFF layer adhesion mechanism makes FFF parts inherently anisotropic.

Because of these reasons, FFF could be useful to manufacture BRS. However FFF machines currently in the market/literature follow a Cartesian Coordinates (Figure 2.25a) a methodology that difficult the BRS manufacturing process. Because of that, a new machine design that involve a new machine methodology is necessary to manufacture BRS stents because of its tubular shape. This new machine/methodology could be based on Cylindrical Coordinates (Figure 2.25b) avoiding the second and third disadvantages of FFF previous mentioned. This new concept has been developed, for the first time, in this thesis work and it is present in Chapter 7.

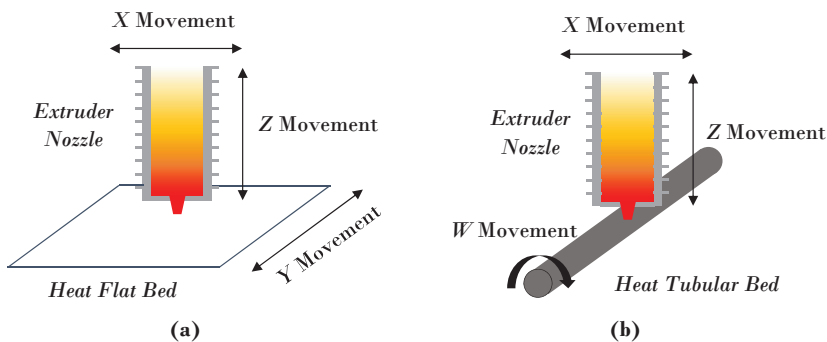


Figure 2.25 FFF Methodologies (a) Cartesian (b) Cylindrical Proposal

2.5.4 Extrusion Melting Physics

FFF is based on extrusion melting method. To understand the process this section presents the physics behind the manufacturing process. According Abeykoon et al. [14] an extruder based system can be illustrated as shown in Figure 2.26.

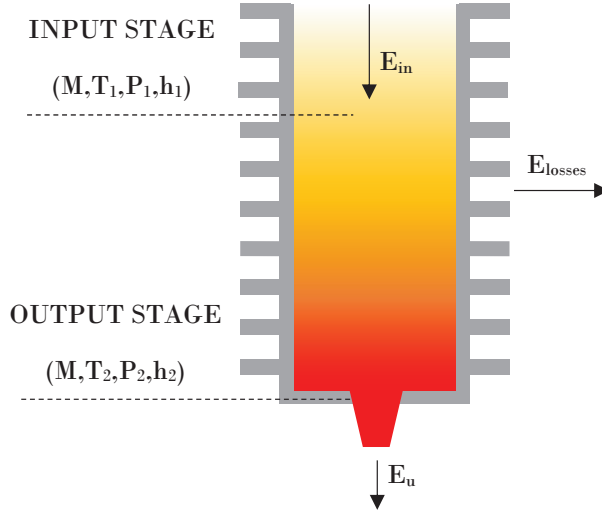


Figure 2.26 Fused Filament Fabrication Extruder Method (Energy Balance)

Then the energy used for useful work (E_u) from an extruder can be given as:

$$(18) \quad E_u = E_{in} - E_{losses}$$

where E_{in} is the total energy supplied to the extruder and E_{losses} is the total amount of energy wasted without involving in any useful work. Therefore, the extruder energy efficiency ($n_{extruder}$) is given by:

$$(19) \quad n_{extruder} = \frac{E_{in} - E_{losses}}{E_{in}} * 100\%$$

Here, the energy inputs (E_{in}) are from the electrical energy supplied to the devices such as drive motor, motor cooling fan, barrel/die heaters, barrel cooling fans, instruments in the control panel, and water pump. The energy losses which may occur in these devices and other mechanical/functional systems such as transmission, forced/natural cooling come under E_{losses} .

The thermodynamic efficiency of an extruder can be determined by comparing the actual energy consumed by the extruder to the theoretical energy required to transform the polymer from initial stage (solid) to the desired output stage (melted).

Usually, the thermodynamic efficiency is calculated under the following assumptions:

- The extruder is under steady state operation.
- The process operates in uniform temperature, pressure and mass flow rate.
- The feed material is assumed to be under uniform temperature and pressure.

The theoretical energy required for melting and forming (E_T) of material in polymer extrusion is:

For semi-crystalline materials:

$$(20) \quad E_{T,SC} = M \int_{T_1}^{T_2} C_p \times dT + M \times H_f + M \int_{P_1}^{P_2} \left(\frac{\partial h}{\partial P} \right)_T \times dP$$

For amorphous materials:

$$(21) \quad E_{T,AM} = M \int_{T_1}^{T_2} C_p \times dT + M \int_{P_1}^{P_2} \left(\frac{\partial h}{\partial P} \right)_T \times dP$$

where M is the mass flow rate, T_1 and T_2 are the feedstock temperatures at the input and output states respectively, P_1 and P_2 are the pressures at the input and output states respectively, C_p is the specific heat capacity of the material, H_f is the enthalpy of heat of fusion of the materials and ρ is the material density.

According to the first law of thermodynamics, the minimum energy required to go from state 1 to state 2 (Figure 2.26) can be calculated from the enthalpy changes (Δh) occur in melting (assumes that these occur at constant pressure) and forming (assumes that this occur at constant temperature) operations:

$$(22) \quad \Delta h = (h_2 - h_1) = \Delta h_1 + \Delta h_2$$

$$(23) \quad \Delta h_1 = \int_{T_1}^{T_2} C_p \times dT + H_f = \bar{C}_p \times (T_2 - T_1) + H_f$$

$$(24) \quad \Delta h_2 = \int_{P_1}^{P_2} \left(\frac{\partial h}{\partial P} \right)_T \times dP = \frac{(P_2 - P_1)}{\bar{\rho}}$$

where h_1 and h_2 are the specific enthalpy values of the materials at the input and output states respectively, Δh_1 and Δh_2 are the enthalpy changes occur at melting and forming operations respectively, C_p is the average specific heat capacity of the polymer and $\bar{\rho}$ is the average density of the material. Then, the thermal efficiency ($n_{extruder,thermo}$) of an extruder is given by:

$$(25) \quad n_{extruder,thermo} = \frac{M \times \Delta h}{E_{in}} * 100\%$$

2.5.5 Fused Filament Fabrication Processing Parameters

FFF is a multi-parameters process. Between the dozen parameters that define this manufacturing process stand out the seven named below.

Nozzle Temperature (N_T)

This parameters define the temperature of the nozzle. It is in charge of melt the material. The control of this parameter becomes crucial to avoid the material properties changes and the final precision of the object.

Bed Temperature (B_T)

This parameter define the temperature of the printing surface bed. Is a really important process parameter due to a bad bed temperature could produce the raising of the object producing irregularly final product.

Layer Height (L_H)

This parameter define the height of the layer that divide the 3D object. The greater height, the faster process but the worst final quality.

Infill

This parameter define the percentage of object that will be solid. The final resistance of the 3D object will depend directly of this parameter.

Printing Speed (P_S)

This parameter define the speed of the printing process. Usually, faster speed leaves lower final quality.

Nozzle Flow Rate ($N_{F\%}$)

This parameter define the amount of material that the nozzle will expel. With this parameter it can be controlled the filament width and the final precision of the object.

Nozzle Retract (N_R)

This parameter define the speed and distance that nozzle will retract when it not be printing. It is an important parameter to avoid rest of material around the object.

The ability to control almost all the parameters involve in the process, becomes 3DP a process in peak in all the industrial sectors, mainly in medical.

2.5.6 3D Printing Technologies in the Medical Sector

Today, the manufacturing industry is an important partner in the medical sector, such as 3D Printing, which even, is being introduced into the hospitals (Figure 2.27).

Each year, healthcare needs and costs grow due to an aging population, the rise in chronic diseases, and more. In fact, global healthcare spending is projected to reach nearly \$9 trillion by 2020. From anatomical models to early bioprinting applications, the use of AM is providing benefits for patients and physicians/institutions including:

- Better patient outcomes
- Less time in the operating room
- Reduced costs

In 2017, collaboration between hospitals, device manufacturers, U.S. Food and Drug Administration (FDA), and partners such as SME, led to extraordinary strides in identifying industry trends, opportunities, challenges and solutions.

These partnerships drive efficiency through best practice sharing as well as accelerate innovation for applications such as bioprinting and tissue fabrication. They also lay the groundwork for 3D printing of organs and scaling up production of tissues which are still decades away.

With millions of patients already directly impacted by the technology, this momentum continues into 2018 and beyond where AM will continue to positively impact public health and drive strong business results.

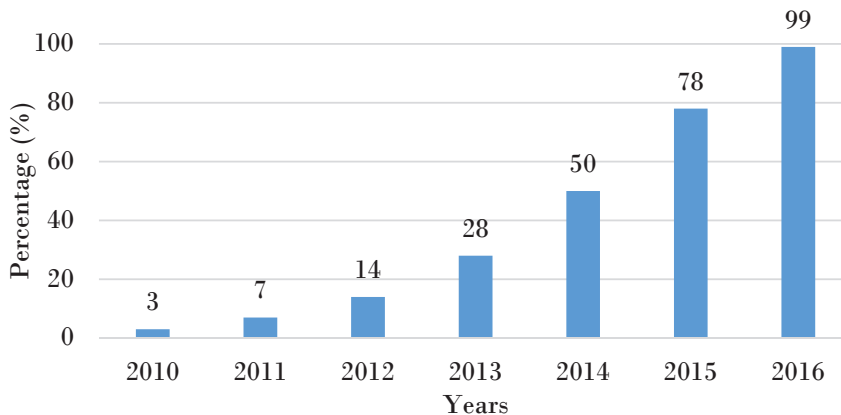


Figure 2.27 Hospital in the U.S. with centralized 3D printing facilities

3D Printing applications in medicine are increasing due to many factors, some of them are:

Precision Medicine: Better patient outcomes and lower costs from developing treatment Plans and devices specifically for the patient.

3D Printing Processes: more accessible technology becomes mainstream.

Materials: Workable materials from polymers to metals allow for varied applications.

Software: Improved software allows for faster and more accurate segmentation of medical imaging files

Resources: Industry rallying behind potential And sharing body of knowledge.

Studies: Growing evidence of patient outcomes and cost-effectiveness

Nevertheless there are some many challenges related to 3D Printing in the medical industry. From a stringent regulatory environment to funding, this burgeoning industry is seeing challenges, which the industry is actively addressing. Some of them are:

Regulatory environment: Regulations are still being formulated. In December 2017, the FDA released guidance on 3D printed medical devices, “preparing for a significant wave of new technologies that are nearly certain to transform medical practice,” according to a statement.

Reimbursement: Costs are not reimbursed through health insurance. Typically, hospitals will cover the cost as it saves time/ costs later. For surgical planning, for instance, it’s cheaper in the long run since it saves time in the operating room.

Technology: Materials, processes and software for 3D printing for medical applications are evolving. Manufacturers are continually learning more about interaction between materials and the 3D printer, biocompatibility, validation processes, creating standards for raw material suppliers, and more. Segmentation is complicated and requires specialized expertise. The segmentation software is costly.

Qualified workforce, recruiting, talent: The blending of biology and engineering is a relatively new need and there is a strong demand. Educators, industry, and medical institutions are working together to make recruiting and training a priority.

Despite the challenges, 3DP is being used nowadays (Figure 2.28). While prototyping remains the top use, anatomical models and surgical instruments are significant application areas. Other applications include microfluidics, education, management support, and packaging.

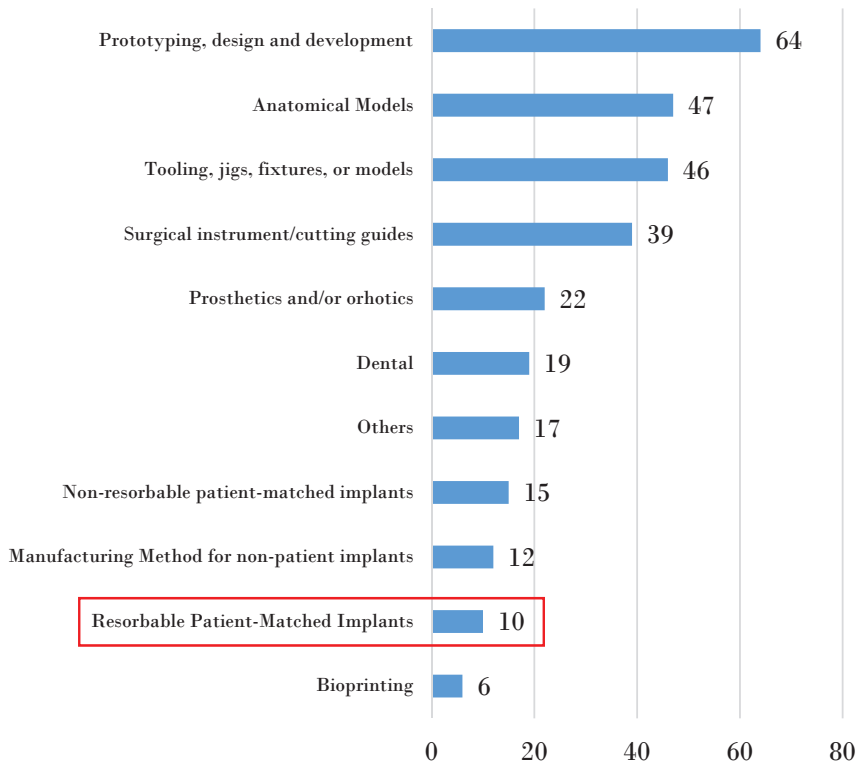


Figure 2.28. Application of 3DP in the Medical Sector

It is interesting to remark the low use of 3DP in resorbable patient-matched implants such as stents are. This fact maybe is motivated by the recent novelty of this technology join with the recent novelty of the BRS concept.

Develop the new FFF methodology based on cylindrical coordinates presented in the section 2.5.3 to study if this novel concept is useful to produce BRS is one on the aims of the present thesis work.

This concept could be open a new stage in the production of BRS made of thermoplastic materials and help to increase the use of AM technologies in the implantable medical sector.

2.6 The state of the art

This closing section try to briefly present the last works done in the stents field, both in the field of permanent stents and in that of absorbable.

As have been demostranted in previous sections, stents have some differences challenges asociated with it; manufacturing process, material, design, medical consideration. In this context, many authors that have been working on the stent field on these different aspects.

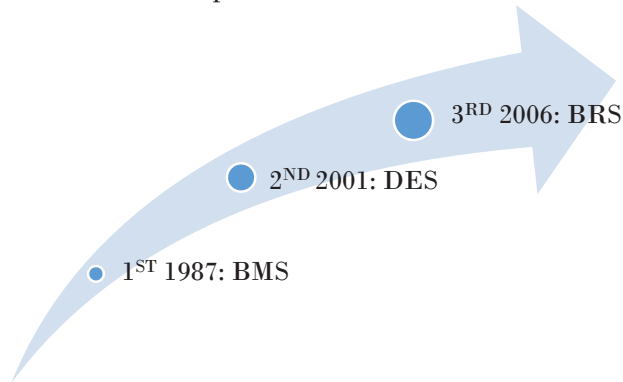


Figure 2.29. Evlution of Stents Industry

One the most investigated field has been the manufacturing field, mainly focus on the laser cutting process because it is the current manufacturing technique to produce stents. Kleine et al. [15] presented micro-cutting results in where the kerf width and the surface quality were analysed. Huang et al. [16] studied the effect of a femtosecond (150 fs) laser machining on the surface and characteristics of nitinol. They result have produced surface roughness of about 0.2 μm on Nitinol. HRSEM and microstructural analyses revealed a HAZ smaller than 70 μm exists on the machined surface. Raval et al. [17] machined a coronary stent after Nd:YAG laser cutting of 316LVM tubing and an assessment of its surface characteristics after electrochemical polishing. One year later, Kathuria [18] described the precision fabrication of metallic stent from stainless steel by using short pulse Nd:YAG laser. They conclude that the processing of stent with desired taper and quality shall still be preferred by the short pulse and higher pulse repetition rate of the laser. Yung et al. [13] performed a qualitative theoretical analysis and experimental investigations of the process parameters on the kerf profile and cutting quality. The result showed that the kerf profile and cutting quality are significantly influenced by the process parameters, with the single pulse energy and pass number having the most significant effects. They obtained debris-free kerf with narrow width ($\approx 25 \mu\text{m}$) and small taper ($\approx 1^\circ$), and concluded that as the single pulse energy is increased and the laser beam velocity is decreased, the kerf width increases.

Shortly after, Shanjin and Yang [19] presented Nd:YAG pulsed laser cutting of titanium alloys sheet to investigate the influence of different laser cutting parameters. The results presented shown that medium pulse energy, high pulse rate, high cutting speed and argon gas at high pressure help to acquire thin HAZ layers. Baumeister et al. [20] presented laser micro-cutting results. Different material thicknesses were evaluated. Processing was carried out with CW operation and with nitrogen and oxygen as assistance gases. Besides the high processing rate of oxygen-assisted cutting, a better cutting performance in terms of a lower kerf width was obtained. Lia et al. [21] studied the femtosecond laser processing of Ni-Ti SMA using a fundamental wavelength of 775 nm from Ti:Sapphire laser and its second and third harmonic irradiations.

Meng et al. [22] analysed the cut parameters with a fibre laser system. They concluded that the high quality coronary stent have been cut with the power of 7 W, pulse length of 0.15 ms, frequency of 1500 Hz, scanning speed of 8 mm/s and oxygen gas at 0.3 MPa as assistance gas. Meng et al. [23] designed a cardiovascular stent cutting system based on fibre laser where the kerf width size was studied for different cutting parameters. Pfeifer et al. [24] pulsed Nd:YAG laser cutting of 1 mm thick Ni-Ti shape memory alloy (SMA). They studied the influence of pulse energy, pulse width and spot overlap on the cut geometry, roughness and HAZ. Compared to short and ultrashort laser processing of SMA, high cutting speeds ($v=2-12$ mm/s) with a sufficient cut quality ($R_z=10-30$ μ m) were achieved.

In 2011, Scintilla et al. [25] presented results of ytterbium fibre laser cutting of Ti6Al4V sheets (1 mm thick) performed with argon as assistance gas. The results show that, with increasing the cutting speed and then decreasing the heat input from 2 kW, an increase of HAZ and recast layer thickness occurs, up to 117 μ m. Powell et al. [26] studied the phenomenon of “striation-free cutting”. They concluded that the creation of very low roughness edges is related to an optimization of the cut front geometry when the cut front is inclined at angles close to the Brewster angle for the laser-material combination. Muhammad et al. [27] studied the capability of picosecond laser micromachining of nitinol and platinum-iridium alloy in improving the cut quality. Process parameters used in the process have achieved dross-free cut and minimum extent of HAZ.

Scintilla and Tricarico [28] analysed the influence of processing parameters and laser source type on cutting edge quality of AZ31 magnesium alloy sheet, and differences in cutting efficiency between fibre and CO₂ laser were studied.

They investigate the effect of processing parameters in a laser cutting of 1 and 3.3 mm thick sheets on the cutting quality. Teixidor et al. [29] carried out an experimental study of fibre laser cutting of 316L stainless steel thin sheets. They analysed the effect of laser parameters on the cutting quality for fixed Nitrogen assistance gas. Besides that, they presented a mathematical model based on energy balance for the cross dimensions. The study showed that increasing the peak pulse power and the cutting speed increases the kerf width, surface roughness and dross deposition. C.H Fu et al. [30] designed an experiment based on laser cutting in order to understand the process capability of fibre laser to cutting Nitinol alloy. They studied the kerf geometry, roughness, topography, microstructure, and hardness to understand the nature of the HAZ and recast layer in fibre laser cutting.

Nevertheless, preventing the thermal damage is impossible in conventional laser process due to the intrinsic characteristics of this production method. Because of that, laser processing in the presence of liquid has been studied for more than 40 years for various applications [31], [32].

Choo et al. [33] carried out an experimental comparison between short pulse laser ablation in air and under-water of silicon. Daminelli et al. [34] performed femtosecond laser irradiation of silicon under-water confinement. They found that debris re-deposition was negligible and the ablated material remained suspended in the water layer. Kruusing [31], [32] listed the advantages of water-assisted processing: light transmission, development of higher plasma pressure due to confinement, water carrying away debris, more effective cooling, useful chemical reactions, and reduced pollution by waste gases, reduced noise level and higher optical breakdown threshold than in air. Water-assisted laser ablation by using femtosecond laser has been done in processing different material under different experimental conditions [34][35][36]. Under-water laser micromachining for tubes specifically for coronary stent applications received less attention.

Work by Muhammad et al [37] directed a water flow through the tubes during the fibre laser micromachining to reduce HAZ, as well as protecting the opposite surface of the tube. Yan et al [38] reported underwater machining of deep cavities in alumina ceramic. They found that underwater machining has the capability of preventing crack initiation, reducing heat damage and giving an insignificant recast layer. In other work, Muhammad et al [39] studied the underwater femtosecond laser micromachining of thin Nitinol Tubes.

However, all these works have been carried out with permanent stent. The motivation for the development of bioabsorbable stents is driven by the need to solve the limitations of metallic stents. The goal is to design a bioabsorbable stent, which once bioabsorbed, will leave behind only the healed, natural vessel allowing restoration of vaso-reactivity with the potential for vessel remodeling. In this context, there are many researcher that have focused their works, mainly in polymers due to there are the most promised materials in BRS future.

Lootz et al. [40] analyzed the influence of laser cutting process with CO₂ lasers on the morphological and physicochemical properties of polyhydroxybutyrate. Results showed that cells preferred laser-machined areas. They concluded that, not only were the material properties altered as a result of processing, but also the biological response was affected. Grabow et al. [41] studied the effect of laser cutting on Poly-L-Lactide (PLLA). The results showed the dramatic influence of the plasticizer content and sterilization procedure on the mechanical properties of the material. Laser cutting had a lesser effect. Hence the effects of processing and sterilization must not be overlooked in the material selection and design phases of the development process leading to clinical use. Caiazzo et al. [42] investigated the application of the CO₂ laser cutting process to three thermoplastic polymers (PE, PP and PC) in different thicknesses ranging from 2 to 10 mm.

Tiaw et al. [43] studied the effect of Nd:YAG laser on micro-drilling and micro-cutting of thin PCL films. Melting and tearing of the thin polymer film were not much of an issue for the thin spin-cast film but a slight extent of melting was observed in the thicker biaxial drawn film. As for the thick polymer sheet of 1 mm thickness, laser singulation was carried out with clear neat edge without too much heat affected zone at a much higher singulation speed. Masmiasi and Philip [44] carried out investigations about the optimum ranges of parameters for drilling of polymer using a CO₂ laser. Baer et al. [45] described the fabrication of a laser-activated Shape Memory Polymer (SMP) stent and demonstrated photothermal expansion of the stent in an in vitro artery model.

In 2008 Paulo et al. [46] realized some experimental studies on CO₂ laser cutting of polymeric materials. Their results showed that HAZ increases with the laser power and decreases with the cutting velocity. Choudhury and Shirley [47] employed CO₂ laser to cut three polymeric materials (PP, PC and PMMA) and developed a model equation relating input process parameters with the output.

Yee et al. [48] analyzed the effect of Femtosecond Laser Micromachining on Poly-E-Caprolactone (PCL). Rocio Ortiz et al. [49] examined the picosecond laser ablation of PLLA as a function of laser fluence and degree of crystallinity. High quality micro-grooves were produced in amorphous PLLA, revealing the potential of ultra-fast laser processing technique. In 2013 Schneider and Petring [50] employed a high power laser to cut fiber reinforced thermoplastic polymers with continuous and pulsed wavelength. Result shows that HAZ could be significantly reduced by multipass at high processing cutting speed.

Stepak et al. [51] presented the impact of the KrF excimer laser irradiation above the ablation threshold on physicochemical properties of biodegradable PLLA. It could be concluded that usage of the 248 nm wavelength resulted in simultaneous ablation at the surface and photo degradation within the entire irradiated volume due to high penetration depth. Furthermore, the thermal activation originating from relaxation of excited chromophores to vibrationally excited ground states, enhances the degradation process. Stepak et al. [52] fabricated a polymer-based biodegradable stent using a CO₂ laser. They noted that the high temperature gradient during the process altered the properties of the material within the heat affected zone (HAZ).

After a deep literature review some of the stents challenges in the BRS field can be enumerated as follow:

- Study the feasibility of other type of laser for BRS production.
- Study new manufacturing technologies for BRS production.
- Study the effects the manufacturing process have on BRS properties.
 - Degradation Rate
 - Cell Proliferation
 - Radial Behaviour
- Study the effects the sterilization have on BRS properties.
- Develop a new concept of BRS to solve the current limitations.

In this context begins the present thesis work at the end of 2015 which aimed to contribute to all the abovementioned challenges.

Chapter 3

Fibre Laser Cutting of Polymer Sheets

Abstract

The adaptation of the laser manufacturing industry to BRS materials is costly, thus further studies employing different sorts of lasers are necessary.

Chapter 3 aims to explore the feasibility of 1.08 μm wavelength fibre laser to cut Polycaprolactone sheet, which is especially interesting for long-term implantable devices, such as stents. The laser cut samples were analysed by Differential Scanning Calorimetry (DSC), Tensile Stress Test, and Optical Microscopy in order to study the effects the laser process has on the workpiece. The parameters measured were: taper angle, dimensional precision, material structure changes and mechanical properties changes.

Results showed a dimensional precision above 95.75 % with a taper angle lower than 0.033° . The laser ablation process has exhibited a minor influence upon material properties. Results exhibit the feasibility of fibre laser to cut polycaprolactone sheet, nevertheless it is need further studies with Polycaprolactone tubes to be sure that fibre laser process is a good manufacturing method for BRS based on polymers.

This chapter had been published in the Journal of Optics & Laser Technology.



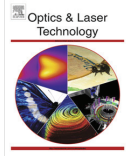
Antonio J. Guerra, Jordi Farjas, Joaquim Ciurana.
“Fibre Laser Cutting Of Polycaprolactone Sheet For Stents Manufacturing: A Feasibility Study”. **2017**, 95, 113-123. Optics & Laser Technology



ELSEVIER

Contents lists available at ScienceDirect

Optics and Laser Technology

journal homepage: www.elsevier.com/locate/jolt

Full length article

Fibre laser cutting of polycaprolactone sheet for stents manufacturing: A feasibility study

Antonio J. Guerra^a, Jordi Farjas^b, Joaquim Ciurana^{a,*}^a Department of Mechanical Engineering and Civil Construction, Universitat de Girona, Maria Aurèlia Capmany, 61, 17003 Girona, Spain^b Department of Physics, Universitat de Girona, Maria Aurèlia Capmany, 61, 17003 Girona, Spain

ARTICLE INFO

Article history:

Received 11 October 2016

Received in revised form 19 January 2017

Accepted 25 March 2017

Keywords:

Fibre laser

Laser cutting

Stent

Biodegradable

Polymer

ABSTRACT

The role of the stent is temporary and it is limited to the intervention and shortly thereafter. Bioresorbable polymer stents were introduced to overcome this problem, making the stent manufacturing process rather difficult considering the complexity of the material. The stent forecast sale makes constant technology development necessary on this field. The adaptation of the laser manufacturing industry to these new materials is costly, thus further studies employing different sorts of lasers are necessary. This paper aims to explore the feasibility of 1.08 μm wavelength fibre laser to cut *polycaprolactone sheet*, which is especially interesting for long-term implantable devices, such as stents. The laser cut samples were analysed by *Differential Scanning Calorimetry (DSC)*, *Tensile Stress Test*, and *Optical Microscopy* in order to study the effects of the laser process over the workpiece. The parameters measured were: taper angle, dimensional precision, material structure changes and mechanical properties changes. Results showed a dimensional precision above 95.75% with a taper angle lower than 0.033°. The laser ablation process has exhibited a minor influence upon material properties. Results exhibit the feasibility of fibre laser to cut *polycaprolactone*, making the fibre laser an alternative to manufacture stents.

© 2017 Elsevier Ltd. All rights reserved.

1. Introduction

Nowadays, stents are the main treatment modality for atherosclerosis. The coronary stent global market, primarily balloon-expanded, bare metal, and drug eluting stents (BMS and DES), was approximately \$7.5 billion in 2015 and forecast stent sales will grow at double digit rates as a result of constant innovations, increasing coronary atherosclerotic diseases, and emerging market update [1]. These facts, have made that many authors focus their research in this field, such as [2] whom studied the effect of a femtosecond (150 fs) laser machine on the surface and the characteristics of Nitinol to stent applications, or [3] whom studied the capability of picosecond laser micromachining of Nitinol and platinum-iridium alloy to improve the cut quality. Process parameters used in the process have achieved cross-free cut and minimum extent of Heat Affected Zone (HAZ).

Although metallic stents are effective in preventing acute occlusion and reducing late restenosis after coronary angioplasty, many concerns still remain. Nowadays, the major medical limitations of stents are thrombosis and restenosis [1]. Bioresorbable stents

(BRSs) were introduced to overcome these limitations with important advantages: complete bioresorption, mechanical flexibility, they do not produce imaging artefacts in non-invasive imaging modalities, etc. Several types of materials are currently been investigated: poly-L-lactic acid (PLLA) and magnesium have been the most promising materials [4]. Other polymers suggested as material for bioabsorbable stents include polyglycolic acid (PGA) and polycaprolactone (PCL) [5]. Biodegradable stents offer the potential of improving long-term patency rates by providing support just long enough for the artery to heal, offering the potential to establish a vibrant market. However, designing a biodegradable structure for an intended period of support is rather difficult, considering the complexity of the material, the stent geometries, the manufacturing process, etc.; making the application of biodegradable materials a particularly difficult challenge.

Nowadays the main efforts have been focused on analysing the mechanical and medical considerations of new biodegradable materials. Hideo Tamai et al. [6] evaluated the feasibility, safety, and efficacy of the PLLA stent in humans. Fifteen patients electively underwent PLLA Igaki-Tamai stent implantation for coronary artery stenosis. The results were promising. Unverdorben et al. [7] developed a polyhydroxybutyrate biodegradable stent and carried out preliminary experiments with rabbits. Zilberman et al. [8] focused their studies on the mechanical properties of bioresorbable

* Corresponding author.

E-mail addresses: antonio.guerra@udg.edu (A.J. Guerra), jordi.farjas@udg.edu (J. Farjas), joaquin.ciurana@udg.edu, joaquin.ciurana@gmail.com (J. Ciurana).

fibres. PLLA, Polydioxanone (PDS) and poly (glycolide-co- ϵ -caprolactone) PGACL were studied in vitro. The three fibres combined a relatively high initial strength and modulus together, with sufficient ductility. Venkatraman et al. [9] reported, for the first time, the development of a fully biodegradable polymeric stent that can self-expand at body temperatures. Niels Grabow et al. [10] designed and produced a biodegradable slotted tube stent for rapid balloon-expansion. Based on PLLA and prolyl 4-hydroxylase (P4HB) polymers, carried out mechanical and degradation experiment. The results showed that the PLLA/P4HB stent allows rapid balloon-expansion and exhibited adequate mechanical scaffolding properties suitable for a broad range of vascular and nonvascular applications. Liang et al. [11] designed a biodegradable shape-memory block co-polymers (PCTBV-25) for fast self-expandable stents. The stent made from PCTBV-25 film showed nearly complete self-expansion at 37 °C within only 25 s. Vieira et al. [12] studied the evolution of mechanical properties during degradation based on experimental data. The decrease of tensile strength followed the same trend as the decrease of molecular weight.

Although the mechanical and medical properties of the material are important, finding the best manufacture process to this kind of material has to be considered as well. Lasers appear to be the perfect tool for this purpose because of non-contact material removal and high precision. Therefore, some authors have been focusing their studies on the laser process of polymers. Grabow et al. [13] studied the effect of CO₂ laser cutting, and sterilization on PLLA. The results showed the dramatic influence of the sterilization procedure on the mechanical properties of the material. In 2008 Tiaw et al. [14] studied the effect of Nd:YAG laser on micro-drilling and micro-cutting of thin PCL films. The melting and tearing of the thin polymer film were not much of an issue for the thin spin-cast film, but a slight extent of melting was observed in the thickest biaxial drawn film. Choudhury and Shirley [15] employed CO₂ laser to cut three polymeric materials and developed a model equation regarding input process parameters with the output. Rocio Ortiz et al. [16] examined the picosecond laser ablation of PLLA as a function of laser fluence and degree of crystallinity. High quality micro-grooves were produced in amorphous PLLA, revealing the potential of the ultra-fast laser processing technique. Luigi et al. [17] modelled the evolution of PLA density under ultra-high pressure/temperature in the region of alpha relaxation. Azhikannickal et al. [18] characterized the magnitude and distribution of reflected light from thermoplastics as a function of thickness, laser incidence angle, and surface roughness. In 2013 Schneider and Petring [19]

employed a high power laser to cut fibre reinforced thermoplastic polymers with continuous and pulsed wavelength. The result shows that HAZ could be significantly reduced by multi-pass processing at high processing cutting speed. Leone et al. [20] employed a 30 W MOPA Q-switched short pulsed Yb:YAG with multi-passes to cut Carbon Fibre Reinforced Polymeric Composite (CFRP) thin Sheet. Their results pointed out that the main factors to obtain an effective cut were the scanning speed and pulse power. Stepak et al. [21] presented the impact of the KrF excimer laser irradiation above the ablation threshold on physicochemical properties of biodegradable PLLA. They concluded that usage of the 248 nm wavelength resulted in simultaneous ablation at the surface and photo degradation within the entire irradiated volume due to high penetration depth. Stepak et al. [5] fabricated a polymer-based biodegradable stent using a CO₂ laser. Tamrin et al. [22] determined an optimized set of cutting parameters for CO₂ laser for three different thermoplastics employing grey relational analysis. Genna et al. [23] assessed a simple procedure to determine the rates of absorbed, reflected, transmitted and scattered energy in the case of an unfilled High Density Polyethylene (HDPE) plate. Their results showed that about 47% of power was lost employing a 975 nm laser.

Although the effect of laser process over different polymers has been studied, nowadays, further studies about the laser cutting process of biodegradable materials are would be helpful to expand the laser stents manufacturing possibilities. The semi-transparent behaviour of most organic polymers at high wavelengths, hinders their manufacturing process with some sort of lasers, making the adaptation of this industry to these new materials costly. The use of fibre laser with high wavelength, short pulse laser with Galvano-mirror [20], among other, could open an interesting research line in the stent manufacturing field. This work shows experimental and parametrically the feasibility of 1.08 μ m wavelength fibre laser to cut *polycaprolactone*. The effects of peak pulse power, cutting speed, and number of passes upon dimensional and material properties is presented.

2. Material and methods

2.1. Cutting system

Experiments were carried out with a CNC Machine KONDIA. The laser employed was a Fibre Laser Rofin FL x50s that is able to provides a 1.08 μ m wavelength, a pulse width from 26 μ s to continu-

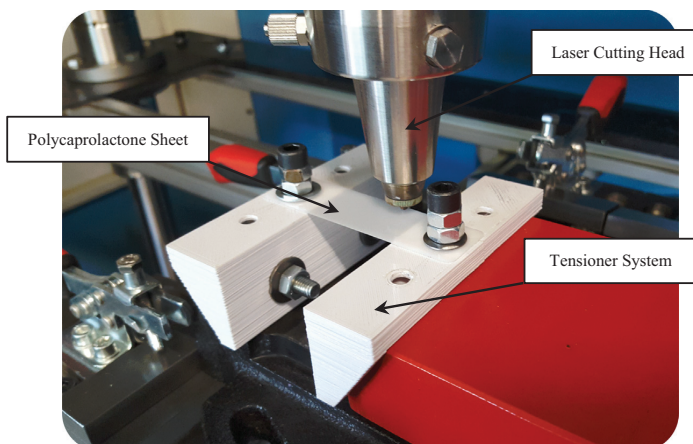


Fig. 1. Cutting system.

Table 1
Polycaprolactone CAPA 6500® properties supplied by Perstorp.

Molecular weight	Melting temperature	H ₂ O Content	Yield stress	Young modulus	Strain at break	Heat of fusion ΔH _{fc}	Absorption coefficient α
50,000 g/mol	60 °C	<1%	17.5 MPa	470 MPa	>700%	137.32 J/g	0.003

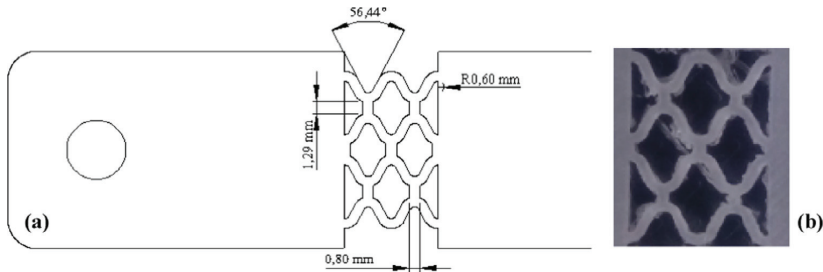


Fig. 2. Experimental geometry (a) CAD geometry. (b) Images of optical microscopy.

Table 2
Screening experiment parameter levels.

Level	PPP (W)	CS (mm/min)	NP
Low	100	350	2
High	250	1150	20

Table 3
Full factorial design levels.

Level	PPP (W)	CS (mm/min)	NP
Low	195	600	10
Medium	205	700	14
High	215	800	18

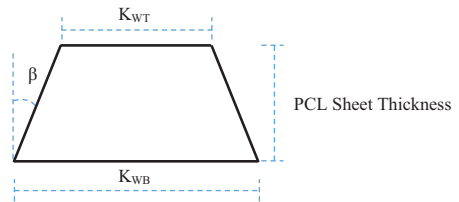


Fig. 3. Taper angle measurements procedure.

ous wavelength (CW), 500 W of peak pulse power, a frequency from CW to 5000 Hz with a 1.1 of beam quality. The process fibre used had 150 μm of diameter, which was mounted in a focusing optics consisted of a *Precitec Fine Cutting Head* with a 50 mm length collimation lens and a 50 mm focal length objective. The coaxial assist gas nozzle had an exit diameter of 0.5 mm. The samples were clamped and prestressed to avoid its deformation and kept at a constant standoff distance of 0.2 mm (Fig. 1).

2.2. Materials and geometry

Polycaprolactone (PCL) CAPA 6500® supplied by Perstorp was used as the material because of its properties (Table 1). PCL is a biodegradable polyester with a low melting point (60 °C) and a glass transition of about -60 °C. Degradation is produced by hydrolysis of its ester linkages in physiological conditions and

has therefore received a great deal of attention for using it as an implantable biomaterial. In particular it is especially interesting for the preparation of long term implantable devices, such stents, due to its degradation which is even slower than that of *polylactide*. The sheets were manufactured taking advantage of 3D technology employing a RepRap BCN 3D printer obtaining a 400 μm of thickness. The sheet were kept at 60 °C for 10 min to remove the wires separation produced by the 3D printer and obtain a smooth surface avoiding the possible problems [24]. A simplify sub unit of the stent version was selected for the experiment (Fig. 2).

2.3. Pretesting

Screening experiments were carried out to determine the appropriate cutting speed (CS), peak pulse power (PPP), pulse width (PW), frequency (FQ), gas pressure (GP), and number of passes (NP) to achieve a complete penetration of the material. Higher frequency (5000 Hz) and short pulse width (0.10 ms) gave the best results, thus, were kept constants. Regarding assistance

Table 4
DOE.

#	PPP (W)	CS (mm/min)	NP	#	PPP (W)	CS (mm/min)	NP	#	PPP (W)	CS (mm/min)	NP
01	195	600	10	10	205	600	10	19	215	600	10
02	195	600	14	11	205	600	14	20	215	600	14
03	195	600	18	12	205	600	18	21	215	600	18
04	195	700	10	13	205	700	10	22	215	700	10
05	195	700	14	14	205	700	14	23	215	700	14
06	195	700	18	15	205	700	18	24	215	700	18
07	195	800	10	16	205	800	10	25	215	800	10
08	195	800	14	17	205	800	14	26	215	800	14
09	195	800	18	18	205	800	18	27	215	800	18

Table 5
Tensile stress test conditions.

Test condition	Value	Units
Speed	10	mm/min
Temperature	21	°C
Rel. hum	47	%
Load cell	5	kN

Table 6
DSC test conditions.

Test condition	Value	Units
Initial temp.	25	°C
Final temp.	80	°C
Heating rate	10	°C/min
Flowing gas N ₂	50	ml/min
Pan material	Al	-

gas, high pressure produced a vibration of the workpiece that made it difficult to keep a constant standoff distance, therefore, it was kept constant at 0.2 MPa. To reach the appropriate cutting speed, peak pulse power, and number of passes we carried out a full factorial design. The parameter levels employed in the experiments are listed in Table 2.

2.4. Design of experiment (DOE)

125 pretesting cuts were made to find the proper cutting parameters range, namely, the higher cutting speed, lower peak

pulse power, and lower number of passes possible that allow a complete penetration of the material. From the observations, beyond 215 W, the heat accumulated in laser nozzle produced the melting of adjacent zones, affecting the structural integrity, while below 195 W, the cutting speed needs to achieve complete penetration was too much slow which is unsuitable from the manufacture point of view. The parameters range selected are listed in Table 3.

Once the appropriate parameters range were enclosed, a Full Factorial Design (FFD) was used (Table 4).

2.5. Characterization

In order to study the feasibility of fibre laser to cut PCL sheets, four characteristics were measured, the dimensional precision (DP), taper angle (β), mechanical properties changes (MP), and material structure changes (MS). To measure the mechanical properties and the material structures changes we selected the more representative samples based on the input energy density employed to cut them, namely, the samples cut at lower, middle, and higher energy. With regards to the dimensional precision and taper angle, were measured for all FFD samples. In order to obtain greater reliability results, 2 samples were cut to measure the dimensional precision, taper angle, and material structure changes and 6 samples to properties quality factors.

2.5.1. Dimensional precision and taper angle

These quality parameters were measured with an optical microscope Nikon SMZ – 745T attached to a digital camera CT3 ProgRes

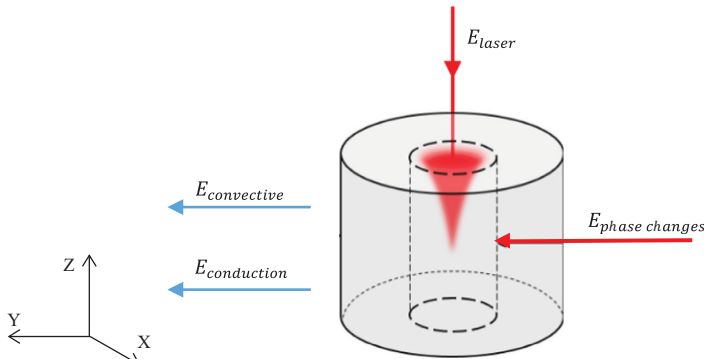


Fig. 4. Scheme of laser ablation process based on energy balance.

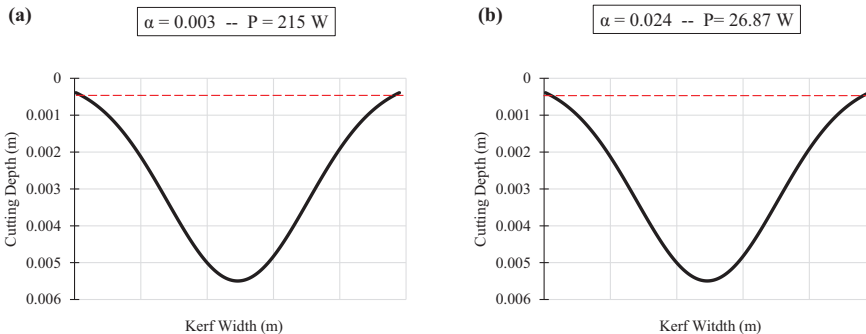


Fig. 5. Cutting profile compensation (a) lower absorption – higher power, (b) higher absorption – lower power.

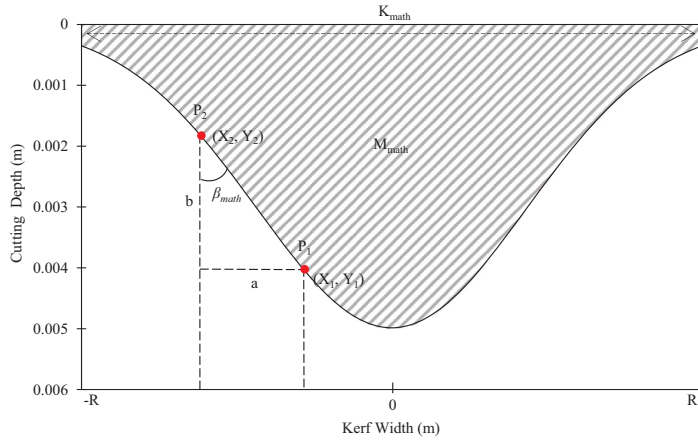


Fig. 6. Laser cutting profile.

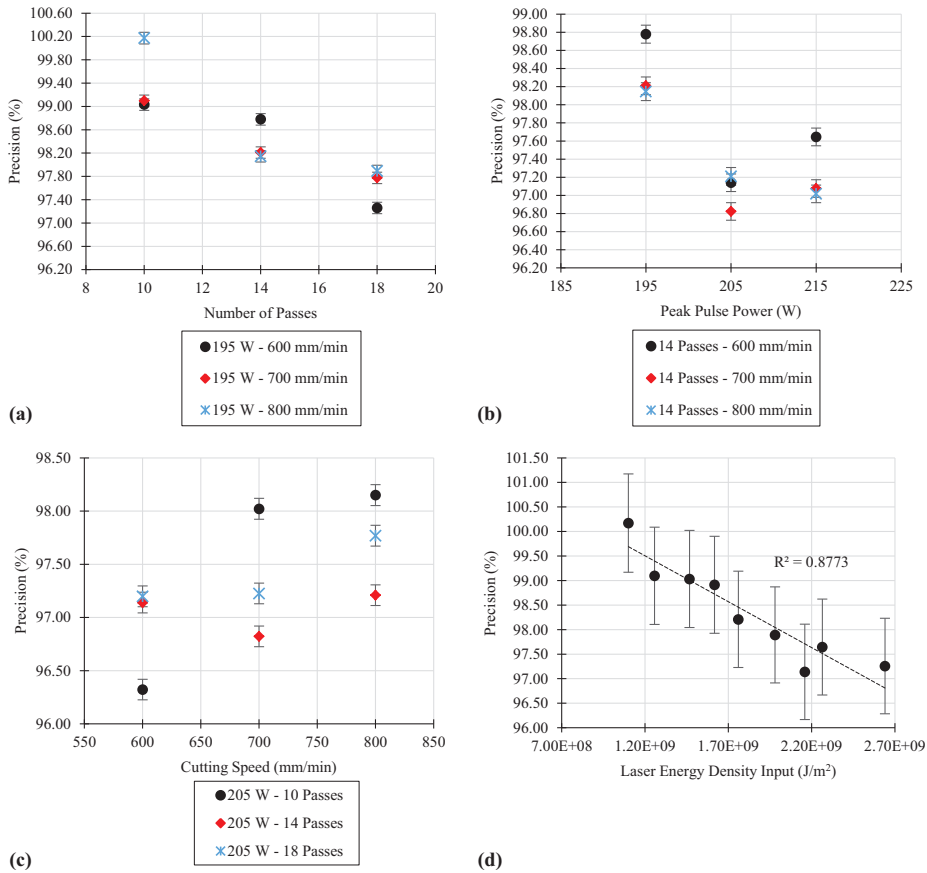


Fig. 7. Precision according to (a) Number of passes, (b) Peak pulse power, (c) Cutting speed (d) E_{laser} .

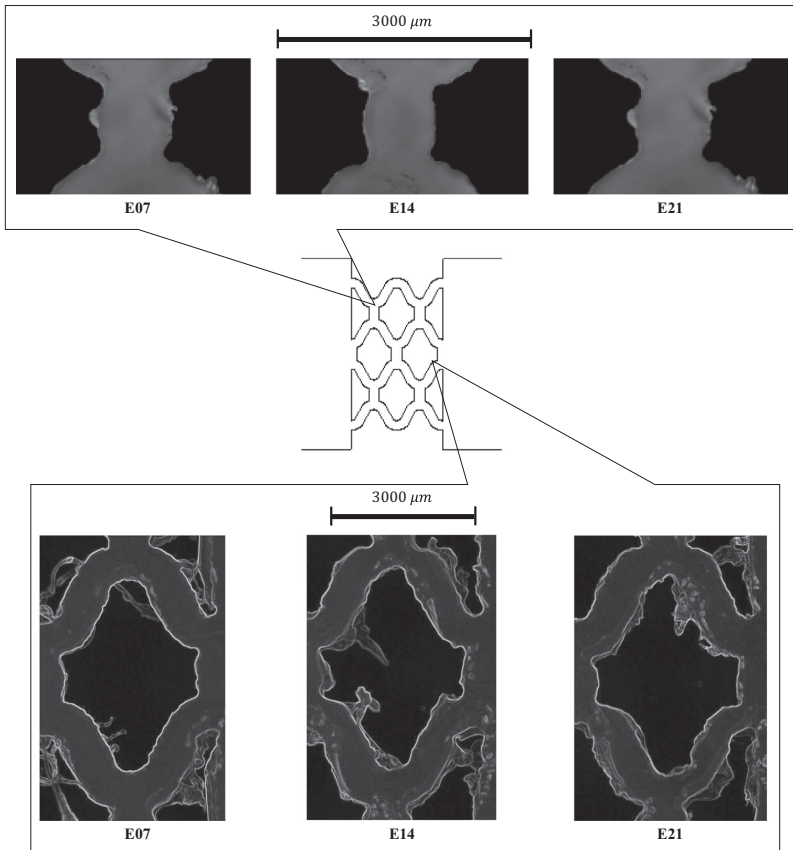


Fig. 8. Precision according E_{laser} (E07) $1.10E + 09 \text{ J/m}^2$ (E14) $1.85E + 09 \text{ J/m}^2$ (E21) $2.91E + 09 \text{ J/m}^2$.

for the collection of digital images. Image J software was employed to the images processing, and measurements.

The dimensional precision measure were determined comparing the geometrical aspect from the cut samples with the CAD programmed geometry, where CAD radius, lengths, area, and strut width are considered the 100% of precision. The average precision of these geometrical aspects was used for the precision figures.

Taper angle (β) were determined by the measurement of the kerf width in the top (K_{WT}) and the bottom (K_{WB}) faces of the sheets (Fig. 3).

2.5.2. Material properties

Mechanical properties changes measurements were conducted with a MTS Insight TENSILE STRESS Machine under the conditions summarised in Table 5.

Material structure changes was measured using Differential Scanning Calorimetry (DSC) under the conditions summarised in Table 6. We conducted the measurements with a DSC Q2000 Machine.

3. Mathematical study

The motivation of the mathematical section was to demonstrated the capability of Nd:YAG with $1,08 \mu\text{m}$ of wavelength to cut PCL as a laser specialized on cutting this kind of material. In polymers the laser ablation may take place due to several mecha-

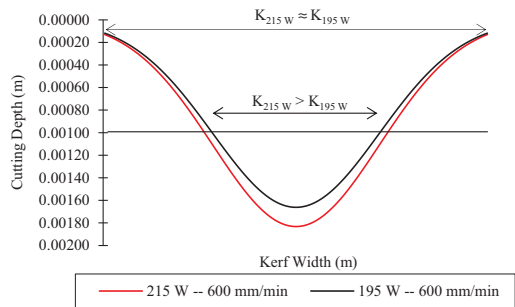


Fig. 9. Taper angle behaviour according cutting parameters.

nisms; photochemical, photothermal, photo physical or combination of all these. In photochemical mechanism the electronic excitation is responsible for direct bond breaking, whereas in photothermal ablation the electronic ablation is thermalized on ps time scale and the thermal bond breaking may take place. In the photo physical process both thermal and non-thermal processes play a vital role and two different bond breaking energies for ground state and electronically excited states are applied [25]. The different equations that govern the laser ablation process are

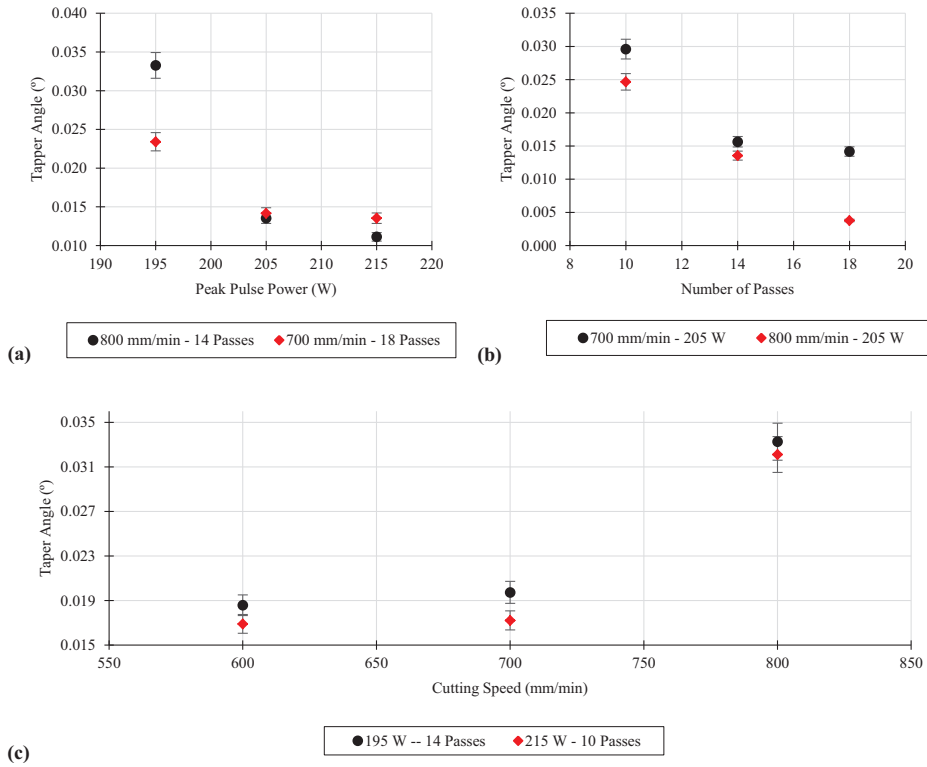


Fig. 10. Taper angle according to (a) Peak pulse power. (b) Number of passes. (c) Cutting speed.

presented based on energy balance (Fig. 4). Similar approach to [26] was followed with modification as the following:

$$E_{laser}dxdy - E_{conduction}dA - E_{convection}dA = E_{phase\ change}dxdy \quad (1)$$

where E_{laser} is the energy density input produced by the beam, $E_{convection}$ is the energy loss by convection, $E_{conduction}$ is the energy conducted across material, and $E_{phase\ changes}$ is the energy necessary to achieve the phase change. Considering the laser as a Gaussian distributed pulse moving in the positive x direction with uniform velocity v , the laser input energy density is given by:

$$E_{laser}dA = \int_{-\infty}^{\infty} I(x, y, z) \frac{dx}{v} dA = \frac{\alpha P}{vR\sqrt{\pi}} e^{-y^2/R^2} dxdy \quad (2)$$

Where, α is the absorption coefficient of the material at laser wavelength and R is the laser beam radius. The energy lost by conduction into the surface is given by:

$$E_{conduction}dA = \left[\int_{-\infty}^{\infty} K \left(\frac{dt}{dn} \right) \frac{dx}{v} \right] dA = \rho C_p (T_s - T_a) D(y) dxdy \quad (3)$$

Where, ρ is the material density, C_p is the thermal capacity of the material, T_s is the temperature in the cut-off point, T_a is the ambient temperature, and $D(y)$ is the cutting depth. The energy loss by convection is given by:

$$E_{convection}dA = \left[\int_{-\infty}^{\infty} h dt \frac{dx}{v} \right] dA = \frac{h}{v} (T_s - T_1) D(y) dxdy \quad (4)$$

where h is the convective heat transfer coefficient of the surrounded media, which depends on the type of media (gas or liquid), the flow

velocity, viscosity, etc. T_1 is the media temperature. The energy needed to achieve the phase change is given by:

$$E_{phase\ change}dA = \rho L_m D(y) dxdy \quad (5)$$

where ρ is the material density, and L_m is the latent heat of fusion. In conventional laser ablation process (gas assisted) conduction and convection losses are usually negligible, the laser cutting process can be depicted as the following:

$$\frac{\alpha P}{vR\sqrt{\pi}} e^{-y^2/R^2} dxdy = \rho L_m D(y) dxdy \quad (6)$$

To achieve a complete penetration of the material ($D(y) \geq d$), where d is the workpiece thickness, the laser power must be:

$$P \geq \frac{\rho L_m d v R \sqrt{\pi}}{\alpha} \quad (7)$$

Due to the semi-transparent behaviour of most organic polymers at our working wavelength, higher power would be required to achieve a complete penetration. This fact will not affect over the cutting profile due to the fact that the laser power can compensate the absorption coefficient, thus, it will not affect the dimensional precision. Fig. 5 shows the theoretical curves, derived from different parameters that exhibit as is compensated the low absorption increasing the power.

From the mathematical model we can calculate the expected taper angle (β_{math}), and molten area (M_{math}) (Fig. 6). These values are given by Eqs. (8) and (9), as shown:

$$\beta_{math} = \arctan\left(\frac{a}{b}\right) = \arctan\left(\frac{x_2 - x_1}{y_2 - y_1}\right) \quad (8)$$

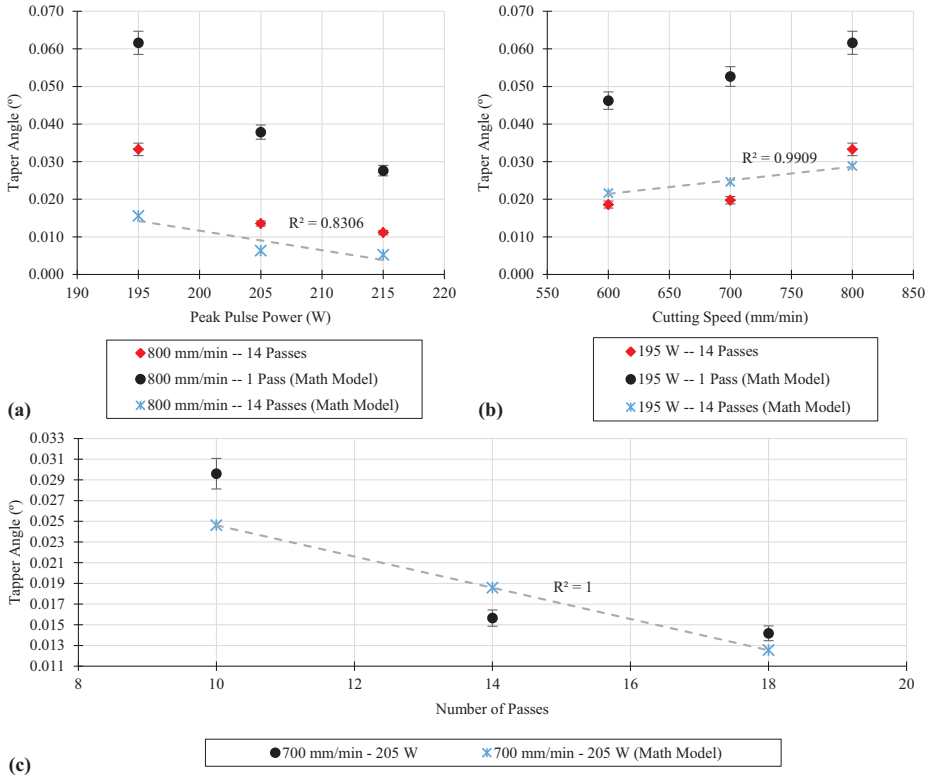


Fig. 11. Math model Vs experimental results (a) Peak pulse power. (b) Number of passes. (c) Cutting speed.

$$M_{math} = \int_{-R}^R \frac{\alpha P}{\rho L v R \sqrt{\pi}} e^{-y^2/R^2} dy \quad (9)$$

where P_1 , and P_2 are selected points at 30% and 60% from $-R$. The mathematical model has shown the feasibility of high wavelength fibre laser to cut semi-transparent materials as PCL.

4. Results

This section presents the experimental results for the quality factors. The quality factors were analysed according to process parameters. All data are expressed as mean \pm standard error (SE). Analysis of variance (ANOVA) method was applied to test the statistical significance of the process parameters. The analysis was carried out at a 95% confidence level. The significant parameters ($p < 0.05$) are denoted as *.

4.1. Precision

Results show a downward trend according to number of passes*, and peak pulse power* increases (Fig. 7 (a), and 7 (b)). This trend is reversed in relation to cutting speed increases (Fig. 7 (c)). The increase on the E_{laser} , and the number of passes, lowers the accuracy as a result of the increase in the kerf width and temperature in the cut-off point (Figs. 7(d) and 8). It seems that the heat accumulated in the nozzle produces the melting of adjacent zones generating unpredicted results in some zones. All experimental results were above than 95.75% average precision.

4.2. Taper angle

Taper angle shows a downward trend according to number of passes*, and peak pulse power increases (Fig. 10(a) and (b)). This trend is reversed again according to cutting speed increases (Fig. 10(c)). This is due to the increases on peak pulse power which raises the amplitude of E_{laser} , reducing the taper angle (Fig 9).

From experimental results we developed an equation that allow us to predict the taper angle at n passes (Eq. (10)).

$$\beta_{math(NP)} = \beta_{math} - 0,038NP\beta_{math} \quad (10)$$

Where β_{math} is the taper angle from mathematical model, NP is the number of passes, and $\beta_{math(NP)}$ is the taper angle at NP passes. This equation together with the mathematical model confirmed the experimental results with an average correlation of 97.2% for other set of experiments and not only for the one where the equation came from (Fig 11).

4.3. Material structure

From the DSC curves (Fig. 12a to Fig. 12d) we can obtained the crystallinity percentage of the sample (Fig. 12e) by the follow equation:

$$C_{\%} = \frac{\Delta H_f}{\Delta H_{fc}} \cdot 100 \quad (11)$$

Where, $C_{\%}$ is the crystallinity percentage, ΔH_f is the heat of fusion (area beneath the DSC curve), and ΔH_{fc} is the heat of fusion of the PCL 100% crystalline (Table 1).

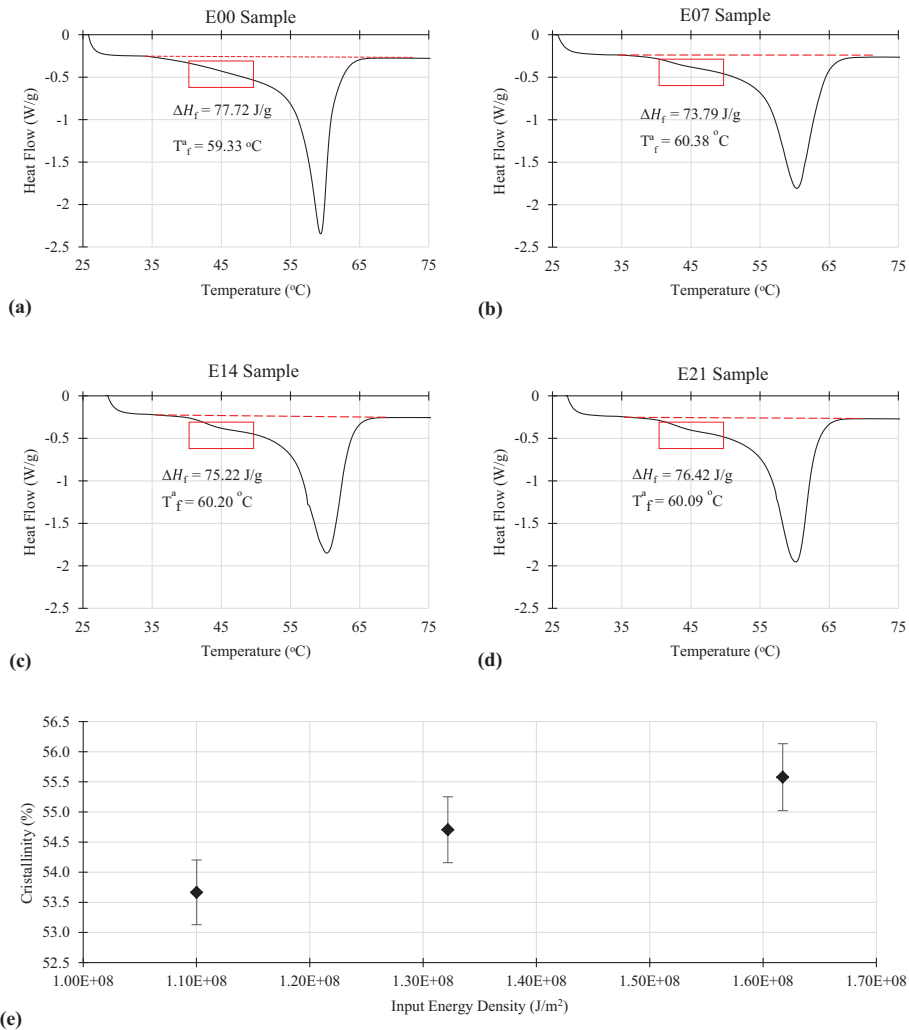


Fig. 12. Material structure (a) E00 sample. (b) E07 sample. (c) E14 sample. (d) E21 sample. (e) MS Vs E_{laser} .

The crystallinity percentage shows an increasing trend when E_{laser} increases (Fig. 12e). The increase of E_{laser} raises the nozzle temperature, reducing the workpiece cooling rate. This fact allows a better placement of the polymer chains, increasing the crystallinity percentage. Results also show a lesser change in the structure distribution (Fig. 12 red squares).

The laser cutting process has reduced the crystallinity percentage in a 2.06×10^{-8} % per J/m^2 . Although is a lesser effect, it must be controlled since it could affects the material degradation [27].

4.4. Mechanical properties

Results show no systematic trend, except for the Young Modulus that decreases steadily with the E_{laser} increases; this seems to indicate a lesser degradation of the polymer (Fig. 13 and Table 7).

5. Discussion

This work has shown the feasibility of 1.08 μm wavelength fibre laser to cut polycaprolactone sheets. The experimental results have supported the mathematical model with an average correlation of 97.2%.

Results have shown the influence of input energy density upon the workpiece quality factors, where the lower E_{laser} left the best results. The correct relationship between the laser power and cutting speed that generate just the energy to reach phase change becomes crucial.

From the statistical and experimental results, the number of passes ($p < 0.05$) has demonstrated a strong influence on the process. Like all semi-crystalline polymers, when the laser pass through the PCL, the beam energy is reflected, scattered, absorbed and transmitted [23]. The part of energy scattered inside the materials is reflected inside the thickness by the boundary surfaces,

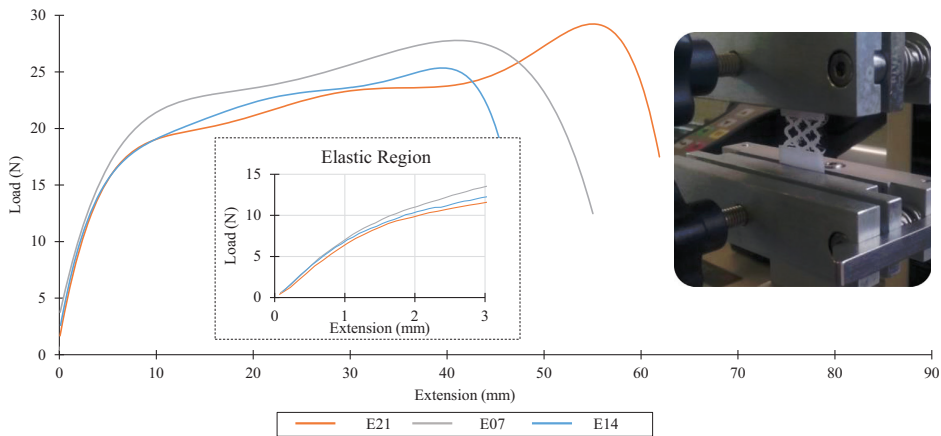


Fig. 13. Tensile stress test results.

Table 7
Mechanical properties.

Sample	Yield stress (MPa)	Maximum stress (MPa)	Young modulus (MPa)	Strain at break (%)	Elongation at yield (%)
E07	6.5	9.1	23.2	453.3	89.21
E14	5.6	8.2	22.3	374.5	74.50
E21	6.1	9.4	21.3	586.7	100.5

included the kerf surfaces. Due to the different impact angle and roughness (due to the previous laser passes) according to [18,23] the scattered power produces an increase on the kerf surfaces temperature, even more so between two close cut areas. So, the accuracy decreases increasing the number of passes. Although the increase of the number of passes reduced the dimensional precision, this increase, also reduced the taper angle.

The thermal sensibility of the polycaprolactone has been a rough path during the experiments making the nozzle temperature a significant factor in the process. Although, if the laser is correctly aligned should not interact with the nozzle at all, the energy reflected for the sheets, joins with the lower glass-transition temperature of the PCL make that the lowest nozzle temperature changes affect the material. The increase on the input energy density raised the nozzle temperature affecting the surrounding cut-off zones and producing unexpected damages upon both outer properties (i.e. kerf width) and inner properties (i.e. crystalline structure). The inclusion of some cooling technique could be helpful to keep the nozzle temperature constant independently of the cutting parameters avoiding the material changes, and therefore, the subsequent techniques. Also, the inclusion of some cooling technique have demonstrated their efficacy reducing the thermal damages associate with laser process, such as, HAZ, dross, recast layer, etc. [28,29].

With regards to the material properties, laser process has exhibited a lesser effect upon them [13], surely, because of the lower absorption coefficient at our laser wavelength, that reduced the thermal effect over the material structure, and thus, over their properties. PCL has exhibited good mechanical properties for stent applications, however it would be advantageous to do some additional tests in the tubular case, in which the radial and compression strength are investigated. For balloon expandable stents, an infinite elastic modulus prevents recoil. A low yield strength is preferred to allow stent expansion at acceptable balloon pressures and facilitates crimping of the stent on the delivery system. High tensile properties after expansion help to achieve radial strength with

a minimal volume of implanted foreign material. Higher tensile properties also permit the use of thinner struts for an overall lower profile, thus improving flexibility, deliverability, and access to smaller vessels. A steep work-hardening rate leads to a desirable rise in strength during expansion. Finally, a high ductility is needed to withstand deformation during expansion. These properties are interrelated and sometimes contradictory, requiring careful compromise. For example, higher tensile strength materials typically also have higher yield strengths. Although the higher tensile strength is desirable for bolstering radial strength as outline above, the associated higher yield strength promotes the undesired acute recoil upon balloon deflection. Similarly, a small grain size that is known to favour fatigue resistance and the ability to achieve a favourable polish, usually raises yield strength leading to excessive acute recoil [30].

Although the results have been demonstrated the potential of fibre laser to cut PCL sheet accurately with lesser effect over the material properties, the cutting of sheet is rather different than tubes. In tubes, the problems can be quite different, e.g. back damages. These facts make necessary further studies in this field, which study the effect of laser cutting parameters upon the thermal damages.

6. Conclusions

The feasibility of 1.08 μm fibre laser to cut polycaprolactone has been reported, analysing how the manufacturing process parameters affect over the workpiece. Dimensional precision, taper angle, material structural changes, and mechanical properties changes have been evaluated. A mathematical study has been proposed supported by the experimental results.

Based on mathematical and experimental results, we can conclude that fibre laser process is able to achieve dimensional precisions above than 95.75% with a taper angle lower than 0.033°. The laser process has exhibited a lesser influence upon the material

properties, owing to the lower absorption of PCL at this wavelength.

Fibre laser of 1.08 μm of wavelength has been shown to be a profitable and thrifty tool to cut polycaprolactone sheet.

Acknowledgments

The authors acknowledge the financial support from Ministry of Economy and Competitiveness (MINECO), Spain for its PhD scholarship and grants from DPI2013-45201-P and University of Girona (UdG), Spain MPCUdG2016/036. The authors would like to thank the technical support offered by the Analysis and Advanced Material for Structural Design research group (AMADE) and the Technical Services of the University of Girona. As well as the language assessment of Araceli Ferreira.

References

- [1] J.S. Soares, J.E. Moore, Biomechanical challenges to polymeric biodegradable stents, *Ann. Biomed. Eng.* (2015).
- [2] H. Huang, H.Y. Zheng, G.C. Lim, Femtosecond laser machining characteristics of Nitinol, *Appl. Surf. Sci.* 228 (1–4) (2004) 201–206.
- [3] N. Muhammad, D. Whitehead, a. Boor, W. Oppenlander, Z. Liu, and L. Li, Picosecond laser micromachining of nitinol and platinum-iridium alloy for coronary stent applications, *Appl. Phys. A Mater. Sci. Process.*, vol. 106, no. 3, pp. 607–617, 2012.
- [4] E. Tenekecioglu, C. Bourantas, M. Abdelghani, Y. Zeng, R.C. Silva, H. Tateishi, Y. Sotomi, Y. Onuma, M. Yilmaz, P.W. Serruys, From drug eluting stents to bioresorbable scaffolds; to new horizons in PCI, *Expert Rev. Med. Devices* 13 (3) (2016) 271–286.
- [5] B. Stepak, a. J. Antończak, M. Bartkowiak-Jowska, J. Filipiak, C. Pezowicz, and K. M. Abramski, Fabrication of a polymer-based biodegradable stent using a CO₂ laser, *Arch. Civ. Mech. Eng.*, vol. 14, no. 2, pp. 317–326, 2014.
- [6] H. Tamai, K. Igaki, E. Kyo, K. Kosuga, A. Kawashima, S. Matsui, H. Komori, T. Tsuji, S. Motohara, H. Uehata, Initial and 6-month results of biodegradable poly-L-lactic acid coronary stents in humans, *Circulation* 102 (4) (2000) 399–404.
- [7] M. Unverdorben, a. Spielberger, M. Schywalsky, D. Labahn, S. Hartwig, M. Schneider, D. Loozt, D. Behrend, K. Schmitz, R. Degenhardt, M. Schaldach, C. Vallbracht, and W. Yoon, A polyhydroxybutyrate biodegradable stent: preliminary experience in the rabbit, *Cardiovasc. Intervent. Radiol.*, vol. 25, no. 2, pp. 127–132, 2002.
- [8] M. Zilberman, K.D. Nelson, R.C. Eberhart, "Mechanical properties and in vitro degradation of bioresorbable fibers and expandable fiber-based stents", *J. Biomed. Mater. Res. - Part B Appl. Biomater.*, vol. 74, no. 2, pp. 792–799, 2005.
- [9] S.S. Venkatraman, L.P. Tan, J.F.D. Jose, Y.C.F. Boey, X. Wang, Biodegradable stents with elastic memory, *Biomaterials* 27 (8) (2006) 1573–1578.
- [10] N. Grabow, C.M. Bünger, C. Schultze, K. Schmohl, D.P. Martin, S.F. Williams, K. Sternberg, K.P. Schmitz, A biodegradable slotted tube stent based on poly(L-lactide) and poly(4-hydroxybutyrate) for rapid balloon-expansion, *Ann. Biomed. Eng.* 35 (12) (2007) 2031–2038.
- [11] L. Xue, S. Dai, Z. Li, Biodegradable shape-memory block co-polymers for fast self-expandable stents, *Biomaterials* 31 (32) (2010) 8132–8140.
- [12] A.C. Vieira, J.C. Vieira, J.M. Ferra, F.D. Magalhães, R.M. Guedes, A.T. Marques, Mechanical study of PLA-PCL fibers during in vitro degradation, *J. Mech. Behav. Biomed. Mater.*, vol. 4, no. 3, pp. 451–460, 2011.
- [13] N. Grabow, M. Schlun, K. Sternberg, N. Hakansson, S. Kramer, and K.-P. Schmitz, "Mechanical properties of laser cut poly(L-lactide) micro-specimens: implications for stent design, manufacture, and sterilization.", *J. Biomech. Eng.*, vol. 127, no. February 2005, pp. 25–31, 2005.
- [14] K.S. Tiaw, M.H. Hong, S.H. Teoh, Precision laser micro-processing of polymers, *J. Alloys Compd.* 449 (1–2) (2008) 228–231.
- [15] I.A. Choudhury, S. Shirley, Laser cutting of polymeric materials: an experimental investigation, *Opt. Laser Technol.* 42 (3) (2010) 503–508.
- [16] R. Ortiz, I. Quintana, J. Etxarri, A. Lejardi, and J. R. Sarasua, "Picosecond laser ablation of poly-L-lactide: Effect of crystallinity on the material response", *J. Appl. Phys.*, vol. 110, no. 9, 2011.
- [17] L. Grassia, M.G. Pastore Carbone, G. Mensitieri, A. D'Amore, Modeling of density evolution of PLA under ultra-high pressure/temperature histories, *Polymer (Guildf)* 52 (18) (2011) 4011–4020.
- [18] E. Azhikannickal, P.J. Bates, G. Zak, Use of thermal imaging to characterize laser light reflection from thermoplastics as a function of thickness, laser incidence angle and surface roughness, *Opt. Laser Technol.* 44 (5) (2012) 1491–1496.
- [19] F. Schneider, N. Wolf, D. Petring, High power laser cutting of fiber reinforced thermoplastic polymers with cw- and pulsed lasers, *Phys. Procedia* 41 (2013) 415–420.
- [20] C. Leone, S. Genna, V. Tagliaferri, Fibre laser cutting of CFRP thin sheets by multi-passes scan technique, *Opt. Lasers Eng.* 53 (2014) 43–50.
- [21] B.D. Stepak, A.J. Antończak, K. Szustakiewicz, P.E. Koziol, K.M. Abramski, Degradation of poly(L-lactide) under KrF excimer laser treatment, *Polym. Degrad. Stab.* 110 (2014) 156–164.
- [22] K.F. Tamrin, Y. Nukman, I.a. Choudhury, S. Shirley, Multiple-objective optimization in precision laser cutting of different thermoplastics, *Opt. Lasers Eng.* 67 (2015) 57–65.
- [23] S. Genna, C. Leone, V. Tagliaferri, Characterization of laser beam transmission through a high density polyethylene (HDPE) plate, *Opt. Laser Technol.* 88 (2017) 61–67.
- [24] D. Drummer, S. Cifuentes-Cuellar, D. Rietzel, Suitability of PLA/TCP for fused deposition modeling, *Rapid Prototyp. J.* 18 (6) (2012) 500–507.
- [25] S. Mishra, V. Yadava, Laser Beam MicroMachining (LBMM) - A review, *Opt. Lasers Eng.* 73 (2015) 89–122.
- [26] D. Yuan, S. Das, Experimental and theoretical analysis of direct-write laser micromachining of polymethyl methacrylate by CO₂ laser ablation, *J. Appl. Phys.* 101 (2007) (2007) 024901.
- [27] E. Passaglia, M. Bertoldo, S. Coiai, S. Augier, S. Savi, F. Ciardelli, The effect of crystalline morphology on the degradation of polycaprolactone in a solution of phosphate buffer and lipase, *Polym. Adv. Technol.* 19 (April) (2008) 560–568.
- [28] N. Muhammad, D. Whitehead, a. Boor, and L. Li, "Comparison of dry and wet fibre laser profile cutting of thin 316L stainless steel tubes for medical device applications", *J. Mater. Process. Technol.*, vol. 210, no. 15, pp. 2261–2267, 2010.
- [29] N. Muhammad, L. Li, Underwater femtosecond laser micromachining of thin nitinol tubes for medical coronary stent manufacture, *Appl. Phys. A Mater. Sci. Process.* 107 (4) (2012) 849–861.
- [30] P. Poncin and J. Proft, "Stent Tubing: Understanding the Desired Attributes", *Proc. ASM Conf. Mater. Process. Med. Devices*, no. September, pp. 253–259, 2003.

Chapter 4

Effect of Fibre Laser on Degradation

Abstract

The degradation rate of biodegradable stents is one of the most important factor upon making these devices, due to it is the property in charge to provide the appropriate period of time to heal the atherosclerosis. The research for a degradable material that shows mechanical properties similar to the current permanent stents in the market and an appropriate degradation rate is still an open challenge. The literature has shown the degradation rate of some biodegradable materials before stent manufacturing's process employing in-vitro degradation methods in static flow conditions which does not match properly with the real body conditions where the blood flow circulate by the vessel.

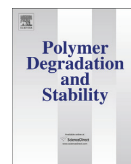
Chapter 4 presents the effect the fibre laser cutting process upon the degradation rate of polycaprolactone. Degradation study were carried out with a novel in-vitro method (dynamic) closer to body conditions and were compared with the traditional in-vitro method (static). This approach was not presented in the literature. The laser cut samples were analysed by Scanning Electron Microscopy (SEM), Optical Microscopy, and Weighing in order to study the effects the laser process, and degradation method have on the degradation rates, surface morphology changes, and geometric pattern changes in the stent.

Results had shown the influence the laser process over the degradation rates, accelerating it according the input energy density increases. The dynamic degradation method has increased the weight of samples, fact that will accelerate the degradations rate in a medium period of time. This fact has proved the differences that will exist in body conditions.

This chapter has been published in the Journal Polymer Degradation & Stability (Under Journal Guidelines).



Antonio J. Guerra, Joaquim Ciurana. “Effect Of Fibre Laser Process On In-Vitro Degradation Rate Of A Polycaprolactone Stent A Novel Degradation Study Method”. **2017**, 142, 42-49. Polymer Degradation and Stability.



Effect of fibre laser process on in-vitro degradation rate of a polycaprolactone stent a novel degradation study method



Antonio Jesús Guerra, Joaquim Ciurana*

Department of Mechanical Engineering and Industrial Construction, Universitat de Girona, Avinguda Lluís Santaló s/n, 17071 Girona, Spain

ARTICLE INFO

Article history:

Received 14 February 2017

Received in revised form

22 May 2017

Accepted 29 May 2017

Available online 30 May 2017

Keywords:

Fibre laser

Cutting

Biodegradable stent

Degradation rate

ABSTRACT

In this paper, the authors present the effect of input energy density of Nd:YAG fibre laser upon the degradation rate of the polycaprolactone. The degradation study were carried out with a novel *in-vitro* method closer to body conditions and were compared with the traditional *in-vitro* method. This approach was not presented in the available literature. The degradation rate of biodegradable stents is one of the most importance factor upon making these devices, due to it is the property in charge to provide the appropriate period of time to heal the atherosclerosis. The research for a degradable material that shows mechanical properties similar to the current permanent stents in the market and an appropriate degradation rate is still an open challenge. The literature has shown the degradation rate of some biodegradable materials before stent manufacturing's process employing *in-vitro* degradation methods in static flow conditions which does not match properly with the real body conditions where the blood flow circulate by the vessel. The laser cut samples were analysed by Scanning Electron Microscopy (SEM), Optical Microscopy, and weighing in order to study the effect of laser process, and degradation method over the degradation rates, surface morphology changes, and geometric pattern changes in the stent. Results have shown the influence of the laser process over the degradations rate, accelerating it according the input energy density increases. The dynamic method has increased the weight of samples, fact that will accelerate the degradations rate in a medium period of time that prove the differences that will exist in body conditions.

© 2017 Elsevier Ltd. All rights reserved.

1. Introduction

Since their introduction in the market in the early 1990s, nobody was able to predict the advantages that will occur in stent technology over the upcoming decades. Since PCI appearances it became evident that this approach has significant limitations, such as vessel occlusion, restenosis or migration of the prosthesis. These problems have improved with the development of bare metal stents (BMS) and more recently, the drug eluting stents (DES). Despite the improvements, the role of stenting remains temporary and it is limited to the intervention and shortly thereafter. This need require the development of biodegradable stents, which are completely absorbed by the body once the medical disease has been healed, solving the PCI's limitations.

In the design of biodegradable stents, it is advantageous to consider materials that have received regulatory approval for other

* Corresponding author.

E-mail address: quim.ciurana@udg.edu (J. Ciurana).

applications, such as, polylactide acid (PLLA), polycaprolactone (PCL), polyglycolic acid (PGA), magnesium (Mg), and zinc (Zn), among others. Regardless of material choice, the challenges associated with biodegradable materials remain similar; the mechanical properties, manufacturing process, and biocompatibility. The most important it is not only to know the properties of the stent's material before manufacturing's process, but also how do this process affect upon their properties, primarily the degradation rate because it is the head of provide the appropriate period of time to heal the *atherosclerosis*. There is a need to develop techniques for evaluating the ability of biodegradable stents to provide not only acute support, but also reliable structural integrity for an appropriate period of time that allows to the stent to achieve their goal.

Due to these needs, there are numerous authors whose have been analysing the degradation rate before manufacturing's process relating to different biodegradable materials. Wiggins et al. [1] found that the degradation rate of polyurethane increased with cyclic strain rate, whereas strain magnitude has essentially no effect employing a circular membrane devices in which vacuum was

applied to one side of the membrane. This device applied bi-axial strain to the membrane in the middle region, and largely uniaxial strain in the outer region. Zilberman et al. [2] studied the effect of degradation on tensile mechanical properties and morphology of PLLA, PDS, and PGACL where PLLA emerged as the most promising materials of the study. Kannan et al. [3] demonstrated that the addition of POSS nanocores to the PU imparts a type of protective, extending its resistance to degradation. Niels Grabow et al. [4] designed and produced a biodegradable slotted tube stent based on PLLA and P4HB polymers, carried out mechanical and degradation experiment. The results showed that the PLLA/P4HB stent allows rapid balloon-expansion and exhibited adequate mechanical scaffolding properties suitable for a broad range of vascular and nonvascular applications. Yang et al. [5,6], studied the effect of cyclic loading on the in vitro degradation of PLGA scaffolds for 12 weeks. Their mode of deformation was unconfined compression of <5% strain at 1 Hz for 8 h per day for 12 weeks and compared results with static controls. The authors have found that water absorption was higher in dynamic conditions and observed markedly higher reductions in mass, dimensions, and molecular weight when compared with static conditions. Vieira et al. [7] studied the evolution of mechanical properties during degradation based on experimental data. The decrease of tensile strength followed the same trend as the decrease of molecular weight. Mostaed et al. [8] studied the degradation behaviour of Zn and Zn binary alloys in Hanks' modified solution which simulates the ionic composition of blood plasma.

In order to accomplish the best process from the economic point of view, efforts to understand the material's properties and finding the best manufacture process to this kind of material have been considered. The lasers appear to be the perfect tool for this purpose because of non-contact material removal and high precision. Because of that, some authors have been focusing their studies in the laser manufacturing process of biodegradable materials. Grabow et al. [9] studied the effect of CO₂ laser cutting, and sterilization on Poly-L-Lactide (PLLA). The results showed the dramatic influence of the sterilization procedure on the mechanical properties of the material. In 2008 Tiaw et al. [10] studied the effect of Nd:YAG laser on micro-drilling and micro-cutting of thin PCL films. Melting and tearing of the thin polymer film were not much of an issue for the thin spin-cast film, but a slight extent of melting was observed in the thickest biaxial drawn film. Choudhury and Shirley [11] employed CO₂ laser to cut three polymeric materials, and developed a model equation regarding input process parameters with the output. Rocio Ortiz et al. [12] examined the picosecond laser ablation of PLLA as a function of laser fluence and degree of crystallinity. High quality micro-grooves were produced in amorphous PLLA, revealing the potential of the ultra-fast laser processing technique. In 2013 Schneider et al. [13] employed a high power laser to cut fibre reinforced thermoplastic polymers with continuous and pulsed wavelength. The result shows that HAZ could be significantly reduced by multi-pass processing at high processing cutting speed. Stepank et al. [14,15], presented the impact of the KrF laser and CO₂ laser irradiation on physicochemical properties of biodegradable PLLA. Stepank et al. [16] fabricated a polymer-based biodegradable stent using a CO₂ laser. Tamrin et al. [17] determined an optimized set of cutting parameters for CO₂ laser for three different thermoplastics employing grey relational analysis. Guerra et al. [18] demonstrated the feasibility of fibre lasers of 1.8 μm of wavelength to cut polycaprolactone sheet with higher precisions. The process barely affected over the material properties due to the lower material absorbance at this wavelength.

Despite the numerous studies about biodegradable materials to stent's application both in material's properties, as in the laser manufacturing process, nowadays it is unknown the effect of laser

process upon degradation rate of other promising material such as polycaprolactone [19]. For this reason, this paper aims to study the effect of input energy density of Nd:YAG fibre laser upon degradation rate of the polycaprolactone. The degradation studies were carried out with a novel *in-vitro* method closer to the body conditions and were compared with the traditional *in-vitro* method. This approach was not presented in the available literature. Degradation rates, surface morphology changes, and geometric pattern changes in the stents were studied according to the laser process, and the degradation method employed.

2. Material and methods

2.1. Laser cutting process

Samples were cut employing a Fibre Laser RoFin FL x50s that provides: 1.08 μm of wavelength, a shorter pulse width of 26 μs, 500 W of maximum power, a maximum frequency of 5000 Hz, and 1.1 of beam quality. The process fibre used had 150 μm of diameter, which was mounted in a focusing optics consisted of a *Precitec Fine Cutting Head* with a 50 mm length collimation lens and a 50 mm focal length objective.

Screening experiments were carried out to determine the appropriate E_L range to achieve a complete cut of PCL sheets. After analyzing the screening results, we decided to set up; a frequency of 5000 Hz, 0.2 MPa of pressure air, 0.10 ms of pulse width, and 0.2 mm of standoff distance. 14 samples were studied in this work (Table 1), 13 of them cut at different E_L and the original uncut sample E00. Four replicas of each sample were cut to carry out the degradation studies, two for each degradation conditions. A simplify sub unit of the stent version was selected for the experiment (Fig. 1).

2.2. Material

Experiment were performed using *Polycaprolactone* (PCL) Capa 6500[®] supplied by Perstorp (Table 2). PCL sheets of 400 μm thickness were prepared taking advantage of 3D technology employing a RepRap BCN 3D printer. Before printing, the sheets were kept at 60 °C for 10 min to homogenize the surface and dried in for 24 h at 37 °C. PCL is a hydrophobic, semi-crystalline polymer; its crystallinity tends to decrease with increasing molecular weight. The good solubility of PCL, its low melting point (59–64 °C) and exceptional blend-compatibility has stimulated extensive research into its potential application in the biomedical field. In particular it is especially interesting for the preparation of long-term implantable devices, such stents, due to its degradation, which is even slower than that of polylactide.

2.3. Characterization

2.3.1. Degradation analysis

The degradation study was carried out with a novel system

Table 1
Design of experiment.

Sample	E _L (J/m ²)	Sample	E _L (J/m ²)
E00	Uncut	E07	1,85 × 10 ⁹
E01	1,10 × 10 ⁹	E08	1,94 × 10 ⁹
E02	1,21 × 10 ⁹	E09	1,98 × 10 ⁹
E03	1,45 × 10 ⁹	E10	2,16 × 10 ⁹
E04	1,51 × 10 ⁹	E11	2,18 × 10 ⁹
E05	1,64 × 10 ⁹	E12	2,64 × 10 ⁹
E06	1,76 × 10 ⁹	E13	2,91 × 10 ⁹

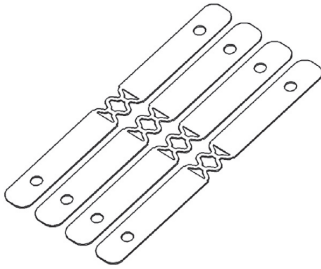


Fig. 1. Experimental geometry.

(Fig. 2). The phosphate buffered solution (PBS) at 37 °C (pH 7.4 ± 0.1) is collecting in the superior distribution chamber, the PBS flow by the pipes, where the stent is placed, simulating the blood flow. The PBS is recollected in the inferior tank where a peristaltic pump ($Q = 2000 \text{ L/h}$) keeps coming back to the superior tank. The pipes have a closure system that allows us to extract the stent weekly to related testing. This novel method is closer to body conditions, allowing us a better understanding of the degradation rate.

To compare the degradation rates, both, in dynamic as in static conditions, a separate group of samples too were analysed in traditional *in-vitro* conditions in plastic vessels with 4 ml of PBS. All samples were recovered after, 2, 4, 6, and 8 weeks under the same conditions. The water absorption and weight loss were evaluated by weighing in a METTLER TOLEDO Sartorius 2 MP Scale, taking into account the original stent's weight after cutting process (W_0), the weight of the wet/swallow sample (W_w), and the residual weight,

after degradation that had completely dried (W_d) in oven for 24 h. The water absorption rate, $W_a\%$, was evaluated by the following equation:

$$W_a\% = \frac{W_w - W_d}{W_d} \cdot 100 \quad (1)$$

Weight loss percentage, $W_l\%$ was estimated with the following equation:

$$W_l\% = \frac{W_0 - W_d}{W_0} \cdot 100 \quad (2)$$

The phosphate buffered solution was changed often in order to keep the pH as constant as possible.

2.3.2. Physical and morphologic analysis

To analyse the changes in the stent's surface morphology, the samples were examined by Scanning Electron Microscopy (SEM) with a Hitachi S-4100 in the 0, 4, and 8 weeks. Prior to analysis, the samples were coated with a layer of evaporated carbon in an Emitech K950 turbo evaporator. The physical aspects were analysed by the Optical Microscope Nikon SMZ – 745T attached to a digital camera CT3 ProgRes to study the changes in the stent geometry during the degradation process. This study was carried out in the 0, 4, and 8 weeks. Image J[®] software was used to process, both, the SEM as the OPTICAL images.

3. Results and discussion

This section presents the experimental results. The degradation rates, the surface morphology changes, and the geometry's changes have been analysing according to the E_L of the fibre laser source and

Table 2
Polycaprolactone properties.

Molecular Weight	Melting Temperature	H ₂ O Content	Yield Stress	Young Modulus	Strain at Break	Degradation Time
50000 g/mol	60 °C	<1%	17.5 MPa	470 MPa	>700%	>24 Months

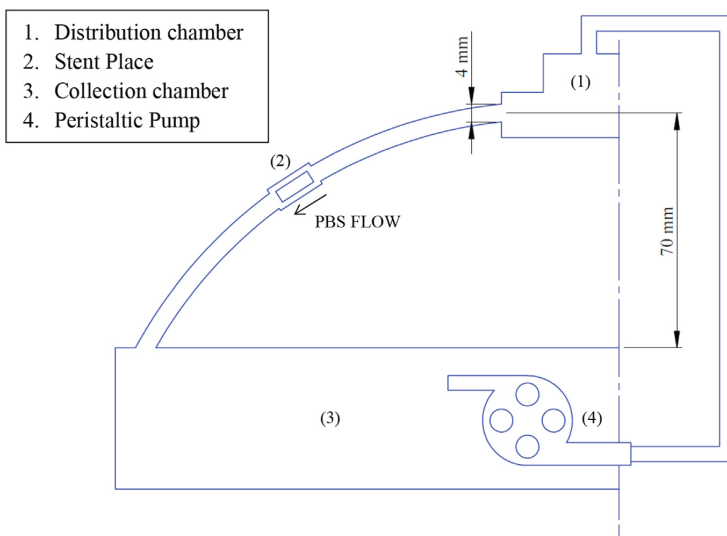


Fig. 2. Degradation system.

the degradation method employed. Due to the number of replicas employed, results just showed tendencies of the samples to show that indeed the laser process and the degradation conditions affect the degradation behaviour. All data are expressed as mean \pm standard error (SE).

3.1. Degradation rate

The mechanisms of degradation of PCL is well-known. Degradation occurs when water penetrates the PCL bulk, causing hydrolysis throughout the entire polymer matrix. From the literature it can be concluded that PCL undergoes a two-stage degradation process: first, the non-enzymatic hydrolytic cleavage of ester groups, and second, when the polymer is more highly crystalline and of low molecular weight, the polymer is shown to undergo intracellular degradation and it may be completely resorbed and degraded via intracellular mechanism [19].

With regards to the degradation process employed, results have shown two different behaviours (Fig. 3). In the static case, samples have gone losing weight according to literature [19]. In the dynamic case, the samples have shown an increase of weight (Fig. 3). It seems that the PBS flow is introduced into the samples causing higher water absorption, and then, an increase of their weight. This water absorption endured by the samples could imply an alteration of their properties. In general will reduce the resistance and the hardness, increasing its tenacity, besides the acceleration of degradation rate in a medium-large period of time [19]. Besides, a faster water absorption will leave a faster degradation of the samples, thus, the stent will fail before. These facts reveal the lacks in the traditional *in-vitro* method employed to study the degradation rates. This new method could help us a better understand of the degradation rates of biodegradable material in conditions closer to human body. Even, it could be useful to study the effect of tortuous vessels over the weight loss of the stent.

According to laser process, the degradation rate seems to be affected by the E_L . In the static case, the increase of E_L accelerates the degradation rate (Fig. 4), because of the chains breakups produced by the laser source that reduced the molecular weight of the samples [14], accelerating their weight loss. Although the

differences seem negligible, the samples cut at $1.21 \times 10^9 \text{ J/m}^2$ lost the half weight than the samples cut at $2.91 \times 10^9 \text{ J/m}^2$. This difference will be an important factor that will cause the premature fail of the stent. In the dynamic case (Fig. 4), the sample's weight increases with a linear trend according to the E_L increases confirmed by the relation between molecular weight and porosity. This fact will accelerate the degradation rate in a medium-large period of time [19].

3.2. Geometry changes

Samples have not exhibited significant changes in the geometrical aspects during the degradation studies (Fig. 5). Samples degraded by dynamics conditions show a relative cleanliness of the superficial burr, but they not show changes in the stent's structure (Fig. 5 Red Squares). These facts allow us to believe that difference between samples degraded under dynamic conditions and static conditions are caused by the water absorption, since dynamics conditions allow a faster inclusion of water inside the material.

The differences between degradation rates could be influenced by much more circumstances, for that, it would be interesting to carry out further studies about the influence of the stent's shape, temperature, material, etc., in their degradation rates. Previous section has proved the difference produced in the degradation rates due to the PBS flow, which allow us to confirm that the fluid speed will affect the degradation rates of the samples, because of, the stent's shape will affect the fluid conditions (speed, boundary layer, pressure, etc.) and then, it will change the degradation rates.

3.3. Surface morphology changes

The main intention behind the surface morphology SEM study was to visualize the possible mechanisms involved, both, in the laser cutting process, as in the degradation process on the polycaprolactone sheets. Besides identifying the effect of laser process during the experiments, the surface morphology study aimed to evaluate the effect of two different degradation process employed over the workpieces. Figs. 6 and 7 present the SEM images of the top surface in the Heat Affected Zone (HAZ).

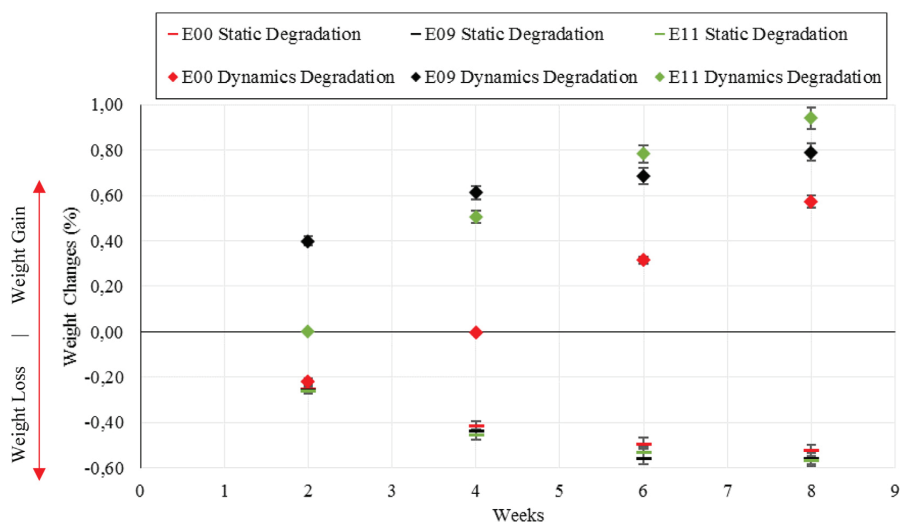


Fig. 3. Weight changes according weeks.

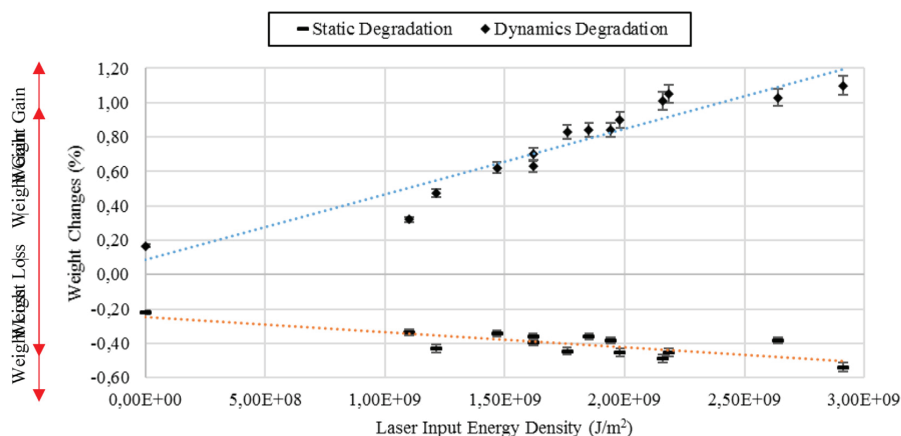


Fig. 4. Average weight changes after 8 weeks according to E_L employed to cut samples.

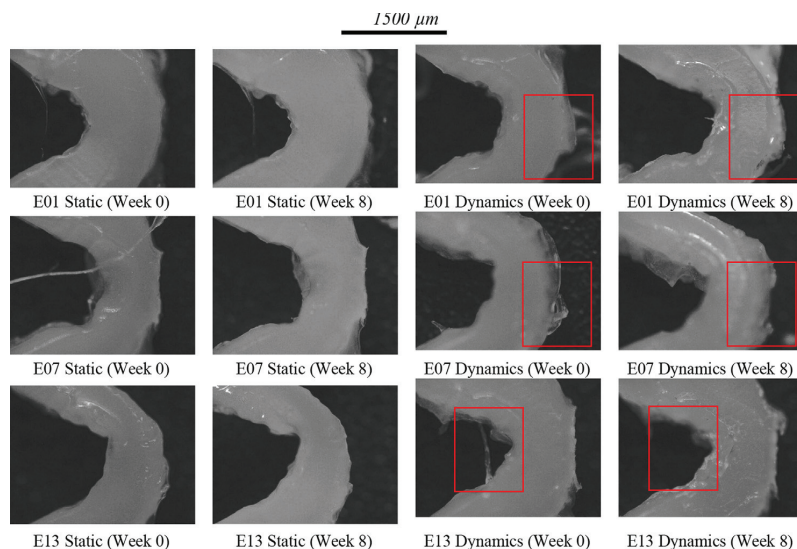


Fig. 5. Geometrical changes during the degradation studies.

With regards to the degradation process, dynamics and statics conditions have shown strong differences. Fig. 6 shows the difference between the samples before and after the two degradation processes.

It seems the higher surface erosion that the dynamics method produced in the samples. This fact could make it think that samples degraded under dynamics conditions will lose weight faster than samples degraded under static conditions. Nevertheless Figs. 3 and 4 showed the opposite, corroborating that the weight gain suffered by this samples was caused by the water absorption. The erosion raises the samples porosity allowing a better water absorption.

Surface degradation or erosion involves the hydrolytic cleavage of the polymer backbone only at the surface [18]. This situation arises when the rate of hydrolytic chain scission and the production of oligomers and monomers, which diffuse into the surroundings, is faster than the rate of water intrusion into the polymer bulk

(static conditions method). This typically results in thinning of the polymer over time without affecting the molecular weight. The advantage to this type of erosion is the predictability of the process, giving desirable release vehicles for drugs, as release rates can be predetermined [18].

According to Woodruff et al. [19], if water molecules can diffuse into the polymer bulk (dynamics degradation method), hydrolyze the chains enabling the monomers or oligomers to diffuse out, erosion will occur gradually and equilibrium for this diffusion–reaction phenomenon would be achieved. If this equilibrium is disturbed, the degradation mechanism could provoke internal autocatalysis, via the carboxyl and hydroxyl end group by-products. Whereas surface oligomers and carboxyl groups may freely diffuse into the surroundings (surface erosion situation), in the case of bulk degradation the internal concentration of autocatalysis products can produce an acidic gradient as the newly generated carboxyl end

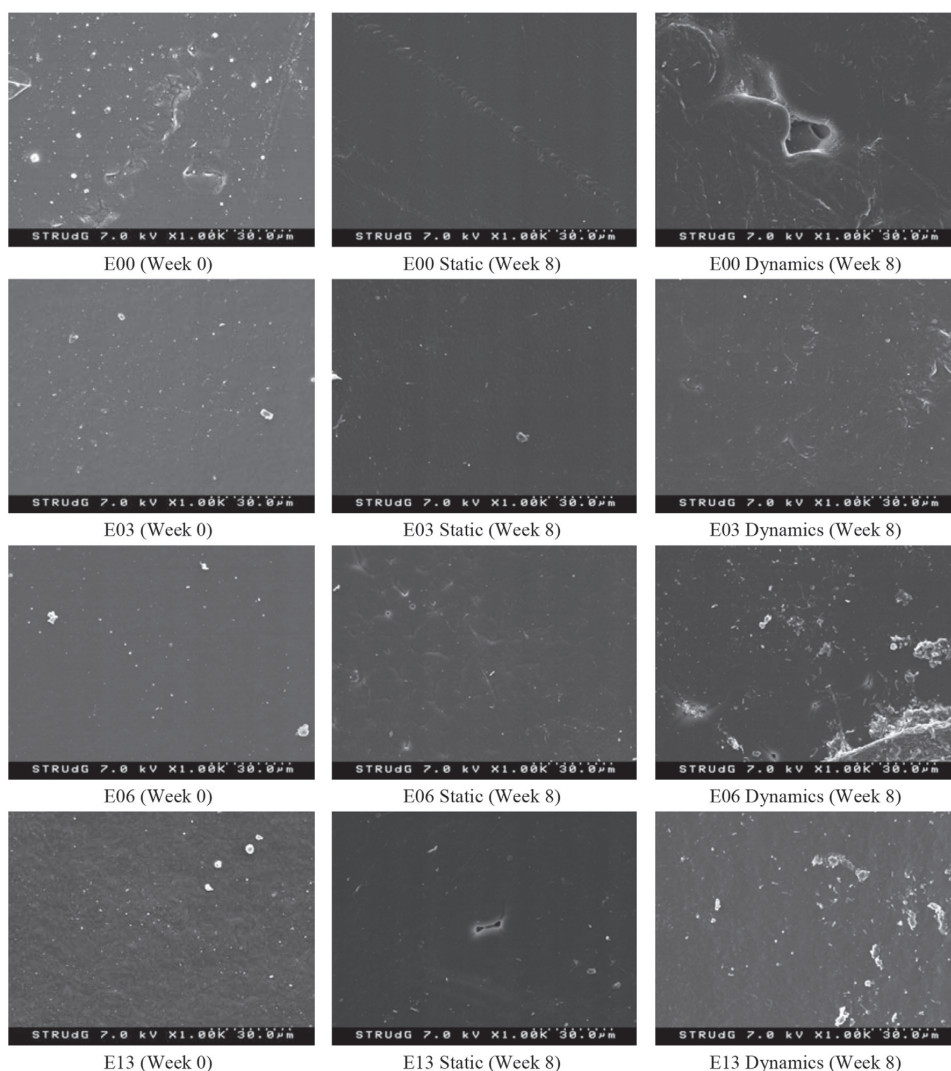


Fig. 6. Surface morphology SEM images.

group formed during ester bond cleavage accumulate. This in turn accelerates the internal degradation compared to the surface, leaving an outer layer of higher molecular weight skin with a lower molecular weight, degraded, interior. The degradation mechanism thus becomes defined by bimodal molecular weight distribution, being unpredictable.

According to laser cutting process, SEM images show a decrease in the surface imperfections in the HAZ. Like all semi-crystalline polymers, when the laser pass through the PCL, the beam energy is reflected, scattered, absorbed and transmitted [20]. The part of energy reflected towards the nozzle raises their temperature, affecting the surrounded areas of the cut-off point (Fig. 7).

4. Conclusions

The effects of laser cutting process over the degradation rate of

polycaprolactone (PCL) sheet have been studied. The influence of the input energy density (E_L) and degradation method over the degradation rate, the geometrical changes, and the surface morphology has been analysed during 8 weeks. This work shows the influence of E_L at *in-vitro* degradation in static conditions and *in-vitro* degradation in dynamic conditions with novel degradation system described in this paper.

Results allow us to conclude that the usage of 1.08 μm wavelength Nd:YAG fibre laser affect the PCL degradation rate by accelerating it according the E_L level increases. This fact is mainly produced by the chains breakup that the laser irradiation produces in the material. These effects make us affirm that although the laser appears to be the perfect tool for stent manufacture process because of their high precision, we must be thorough with the effect that this process cause in the material properties.

Regards to the degradation method employ, results have

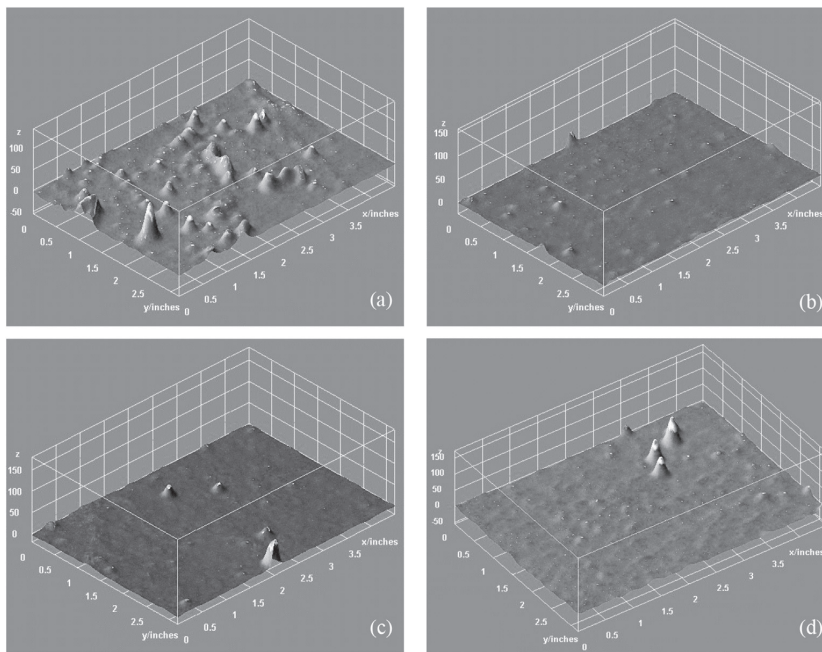


Fig. 7. Surface morphology images processed by Image J[®] (a) E00 (b) E01 (c) E07 (d) E13.

exhibited the strong differences between the static method and the dynamic method, whom is closer to body conditions. Whereas the static method have given degradation curves according with the literature [19], the dynamic method has shown an increases in the water absorption, fact that will accelerate the degradation rate in a medium-large period of time, besides the material alteration that will reduce the resistance and the hardness of the stent, increasing it tenacity [19].

The differences between degradation rates could be influences by much more circumstances, for that, it would be interesting to carry out further studies about the effects of different lasers over the stent material properties, as well as, studies about the dynamics degradation method that analyse the effect of flow speed, stent shape, etc., would be interesting.

Acknowledgements

The first authors acknowledge the financial support from University of Girona (UdG) and the Ministry of Economy and Competitiveness (MINECO), Spain for its PhD scholarship and grants from DPI2013-45201-P. The authors are grateful for the financial support from the University of Girona (Spain) MPCUdG2016/036.

References

- [1] M.J. Wiggins, J.M. Anderson, A. Hiltner, Effect of strain and strain rate on fatigue-accelerated biodegradation of polyurethane, *J. Biomed. Mater. Res. A* 66 (3) (2003) 463–475.
- [2] M. Zilberman, K.D. Nelson, R.C. Eberhart, Mechanical properties and in vitro degradation of bioresorbable fibers and expandable fiber-based stents, *J. Biomed. Mater. Res. - Part B Appl. Biomater.* 74 (2) (2005) 792–799.
- [3] R.Y. Kannan, H.J. Salacinski, M. Odyha, P.E. Butler, A.M. Seifalian, The degradative resistance of polyhedral oligomeric silsesquioxane nanocore integrated polyurethanes: an in vitro study, *Biomaterials* 27 (9) (2006) 1971–1979.
- [4] N. Grabow, C.M. Bünger, C. Schultze, K. Schmohl, D.P. Martin, S.F. Williams, K. Sternberg, K.P. Schmitz, A biodegradable slotted tube stent based on poly(L-lactide) and poly(4-hydroxybutyrate) for rapid balloon-expansion, *Ann. Biomed. Eng.* 35 (12) (2007) 2031–2038.
- [5] Y. Yang, Y. Zhao, G. Tang, H. Li, X. Yuan, Y. Fan, In vitro degradation of porous poly(L-lactide-co-glycolide)/??-tricalcium phosphate (PLGA/??-TCP) scaffolds under dynamic and static conditions, *Polym. Degrad. Stab.* 93 (10) (2008) 1838–1845.
- [6] Y. Yang, G. Tang, Y. Zhao, X. Yuan, Y. Fan, Effect of cyclic loading on in vitro degradation of poly(L-lactide-co-glycolide) scaffolds, *J. Biomater. Sci. Polym. Ed.* 21 (1) (2010) 53–66.
- [7] a. C. Vieira, J.C. Vieira, J.M. Ferra, F.D. Magalhães, R.M. Guedes, a. T. Marques, Mechanical study of PLA-PCL fibers during in vitro degradation, *J. Mech. Behav. Biomed. Mater.* 4 (3) (2011) 451–460.
- [8] E. Mostaed, M. Sikora-Jasinska, a. Mostaed, S. Loffredo, a. G. Demir, B. Previtali, D. Mantovani, R. Beanland, M. Vedani, Novel Zn-based alloys for biodegradable stent applications: design, development and in vitro degradation, *J. Mech. Behav. Biomed. Mater.* 60 (2016) 581–602.
- [9] N. Grabow, M. Schlun, K. Sternberg, N. Hakansson, S. Kramer, K.-P. Schmitz, Mechanical properties of laser cut poly(L-lactide) micro-specimens: implications for stent design, manufacture, and sterilization, *J. Biomech. Eng.* 127 (February 2005) (2005) 25–31.
- [10] K.S. Tiaw, M.H. Hong, S.H. Teoh, Precision laser micro-processing of polymers, *J. Alloys Compd.* 449 (1–2) (2008) 228–231.
- [11] I. a. Choudhury, S. Shirley, Laser cutting of polymeric materials: an experimental investigation, *Opt. Laser Technol.* 42 (3) (2010) 503–508.
- [12] R. Ortiz, I. Quintana, J. Etxarr, A. Lejardi, J.R. Sarasua, Picosecond laser ablation of poly-L-lactide: effect of crystallinity on the material response, *J. Appl. Phys.* 110 (9) (2011).
- [13] F. Schneider, N. Wolf, D. Petring, High power laser cutting of fiber reinforced thermoplastic polymers with cw- and pulsed lasers, *Phys. Procedia* 41 (2013) 415–420.
- [14] B.D. Stepak, A.J. Antończak, K. Szustakiewicz, P.E. Koziol, K.M. Abramski, Degradation of poly(L-lactide) under KrF excimer laser treatment, *Polym. Degrad. Stab.* 110 (2014) 156–164.
- [15] A.J. Antończak, B.D. Stepak, K. Szustakiewicz, M.R. Wojcik, K.M. Abramski, Degradation of poly(L-lactide) under CO₂ laser treatment above the ablation threshold, *Polym. Degrad. Stab.* 109 (2014) 97–105.
- [16] B. Stepak, a. J. Antończak, M. Bartkowiak-Jowska, J. Filipiak, C. Pezowicz, K.M. Abramski, Fabrication of a polymer-based biodegradable stent using a CO₂ laser, *Arch. Civ. Mech. Eng.* 14 (2) (2014) 317–326.

- [17] K.F. Tamrin, Y. Nukman, I. a. Choudhury, S. Shirley, Multiple-objective optimization in precision laser cutting of different thermoplastics, *Opt. Lasers Eng.* 67 (2015) 57–65.
- [18] A.J. Guerra, J. Farjas, J. Ciurana, Fibre laser cutting of polycaprolactone sheet for stents manufacturing: a feasibility study, *Opt. Laser Technol.* 95 (2017) 113–123.
- [19] M.A. Woodruff, D.W. Hutmacher, The return of a forgotten polymer - polycaprolactone in the 21st century, *Prog. Polym. Sci.* 35 (10) (2010) 1217–1256.
- [20] S. Genna, C. Leone, V. Tagliaferri, Characterization of laser beam transmission through a High Density Polyethylene (HDPE) plate, *Opt. Laser Technol.* 88 (2017) 61–67.

Chapter 5
Stents Tubes Fabrication by Dip Coating

Abstract

Once the feasibility of fibre laser to cut bioabsorbable polymers such as polycaprolactone with simples conditions has been demonstrated it is necessary the study of fibre laser cutting process over real stent's tubes.

The literature has proved material such as PLLA, PCL, PGA, Mg Alloys, etc., nevertheless these material needs some modifications to obtain the medical and mechanical properties required to stent purpose. In the stent industry many steps are require until achieve an implantable stent. In the case of polymer's stent, the material should be dissolved to make the tube, by dip coating, for the subsequent laser cutting process, ending by a cleaner and sterilization processes. The effect of the parameter involved in these processes over the material properties are still unclear.

Chapter 5 presents the effects the Dip Coating process have over the tubes features to obtain a PCL, PLA and PCL/PLA tubes for stent manufacturing purpose. The effects of withdrawal speed, number of cycles, and solutions concentration were studied.

Tubes were analysed by Dynamic Mechanical Analysis (DMA), Degradation Rate, Surface Roughness, Thickness, and Uniformity. Results have shown the strong influence of withdrawal speed and polymer's concentration over the tube's features. DMA and degradation results showed the limitations of PCL and PLA as material for the stent purpose, meanwhile the PCL/PLA composite tube showed a behaviour closer to the stents requirements.

This chapter had been published in the Journal Procedia CIRP (Under Journal Guidelines).



Antonio J. Guerra, San, J., Joaquim Ciurana.
“Fabrication of PCL/PLA Composite Tube for Stent Manufacturing”. 2017, 65, 231-235. Procedia CIRP.

3rd CIRP Conference on Bio Manufacturing

Fabrication of PCL/PLA composite tube for stent manufacturing

Antonio J. Guerra^a, Joan San^b, Joaquim Ciurana^{a*}

^aDepartment of Mechanical Engineering and Industrial Construction - University of Girona, Maria Aurèlia Capmany 61, 17003 Girona, Spain

^bDepartment of Medical Sciences - Faculty of Medicine - University of Girona, Emili Grahit 77, 17003 Girona, Spain

* Corresponding author. Tel.: +34 972418265; fax: +34 972418098. E-mail address: quim.ciurana@udg.edu

Abstract

This work presents the effect of Dip Coating process over the tube's features to obtain a PCL/PLA tube to stent purpose. The effects of withdrawal speed, number of cycles, and solutions concentration were studied. Four different tubes were fabricated and analyzed by Dynamic Mechanical Analysis (DMA), Degradation Rate, Surface Roughness, Thickness, and Uniformity.

Results have shown the strong influence of withdrawal speed and polymer's concentration over the tube's features. DMA and degradation results showed the limitations of PCL and PLA as material for the stent purpose, meanwhile the PCL/PLA composite tube showed a behavior closer to the stents requirements.

© 2016 The Authors. Published by Elsevier B.V. This is an open access article under the CC BY-NC-ND license (<http://creativecommons.org/licenses/by-nc-nd/4.0/>).

Peer-review under responsibility of the scientific committee of the 3rd CIRP Conference on BioManufacturing 2017

Keywords: Dip Coating, Biodegradable Stent, Composite

1. Introduction

Since their introduction in the market in the early 1990s, nobody was able to predict the advantages that will occur in stent technology over the upcoming decades. Nowadays, stents are the main treatment modality for atherosclerosis. The coronary stent global market, primarily balloon-expanded, bare metal (BMS), and drug eluting stents (DES), was approximately \$7.5 billion in 2015 and forecast stent sales will grow at double digit rates [1]. Since stenting appearances it became evident that this approach has significant limitations, such as vessel occlusion, restenosis or migration of the prosthesis. These problems have improved with the development of BMS and more recently, the DES both based on metallic structures.

Although metallic stents are effective in preventing acute occlusion and reducing late restenosis after coronary angioplasty, many concerns still remain, such as thrombosis and restenosis. Bioresorbable stents (BRS) were introduced to overcome these limitations with important advantages: complete bioresorption, mechanical flexibility, etc.

In the design of biodegradable stents several types of materials are currently been investigated: poly-L-lactic acid

(PLLA) and magnesium have been the most promising materials [2], although there are other polymers suggested such as polycaprolactone (PCL) [3]. Regardless of material choice, the challenges associated with biodegradable materials remain similar; the mechanical properties, manufacturing process, and biocompatibility.

Due to these needs, there are numerous authors whose have been analyzing the properties of some different polymeric biodegradable materials. Wiggins et al. [4] found that the degradation rate of polyurethane increased with cyclic strain rate, whereas strain magnitude has essentially no effect employing a circular membrane devices in which vacuum was applied to one side of the membrane. This device applied bi-axial strain to the membrane in the middle region, and largely uniaxial strain in the outer region. Meital et al. [5] studied the effect of degradation on tensile mechanical properties and morphology of PLLA, PDS, and PGACL where PLLA emerged as the most promising materials of the study. Ruben et al. [6] demonstrated that the addition of POSS nanocores to the PCU imparts a type of protective, extending its resistance to degradation. Niels Grabow et al. [7] designed and produced a biodegradable slotted tube stent based on PLLA and P4HB polymers, carried out mechanical and degradation experiment.

The results showed that the PLLA/P4HB stent allows rapid balloon-expansion and exhibited adequate mechanical scaffolding properties suitable for a broad range of vascular and nonvascular applications. Yang et al. [8, 9] studied the effect of cyclic loading on the in vitro degradation of PLGA scaffolds for 12 weeks. Their mode of deformation was unconfined compression of <5% strain at 1Hz for 8 h per day for 12 weeks and compared results with static controls. The authors have found that water absorption was higher in dynamic conditions and observed markedly higher reductions in mass, dimensions, and molecular weight when compared with static conditions. Vieira et al. [10] studied the evolution of mechanical properties of PLA-PCL fibers during degradation based on experimental data. The decrease of tensile strength followed the same trend as the decrease of molecular weight. More recently, Chu et al. [11], have analyzed the effect of fluid shear stress in the in vitro degradation rate of PLGA membranes. Their work showed that the fluid shear stress affects over the viscosity of the degradation solution, the ultimate strength and has a great effect on the surface morphology of PLGA membranes.

Despite, the efforts for understand and develop news fully biodegradable materials for medical applications, nowadays is still necessary to continue the study of new material or configuration of them, and the employed manufacturing process. In the stent industry, many steps are require until achieve an implantable stent. The original material should be dissolved to make the tube, by dip coating, for the subsequent laser cutting process, ending by a cleaner and sterilization processes. The effect of the parameter involved in these processes over the material properties are still unclear.

The ideal stent should be uniform, has smooth surface for a better vessel placing, fully corrosion resistant, vascular compatible, fatigue resistant, and visible using standard X-Ray and MRI methodology, and a good relation between hardness and soft. The above properties are interrelated and sometimes contradictory, requiring careful compromise.

The authors aim to analyze the effect of process parameters over the tube's physical features to obtain a PCL/PLA composite tube that accomplish with the stents requirement. The effect of withdrawal speed, the number of cycles, and the solutions concentration was studied. Four different tubes were made, namely, PCL, PLA, PCL/PLA, and PLA/PCL. The tubes were analyzed by Dynamic Mechanical Analysis (DMA), Surface Roughness, Dimensional Uniformity, in order to find the best tube for the stent purpose.

2. Material and Method

2.1. Dip Coating Machine

Dip coating techniques can be described as a process where the substrate to be coated is immersed in a liquid and then withdrawn with a well-defined withdrawal speed under controlled temperature and atmospheric conditions. Taking advantage of a 3D Printer Machine, we developed a Dip Coating Machine. A male stainless steel cores of 4 mm outer diameter are lodged in a superior support grip to the vertical axis. The process is defined by the start-up time, withdrawal speed, evaporation time, and number of cycles (**Fig. 1**).

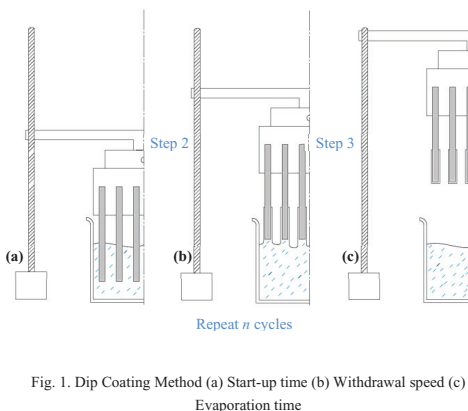


Fig. 1. Dip Coating Method (a) Start-up time (b) Withdrawal speed (c) Evaporation time

2.2. Materials

Polycaprolactone (PCL) Capa 6500[®] supplied by Perstorp and Polylactide (PLA) 3251D[®] supplied by NatureWorks were used as material for the experiments. PCL is a biodegradable polyester with a low melting point (60°C) and a glass transition of about -60°C. PLLA is a biodegradable thermoplastic aliphatic polyester derived from renewable resources, such as corn starch, or sugarcane. Their melting point is about 173–178 °C with a glass transition of 60–65 °C. Both PCL and PLA degradation is produced by hydrolysis of its ester linkages in physiological conditions and has therefore received a great deal of attention for using it as an implantable biomaterial for long term implantable devices, such stents, because of their properties (**Table 1**). The solvent employed were CHCl₃.

Table 1. Material Properties.

Material	Molecular Weight [g/mol]	Young Modulus [MPa]	Strain at Break [%]	Degradation Time [Months]
PCL	50000	470	700	>24
PLA	90000	108	3.5	12-24

2.3. Characterization

2.3.1. Physical Properties

To study the physical tube’s characteristics, the samples were examined using Roughness Mitutoyo SurfTest SV-2000 Machine to measure the R_a along the longitudinal axis, Optical Microscope Nikon SMZ – 745T attached to a digital camera CT3 ProgRes to check the radial uniformity, and Micrometer Micromar 40EWW to measure the tube’s thickness. Three measurements of each test were carried out to obtain more accurate results.

2.3.2. Mechanical Properties

The mechanical characteristic were measured by DMA employing the METTLER TOLEDO SDTA861e Machine. The dynamic storage modulus (E') are analyzed. The loss tangent is the ratio of loss modulus and storage modulus, which indicate the viscosity and elastic properties of material, respectively. The peak of loss tangent curve appears and can be defined as the glass transition temperature (T_g) of material. Three measurements of each sample were carried out to obtain more accurate results.

2.3.3. Degradation Rate

The degradation study were carried out submerging the samples in Phosphate Buffered Solution (PBS) at 37 °C during 6 weeks. The samples were recovered after, 2, 4, and 6 weeks under the same conditions. Weight loss were evaluated by weighing in a METTLER TOLEDO Sartorius 2MP Scale, taking into account the original tube’s weight after dip coating process (W_0), and the residual weight, after degradation that had completely dried (W_r). Weight loss percentage, $W_L\%$ was estimated with the following equation:

$$W_L\% = \frac{W_0 - W_r}{W_0} \cdot 100 \quad (1)$$

2.4. Design of Experiment

Based on a Central Composite Design (CCD) with 6 center points and alpha 1.22, 20 PCL tubes and 20 PLA tubes were made, (3 replicas of each one). Table 2 collects the levels selected. Analyzing the physical properties we selected the best parameters to obtain a tube for the stent purpose, namely, a uniform tube with the minimal R_a . All experiment were conducted in controlled room condition at 25 °C and 50 % of humidity. The samples were dried in oven at 35 °C for 48 hours to remove all the solvent content.

Table 2. Design of Experiment Levels.

Level	Withdrawal Speed (mm/min)	Polymer Concentration (w/v)	Cycles (#)
Low	50	3	40
Med	250	5	50
High	450	7	60

3. Results and discussion

3.1. Dip Coating Parameter Effects

Results have shown the strong influence of withdrawal speed over the layer thickness (Figure 2a). Both the PCL and the PLA have shown similar behavior. At low speeds the $CHCl_3$ contained in the solution dissolves part of the previous layer, making impossible the formation of a uniform wall. On the contrary, at fast speeds, the slight vibrations produced in the axis, generate inequalities on the tube’s radial shape as can be seen from Figure 3. With regard to the polymer’s concentration, its increase, raises the layer thickness following a near linear trend (Figure 2b). The best results were achieved with a concentration of 5% (w/v) both for PCL and PLA. Lastly, for a polymer concentration and withdrawal speed fixed, the number of cycles, seem to do not affect over the layer thickness directly, due to it mainly depends both on the polymer concentration and the withdrawal speed.

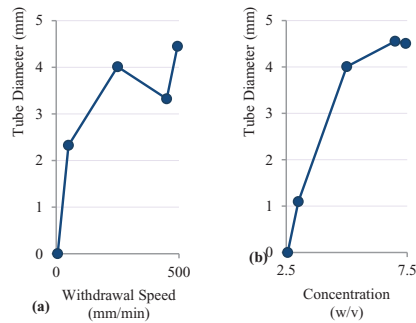


Fig. 2. Main effect plot for thickness (a) Withdrawal speed (b) Polymer concentration

Analyzing the roughness, its shows a downward trend according to withdrawal speed increases. With regards to the polymer’s concentration, its reduction, lower the solution viscosity, helping to a better layers deposition, thus a minor roughness. According to the number of cycles, the results show an increases of the superficial roughness according to cycles raise. The increase of cycles, makes that the solution is exposed longer, increasing their concentration due to the $CHCl_3$ evaporation.

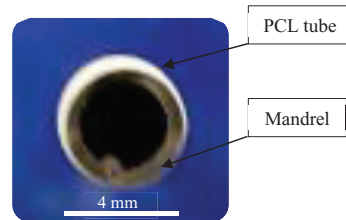


Fig. 3. Front View of the tube (tube’s radial shape)

With regards to the uniformity, the samples have been strongly influenced by the withdrawal speed and solution concentration, where the lower data have left the best results.

3.2. PCL-PLA Composite fabrication

Based on the previous results, the parameter selected to develop the PCL – PLA composite tubes were 250 mm/min withdrawal speed both for PCL and PLA, 5 % (w/v), 10 cycles per layer, both for PCL and PLA to obtain 100 μm layers. Table 3 shows the tubes composition.

Table 3. Tubes Composition Layer

Sample	Layer 1 (100 μm)	Layer 2 (100 μm)	Layer 3 (100 μm)	Layer 4 (100 μm)
1	PCL	PCL	PCL	PCL
2	PLA	PLA	PLA	PLA
3	PCL	PCL	PLA	PLA
4	PLA	PLA	PCL	PCL

3.3. Physical Properties

The results have corroborated the behavior described in the section 3.1. Dip Coating Parameter Effects. Nevertheless, it seems that the order of the layer deposition affect over the union of PCL - PLA. When the first layers are PCL (sample number 3) the resultant tubes have a largest R_a and a visible heterogeneity on their surface than the tubes which have PLA as first layer (sample number 4).

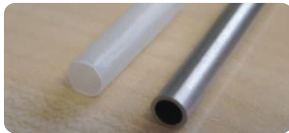


Fig. 4. PLA tube (left) and Dip Coating 316 SS mandrel

3.4. Dynamics Mechanical Analysis

The DMA results (Figure 5) have shown the strong different between PCL and PLA make clear their difficulty for the stent purpose. Nevertheless, the PCL – PLA composite has shown a middle E' that would be more appropriate for stent manufacture [12]. In this case, the order in the deposition layer did not show any influence over the dynamic modulus E' .

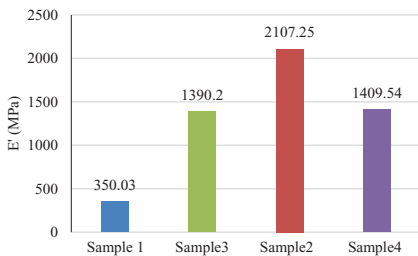


Figure 5. DMA Results

3.5. Degradation Rate

Results have shown the differences between PCL and PLA degradation rates. The composite tubes, both PCL-PLA as PLA-PCL have shown a medium weight losses, which make them, a good material for the stent purpose.

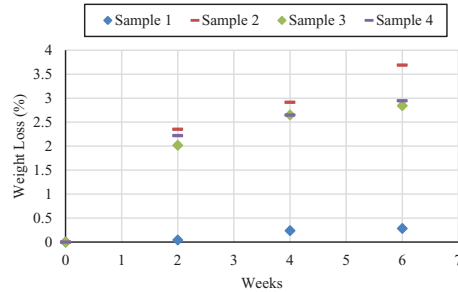


Fig. 6. Degradation rate of tubes

4. Conclusions

In this study, the dip coating parameters has been studied and selected to fabricate a PCL/PLA composite tube for stent manufacture.

The effect of withdrawal speed, the number of cycles, and the solution’s concentration over the physical properties were studied. The results have shown the strong influence of withdrawal speed and polymer’s concentration over the layer thickness and superficial roughness.

Four different tubes were fabricated with different order of layers, namely, PCL, PLA, PCL/PLA, and PLA/PCL. The tubes were analyzed by Dynamic Mechanical Analysis (DMA), Surface Roughness, Dimensional Uniformity, and Degradation Study in order to find the best tube for the stent purpose.

DMA results showed the limitations of PCL and PLA as material for the stent purpose, meanwhile the composite PCL/PLA tube showed a behavior close to the stent requirements. The degradation study corroborated the statement that the PCL/PLA composites could be a promise material for the biodegradable stents purpose.

This work is only a preliminary study that allow us to believe that a composite tubes made from PCL and PLA would be a good solution for the biodegradable stent market. Although the tests carried out are only one of many test that a stent should be go through to say that their properties are adequate, the work present is a good approximation of the potential of composite tubes.

Acknowledgements

The authors acknowledge the financial support from Ministry of Economy and Competitiveness (MINECO), Spain for its PhD scholarship and grants from DPI2013-45201-P and University of Girona (UdG), Spain MPCUdG2016/036.

References

- [1] Soares JS, Moore JE. Biomechanical Challenges to Polymeric Biodegradable Stents. *Ann. Biomed. Eng.* 2015.
- [2] Tenekecioglu E, Bourantas C, Abdelghani M, Zeng Y, Silva RC, Tateishi H, Sotomi Y, Onuma Y, Yilmaz M, Serruys PW. From drug eluting stents to bioresorbable scaffolds; to new horizons in PCI. *Expert Rev. Med. Devices*, 2016; 13(3):271–86.
- [3] Stepak B, Antończak AJ, Bartkowiak-Jowska M, Filipiak J, Pezowicz C, Abramski KM. Fabrication of a polymer-based biodegradable stent using a CO₂ laser. *Arch. Civ. Mech. Eng.* 2014;14(2):317–26.
- [4] Wiggins MJ, Anderson JM, Hiltner A. Effect of strain and strain rate on fatigue-accelerated biodegradation of polyurethane. *J. Biomed. Mater. Res. A* 2003;66(3):463–75.
- [5] Zilberman M, Nelson KD, Eberhart RC. Mechanical properties and in vitro degradation of bioresorbable fibers and expandable fiber-based stents. *J. Biomed. Mater. Res. - Part B Appl. Biomater.* 2005;74(2):792–9.
- [6] Kannan RY, Salacinski H, Odlyha M, Butler PE, Seifalian AM. The degradative resistance of polyhedral oligomeric silsesquioxane nanocore integrated polyurethanes: An in vitro study. *Biomaterials* 2006;27(9):1971–9.
- [7] Grabow N, Bünger CM, Schultze C, Schmohl K, Martin DP, Williams SF, Sternberg K, Schmitz KP. A biodegradable slotted tube stent based on poly(L-lactide) and poly(4-hydroxybutyrate) for rapid balloon-expansion. *Ann. Biomed. Eng.* 2007;35(12):2031–8.
- [8] Yang Y, Zhao Y, Tang G, Li H, Yuan X, Fan Y. In vitro degradation of porous poly(L-lactide-co-glycolide)/β-tricalcium phosphate (PLGA/β-TCP) scaffolds under dynamic and static conditions. *Polym. Degrad. Stab.* 2008; 93(10):1838–45, 2008.
- [9] Yang Y, Tang G, Zhao Y, Yuan X, Fan Y. Effect of cyclic loading on in vitro degradation of poly(L-lactide-co-glycolide) scaffolds. *J. Biomater. Sci. Polym. Ed.* 2010;21(1):53–66.
- [10] Vieira AC, Vieira JC, Ferra JM, Magalhães FD, Guedes RM, Marques AT. Mechanical study of PLA-PCL fibers during in vitro degradation. *J. Mech. Behav. Biomed. Mater.* 2011;4(3):451–60.
- [11] Chu Z, Zheng Q, Guo M, Yao J, Xu P, Feng W, Hou Y, Zhou G, Wang L, Li X, Fan Y. The effect of fluid shear stress on the in vitro degradation of poly(lactide-co-glycolide) acid membranes. *J. Biomed. Mater. Res. Part A* 2016;104(9):2315–24.
- [12] P. Poncin and J. Prof. Stent Tubing: Understanding the Desired Attributes. *Proc. ASM Conf. Mater. Process. Med. Devices* 2003:253–9.

Chapter 6
Fibre Laser Cutting of Polymer Tubes

Abstract

Once the feasibility of fibre laser to cut bioabsorbable polymers such as polycaprolactone with simples conditions has been demonstrated it is necessary the study of fibre laser cutting process over real stent's tubes.

Chapter 6 aims to study the effects the fiber laser cutting process has on polycaprolactone (PCL), polylactide acid (PLA), and PLA-PCL tubes for stent manufacturing. The effect of Power, Cutting Speed, and Number of Passes over Penetration, Precision, and Dross is presented.

Results have shown the difficulties to cut PLA with 1.08 μm wavelength lasers, being impossible to achieve a complete penetration both the PLA tubes, as PLA-PCL composite tubes. Nevertheless, with PCL tubes, fibre laser has been able to achieve dimensional precisions above than 95.75 %.

Fibre laser had been shown to be a useful tool to manufacture polycaprolactone stents with precision but have problem to cut other polymeric materials.

This chapter has been published in the Journal Procedia Manufacturing (Under Journal Guidelines).



Antonio J. Guerra, Joaquim Ciurana. “Fibre Laser Cutting of Polymer Tubes for Stents Manufacturing”. 2017, 13, 190-196. Procedia Manufacturing.



Manufacturing Engineering Society International Conference 2017, MESIC 2017, 28-30 June
2017, Vigo (Pontevedra), Spain

Fibre laser cutting of polymer tubes for stents manufacturing

A. Guerra, J. de Ciurana

Department of Mechanical Engineering and Industrial Construction, University of Girona, Maria Aurèlia Capmany 61, Girona 17003, Spain,

Abstract

Nowadays, stents are the main treatment modality for atherosclerosis. Although metallic stents are effective many concerns still remain. Bioresorbable stents (BRSs) were introduced to overcome these limitations with important advantages. In this paper the authors aim to study the effect of fiber laser cutting over polycaprolactone (PCL), polylactide acid (PLA), and PLA-PCL tubes for stent manufacturing. The effect of Power, Cutting Speed, and Number of Passes over Penetration, Precision, and Dross is presented. Results have shown the difficulty of cut PLA with 1.08 μm wavelength lasers, being impossible to achieve a complete penetration both the PLA tubes, as composite tubes. Nevertheless, with PCL tubes, fibre laser has been able to achieve dimensional precisions above than 95.75 %. Fibre laser has been shown to be a profitable tool to manufacture polycaprolactone stents.

© 2017 The Authors. Published by Elsevier B.V.

Peer-review under responsibility of the scientific committee of the Manufacturing Engineering Society International Conference 2017.

Keywords: Fiber Laser, Cutting, Polymers, Tube, Stent

1. Introduction

Nowadays, stents are the main treatment modality for atherosclerosis. Although current stents are effective, many concerns still remain. Recently, bioresorbable stents (BRS) were introduced to overcome these limitations with important advantages: complete bioresorption, mechanical flexibility, etc. Several types of materials are currently been investigated: poly-L-lactic acid (PLLA) and magnesium have been the most promising materials although other polymers suggested as material for bioabsorbable stents include polyglycolic acid (PGA) and polycaprolactone (PCL)[1].

The main efforts have been focused on analysing the mechanical and medical considerations of new biodegradable materials. Hideo Tamai et al [2] evaluated the feasibility, safety, and efficacy of the PLLA stent in humans. Fifteen patients electively underwent PLLA Igaki-Tamai stent implantation for coronary artery stenosis with promising results. Venkatraman et al. [3] reported, for the first time, the development of a fully biodegradable polymeric stent

that can self-expand at body temperatures. Liang et al. [4] designed a biodegradable shape-memory block co-polymers (PCTBV-25) for fast self-expandable stents. The stent made from PCTBV-25 film showed nearly complete self-expansion at 37°C within only 25 s, which is much better and faster than the best-known self-expandable stents. Vieira et al. [5] studied the evolution of mechanical properties during degradation based on experimental data. The decrease of tensile strength followed the same trend as the decrease of molecular weight.

Although the mechanical and medical properties of the material are important, finding the best manufacture process to this kind of material has to be considered as well. Lasers appear to be the perfect tool for this purpose. Therefore, some authors have been focusing their studies in the laser manufacturing process of polymers. Grabow et al. [6] studied the effect of CO₂ laser cutting, and sterilization on Poly-L-Lactide (PLLA). The results showed the dramatic influence of the sterilization procedure on the mechanical properties of the material. Rocio Ortiz et al. [7] examined the picosecond laser ablation of PLLA as a function of laser fluence and degree of crystallinity. Their results revealed the potential of the ultra-fast laser processing technique. Leone et al. [8] employed a 30 W MOPA Q-switched pulsed Yb:YAG to cut Carbon Fibre Reinforced Polymeric Composite (CFRP) thin Sheet. Stepan et al. [1] fabricated a polymer-based biodegradable stent using a CO₂ laser. Tamrin et al. [9] determined an optimized set of cutting parameters for CO₂ laser for three different thermoplastics employing grey relational analysis.

Although the effect of laser process over different polymers has been studied, nowadays, further studies about the laser cutting process of biodegradable materials are would be helpful to manufacture stents, which expands the laser manufacturing possibilities. The semi-transparent behaviour of most organic polymers at high wavelengths, hinders their manufacturing process with some sort of lasers, making the adaptation of this industry to these new materials costly. This work shows experimentally the feasibility of 1.08 μm wavelength fibre laser to cut polymers, which can open a new market opportunity to laser cutting firms. In this paper the authors aim to study the effect of fiber laser cutting over PCL, PLA, and PLA-PCL tubes for stent manufacturing. The effect of pulse power, cutting speed, and number of passes over complete penetration, dimensional precision, and dross is presented.

2. Material and Method

2.1. Laser Cutting System

Experiments were carried out with a CNC lathe machine. The laser employed was a Fibre Laser Rofin FL x50s that provides: a 1.08 μm of wavelength, 26 μs of shorter pulse width, 500 W of maximum power, a higher frequency of 5000 Hz and 1.1 of beam quality with 150 μm of fiber diameter (Fig. 1). The coaxial assist gas nozzle had an exit diameter of 0.5 mm. Pressure air at 0.4 MPa was used for the experiments.

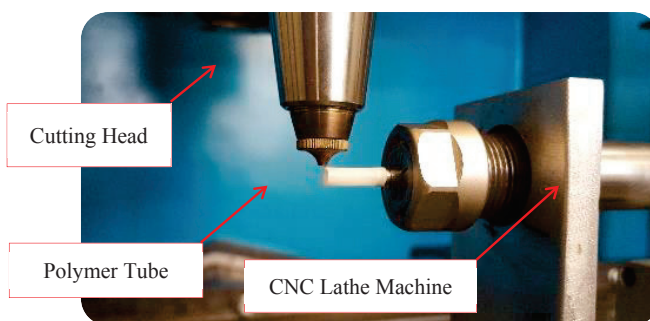


Fig. 1. Laser cutting system

2.2. Materials

Polycaprolactone (PCL) Capa 6500® supplied by Perstorp and Poly lactide (PLA) 3251D® supplied by NatureWorks were used as material for the experiments. PCL is a biodegradable polyester with a low melting point

(60°C) and a glass transition of about -60°C. PLA is a biodegradable thermoplastic aliphatic polyester derived from renewable resources, such as corn starch, or sugarcane. Their melting point is about 173–178 °C with a glass transition of 60–65 °C. Both PCL and PLA degradation is produced by hydrolysis of its ester linkages in physiological conditions and has therefore received a great deal of attention for using it as an implantable biomaterial for long term implantable devices, such stents, because of their properties (Table 1).

Table 1. Materials properties

Material	Molecular weight (g/mol)	Young modulus (MPa)	Strain at break (%)	Degradation time (Months)
PCL	50000	470	700	> 24
PLA	90000	108	3.5	12 – 24

Tubes were made by dip coating process employing CHCl₃ as solvent of the 5% (w/v) solution for both polymers. The tubes have an inner diameter of 4 mm and a wall thickness of 200 ± 10 µm (Fig. 2).



Fig. 2. PLA Tube and its core

2.3. Design of experiment

Screening experiment were carried out to know the input energy density necessary to achieve a complete penetration of the samples without affect the surrounded zones employing the levels of the Table 2.

Based on results, we are able to concluded that PCL needs an energy between $3 \cdot 10^8$ and $7 \cdot 10^8$ J/m² to obtain the complete penetration of samples. PLA and composite tubes were not completed penetrate without affect the surrounded zones due to the absorption coefficient of PLA.

Table 2. Design of experiments

Parameter	Low level	High level
Pulse power (W)	40	120
Cutting speed (mm/min)	300	700
Number of passes (#)	4	16

2.4. Characterization

Dimensional features of the samples were analyzed by the Optical Microscope Nikon SMZ – 745T attached to a digital camera CT3 ProgRes. Image J® was used to process the images and collect the data.

3. Results and discussion

Results have shown the influence of input energy density upon quality parameters, where a middle energy density left the best results. The correct relationship between the laser power, cutting speed, and number of passes becomes important to reach desired final geometry. All data are expressed as mean ± standard error (SE).

Analysis of variance (ANOVA) method was applied to test the statistical significance of the process parameters. The analysis was carried out at a 95% confidence level ($\alpha=0.05$). The ANOVA results showed that the main factors were cutting speed and number of passes.

3.1. Dimensional Precision

The dimensional precision measures were determined comparing the geometrical aspect from the cut samples with the CAD programmed geometry (Fig. 3). CAD lengths, and areas were considered the 100% of precision. The average precision of these geometrical aspects was used for the precision figures.

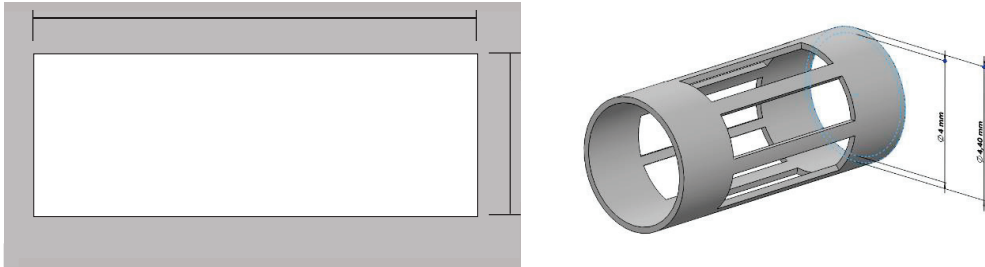


Fig. 3. Experiment Geometry (a) 2D View (b) 3D View

Results showed an increasing trend when kerf width is compared with the number of passes raises. That increasing trend is due to the increases of the input energy density accumulated in the cut-off point (Fig. 4).

In concordance with that, the increases of peak pulse power as well as the reduction of cutting speed left an increases on the kerf with (Fig. 5).

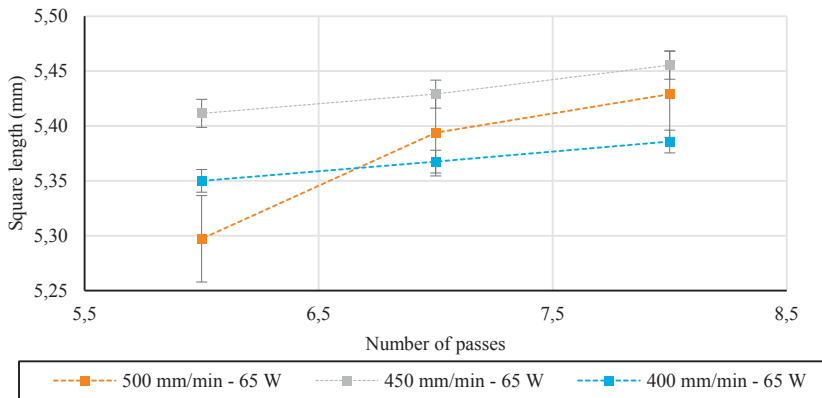


Fig. 4. Number of passes Vs Square length and Cutting speed Vs Square length

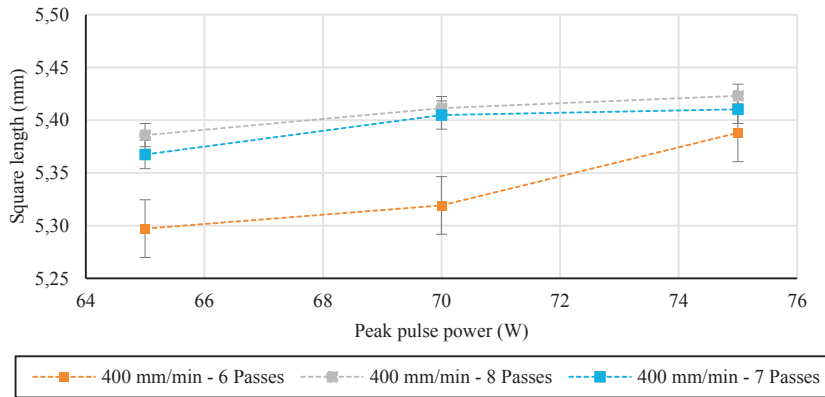


Fig. 5. Peak pulse power Vs Square length and number of passes Vs Square length

Analysing the results according to the input energy density, we can concluded that employing a cutting energy between $5 \cdot 10^8$ and $6 \cdot 10^8$ J/m² gave the best precision results (Fig. 6).

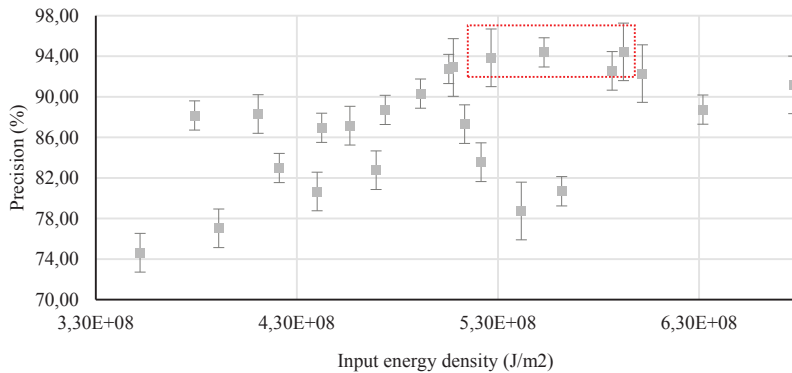


Fig. 6. Precision results Vs Input energy density

The 3 dimensional regression plot shows to us that lower cutting speed joins with lower passes at max peak pulse power (75 W) will gave the best dimensional precision, reaching the 98% of accuracy.

3.2. Dross Analysis

Fig. 7 shows the influence of the process parameter on the resultant dross (red market areas). The results show how the average dross area is reduced according to the cutting speed reduces. According to power results, a downward trend according to power increases is seen.

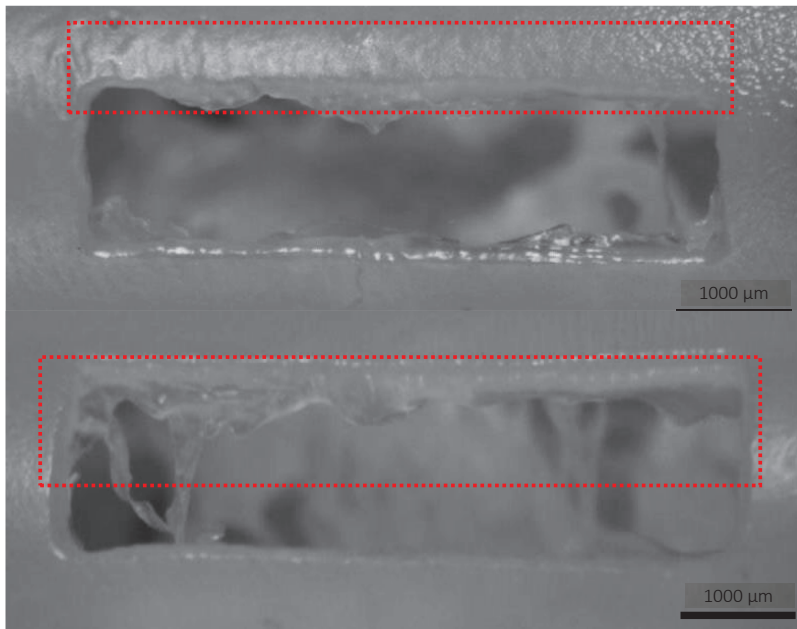


Fig. 7. Dross deposition (a) Sample cut at 400 mm/min – 7 Passes – 75 W (b) Sample cut at 450 mm/min – 7 Passes – 70 W

4. Conclusions

This work has demonstrated the feasibility of fiber laser to manufacture polycaprolactone tubes for stents purpose. The thermal sensibility of the polymers has been a rough path during the experiments. The increase of the nozzle temperature affects the surrounding cut-off zones and produces unexpected damages, making impossible the correct cutting process of the PLA tubes.

To PCL tubes, fibre laser process is able to achieve dimensional precisions above than 95.75 %. The lower absorption of PCL at this wavelength, although it hinders the cutting process, would reduce the scattering, reducing the material property affectation.

Fibre laser of 1.08 μm of wavelength has been shown to be a profitable and thrifty tool to cut polycaprolactone and, therefore, it is a great and efficient tool to manufacture stents.

Acknowledgements

The authors acknowledge the financial support from Ministry of Economy and Competitiveness (MINECO), Spain for its PhD scholarship and grants from DPI2013-45201-P and University of Girona (UdG), Spain MPCUdG2016/036.

References

- [1] B. Stepak, a. J. Antończak, M. Bartkowiak-Jowska, J. Filipiak, C. Pezowicz, K. M. Abramski, *Arch. Civ. Mech. Eng.* 14 (2014) 317–326.
- [2] H. Tamai, K. Igaki, E. Kyo, K. Kosuga, A. Kawashima, S. Matsui, H. Komori, T. Tsuji, S. Motohara, H. Uehata, *Circulation*. 102 (2000) 399–404.
- [3] S. S. Venkatraman, L. P. Tan, J. F. D. Joso, Y. C. F. Boey, X. Wang, *Biomater.* 27 (2006) 1573–1578.
- [4] L. Xue, S. Dai, Z. Li, *Biomater.* 31 (2010) 8132–8140.
- [5] a. C. Vieira, J. C. Vieira, J. M. Ferra, F. D. Magalhães, R. M. Guedes, a. T. Marques, *J. Mech. Behav. Biomed. Mater.* 4 (2011) 451–460.
- [6] N. Grabow, M. Schlun, K. Sternberg, N. Hakansson, S. Kramer, K.-P. Schmitz, *J. Biomech. Eng.* 127 (2005) 25–31.

- [7] R. Ortiz, I. Quintana, J. Etxarri, A. Lejardi, J. R. Sarasua, *J. Appl. Phys.* 110 (2011).
- [8] C. Leone, S. Genna, V. Tagliaferri, *Opt. Lasers Eng.* 53 (2014) 43–50.
- [9] K. F. Tamrin, Y. Nukman, I. a. Choudhury, S. Shirley, *Opt. Lasers Eng.* 67 (2015) 57–65.

Chapter 7
Novel 3D Additive Manufacturing Machine

Abstract

Previous results have demonstrated that laser micro cutting is able to produce BRS. Nevertheless in the case of polymeric stents, the 3D additive manufacturing techniques could be a more economical solution.

Chapter 7 aims to design and implement a novel 3D Additive Manufacturing Machine to Biodegradable Stent Manufacture. This machine have been never reported previously. A proof of concept is perform and the effects of nozzle temperature, fluid flow, and printing speed over the polycaprolactone stent's precision is studied.

Results allow us to think that the novel technology presented in this chapter will be an interesting future research line for BRS production. Results had shown the strong influence of temperature and flow rate over the printing precision. Printing speed did not had a clear tendency.

This chapter had been published in the Journal Procedia Manufacturing (Under Journal Guidelines), in the Catalonian Government ACCIÓ Website, and in the European Enterprise Europe Network.



Antonio J. Guerra, Roca, A., Joaquim Ciurana. “A Novel 3D Additive Manufacturing Machine To Biodegradable Stents”. 2017, 13, 718-723. Procedia Manufacturing.



Available online at www.sciencedirect.com

ScienceDirect

Procedia Manufacturing 13 (2017) 718–723

Procedia
MANUFACTURING

www.elsevier.com/locate/procedia

Manufacturing Engineering Society International Conference 2017, MESIC 2017, 28-30 June
2017, Vigo (Pontevedra), Spain

A novel 3D additive manufacturing machine to biodegradable stents

A. Guerra, A. Roca, J. de Ciurana

Department of Mechanical Engineering and Industrial Construction, University of Girona, Maria Aurèlia Capmany 61, Girona 17003, Spain

Abstract

Biodegradable stents offer the potential to improve long-term patency rates by providing support just long enough for the artery to heal. However, design a biodegradable structure for an intended period of support is rather difficult. Nowadays in the stent industry the manufacture process par excellence is the laser micro cutting. Nevertheless in the case of polymeric stents, the 3D additive manufacturing techniques could be a more economical solution.

This work aim to design and implement a novel 3D Additive Manufacturing Machine to Biodegradable Stent Manufacture. The effects of nozzle temperature, fluid flow, and printing speed over the polycaprolactone stent's precision is studied. Results have shown the strong influence of temperature and flow rate over the printing precision. Printing speed did not had a clear tendency. The results allow us to believe that the novel technology presented in this paper will be an interesting future research line.

© 2017 The Authors. Published by Elsevier B.V.

Peer-review under responsibility of the scientific committee of the Manufacturing Engineering Society International Conference 2017.

Keywords: Additive Manufacturing, Cylindrical, 3D Printing, Biodegradable Stent, Polymer

1. Introduction

Although metallic stents are effective in preventing acute occlusion and reducing late restenosis after coronary angioplasty, many concern still remain. The role of stenting is temporary and is limited to the intervention and shortly thereafter, until healing and re-endothelialization are obtained. Bioresorbable stents (BRS) were introduced to overcome these limitations with important advantages: complete bioresorption, mechanical flexibility, does not produce imaging artefacts in non-invasive imaging modalities, etc. [1]

Biodegradable stents offer the potential to improve long-term patency rates by providing support just long enough for the artery to heal, offering the potential to establish a vibrant market. However, design a biodegradable structure for an intended period of support is rather difficult. Nowadays in the stent industry the manufacture process par

excellence is the laser micro cutting. Nevertheless in the case of polymeric stents, the 3D additive manufacturing techniques could be a more economical solution [2].

Recently, three-dimensional (3D) printing, a specific technique in the biomedical field, has emerged as an alternative system for producing biomaterials. The 3D printing system, applied to rapid prototyping in structural fabrication can easily manufacture biomaterials, such as BRS, better than other devices. Additionally, 3D-printing offers a more efficient process for assembling all of the necessary components, such as the vascular artificial scaffold. For the past decade, biomedical stents have received much attention for their prevention of coronary thrombosis. Conventionally used BMS, such as stainless steel and titanium, can cause after effects, as they remain in situ even after vascular repair. Thus, there is a need for residue-free alternatives [2].

Some authors have been focused their research in the field of stent manufacture. Stepak et al. [3] presented the impact of the KrF excimer laser irradiation above the ablation threshold on physicochemical properties of biodegradable PLLA. It could be concluded that usage of the 248 nm wavelength resulted in simultaneous ablation at the surface and photo degradation within the entire irradiated volume due to high penetration depth. Stepak et al. [4] fabricated a polymer-based biodegradable stent using a CO₂ laser.

Nevertheless, with the best author's knowledge, the use of cylindrical 3D printing for stent purpose have been never reported before. This work aim to design and implement a novel 3D Additive Manufacturing Machine to Biodegradable Stent Manufacture. The effects of nozzle temperature, fluid flow, and printing speed over the stent's precision is studied and compared with the laser cutting technology.

2. Material and method

2.1. 3D Printer machine

The 3D Additive Manufacturing Machine developed is based in the Fused Filament Fabrication (FFF) and the 3-axis 3D printing technologies. The filament is melted into the extruder nozzle, which deposited the material onto a heated computer-controlled rotatory Cartesian platform (Fig. 1). The machine developed is based in the Fused Filament Fabrication (FFF) method and the 3-axis 3D printing technology. The filament is melted into the extruder nozzle, which deposited the material onto a computer-controlled rotatory platform. The machine provides a precision of 0.9375 μm in the X axis, 0.028125° in the W axis, 0.3125 in the Z axis, and 0.028125° in the extruder. The nozzle provides 0.4 mm of diameter.

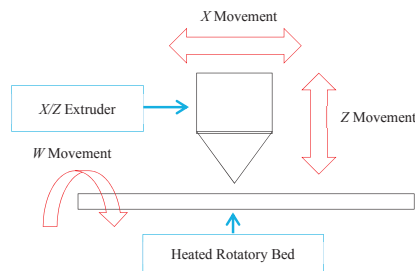


Fig. 1. 3D Machine methodology.

2.2. Material and geometry

Polycaprolactone (PCL) Capa 6500® supplied by Perstorp was used as material. PCL is a biodegradable polyester with a low melting point (60°C) and a glass transition of -60°C. PCL degradation is produced by hydrolysis of its ester linkages in physiological conditions and has therefore received a great deal of attention for using it as an implantable biomaterial, such stents, because of their properties (Table 1).

Table 1. Polycaprolactone (PCL) Capa 6500 properties.

Molecular Weight	Young Modulus	Strain at Break	Degradation Time
50000 g/mol	470 MPa	700 %	> 24 Months

The stent model used for the experiments was a diamond-cells stent. The stent parameters were the following: inner diameter (I_0), stent thickness (S_T), number of circumferential cells (N_C), width and length of the cell (W_C , L_C), strut width (S_W) (Fig. 2). These parameters determine the behavior of the stent, the correct adjustment of them is crucial for calibrating the stent to the particular needs of each patient.

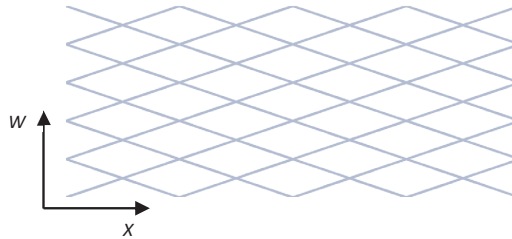


Fig. 2. Experiment geometry.

2.3. Design of experiment

Screening experiment were carried out to find the correct process parameters level to achieve a complete stents. The process parameter studied were; of nozzle temperature (N_T^{a} : 80/250°C), fluid flow rate (FR%: 75/200%), printing speed (PS: 200/1440 mm/min). Based on the screening results we selected the experiment parameters (Table 2).

Table 2. Design of experiments.

Parameter	Low Level	High Level
Printer Speed (mm/min)	480	880
Printer Temperature (°C)	200	250
Fluid Flow Rate (%)	100	200

2.4. Characterization

Dimensional features (S_T , W_C , L_C , and S_W) of each of the 60 samples were analyzed by the Optical Microscope Nikon SMZ – 745T attached to a digital camera CT3 ProgRes. Image J® was used to process the images and collect the data. Micrometer Micromar 40EWW was used to measure S_T .

3. Results and discussion

The results have shown the strong influence of flow rate and temperature over the strut width while speed did not had a clear tendency. Temperature results have showed the influence over the dimensional features. At highest temperatures, the viscosity decreases according to the equation below [5]:

$$\mu(T) = \mu_0 \exp(-bT) \quad (1)$$

Where T is the temperature and μ_0 and b are coefficients. That fact makes that PCL flow better by the nozzle which originates a mayor strut width (Fig. 3a).

The effect of the speed did not show a clear tendency (Fig. 3b). It seems that the combinations of speed-flow (Fig. 4a) or speed-temperature (Fig. 4b) are influential. The printing speed affect over the material accumulations and the axis micro-vibrations. At higher speeds the filament flows faster through the nozzle, acquiring more inertia and reducing the filament torsion when it is deposited on the bed of the printer. The increase of printing speed also derives in a reduction of PCLs cooling rate, the heated nozzle leaves faster the printer-off point and heat can be dissipated more effectively. This fact will change the material properties.

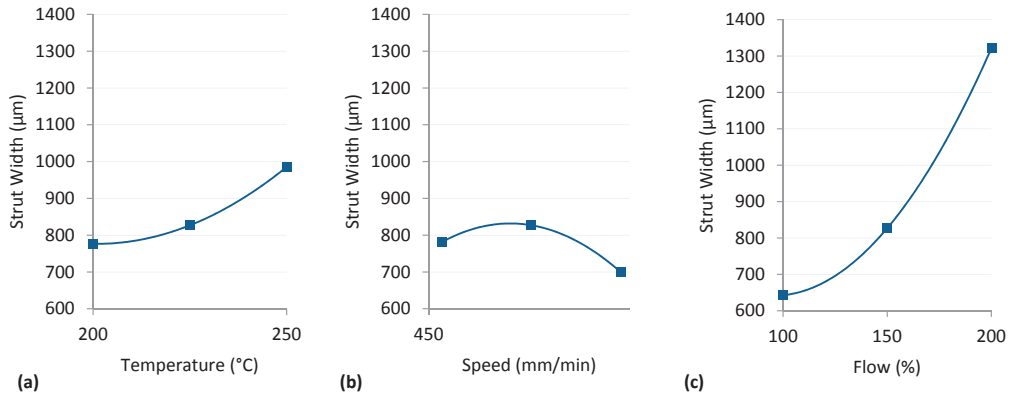


Fig. 3. Main effect plot for strut width (a) Temperature effects; (b) Printer speed effects; (c) Fluid flow rate effects.

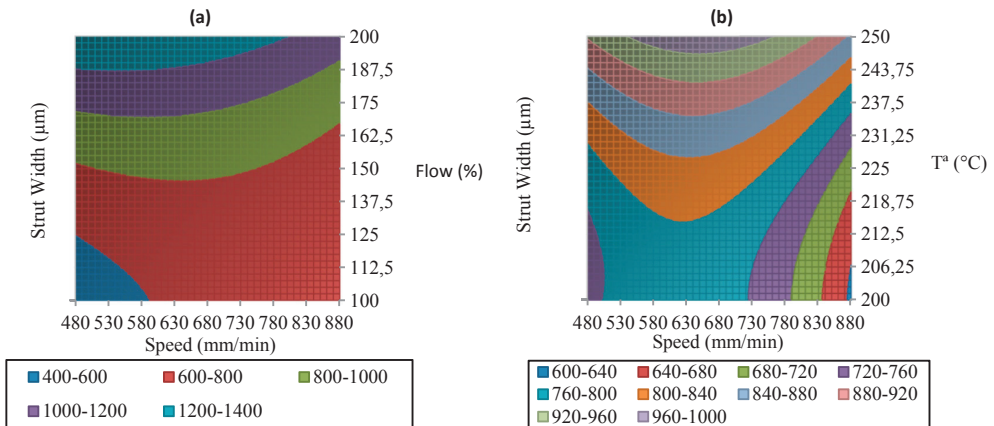


Fig. 4. Surface plots (a) Printer speed vs fluid flow rate; (b) Printer speed vs printer T^a .

Regards to the flow rate, has shown a growth nearly linear behavior of the strut width according to it increases. It is observed that the stents printed with highest flow rates had a top flat face (Fig. 5). This fact is due to an excessive stream of material thus squashing the filament as the nozzle is moving, increasing its diameter (Fig. 3c).

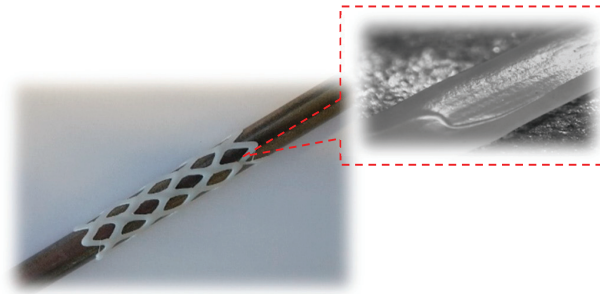


Fig. 5. Effect of the over fluid flow rate over the stent's top face.

Furthermore, the area results have been corroborated the previous results. As is to be expected, when the filament diameter increases the area gets smaller (Fig. 6 and Fig. 7).

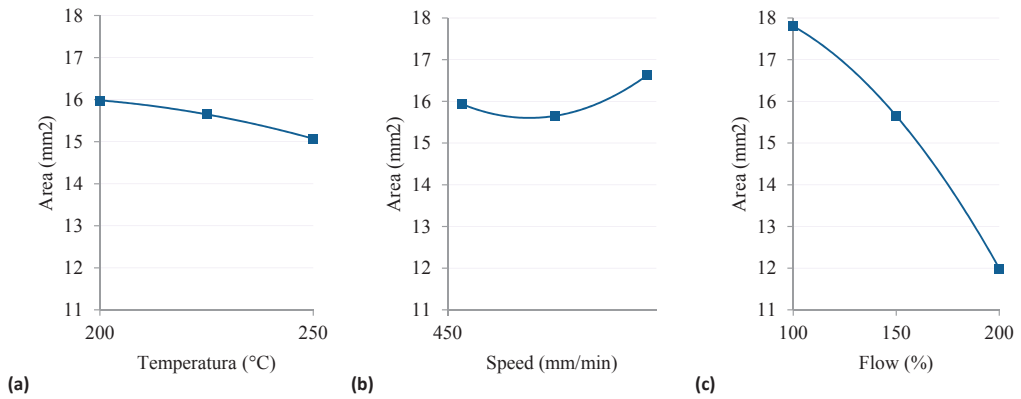


Fig. 6. Main effect plot for area (a) Printer T³ effects; (b) Printer speed effects; (c) Fluid flow rate effects.

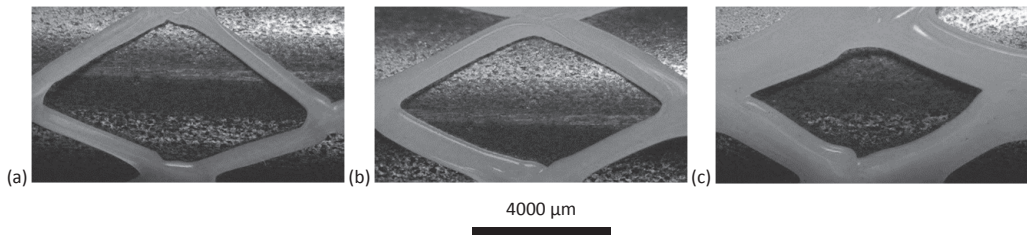


Fig. 7. Optical images of printer samples (a) 100 % Fluid flow rate; (b) 150% Fluid flow rate; (c) 200 % Fluid flow rate.

4. Conclusion

This work has demonstrated the feasibility of cylindrical 3D printing technology to the polymer stent manufacture. The effect of temperature, printing speed, and polymer flow rate have been reported. The strong influence of temperature and flow rate over the printing precision has been shown. The potential of cylindrical 3D printing on the micro medical devices manufacture, such as stents, have been introduced. Further studies about the effect of other printing parameters, materials, etc., would be interesting. The results allow us to believe that the novel technology presented in this paper will be an interesting future research line.

Acknowledgements

The authors acknowledge the financial support from Ministry of Economy and Competitiveness (MINECO), Spain for its PhD scholarship and grants from DPI2013-45201-P and University of Girona (UdG), Spain MPCUdG2016/036.

References

- [1] E. Tenekecioglu, C. Bourantas, M. Abdelghani, Y. Zeng, R. C. Silva, H. Tateishi, Y. Sotomi, Y. Onuma, M. Yılmaz, P. W. Serruys, *Expert Rev. Med. Devices*. 13-3 (2016) 271–286.
- [2] S. a. Park, S. J. Lee, K. S. Lim, I. H. Bae, J. H. Lee, W. D. Kim, M. H. Jeong, J. K. Park, *Mater. Lett.* 141 (2015) 355–358.
- [3] B. D. Stepak, A. J. Antończak, K. Szustakiewicz, P. E. Koziol, K. M. Abramski, *Polym. Degrad. Stab.* 110 (2014) 156–164.
- [4] B. Stepak, a. J. Antończak, M. Bartkowiak-Jowska, J. Filipiak, C. Pezowicz, K. M. Abramski, *Arch. Civ. Mech. Eng.* 14-2 (2014) 317–326.
- [5] Reynolds O, *Phil. Trans. Royal Soc. London*. 177 (1886) 157.

Chapter 8

Effect of Printing Process on PCL Stent

Abstract

Previous results have demonstrated that Tubular 3D Printing is able to produce BRS in a easy way. Nevertheless a deep analysis on the printing process is necessary.

Chapter 8 presents the effects of printing process parameters over the physical features of a real polycaprolactone stent.

The effects of printing nozzle temperature, printing flow rate, printing speed, and printing trajectories over polycaprolactone's stents were studied. Printed samples were analysed by Optical Microscopy, Differential Scanning Calorimetry (DSC), and Radial Expansion Test in order to study the effects the printing parameters have over their dimensional precision, material structure distribution, and radial behaviour, respectively.

Results showed the strong influence of printing temperature and printing flow rate over the dimensional precision, in which printing speed did not show any influence. Printing parameters has not exhibited a significant influence over the materials structure. The samples show a good radial behaviour with an average expansion ratio of 320% and around 22% of recoil ratio.

This chapter had been published in the Journal Procedia Manufacturing (Under Journal Guidelines).



Antonio J. Guerra, Joaquim Ciurana. “3D-Printed Bioabsorbable Polycaprolactone Stent: The Effect Of Process Parameters On Its Physical Features”. **2018**, 137, 430–437. Material and Design.



3D-printed bioabsorbable polycaprolactone stent: The effect of process parameters on its physical features



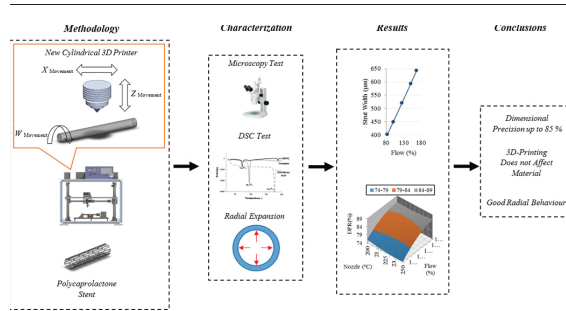
Antonio J. Guerra, Joaquim Ciurana *

Department of Mechanical Engineering and Civil Construction, Universitat de Girona, Maria Aurèlia Capmany, 61, 17003 Girona, Spain

HIGHLIGHTS

- A novel 3D Additive Manufacturing Machine to bioabsorbable polymeric stents is presented.
- The 3D-printing process has leave strong effects over the dimensional precision.
- The 3D-printing process has leave lesser effects over the material structure.
- 3D-printed stents have shown good radial behaviour (320% of expansion and a 22.78% of recoil).

GRAPHICAL ABSTRACT



ARTICLE INFO

Article history:

Received 10 June 2017
 Received in revised form 11 October 2017
 Accepted 14 October 2017
 Available online 16 October 2017

Keywords:

Additive manufacturing
 3D printing
 Biodegradable stent
 Polymer

ABSTRACT

Biodegradable stents (BRS) offer the potential to improve long-term patency rates by providing support just long enough for the artery to heal. However, manufacture BRS is rather difficult. Nowadays 3D additive manufacturing could be an interesting manufacturing method to produce BRS. In this context, this work presents a novel 3D Additive Manufacturing Machine to be used to manufacture BRSs based on polymers and discusses the effect the process parameters have on the physical features of the BRS.

The printing nozzle temperature, flow rate, speed, and trajectories effects on polycaprolactone stents were studied. Printed samples were analysed using Optical Microscopy, Differential Scanning Calorimetry (DSC), and the Radial Expansion Test to study the effects printing parameters have on their dimensional precision, material structure distribution, and radial behaviour, respectively. Results showed that the dimensional precision of a BRS is strongly influenced by printing temperature and flow rate, although printing speed did not exert any influence. Printing parameters did not significantly influence the structure of the materials. Furthermore, the samples, with an average expansion ratio of 320% and around 22% of recoil ratio, showed good radial behaviour.

© 2017 Elsevier Ltd. All rights reserved.

1. Introduction

Conventionally used bare metal stents such as stainless steel and titanium, can cause after-effects because they remain in situ even after

vascular repair [1]. The role of stenting is temporary and is limited to the intervention and shortly thereafter, i.e., until healing and re-endothelialization are obtained. Bioresorbable stents (BRS) were introduced to overcome these limitations and exhibit some significant advantages such as, among others, complete bioresorption, mechanical flexibility or not producing imaging artefacts in non-invasive imaging modalities [2]. BRS offer the potential to improve long-term patency rates by providing support just long enough for the artery to heal,

* Corresponding author.

E-mail addresses: antonio.guerra@udg.edu (A.J. Guerra), quim.ciurana@udg.edu (J. Ciurana).

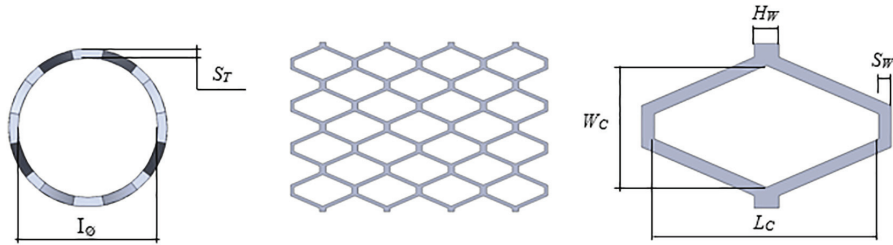


Fig. 1. Stent geometry.

offering the potential to establish a vibrant market and the focus of many research lines. Hideo Tamai et al. [3] evaluated the feasibility, safety, and efficacy of the poly-L-lactic acid (PLLA) stent in humans. Fifteen patients electively had Igaki-Tamai PLLA stent implantations for coronary artery stenosis. Shen et al. [4] studied the degradation of L-lactide (LA) and 5-methyl-5-benzoyloxycarbonyl-1,3-dioxan-2-one (MBC) coated stents and cast films through gel permeation chromatography (GPC), weight loss, light microscopy, scanning electron microscopy (SEM), and immunohistochemical staining in vitro and in vivo tissue. Their work demonstrated similar degradation behaviour of the coating material in vivo conditions. There were no significant differences in extensive endothelialization or the expression of inflammation-associated proteins such as monocyte chemoattractant protein-1 (MCP-1), interleukin-6 (IL-6), and CD3 four weeks after stent implantation. Therefore, the heparin-immobilized copolymer is an excellent candidate material for drug-eluting stents given its lack of permanent existence after drug release and minimal in vivo tissue responses. Kim et al. [5] studied the tissue response to the PLLA/PMB30W blend used for BRS stent purposes. Six months into the study, the samples maintained high density of PMB30W without significant bioabsorption, which let them to conclude that the PMB30W was able to reduce tissue responses. Azaouzi et al. [6] optimized the self-expanding Nitinol stent by employing finite element analysis (FEA). Recently, Guerra et al. [7] studied the effect fibre laser processes have on the degradation rate of polycaprolactone. Employing a novel degradation system that simulated the blood flow in the body, they concluded that fibre laser process has a lesser effect on the degradation rate. Nevertheless, the novel degradation system employed revealed that polycaprolactone will degrade faster in body conditions than the traditional literature data have reported to date.

Although the mechanical and medical properties of the materials are important, finding the best manufacturing process for this kind of material has to be considered as well. Nowadays, the traditional manufacturing process in the stent industry is laser micro cutting, and has been the focus of numerous research projects in the past decades. Demir et al. [8] manufactured CoCr stents using selective laser melting (SLM) as an alternative to the traditional laser micro cutting. Because of the selective laser process, samples needed to be polished electrochemically to achieve a good surface finish. Physical and chemical analysis results showed that SLM can be considered as an adequate manufacturing technique for stents. In 2008 Tiaw et al. [9] studied the effect of Nd:YAG laser on micro-drilling and micro-cutting of thin PCL films. The melting and tearing of the thin polymer film were not much of an issue for the thin spin-cast film, but a slight extent of melting was observed in the thickest biaxial drawn film. Choudhury and Shirley [10] employed a CO₂ laser to cut three polymeric materials (PP, PC and

PMMA) and developed a model equation relating input laser cutting process parameters with the output. In 2013 Schneider and Petring [11] employed a high power laser to cut fibre reinforced thermoplastic polymers using continuous and pulsed wavelengths. The result shows that HAZ could be significantly reduced with multi-pass processing at high processing cutting speed. Stepak et al. [12] fabricated a polymer-based biodegradable stent using a CO₂ laser, meanwhile Genna et al. [13] assessed a simple procedure to determine the rates of absorbed, reflected, transmitted and scattered energy in the case of an unfilled High Density Polyethylene (HDPE) plate. Their results showed that about 47% of power was lost when employing a 975 nm laser. Demir et al. [8] used selective laser melting (SLM) to manufacture a CoCr stent. Their work proved SLM is feasible for stents based on metallic materials. Guerra et al. [14] demonstrated the feasibility of 1.8 μm wavelength fibre lasers to cut polycaprolactone sheet with greater precisions. The process barely affected the material properties.

However, laser processing is a thermal process which results in some thermal damage, such as heat affected zones, striations, recast layers, micro cracks, tensile residuals, and dross deposition. To overcome these problems, a series of subsequent techniques must be applied which, in turn, raises the cost of manufacture. The stent industry needs to make continuous advances towards reducing the costs and the problems of this medical device by developing new technologies. In this context, 3D Additive Manufacturing techniques could be a more economical solution. Recently, three-dimensional (3D) printing has emerged as an alternative system for producing polymeric devices for medical applications. Carneiro et al. [15] studied the potential of polypropylene (PP) for 3D printing technique. They compared the 3D printed samples with samples produced by compression moulding. Their results showed PP's potential for 3D printing manufacture. Abdullah et al. [16] studied the feasibility of 3D printing for manufacturing highly ceramic filled polyamide for craniofacial reconstruction, but the mechanical properties achieved were lower than expected. The 3D printing system can easily manufacture biomaterials, making it a more efficient process. Park et al. [1] evaluated the properties of a 3D-printed drug coated BRS stent in animals and their results were promising. Habibovic et al. [17] employed low-temperature 3D printing to produce brushite and monetite implants. Yang et al. [18] grafted a quaternized chitosan to 3D printed scaffolds in order to design a bone engineering scaffold with antibacterial and osteoconductive properties. To the best of this author's knowledge, the study of 3D printing process parameters for stent manufacture has never before been reported. To manufacture BRSs that will fulfil this medical device's requirements nowadays, new machines and methods based on polymers need to be developed.

Table 1
Stent model parameters.

I_0	S_T	N_C	W_C	L_C	S_W	H_W
5 mm	0.2 mm	8	0.80 mm	5.40 mm	0.4 mm	0.8 mm

Table 2
Polycaprolactone (PCL) CAPA 6500® properties.

Molecular weight	Melting temperature	H ₂ O content	Yield stress	Young modulus	Strain at break	Degradation time
50,000 g/mol	60 °C	<1%	17.5 MPa	470 MPa	>700%	>24 months

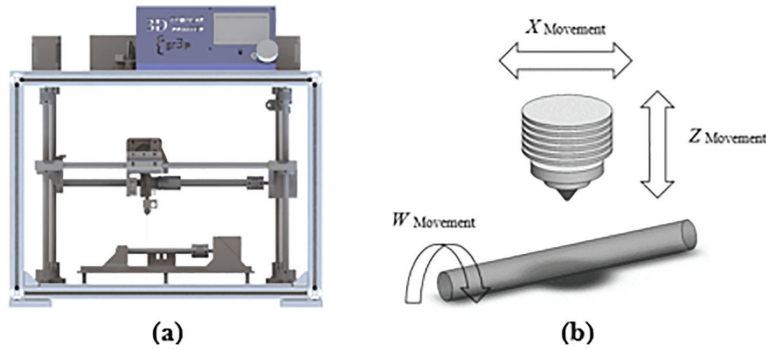


Fig. 2. (a) 3D tubular printer machine (b) machine methodology.

Thus, this work presents a novel 3D Additive Manufacturing Machine to produce BRSs based on polymers and discusses the effect the process parameters have on the physical features of the BRS. The effects nozzle temperature, fluid flow rate, printing speed, and printing trajectory strategies have on the stent's features is presented. Printed samples were analysed using *Optical Microscopy*, *Differential Scanning Calorimetry (DSC)*, and the *Radial Expansion Test* to study the effects printing parameters have on their dimensional precision, material structure distribution, and radial behaviour, respectively. Also presented here is a dimensional prediction model designed to optimize the printing process and achieve greater dimensional precision results.

2. Material and methods

2.1. Stent model

The stent model used for the experiments was a tube-based stent with closed diamond-shaped cells with the following parameters: inner diameter (I_{θ}), stent thickness (S_T), number of circumferential cells (N_C), width and length of the cell (W_C , L_C), strut width (S_W), and hinge widths (H_W), (Fig. 1). These parameters determine the behaviour of the stent, so the correct adjustment of them is crucial to calibrate the stent to the particular needs of each patient [19].

As the aim of this present work is to analyse the manufacturing process using 3D printing, the parameters were kept constant (Table 1).

2.2. Materials

Polycaprolactone (PCL) CAPA 6500® supplied by Perstorp was used as the material (Table 2). PCL is a biodegradable polyester with a low melting point (60 °C) and a glass transition of about -60 °C. Degradation is produced by hydrolysis of its ester linkages in physiological conditions and has, therefore, received a great deal of attention as a possible implantable biomaterial.

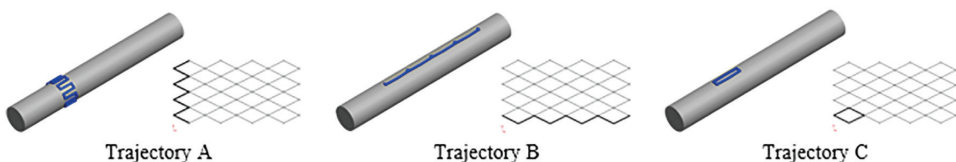


Fig. 3. Printing trajectories strategies.

2.3. Printer machine

The 3D Additive Manufacturing Machine developed is based on the Fused Filament Fabrication (FFF) and the 3-axis 3D printing technology. The filament is melted into the extruder, which deposits the material onto a computer-controlled rotatory platform. The machine provides a precision of $0.9375 \mu\text{m}$ on the X axis, 0.028125° on the W axis, 0.3125 on the Z axis, and 0.028125° in the extruder. The nozzle is 0.4 mm in diameter (Fig. 2).

2.4. Design of experiments (DOE)

Screening experiments were carried out to find the correct process parameter levels to produce complete stents. The following process parameters were studied: nozzle temperature (N_T : 80/250 °C), fluid flow rate (F_{RK} : 75/150%), printing speed (P_S : 480/1440 mm/min), and the printing trajectory strategies (P_T : A/C). A Matlab® script was written to generate the G Code for the machine (Fig. 3). Trajectory A along the W axis, trajectory B along the X axis, and trajectory C completing diamond cells.

Based on the screening results the printing process parameters were selected. Trajectory A was selected because it was the only one capable of completing the stent uniformly. Employing a *Central Composite Design (CCD)* DOE with 6 centre points* and alpha 1.682, (3 replicas) 60 samples were printed (Table 3).

2.5. Characterization

2.5.1. Dimensional features

The dimensional features (S_T , W_C , L_C , S_W , and H_W) of each of the 60 samples were analysed with an Optical Microscope Nikon SMZ – 745T attached to the digital microscope camera CT3 ProgRes. Image J® was used to process the images and collect the data. A Micrometre Micromar 40EWW digital micrometre was used to measure S_T . The dimensional data were averaged and compared with the CAD designed dimensions. By calculating the deviation as a percent difference,

Table 3
CCD design of experiment.

Sample	1	2	3	4	5	6	7	8	9	10	11	12	13	14	15*	16*	17*	18*	19*	20*
N _T	200	200	200	200	250	250	250	250	182	267	225	225	225	225	225	225	225	225	225	225
F _{R%}	100	100	150	150	100	100	150	150	125	125	83	167	125	125	125	125	125	125	125	125
P _S	480	960	480	960	480	960	480	960	720	720	720	720	316	1123	720	720	720	720	720	720

the dimensional precision ratio (DPR) was defined to quantify the distortion as follows:

$$D_{\%}(p) = 100 - \left| 100 - \frac{p \cdot 100}{p_{CAD}} \right| \tag{1}$$

$$DPR = \bar{X}(D_{\%}(S_T), D_{\%}(W_C), D_{\%}(W_L), D_{\%}(S_W), D_{\%}(H_W)) \tag{2}$$

where $D_{\%}(p)$ is the dimensional precision of each stent's parameters (S_T , C_W , etc.), p is the parameter measured by Optical Microscopy, and p_{CAD} is the CAD designed dimension.

2.5.2. Material structure

Changes in the structure of the material were measured using *Differential Scanning Calorimetry (DSC)* following the conditions summarised in **Table 4**. Measurements were performed with a Q2000 *Differential Scanning Calorimeter*.

2.5.3. Radial behaviour

Samples were expanded radially from their original diameter (O_{θ}) until their maximum diameter (M_{θ}) was achieved. Next, the radial forces applied were removed and the diameter's measurement was then taken to determine the recoil ratio (R_{θ}).

3. Results & discussion

The experimental results for the quality factors are presented. The *analysis of variance (ANOVA)* method was applied to test the statistical significance of the process's parameters (N_T , $F_{R\%}$ and P_S) for the dimensional quality factors (S_T , W_C , L_C , S_W , H_W). The analysis was carried out at a 95% confidence level ($\alpha = 0.05$) and shown (parameter denoted as *) in results when significance is reached.

DSC tests were carried out for all 60 samples. Finally, the *Radial Expansion Tests* were carried out to connect the dimensional features and the material's structural features with the radial expansion behaviour of the samples.

3.1. Stent thickness

S_T showed a uniform behaviour for all DOE configurations. This is caused by the stand-off distance between the nozzle and cylindrical bed surface. Since it is constant, the stent thickness remains almost constant and it is only modified by the amount of material that the nozzle expels; a parameter that depends directly on the $F_{R\%}$ and N_T (Fig. 4.a and b).

As *polycaprolactone's* viscosity is inversely proportional to its temperature, the N_T affects the material's ability to spread along the cylindrical surface, thus reducing the S_T , but increasing the S_W and

H_W . For S_T , the $F_{R\%}$, with its linear behaviour, has demonstrated its strong influence, while, P_S has exhibited a low influence (Fig. 4.c).

S_T is mainly responsible for the stiffness of the stent [20]. According to [21], the stent's thickness influences the stresses within a vessel. The stresses induced in the vessel on unloading, particularly in the intima, may act as a chronic stimulus for cell proliferation where the artery attempts to lower these stresses by vessel thickening. The lower lumen gain, but lower acute and chronic stresses, in the thinner strut stented vessel may ultimately result in less injury and a less aggressive healing response. Expansion of the thinner strut stent to a higher diameter to achieve the same final maximum stent diameter as the thicker strut stent results in considerably higher acute stresses at loading, however, at unloading the thicker strut stent induces 23% higher intimal stresses. Clearly, therefore, many stent designs, even thick-strut stents, could potentially offer a solution to restenosis if the optimum expansion diameter was considered such that stresses in the vessel were kept low. Several clinical trials have identified S_T as an independent predictor of restenosis [22–24], concluding that stents with thinner walls have a lower restenosis rate. Achieving a different thickness in a stent is very simple with 3DP since this parameter is controlled by the stand-off distance between the nozzle and the cylindrical bed surface, as well as the number of layers.

3.2. Cell width & cell length

C_W , has been mainly affected by $F_{R\%}$ and N_T (Fig. 5.d and e), while C_L is only affected by $F_{R\%}$ (Fig. 5.f). Once again, the combination of $F_{R\%}$ and N_T affects the ability of *polycaprolactone* to spread along the bed, raising the S_W and, consequently, affecting the cell geometry.

Despite having programmed a defined corner (Fig. 1), the fluency of the *polycaprolactone* at experiment temperatures meant that the cell geometry presented rounded corners (Fig. 5.a to c). This unexpected fact could be beneficial to the stenting procedure because rounded corners produce less damage to the vessel wall.

Puértolas et al. [19] demonstrated that it is possible to calibrate the stent's response by varying the C_L , which is one of the most flexible and effective design parameters of the stent.

3.3. Strut width & hinge width

S_W , and consequently H_W , have been affected by all the process parameters (Fig. 6.d to f). With average S_W of 519.822 μm and average H_W of 1039.64 μm , these quality parameters have been distanced 29.95% from the target. The S_W changes the contact pressure between the strut and the intimal surface [20]. The pressure, which occurs between the contact area of the stent struts and the intimal surface of the artery wall, is determinant for restenosis. Stent struts may cause deep vascular focal and endothelial cell denudation.

Both parameters are affected by all the process parameters, albeit $F_{R\%}$ being dominant. The correct adjustment of the 3DP process parameters to achieve a precise S_W and then a precise stent is crucial because of the effect S_W has on all the other dimensional features.

Although S_W and H_W have shown an error close to 30% from the target, both quality parameter shave exhibited excellent uniformity along all the stent geometry (Fig. 6.a to c), a highly important factor for the correct radial behaviour of the stent.

Table 4
DSC test conditions.

Initial temp.	Final temp.	Heating rate	Flowing gas N ₂	Pan material
25 °C	80 °C	10 °C/min	50 ml/min	Al

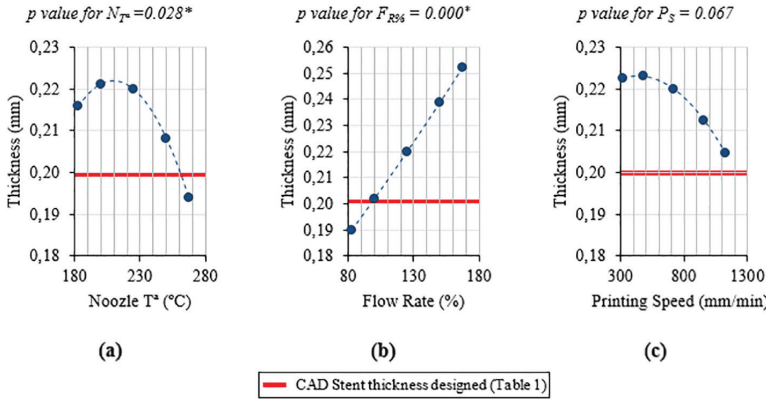


Fig. 4. Stent thickness main effect plot for (a) printing T* at 125% of flow rate and 720 mm/min of printing speed (b) flow rate at 225 °C of printing T* and 720 mm/min of printing speed (c) printing speed at 225 °C of printing T* and 125% of flow rate.

3.4. Average dimensional accuracy & prediction model

Employing Eqs. (1) and (2) described in Section 2.5.1, the average dimensional precision that the 3D printing process can reach was evaluated. With an average precision between 80% and 90% it can be concluded that 3D printing could be an efficient tool for stent manufacturing (Fig. 7). The 3D-surface plot shows the strong influence FR% has on the DDR.

Samples from the DOE central point (E15 to E20) have shown a uniform average precision, which demonstrates the stability of the 3DP process and its replicability. After the Regression Analysis was optimized by removing all of the not influenced parameters (p > 0.05), prediction model equations for all the dimensional quality factors were developed as follows:

$$S_T = 0.2186 - 0.0065N_{T^*} + 0.0185F_{R\%} - 0.0054P_S - 0.0052N_{T^*}^2 \quad (3)$$

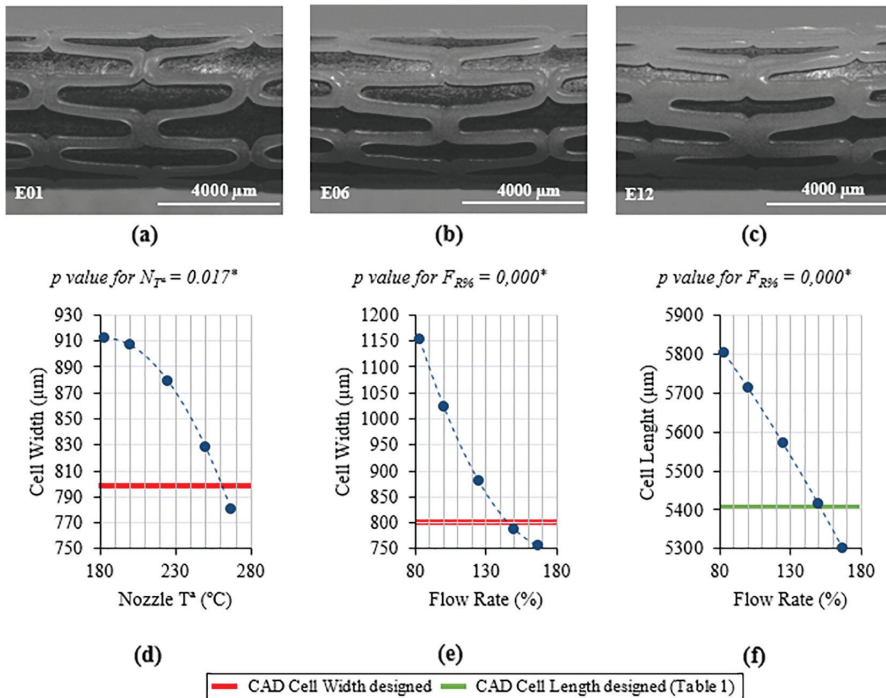


Fig. 5. Cell width and cell length results (a) stent printed at 200° of printing T*, 100% of flow rate, and 480 mm/min of printing speed (b) stent printed at 250° of printing T*, 100% of flow rate, and 960 mm/min of printing speed (c) stent printed at 225° of printing T*, 167.05% of flow rate, and 720 mm/min of printing speed. (d) Main effect plot for printing T* at 125% of flow rate and 720 mm/min of printing speed (e) main effect plot for flow rate at 225 °C of printing T* and 720 mm/min of printing speed (f) main effect plot for flow rate at 225 °C of printing T* and 720 mm/min of printing speed.

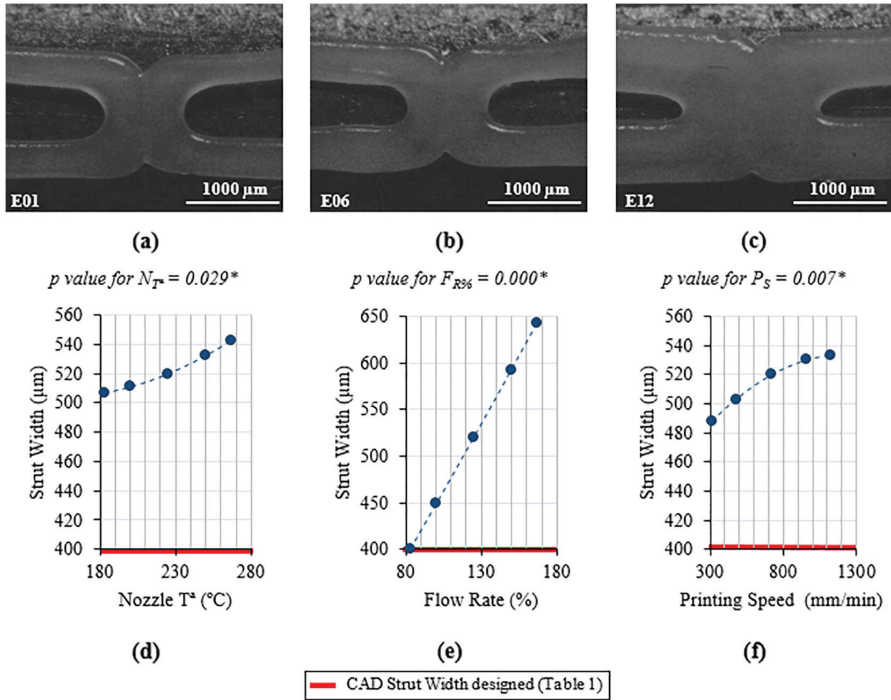


Fig. 6. Strut width and hinge width results (a) stent printed at 200 °C of printing T_p, 100% of flow rate, and 480 mm/min of printing speed (b) stent printed at 250 °C of printing T_p, 100% of flow rate, and 960 mm/min of printing speed (c) stent printed at 225 °C of printing T_p, 167.05% of flow rate, and 720 mm/min of printing speed. (d) Main effect plot for nozzle T_p at 125% of flow rate and 720 mm/min of printing speed (e) main effect plot for flow rate at 225 °C of printing T_p and 720 mm/min of printing speed (f) main effect plot for printing speed at 225 °C of printing T_p and 125% of flow rate.

The S_T equation shows its reliance on N_{T_p} and F_{R%}. Also, P_S has a lesser effect on this dimensional parameter.

$$C_W = 867.062 - 39.234N_{T_p} + 118.022F_{R\%} + 28.041F_{R\%}^2 \quad (4)$$

The C_W equation shows its reliance on N_{T_p} and F_{R%}.

$$C_L = 5573.52 - 149.703F_{R\%} \quad (5)$$

The C_L equation shows its reliance on F_{R%}.

$$S_W = 519.281 - 10.631N_{T_p} + 71.697F_{R\%} + 13.444P_S - 11.614N_{T_p}F_{R\%}P_S \quad (6)$$

The S_W equation shows its reliance on all process parameters and their combination

$$H_W = 2S_W \quad (7)$$

Lastly, H_W, defined by stent design (Section 2.1) as two times S_W, this parameter depends directly on the process parameters that affect the S_W dimensions.

These equations reveal the influence the process parameters have on the dimensional quality factors, and allow us to manufacture a stent with predicted dimensions.

Despite the gap that exists before achieving 100% precision, the prediction model allows us to believe that mayor precision could be reached. Because the 3DP process does not produce dross, heat affected

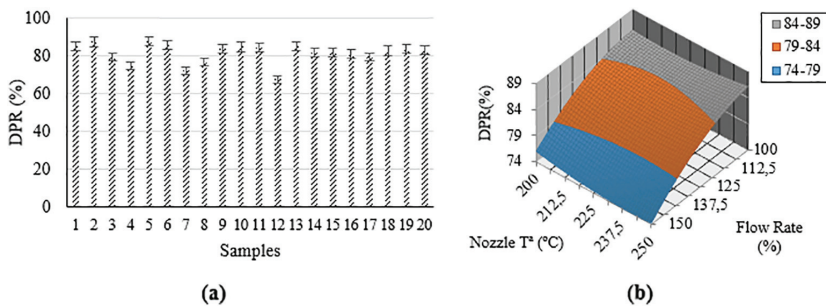


Fig. 7. Average dimensional accuracy results (a) Dimensional Precision Rate (DPR) of all 20 samples. (b) 3D-surface plot for printing T_p and flow rate at 720 mm/min of printing speed.

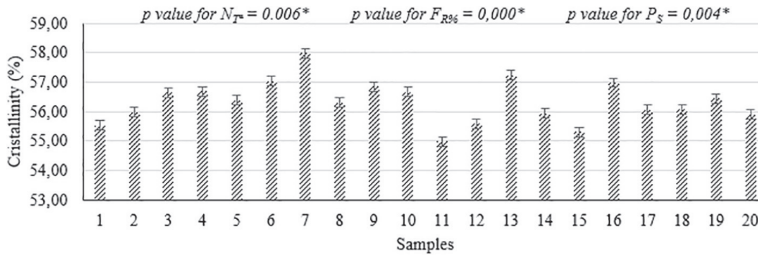


Fig. 8. Material structure results.

zones, recasts, or interior damage, etc., it is presented as an economical way to manufacture stents in just one step. The precision of the 3DP process could be improved by performing a calibration of the machine, and, above all, by studying the design of the extruder to achieve higher torque. Higher torque will allow the stents to be manufactured using lower temperatures.

3.5. Material structure

ANOVA results have shown the influence of all parameters, and their combination, over the crystallinity percentage of the samples. The material's structure depends directly on the cooling rate employed to manufacture the material, thus, N_T , $F_{R\%}$, and P_S affect this. The increase of N_T , $F_{R\%}$, combined with a reduction of P_S raises the material's temperature, reducing the stent's cooling rate. This allows for a better placement of the polymer chains which, in turn, increases the percentage of crystallinity. The degree of crystallinity and the morphology of the crystalline material have significant effects on the polymer's mechanical behaviour. Crystallinity of a polymer affects its mechanical strength and degradation rate. A higher degree of crystallinity means a lower free volume content (low porosity) leading to an increase in stiffness and material strength [25]. This will affect the degradation rates of samples, because if water molecules can diffuse into the polycaprolactone (high porosity) and hydrolyze the chains enabling the monomers or oligomers to diffuse out, erosion will occur gradually and equilibrium for this

diffusion–reaction phenomenon would be achieved. If this equilibrium is disturbed, the degradation mechanism could provoke internal autocatalysis [26].

The reduced effect that the 3DP process has on the material's structure (Fig. 8), makes 3DP a fast method to manufacture these medical devices because, unlike the post-processing methods required by other technologies (e.g. laser micro cutting) to recover the material's properties, these are unnecessary for 3DP. When manufacturing devices, and in order to save costs in post-processing technique, it is important to choose manufacturing processes that accomplish the dimensional precision requirements without adversely affecting the properties of the material.

3.6. Radial behaviour

With an average maximum expansion of 15.95 mm (320% of expansion) and an average recoil of 22.78%, all the samples showed good radial behaviour.

Regardless of the parameters of the 3DP process, all the samples (except E01, E05, E06, and E11) exhibited similar behaviour (Fig. 9.b). Samples E01, E05, E06, and E11 are characterized by their different dimensional features because they show a weaker structure than the other samples. Once again, the stability demonstrated by the six central samples prove the value of the 3DP process. All the samples showed a uniform radial expansion. The high flexibility of polycaprolactone

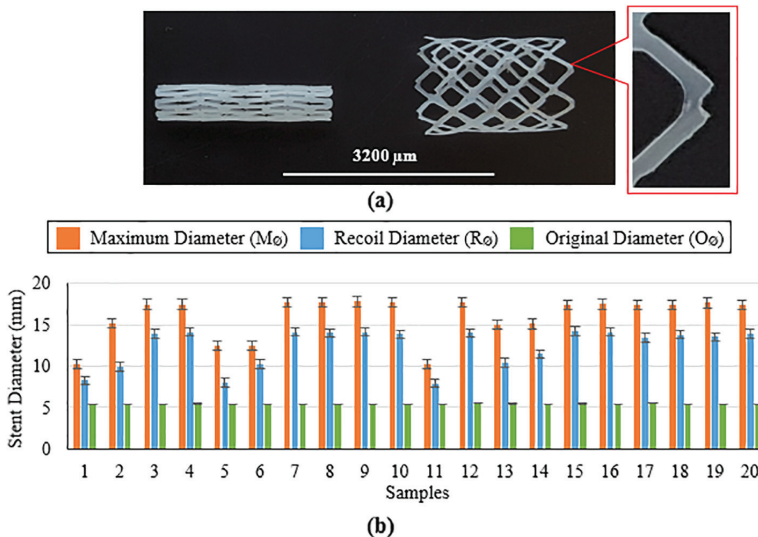


Fig. 9. Radial behaviour results (a) digital images before and after expansion (b) stent diameter results.

prevented the sudden break of the stent, which was commenced by a stretching of the strut width. This stretching mainly originated in the hinges between the longitudinal cells (Fig. 9.a). Narrower struts will cause a premature break of the sample, as in the samples E01, E05, E06, and E11. Radial expansion of the stent produces a longitudinal shrinking. The higher C_L is, the greater radial expansion. Therefore, the stent's radial response can be controlled by calibrating this parameter [19].

Analysing the relationship between radial expansion behaviour and material structure distribution, it can be concluded that the differences observed in the radial behaviour are related to dimensional aspects of samples and not to material structure distribution. Samples printed with an $F_{R\%}$ superior to 100% have presented higher radial expansion, because higher $F_{R\%}$ (the dimensional parameters responsible for radial stability) produces wider struts and hinges [19].

4. Conclusions

This work has demonstrated the feasibility of 3D printing technology to manufacture stents from polymeric materials.

The effect of nozzle temperature, printing speed, printing flow rate, and printing trajectories have been reported and related to the dimensional precision and material structure distribution of the samples. Printing temperature and printing flow rate have been shown to have a strong influence over the dimensional precision of the printing process. Despite the gap that exists to achieving 100% precision, the prediction model developed allows us to believe that mayor precision could be reached. The precision of the 3DP process could be improved by calibrating the machine and, above all, studying the design of the extruder to achieve higher torque. Higher torque will allow the stents to be manufactured at lower temperatures.

The 3D printing process leaves smaller effects on the structure of the material, which is an important fact to save post-processing method costs. Regardless of the printing process's parameters, stents have, with an average of 320% of radial expansion and an average of 22.78% of recoil, shown good radial behaviour. The small differences in the material structure distribution corroborate that the differences in the radial expansion behaviour of the samples are produced by the geometrical aspects of the stents.

The potential 3D printing has for micro medical device manufacture has been introduced. The results allow us to believe that the novel technology presented in this paper will be an interesting line of future research and, because the 3DP process does not produce dross, heat affected zones, recast, interior damages, etc., and because it is a one-step process, it will reduce stent manufacturing costs and make the process much more economical.

Acknowledgements

The authors acknowledge the financial support from the MPCUdG2016/036 grant from the University of Girona (UdG), Spain, and the PhD scholarship and DPI2013-45201-P grant from the Ministry of Economy and Competitiveness (MINECO), Spain.

References

- [1] S.A. Park, S.J. Lee, K.S. Lim, I.H. Bae, J.H. Lee, W.D. Kim, M.H. Jeong, J.K. Park, In vivo evaluation and characterization of a bio-absorbable drug-coated stent fabricated using a 3D-printing system, *Mater. Lett.* 141 (2015) 355–358.

- [2] E. Tenekecioglu, C. Bourantas, M. Abdelghani, Y. Zeng, R.C. Silva, H. Tateishi, Y. Sotomi, Y. Onuma, M. Yilmaz, P.W. Serruys, From drug eluting stents to bioresorbable scaffolds; to new horizons in PCI, *Expert Rev. Med. Devices* 13 (3) (2016) 271–286.
- [3] H. Tamai, K. Igaki, E. Kyo, K. Kosuga, A. Kawashima, S. Matsui, H. Komori, T. Tsuji, S. Motohara, H. Uehata, Initial and 6-month results of biodegradable poly-L-lactic acid coronary stents in humans, *Circulation* 102 (4) (2000) 399–404.
- [4] L. Shen, Z. Li, F. Gong, F. Zhang, Q. Qin, S. Cheng, J. Ge, Characterization of tissue responses and degradation behavior of heparin-immobilized copolymer for drug-eluting stents, *Polym. Degrad. Stab.* 98 (5) (2013) 1015–1021.
- [5] H. II Kim, K. Ishihara, S. Lee, J.H. Seo, H.Y. Kim, D. Suh, M.U. Kim, T. Konno, M. Takai, J.S. Seo, Tissue response to poly(L-lactic acid)-based blend with phospholipid polymer for biodegradable cardiovascular stents, *Biomaterials* 32 (9) (2011) 2241–2247.
- [6] M. Azaouzi, N. Lebaal, A. Makradi, S. Belouettar, Optimization based simulation of self-expanding nitinol stent, *Mater. Des.* 50 (2013) 917–928.
- [7] A.J. Guerra, J. Ciurana, Effect of fibre laser process on in-vitro degradation rate of a polycaprolactone stent a novel degradation study method, *Polym. Degrad. Stab.* (2017).
- [8] A.G. Demir, B. Previtali, Additive manufacturing of cardiovascular CoCr stents by selective laser melting, *Mater. Des.* 119 (2017) 338–350.
- [9] K.S. Tiaw, M.H. Hong, S.H. Teoh, Precision laser micro-processing of polymers, *J. Alloys Compd.* 449 (1–2) (2008) 228–231.
- [10] I.A. Choudhury, S. Shirley, Laser cutting of polymeric materials: an experimental investigation, *Opt. Laser Technol.* 42 (3) (2010) 503–508.
- [11] F. Schneider, N. Wolf, D. Petring, High power laser cutting of fiber reinforced thermoplastic polymers with cw- and pulsed lasers, *Phys. Procedia* 41 (2013) 415–420.
- [12] B. Stepak, A.J. Antończak, M. Bartkowiak-Jowska, J. Filipiak, C. Pezowicz, K.M. Abramski, Fabrication of a polymer-based biodegradable stent using a CO₂ laser, *Arch. Civ. Mech. Eng.* 14 (2) (2014) 317–326.
- [13] S. Genna, C. Leone, V. Tagliiferri, Characterization of laser beam transmission through a High Density Polyethylene (HDPE) plate, *Opt. Laser Technol.* 88 (2017) 61–67.
- [14] A.J. Guerra, J. Farjas, J. Ciurana, Fibre laser cutting of polycaprolactone sheet for stents manufacturing: a feasibility study, *Opt. Laser Technol.* 95 (2017) 113–123.
- [15] O.S. Carneiro, A.F. Silva, R. Gomes, Fused deposition modeling with polypropylene, *Mater. Des.* 83 (2015) 768–776.
- [16] A.M. Abdullah, T.N.A. Tuan Rahim, D. Mohamad, H.M. Akil, Z.A. Rajion, Mechanical and physical properties of highly ZrO₂/β-TCP filled polyamide 12 prepared via fused deposition modelling (FDM) 3D printer for potential craniofacial reconstruction application, *Mater. Lett.* (2016).
- [17] P. Habibovic, U. Gbureck, C.J. Doillon, D.C. Bassett, C.A. van Blitterswijk, J.E. Barralet, Osteoconduction and osteoinduction of low-temperature 3D printed bioceramic implants, *Biomaterials* 29 (7) (2008) 944–953.
- [18] Y. Yang, S. Yang, Y. Wang, Z. Yu, H. Ao, H. Zhang, L. Qin, O. Guillaume, D. Eglin, R.G. Richards, T. Tang, Anti-infective efficacy, cytocompatibility and biocompatibility of a 3D-printed osteoconductive composite scaffold functionalized with quaternized chitosan, *Acta Biomater.* 46 (2016) 112–128.
- [19] S. Puértolas, D. Navallas, A. Herrera, E. López, J. Millastre, E. Ibarz, S. Gabarre, J.A. Puértolas, L. Gracia, A methodology for the customized design of colonic stents based on a parametric model, *J. Mech. Behav. Biomed. Mater.* 71 (February) (2017) 250–261.
- [20] G.A. Holzapfel, Changes in the mechanical environment of stenotic arteries during interaction with stents: computational assessment of parametric stent designs, *J. Biomech. Eng.* 127 (1) (2005) 166.
- [21] H. Zahedmanesh, C. Lally, Determination of the influence of stent strut thickness using the finite element method: implications for vascular injury and in-stent restenosis, *Med. Biol. Eng. Comput.* 47 (4) (2009) 385–393.
- [22] C. Briguori, C. Sarais, P. Pagnotta, F. Liistro, M. Montorfano, A. Chieffo, F. Sgura, N. Corvaja, R. Albiero, G. Stankovic, C. Toutouzas, E. Bonizzoni, C. Di Mario, A. Colombo, In-stent restenosis in small coronary arteries, *J. Am. Coll. Cardiol.* 40 (3) (2002) 403–409.
- [23] J. Pache, A. Kastrati, J. Mehili, H. Schühlen, F. Dotzer, J. Hausleiter, M. Fleckenstein, F.J. Neuman, U. Sattlerberger, C. Schmitt, M. Müller, J. Dirschinger, A. Schömig, Intracoronary stenting and angiographic results: strut thickness effect on restenosis outcome (ISAR-STREO-2) trial, *J. Am. Coll. Cardiol.* 41 (8) (2003) 1283–1288.
- [24] J. Pache, A. Kastrati, J. Mehili, J.A. Coll, Intracoronary Stenting and Angiographic Results: Strut Thickness Effect on Restenosis Outcome Evidence for Use of Coronary Stents: A Hierarchical Bayesian Meta-analysis, 2003 2003.
- [25] H.Y. Ang, H. Bulluck, P. Wong, S.S. Venkatraman, Y. Huang, N. Foin, Bioresorbable stents: current and upcoming bioresorbable technologies, *Int. J. Cardiol.* 228 (2017) 931–939.
- [26] M.A. Woodruff, D.W. Hutmacher, The return of a forgotten polymer – polycaprolactone in the 21st century, *Prog. Polym. Sci.* 35 (10) (2010) 1217–1256.

Chapter 9

3D Printing Process on Degradation

Abstract

Previous results have demonstrated that 3D Printing is able to produce BRS with precision. While manufacturing method to produce BRS with the appropriate architecture, material studies, mechanical studies, etc., have received much attention, the effects of the subsequent sterilization methods on the BRS properties have often been overlooked.

Chapter 9 aims to study the effect of 3D printing process over the degradation rate of Polycaprolactone (PCL) stents, due to is one of the most important stent's property to be in charge to provide the appropriate period of time to heal the atherosclerosis. Employing the novel 3D Tubular Printer designed by our research group, this work presents the effects of printing temperature, printing flow rate, and printing speed over the degradation rate of Polycaprolactone (PCL) stents in dynamics and static conditions. Molecular weight, material structure, degradation rate, and radial expansion tests were performed.

Results have shown the influence of the printing process over the degradations rate, accelerating it according the printing temperature and printing flow rate increase. The static method has left a faster degradation rate of the samples. All samples showed a great stability in their radial behaviour, barely changing after 8 weeks of degradation.

This chapter had been published in the 3D Printing & Additive Manufacturing Journal (Under Journal Guidelines).



Antonio J. Guerra, Joaquim Ciurana. “Three Dimensional Tubular Printing of Bioabsorbable Stents: The Effects Process Parameters Have on In Vitro Degradation”. 2019, 6(1), 50-56. 3D Print Addit Manuf.

Antonio J. Guerra, Joaquim Ciurana. "Three Dimensional Tubular Printing of Bioabsorbable Stents: The Effects Process Parameters Have on In Vitro Degradation". *3D Printing and Additive Manufacturing*. Vol. 6, issue 1 (2019) : 50-56.

<https://doi.org/10.1089/3dp.2018.0020>

© Mary Ann Liebert, Inc.

Abstract

Bioresorbable stents (BRSs) offer the potential to improve long-term patency rates by providing support just long enough for an artery to heal. However, producing a BRS for an intended period of support time is rather difficult. Nowadays in the stent industry, the current manufacturing process used is laser microcutting. Nevertheless, in the case of BRSs based on polymers, three-dimensional (3D) additive manufacturing (AM) techniques could be the better solution. Developing AM techniques to produce BRSs and studying how these technologies affect the stents' properties are indispensable nowadays. In this context, the present work aims to study the effect that the 3D printing process has on the degradation rate of polycaprolactone (PCL) stents. This is because degradation rate is one of the most important properties of a stent if the appropriate amount of time to heal atherosclerosis is to be provided. This work employs a 3D tubular printer designed by our group and presents the effects that printing temperature, flow rate, and speed have on the degradation rate of PCL stents in both dynamic and static conditions. Tests on the molecular weight, material structure, degradation rate, and radial expansion were performed. Results showed that the printing process does in fact influence the degradation rate by accelerating it as the printing temperature and flow rate increase. Furthermore, the static method degraded the samples faster. Finally, all samples showed great stability in their radial behavior, barely changing after 8 weeks of degradation. The results encourage us to believe that tubular 3D printing could well be a solution for BRS production.

Keywords

3D-printing, biodegradable, stent, polymer, degradation, manufacturing

Chapter 10
Effects of Sterilization on 3D-Printed Stent

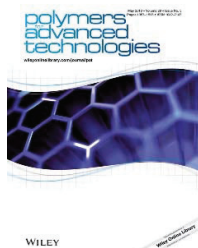
Abstract

Previous results have demonstrated that 3D Printing is able to produce BRS with precision. While manufacturing method to produce BRS with the appropriate architecture, material studies, mechanical studies, etc., have received much attention, the effects of the subsequent sterilization methods on the BRS properties have often been overlooked.

This chapter presents the effects the different sterilization methods and their times of applications have over the properties of 3D-Printed Polycaprolactone (PCL) stent. The effects of Ethanol, Ultraviolet Light, and Antibiotic sterilization processes at 0.5, 1, 2, 4, 8, and 16 hours is presented and discussed. Stents were analysed by Sterility Tests, Scanning Electron Microscopy (SEM), Differential Scanning Calorimetry (DSC), Thermogravimetric analysis (TGS), Molecular Weight, and Degradation Tests (DTS).

Results have shown the efficacy of Ethanol as sterilization treatment, due to, it barely affected the material properties. On the other hand, UV has proved it's strongly influence over the crystallinity and molecular weight, produced mainly by the photodegradation of UV irradiation. Lastly, Antibiotic showed a lesser effect over the crystallinity, but reduced the molecular weight of the samples strongly. Ethanol has presented as the best sterilization method for medical devices with such high material requirement such stents are.

This chapter had been published in the Journal of Polymer for Advanced Technologies (Under Journal Guidelines).



Antonio J. Guerra, Paula Cano, Marc Rabionet, Teresa Puig, Joaquim Ciurana. “The Effect of Sterilization Methods over 3D-Printed Polycaprolactone Stent Properties”. 2018, 29 (8), 2327-2335. Polymer for Advanced Technologies.

Antonio J. Guerra, Paula Cano, Marc Rabionet, Teresa Puig, Joaquim Ciurana. "The Effects Of Different Sterilization Processes On The Properties Of A Novel 3D-Printed Polycaprolactone Stent". *Polymers for Advanced Technologies*. Vol. 29, issue 8 (2018) : 2327-2335.

<https://doi.org/10.1002/pat.4344>

Received: 18 January 2018

Revised: 23 April 2018

Accepted: 23 April 2018

Copyright © 2018 John Wiley & Sons, Ltd.

Abstract

Bioresorbable stents (BRS) offer the potential to improve long-term patency rates by providing support just long enough for the artery to heal itself. While manufacturing methods to produce BRS using the appropriate architecture, material and mechanical studies, etc., have received much attention, the effects subsequent sterilization methods have on BRS properties are overlooked. Sterilization process can change a device's properties. This work presents the effects ethanol, ultraviolet light (UV), and antibiotic sterilization processes at 0.5, 1, 2, 4, 8, and 16 hours have on a novel 3D-printed polycaprolactone stent. The stents were analysed using sterility tests, scanning electron microscopy, differential scanning calorimetry, thermogravimetric analysis, mass spectrometry, for molecular weight, and degradation tests. Results have shown ethanol to be an effective sterilization treatment as it barely affected the material's properties. On the other hand, UV had a considerable influence (mainly produced by the photodegradation of UV irradiation) on crystallinity and molecular weight. Lastly, while antibiotic sterilization did not affect crystallinity to the same degree, it did substantially reduce the molecular weight of the samples. Ethanol results in being the best sterilization method for the high material requirements that medical devices such as stents have.

Keywords

3D-printing, bioresorbable, polymer, stent, sterilization

Chapter 11

3D-Printed Composite BRS

Abstract

Biodegradable stents (BRS) offer enormous potential but first they must meet some specific requirements, such as: (I) their manufacturing process must be precise; (II) degradation should have minimal toxicity; (III) the rate of degradation should match the recovery rate of vascular tissue; (IV) ideally, they should induce rapid endothelialization to restore the functions of vascular tissue, but at the same time reduce the risk of restenosis; and (V) their mechanical behavior should comply with medical requirements. Although the first three requirements have been comprehensively studied, the last two have been overlooked. One possible way of addressing these issues would be to fabricate composite stents using materials that have different mechanical, biological, or medical properties, for instance, Polylactide Acid (PLA) or Polycaprolactone (PCL).

This chapter aims to produce PCL/PLA composite stents using a novel 3D tubular printer based on Fused Deposition Modelling (FDM). The cell geometry (shape and area) and the materials (PCL and PLA) of the stents were analyzed and correlated with 3T3 cell proliferation, degradation rates, dynamic mechanical and radial expansion tests to determine the best parameters for a stent that will satisfy the five strict BRS requirements.

Results proved that the 3D-printing process was highly suitable for producing composite stents (approximately 85–95% accuracy). Both PCL and PLA demonstrated their biocompatibility with PCL stents presenting an average cell proliferation of 12.46% and PLA 8.28% after only 3 days. Furthermore, the PCL/PLA composite stents demonstrated their potential in degradation, dynamic mechanical and expansion tests. Moreover, and regardless of the order of the layers, the composite stents showed (virtually) medium levels of degradation rates and mechanical modulus. Radially, they exhibited the virtues of PCL in the expansion step (elasticity) and those of PLA in the recoil step (rigidity). Results have clearly demonstrated that composite PCL/PLA stents are a highly promising solution to fulfilling the rigorous BRS requirements.



Antonio J. Guerra, Paula Cano, Marc Rabionet, Teresa Puig, Joaquim Ciurana. “3D-printed PCL/PLA composite stents: Towards a new solution to cardiovascular problems”. 2018, 11 (9), 1679. Materials.

Article

3D-Printed PCL/PLA Composite Stents: Towards a New Solution to Cardiovascular Problems

Antonio J. Guerra ¹, Paula Cano ², Marc Rabionet ^{1,2}, Teresa Puig ² and Joaquim Ciurana ^{1,*}

¹ Department of Mechanical Engineering and Civil Construction, Universitat de Girona, C/Maria Aurèlia Capmany 61, 17003 Girona, Spain; antonio.guerra@udg.edu (A.J.G.); m.rabionet@udg.edu (M.R.)

² Department of Medical Sciences, Faculty of Medicine, University of Girona, Emili Grahit 77, 17003 Girona, Spain; paaula.cano@gmail.com (P.C.); teresa.puig@udg.edu (T.P.)

* Correspondence: quim.ciurana@udg.edu; Tel.: +34-972-418-265

Received: 31 July 2018; Accepted: 9 September 2018; Published: 11 September 2018



Abstract: Biodegradable stents (BRS) offer enormous potential but first they must meet five specific requirements: (i) their manufacturing process must be precise; (ii) degradation should have minimal toxicity; (iii) the rate of degradation should match the recovery rate of vascular tissue; (iv) ideally, they should induce rapid endothelialization to restore the functions of vascular tissue, but at the same time reduce the risk of restenosis; and (v) their mechanical behavior should comply with medical requirements, namely, the flexibility required to facilitate placement but also sufficient radial rigidity to support the vessel. Although the first three requirements have been comprehensively studied, the last two have been overlooked. One possible way of addressing these issues would be to fabricate composite stents using materials that have different mechanical, biological, or medical properties, for instance, Polylactide Acid (PLA) or Polycaprolactone (PCL). However, fashioning such stents using the traditional stent manufacturing process known as laser cutting would be impossible. Our work, therefore, aims to produce PCL/PLA composite stents using a novel 3D tubular printer based on Fused Deposition Modelling (FDM). The cell geometry (shape and area) and the materials (PCL and PLA) of the stents were analyzed and correlated with 3T3 cell proliferation, degradation rates, dynamic mechanical and radial expansion tests to determine the best parameters for a stent that will satisfy the five strict BRS requirements. Results proved that the 3D-printing process was highly suitable for producing composite stents (approximately 85–95% accuracy). Both PCL and PLA demonstrated their biocompatibility with PCL stents presenting an average cell proliferation of 12.46% and PLA 8.28% after only 3 days. Furthermore, the PCL/PLA composite stents demonstrated their potential in degradation, dynamic mechanical and expansion tests. Moreover, and regardless of the order of the layers, the composite stents showed (virtually) medium levels of degradation rates and mechanical modulus. Radially, they exhibited the virtues of PCL in the expansion step (elasticity) and those of PLA in the recoil step (rigidity). Results have clearly demonstrated that composite PCL/PLA stents are a highly promising solution to fulfilling the rigorous BRS requirements.

Keywords: 3D-printing; stent; bioabsorbable; bioresorbable; polymer; composite

1. Introduction

Biodegradable stents (BRS) were introduced to overcome the limitations of permanent stents and to offer significant advantages such as, among others, complete bioresorption and/or mechanical flexibility. [1]. BRS have the potential to improve long-term patency rates by providing support just long enough for the artery to heal. Ideally, BRS should meet some exacting requirements.

A large number of authors have contributed to BRS research in recent years. For instance, in terms of manufacturing processes laser cutting and, more recently, additive manufacturing technologies

have been at the center of many studies. Guerra et al. [2] studied the effects laser cutting has on the degradation rate of Polycaprolactone (PCL) stent subunits under dynamic and static conditions. Although their results showed that laser cutting has a negligible effect on degradation, the degradation conditions showed that PCL degrades faster in body conditions (dynamics) than the data found in traditional literature had reported (statics). Meanwhile, Grabow et al. [3] studied the effects CO₂ laser cutting and sterilization have on Poly-L-Lactide (PLLA). Their results revealed the enormous influence sterilization has on the mechanical properties of PLLA (i.e., 40% crystalline modification). Using additive manufacturing, Park et al. [4] produced drug-coated BRS with Fused Deposition Modelling (FDM) and had very promising results in animals (20.7% restenosis). Guerra et al. [5,6] designed and implemented a novel 3D tubular printer that allows the rapid manufacture of BRS based on polymers. Their results suggest that this technology could be the future of BRS manufacturing as they managed to achieve up to 85% precision and manufacturing times under 5 min.

In terms of the abovementioned second (degradation should have minimal toxicity), third (the rate of degradation should match the recovery rate of vascular tissue), and fifth (mechanical behavior should meet medical stipulations) requirements, some authors have focused their studies on potentially suitable materials for producing BRS [7,8]. Hideo Tamai et al. [9] evaluated the feasibility, safety, and efficacy of PLLA stents in humans for coronary artery stenosis with promising results. Shen et al. [10] studied the degradation of L-Lactide (LA) and 5-methyl-5-benzoyloxycarbonate-1,3-dioxan-2-one (MBC) coated stents and cast films. Their results showed similar degradation behavior of the coating materials in *in vivo* conditions and negligible differences in extensive endothelialization or the expression of inflammation-associated proteins after 4 weeks post-stent implantation.

However, there are fewer studies that consider the fourth requirement (BRS should induce rapid endothelialization to restore the functions of vascular tissue but, at the same time, reduce the risk of restenosis). Wang et al. [11] studied the cell adhesion of Human Umbilical Vein Endothelial Cells (HUVEC) on a stent coated with poly-L-lysine and fibronectin. Their work revealed that the metallic-coated stent significantly increased cell adhesion. Meanwhile, Xu et al. [12] developed strategies for improving stent endothelialization by employing a new polymer poly-1,8-octanediol-co-citric acid (POC), anti-CD34 antibody and a vascular endothelial growth factor. Their method significantly improved the proliferation of endothelial progenitor cells (EPC) when compared with PLLA stents. In 2015, Lutter et al. [13] studied the influence the microstructure of a stent's surface has on endothelialization and thrombogenicity using HUVEC and their results demonstrated that, compared to a smooth surface stent, flat cubic elevation improved endothelial cell adhesion. Additionally, Jiang et al. [14] analyzed four polymer coatings for controlling the degradation and HUVEC cell adhesion of Mg stents. Employing PLLA, poly-lactic-co-glycolic-acid (PLGA) (90:10), PLGA (50:50), and PCL, they evaluated surface and biological properties. Their results showed that PLGA (50:50) is a promising coating material for Mg stents. Finally, He et al. [15] studied how to design nanofiber mesh which would allow the attachment and phenotypic maintenance of human coronary artery endothelial cells. Similar work was carried out by Rubert M. et al. [16], who analyzed coaxial electrospun with PCL materials and added poly(ethylene oxide) (PEO) fibers containing basic fibroblast growth factor. The work also focused on fibroblast proliferation by combining cell culture and proliferation with additive manufacturing technologies.

However, many challenges still exist, such as evaluating and understanding the mechanical and biological properties of polymeric BRS. Previous work carried out by our groups [17] has proved that composite stents satisfy some of the requisites. However, composite stents cannot be created easily with conventional laser cutting manufacturing processes [18]. Alternative manufacturing technologies, such as 3D-printing, need to be used. This work aims to develop PCL/PLA (Polylactide Acid) composite stents by employing 3D-printing based on FDM. Both the parameters of the stent, namely, its cell geometry (shape and area) and the materials (PCL and PLA), were analyzed. Stents were subjected to 3T3 cell proliferation, degradation, dynamic mechanical, and radial expansion tests to determine which parameters would best comply with the stringent BRS requirements.

This work presents a proof of concept for the viability of using composites stents in the treatment of cardiovascular disease.

2. Materials and Methods

2.1. Stent Fabrication Method

Stents were manufactured by employing a 3D-printing process in a 3D tubular printer [5]. This 3D additive manufacturing machine is based on the FDM method. The filament is melted into the extruder nozzle, which then deposits the melted material onto a controlled rotatory platform. The machine provides $0.9375\ \mu\text{m}$ precision on the X axis, 0.028125° on the W axis, $0.3125\ \mu\text{m}$ on the Z axis, 0.028125° in the extruder that has a 0.4 mm diameter nozzle (Figure 1).

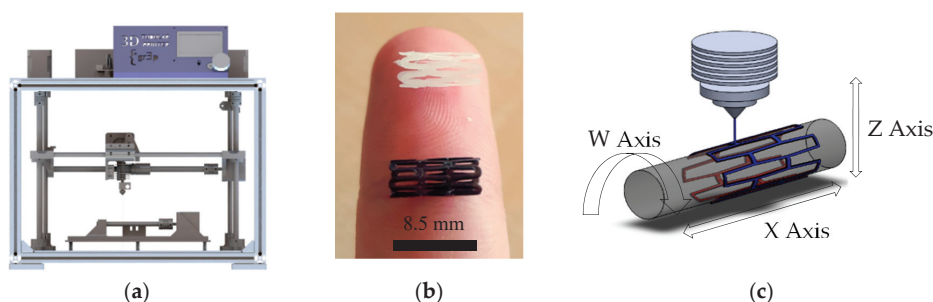


Figure 1. (a) 3D Tubular printer (b) 3D-printed stents [PCL in white, PLA in black] (c) Machine methodology. PCL: Polycaprolactone; PLA: Polylactide Acid.

Stents are defined by their cell geometry shape (C_G :A:C), inner diameter (I_\emptyset : 4 mm), stent thickness (S_T : 0.2 mm), number of circumferential cells (N_C : 4:8), cell area (C_A), strut width (S_W), total length (L: 9.6 mm), and material (M_a :PCL:PLA) (Figure 2). Based on previous work [6], the PCL stents were printed at a temperature of $220\ ^\circ\text{C}$ for nozzle T^a , $25\ ^\circ\text{C}$ for bed T^a , and a printing speed of 300 mm/min, while for the PLA stents, the temperature was $220\ ^\circ\text{C}$ for nozzle T^a , $25\ ^\circ\text{C}$ for bed T^a , and a printing speed of 200 mm/min printing speed. Different printing flow rate percentages (F_R) were also employed for each material to obtain different C_A .

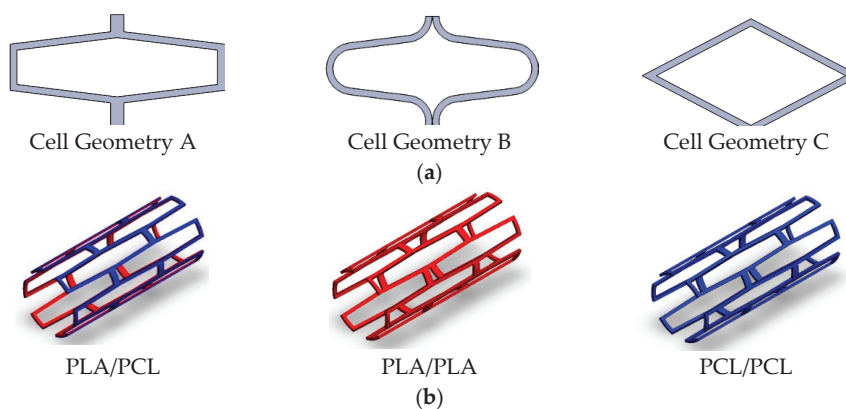


Figure 2. Stent configurations: (a) Stent cell geometries employed; (b) Stent material/layer used.

To study the effects the geometrical and material aspects of the stents have on their final properties, 27 geometries using different combinations of C_G , N_C , F_R , and M_a with a Full Factorial Design (FFD)

were printed (Table 1). Stents were sterilized overnight in a 70% ethanol/water solution, then washed twice with Phosphate Buffered Solution (PBS, Gibco, Waltham, MA, USA) and finally exposed to UV light for 30 min. This sterilization method was followed to avoid any changes in the final properties of the stents [19].

Table 1. Design of Experiments (DOE) of the 54 stents manufactured (27 PCL and 27 PLA).

#	C _G	N _C	F _R PCL *	F _R PLA *	#	C _G	N _C	F _R PCL *	F _R PLA *	#	C _G	N _C	F _R PCL *	F _R PLA *
01	A	4	50	85	10	B	4	50	85	19	C	4	50	85
02	A	4	65	100	11	B	4	65	100	20	C	4	65	100
03	A	4	80	115	12	B	4	80	115	21	C	4	80	115
04	A	6	50	85	13	B	6	50	85	22	C	6	50	85
05	A	6	65	100	14	B	6	65	100	23	C	6	65	100
06	A	6	80	115	15	B	6	80	115	24	C	6	80	115
07	A	8	50	85	16	B	8	50	85	25	C	8	50	85
08	A	8	65	100	17	B	8	65	100	26	C	8	65	100
09	A	8	80	115	18	B	8	80	115	27	C	8	80	115

* Levels of F_R were chosen to obtain the same S_W for PCL and PLA. Three different levels were selected to obtain three different C_A.

2.2. Materials

The materials used were Polycaprolactone CAPA 6500[®] (PCL, Perstorp, Sweden) and Polylactide Acid (PLA, RepRap BCN) (Table 2). PCL is a biodegradable polyester with a low melting point (60 °C) and has a glass transition of about −60 °C. Meanwhile, PLA is a biodegradable thermoplastic aliphatic polyester derived from renewable resources, such as corn starch or sugarcane, and has a melting point of about 173–178 °C with a glass transition of 60–65 °C. Degradation of both PCL and PLA is produced by the hydrolysis of their ester linkages in physiological conditions. White PCL and black PLA were selected so as to easily identify the materials once the printing process had been completed.

Table 2. Material properties.

Material (#)	Molecular Weight (g/mol)	Young's Modulus (MPa)	Strain at Break (%)	Degradation Time (Months)
PCL	50,000	470	700	>24
PLA	30,000	108	3.5	≈12

2.3. Cell Line

Murine 3T3 fibroblasts cells were obtained from the American Type Culture Collection (ATCC, Rockville, MD, USA). The 3T3 cells were cultured in Dulbecco's Modified Eagle's Medium (DMEM; Gibco, Waltham, MA, USA) supplemented with 10% fetal bovine serum, 1% L-glutamine, 1% sodium pyruvate, 50 U/mL penicillin and 50 µg/mL (HyClone, Logan, UT, USA). Cells were kept at 37 °C and 5% CO₂ atmosphere. To obtain more reliable results, a total of 12 replicas for both materials [6 for PCL (3 × 2) and 6 for PLA (3 × 2)] were tested. Two-dimensional (2D) cell culture was also performed to normalize the cell proliferation rates on the stents. Because of their rapid and stable growth kinetic, fibroblast cells were selected to carry out the first proof of concept for the PCL/PLA composite stents. However, further studies with other kinds of cells, such as endothelial human cell, are required and should be performed.

2.4. Culture Methodology

The stents were placed in 24-well non-adherent microplates (Sartstedt, Nümbrecht, Germany), soaked with DMEM and incubated at 37 °C prior to cell seeding. Finally, due to cell growth kinetics and the culture period, the stents were seeded with a 20,000-cell-per-stent concentration and kept at 37 °C in a 5% CO₂ atmosphere for 3 days. Because our aims were to determine whether PCL and PLA are biologically valid and to define the stent geometry that produces the best cell proliferation, cell culture was performed in static conditions. However, further work using dynamic conditions to

simulate a real environment would be beneficial because under dynamic conditions stents would be subjected to pressure and flow conditions that can modify the kinetics of cell proliferation.

2.5. Characterization

2.5.1. Morphological Features

A Nikon SMZ-745T optical microscope (Nikon, Minato, Tokyo, Japan) attached to a ProgRes CT3 digital camera (Jenoptik, Jena, Germany) was used to determine the dimensional features (precision, layer adhesion, etc.) of the samples. Image J[®] (National Institutes of Health, Bethesda, MD, USA) was used to process the images and collect the data.

2.5.2. Cell Proliferation Assay

MTT tests were performed to check the effect the process parameters (C_G , N_C , F_R , and M_a) had on cell proliferation. The subsequent results allowed us to then select the best parameters with which to manufacture the final PCL/PLA composite stents with the best biological response. An MTT (3-(4,5-dimethyl-2-thiazolyl)-2,5-diphenyltetrazolium bromide) assay was selected to test the cell proliferation on the stents. MTT is a yellow tetrazolium salt which can be reduced by the mitochondria of viable cells. This metabolic transformation results in water-insoluble purple crystals of formazan being produced, which can then be solubilized with dimethyl sulfoxide (DMSO) into a colored solution. The absorbance of DMSO solution is related to the number of cells. After incubation, the culture medium was removed, and the stents were put into new wells where they were incubated with 3 mL of DMEM medium and 300 μ L of MTT (Sigma-Aldrich, Saint Louis, MO, USA) for 2.5 h. After this time, the MTT supplemented culture medium was removed, DMSO was added and the stents were shaken to ensure the complete dissolution of the resulting formazan crystals. Four 100 μ L aliquots from each sample were pipetted into a 96-well plate and absorbance was measured at 570 nm using a microplate reader (Bio-Rad, Hercules, CA, USA). Adherent 2D controls were likewise processed with the same number of seeded cells.

2.5.3. Cell Adhesion Assay

To check the cell adhesion on the stents, Confocal Laser Microscopy was performed with a Nikon A1R Microscope. The cultivated samples were dyed as follows: (i) wash samples with phosphate buffered solution (PBS, Gibco, Waltham, MA, USA); then (ii) fix samples with 4% paraformaldehyde at room temperature and wash samples; next (iii) permeabilize cells with 0.2% Triton X-100; and (iv) add blocking buffer at room temperature; then (v) dye cytoskeleton actin with rhodamine-phalloidin (Cytoskeleton Inc., Denver, CO, USA)(1:200) in blocking buffer; and finally (vi) dye the cells nuclei with (4',6'-diamidino-2-phenylindole) (DAPI) (1/1000) in blocking buffer. The adhesion assay was performed simply to obtain qualitative data about cell adhesion.

2.5.4. Mechanical Properties

The PCL, PLA, and PCL/PLA samples were subjected to Dynamic Mechanical Analysis using a METTLER TOLEDO SDTA861e Dynamic Mechanical Analyzer (DMA, METTLER TOLEDO, Columbus, OH, USA). The dynamic storage modulus (E') was analyzed. The loss tangent is the ratio of loss modulus and storage modulus and this indicates the material's viscosity and elastic properties, respectively. The loss tangent curve peak appears and can be defined as the material's glass transition temperature (T_g).

2.5.5. Degradation Rate

The PCL, PLA, and PCL/PLA samples were submerged in phosphate buffered solution (PBS, 7.4 \pm 1 pH) at 37 $^{\circ}$ C for 6 weeks. Samples were recovered after 2, 4, and 6 weeks under the same conditions (25 $^{\circ}$ C). Using a METTLER TOLEDO Sartorius 2MP Scale (METTLER TOLEDO,

Columbus, OH, USA), weight loss was evaluated by measuring the original weight of the sample after the printing process (W_0), and its residual weight after degradation and once it had been completely dried (W_r) in an oven at 30 °C for 24 h. Weight loss percentage, $W_L\%$, was estimated using the following equation:

$$W_L\% = \frac{W_0 - W_r}{W_0} \times 100 \quad (1)$$

The PBS was changed frequently to keep the pH as constant as possible.

2.5.6. Radial Behavior

The PCL, PLA, and PCL/PLA samples were expanded radially from their original diameter (O_0 : 4 mm) until a maximum of 175% of their original diameter (M_0 : 7 mm) was reached. Then, the radial force was removed, and the diameter was measured to determine the recoil ratio (R_0).

2.5.7. Statistics

Results were subjected to regression analysis. The analysis of variance (ANOVA) method was applied to test the statistical significance of the process parameters (C_G , N_C , F_R , and M_a). The analysis was carried out at a 95% confidence level ($\alpha = 0.05$). All observations were confirmed by at least three independent experiments. All data are expressed as mean \pm standard error (SE).

3. Results

In this manuscript, the following steps were executed to perform the experiments (Figure 3).

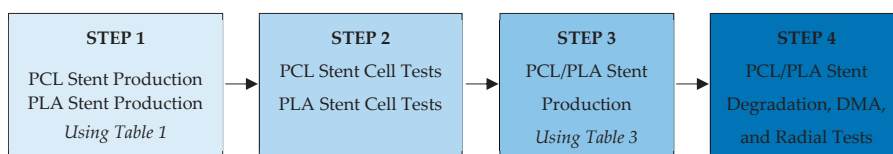


Figure 3. Methodology followed to carry out the experiments. DMA: Dynamic Mechanical Analyzer.

3.1. Cell Proliferation Results

Cell proliferation is mainly related to the molecular weight, stent geometry and the intrinsic porosity of the material [20]. This section presents the effects these parameters had on the final cell proliferation. Murine 3T3 fibroblast culture results (Figure 4a) showed the different biological responses of PCL and PLA. Regardless of the geometrical aspects of the stent, the PCL stents showed a 33.5% greater cell proliferation compared to the PLA stents.

When analyzing the results in terms of input parameters (C_G , N_C , F_R , and M_a), regression analysis showed the considerable statistical influence that flow rate, number of stent radial cells, and material ($p < 0.05$) have on cell proliferation. Stent cell geometry did not show any significant statistical influence on cell proliferation (Figure 4b); however, we hypothesize that geometries with a higher number of pointed corners might well improve cell adhesion and subsequent proliferation. Some previous studies made by others have demonstrated that stent geometry affected the neointima cell proliferation and exerted a substantial influence on thrombosis and restenosis rates [21].

The increase in flow rate and number of cells produced the increase in cell proliferation (Figure 4c,d). This increase is motivated by the reduction in the stent's cell area. The cell area (pore size) of a stent has been recognized as an important parameter that affects the proliferation properties and functions of the scaffolds (stents) because it is directly related to cell migration, vascularization, and mass transport [22]. Moreover, a high flow rate value implies a greater amount of expelled material. Therefore, cells have more material to adhere to and spread to, thus increasing their proliferation rate. Likewise, decreasing the number of stent cells resulted in stents with more material, thus allowing the proliferation of more cells.

Finally, in terms of the decisive effects materials have, lower molecular weights are known to produce poorer cell proliferation [23]. Here, PCL had a M_w of 50,000 g/mol, which is 40% more than PLA had at 30,000 g/mol. This percentage difference closely resembles that obtained in the proliferation results (PCL was 33.5% greater than PLA).

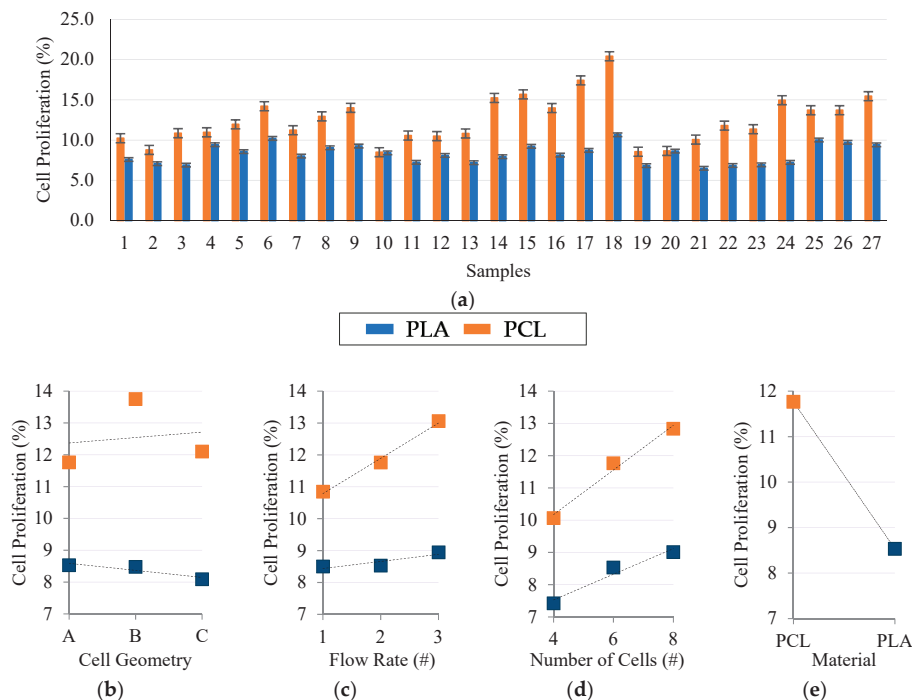


Figure 4. 3T3 Proliferation Results: (a) Average cell proliferation on each sample; (b) Main effect of cell geometry (6 radial cells, 2nd flow rate); (c) Main effect of flow rate (6 radial cells, A Geometry); (d) Main effect of number of cells (A Geometry, 2nd flow rate); (e) Main effect of plot of materials (6 radial cells, A Geometry, 2nd flow rate).

Confocal Laser Microscopy was performed on the PCL and PLA samples to qualitatively determine how 3T3 cells stick to the stents (Figure 5). The objective of this test was to study where the majority of cells adhere to and thus to be able to design stents that produce better proliferation. Figure 5 suggests that cells possess the ability to adhere to any part of the stent, even so, they usually adhered close to the pores and the corners of the stent. Further studies using different stent geometries could be useful to determine how to improve cell proliferation.

The results prove the materials' biological compatibility and encourage us to believe that PCL/PLA composite stents would comply with the fourth requirement, i.e., rapid endothelialization without risk of restenosis. PCL's better cell proliferation may be useful to increase the proliferation of endothelial vessel cells in the external wall of the stents, while an internal PLA wall may help to reduce the proliferation of cells that produce restenosis. However, further studies with other kinds of cells or substances need to be performed to confirm this. The results here show low cell proliferation because of the small amount of material that the stents have. Additional studies that use longer culture times may be beneficial to obtain better proliferation results.

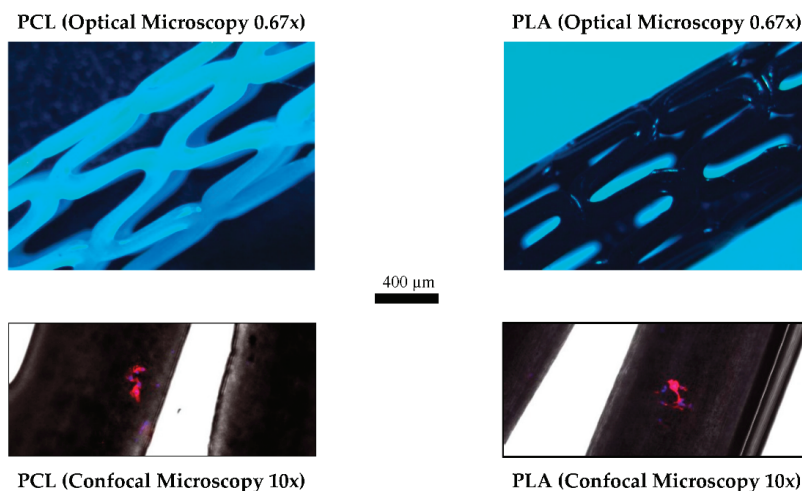


Figure 5. Confocal Laser Microscopy Images: (Left) PCL stent; (Right) PLA stent. Samples cultured with 3T3 fibroblast cells. Nucleus was stained with DAPI (blue) and actin cytoskeleton was stained with rhodamine-phalloidin (red).

3.2. Composite PCL/PLA Stent Manufacturing Results

As the properties of the stents are interrelated and sometimes contradictory, they require a careful compromise. For example, stents should be flexible enough to facilitate their placement but rigid enough to support the vessel. Sometimes higher tensile strength materials, desirable for bolstering radial strength, have higher yield strengths that promote undesired acute recoil. Biological aspects are also contradictory. For example, scaffolds (stents) with smaller pores (cell areas) will give better cell proliferation [24,25]; however, these characteristics will induce poorer radial behavior and vessel support. Therefore, and despite the best cell proliferation being obtained with the 18th DOE configuration (Table 1), other manufacturing parameters were used (Table 3) to produce PCL/PLA composite stents that reach a compromise between biological and mechanical properties. The inner diameter (I_{D} : 4 mm), stent thickness (S_{T} : 0.3 mm [0.15 mm/layer]), total length (L : 19 mm), printer nozzle T^{a} (220 °C), printer bed T^{a} (25 °C), printer infill (100%), and printer speed (300 mm/s for PCL, 200 mm/s for PLA) were kept constant. All the layer sequences were tested to identify if they influenced the properties or not.

Table 3. PCL/PLA Composite stent fabrication parameters*.

#	C_{G}	N_{C}	$F_{\text{R PCL}}$	$F_{\text{R PLA}}$	M_{a} Inner Layer	M_{a} Outer Layer
01	A	6	65	-	PCL	PCL
02	B	6	65	-	PCL	PCL
03	C	6	65	-	PCL	PCL
04	A	6	-	100	PLA	PLA
05	B	6	-	100	PLA	PLA
06	C	6	-	100	PLA	PLA
07	A	6	65	100	PCL	PLA
08	B	6	65	100	PCL	PLA
09	C	6	65	100	PCL	PLA
10	A	6	65	100	PLA	PCL
11	B	6	65	100	PLA	PCL
12	C	6	65	100	PLA	PCL

* Manufacturing parameters selected based on previous results [5,6].

The manufacturing process successfully produced PCL/PLA stents (Figure 6), requiring only 3 min per sample and achieving approximately 85–90% accuracy (depending on the geometry of the stent in question).

The intrinsic properties of 3D-printing based on FDM, make producing an object with pointed corners (geometries A and C) impossible. However, the rounded corners obtained could be useful when stents are being implanted and/or might reduce any potential damage to the endothelial in the vessel wall.

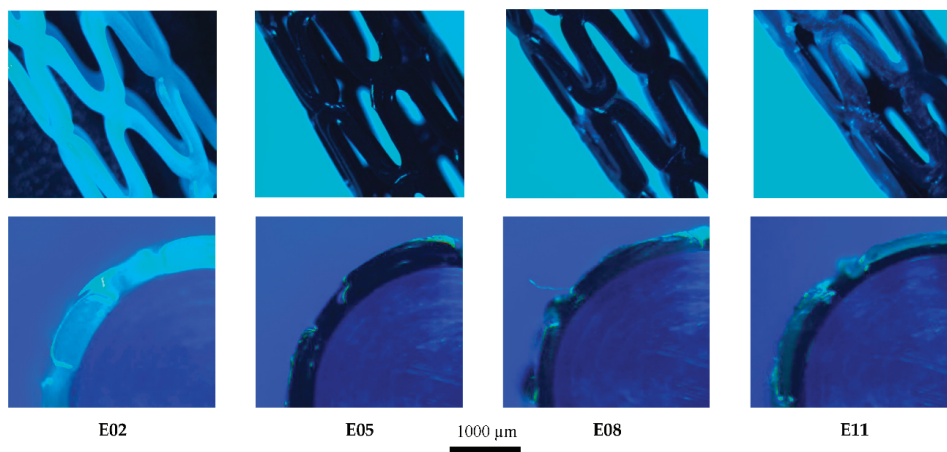


Figure 6. Optical Nikon Microscope images of 3D-printed stents. Superior images show the general 3D view, while inferior images depict the $\frac{1}{4}$ section radial view. Samples numbered according to Table 3. PCL/PLA composite stent fabrication parameters.

3.3. Degradation Rate Results

The mechanisms causing PCL and PLA degradation are well known: degradation occurs when water penetrates the bulk of the material and causes hydrolysis throughout the entire polymer matrix. From the literature it can be concluded that PCL and PLA undergo a two-stage degradation process: first, the non-enzymatic hydrolytic cleavage of ester groups and, second, when the polymer is more highly crystalline and of low molecular weight it experiences intracellular degradation and may be completely resorbed and degraded via an intracellular mechanism [26].

Degradation tests considering all the possible layer configurations were performed to establish if the sequence of layers affected the degradation rate or not. Simple PCL/PLA sheets were printed and tested (leaving aside the effect the stent's cell geometry (C_G , N_C , and F_R) would have). Results have evidenced the variations in degradation rates between PCL and PLA (Figure 7). This difference is produced by the difference in their molecular weights [19]. As is well known, materials with lower molecular weights degrade faster. However, both the PCL/PLA and the PLA/PCL composite stents showed almost medium weight losses, making the composite stent a good option in terms of degradation. Results also proved that the order in which the layers are placed has no effect on the device's degradation rate. However, in real conditions the outermost surface would be placed against the blood vessel wall which could, in turn, produce faster degradation. This is something which should be investigated further.

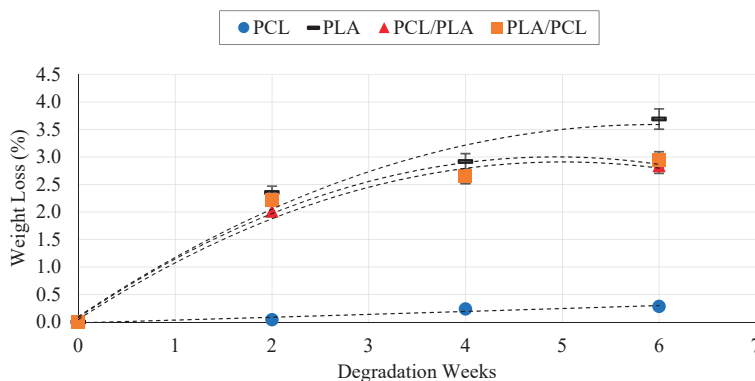


Figure 7. Degradation rate results for PCL, PLA, PCL/PLA, and PLA/PCL stents.

3.4. Dynamics Mechanical Analysis

Again, all the configurations of the layers were tested to determine whether they affected the mechanical behavior of the stents in any way or not. For the DMA tests, simple PCL/PLA sheets were printed and tested (leaving aside the effect the stent's cell geometry has (C_G , N_C , and F_R)). Results (Figure 8) showed the different mechanical behaviors of PCL and PLA and make it clear that alone they cannot be used. Nevertheless, composite PCL/PLA stents have shown a middle E' that would be more appropriate for stent manufacture [12]. As with the degradation rates, the order of the layers did not show any influence on the dynamic modulus.

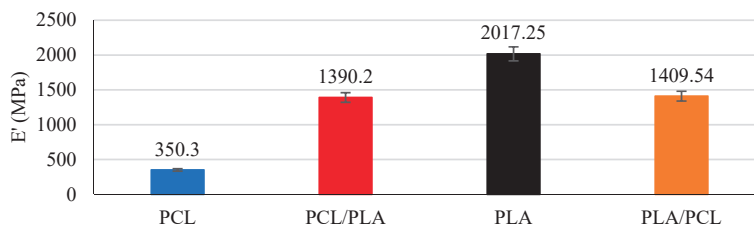


Figure 8. DMA results for PCL, PLA, PCL/PLA and PLA/PCL stents.

3.5. Radial Behavior Results

The radial behavior of stents is one of the most important properties because this is what provides the vessel with the appropriate support it needs. The effects the process parameters (C_G , N_C , F_R , and M_a) and the composition of the layers have on the radial behavior were analyzed.

Unlike in the cell proliferation results, stent cell geometry proved to exert a considerable influence on the radial expansion behavior (Figure 9a,b). The A geometries, with their higher hinges, provided the best results. However, the higher the hinge, the greater the recoil (Figure 8c), which is something that could negatively affect the placement procedure of the stent.

PCL stents (Figure 9a E01 → E03) showed the best radial expansion results; nevertheless, the elasticity of PCL produced higher recoil ratios, which is an undesirable effect. PLA stents (Figure 9a E04 → E06) showed an excellent recoil ratio but an unacceptable radial expansion. Meanwhile, composites stents with either an inner layer of PCL (Figure 9a E07 → E09) or of PLA (Figure 9a E10 → E12) showed very interesting results. Layer order did not affect the radial expansion behavior and exhibited the same results for stents with the same cell geometry. Composite stents exhibited the characteristics of PCL stents in the expansion process as well as the benefits of PLA stents in the recoil. Thanks to the elasticity of PCL, the PLA layer remained unbroken in the expansion process. Furthermore, when the force was removed, the rigidity of PLA hindered the recoil of PCL.

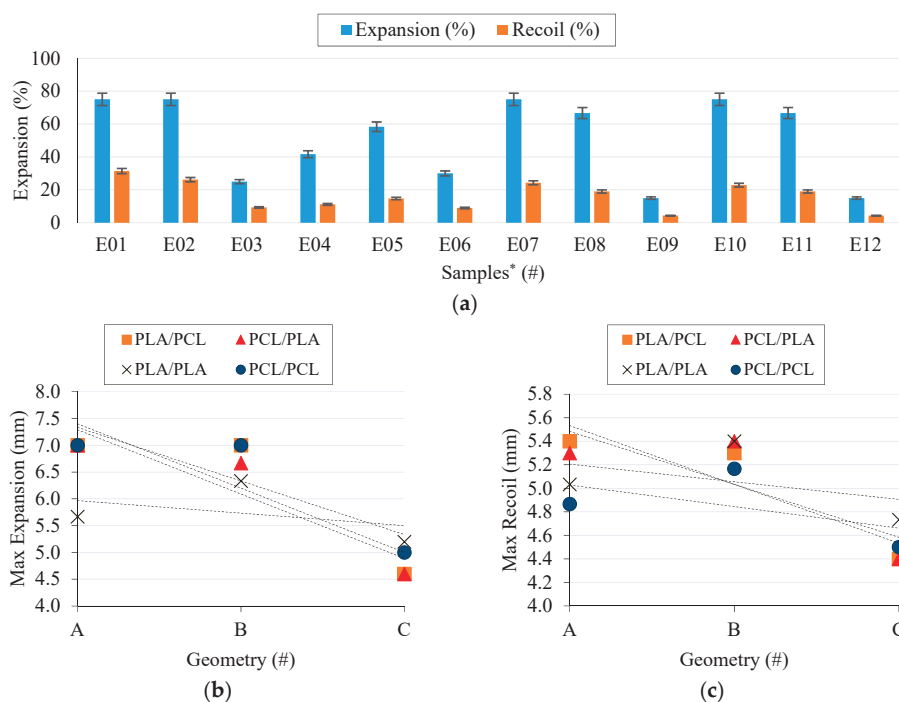


Figure 9. Radial expansion behavior results: (a) Expansion and recoil of each sample, (b) Main effect plot of geometry and layer order on radial expansion, (c) Main effect plot of geometry and layer order on radial recoil. * Samples numbered according to Table 3. PCL/PLA composite stent fabrication parameters.

Results confirm that composite stents can improve the mechanical properties of materials. Their good radial behavior, regardless of the order the layers are placed in, make it possible to produce composite stents with an inner layer of PLA and an outer layer of PCL that comply with the strict BRS requirements.

4. Conclusions

To our knowledge, this is the first work to develop and present composite PCL/PLA stents using a 3D-printing process based on FDM. The effects the cell geometry (shape and area) and materials (PCL and PLA) exert were also analyzed. Samples were subjected to 3T3 cell proliferation, degradation, dynamic mechanical and radial expansion tests to determine the parameters that best meet the rigorous requirements for BRS.

The results have demonstrated the considerable influence the cell area and material of a stent have on 3T3 proliferation. That said, the cell shape of the stent did not show any significant influence at all. Our initial hypothesis was confirmed, i.e., the smaller the cell area of a stent, the better the cell proliferation rate. Meanwhile, as a result of their different molecular weights, PCL demonstrated better cell proliferation than PLA.

The degradation rate results revealed the limitations of PLA for BRS purposes as a consequence of its fast degradation rate, whereas PCL showed a better degradation rate. The composite PCL/PLA stents showed an almost medium degradation for all the layer configurations which was mainly due to PLA degradation. The faster PLA degradation rate would eventually leave a BRS made only of PCL. The differences in their degradation rates are produced by their different molecular

weights, so employing PCL and PLA with similar molecular weights is a must to obtain a homogenous degradation of all the layers.

PCL showed a very low E' modulus in the dynamic mechanical results which, in turn, hinders its sole applicability for stent purposes. On the other hand, PLA showed a high E' modulus and good properties for supporting the artery vessel once in place but its properties hinder its placement. Conversely, composite stents showed a middle E' modulus regardless of the order the layers were made up of.

Finally, the radial behavior results have proved that composite PCL/PLA stents could be used to improve each material's separate limitations. For instance, PCL stents presented overly high recoil ratios but excellent expansion behavior, whereas PLA stents presented inadequate radial expansion, due to their rigidity, but excellent recoil ratio. Composite stents, either with PCL or PLA as the inner layer, demonstrated the virtues of PCL stents (i.e., their radial expansion) and PLA stents (i.e., their recoil ratio) that could be combined to provide a good solution for BRS. Furthermore, their good radial behavior (regardless of the order of the layers) make composite stents a promising concept for cardiovascular problems.

Based on the results presented here, we believe that polymer composite stents manufactured with 3D-printing processes could be a highly effective solution to the current problems that stents made of polymers have. However, FDA rules currently limit the use of 3D-printed stents in real clinical applications and, although PCL and PLA are FDA-approved materials, there are still open challenges to be met before approval for 3D-printed implantable medical devices can be obtained. This manuscript has presented a potential approach for future applications for stents.

Author Contributions: The present work have been developed by A.J.G., P.C., and M.R. under the supervision of J.C. and T.P.

Funding: This research was funded by the Ministry of Economy and Competitiveness (MINECO), Spain, (grant number DPI2016-77156-R), the University of Girona (grant number MPCUdG2016/036) and the Catalan Government (grant 2017SGR00385).

Acknowledgments: The authors acknowledge the financial support received from the Ministry of Economy and Competitiveness (MINECO), Spain, through the PhD scholarship program (grant number DPI2016-77156-R), the University of Girona, Spain, for the support provided by MPCUdG2016/036 and the Catalan Government grant 2017SGR00385

Conflicts of Interest: The authors declare no conflicts of interest.

References

1. Tenekecioglu, E.; Bourantas, C.; Abdelghani, M.; Zeng, Y.; Silva, R.C.; Tateishi, H. From drug eluting stents to bioresorbable scaffolds; to new horizons in PCI. *Expert Rev. Med. Devices* **2016**, *13*, 271–286. [[CrossRef](#)] [[PubMed](#)]
2. Guerra, A.J.; Ciurana, J. Effect of fibre laser process on in-vitro degradation rate of a polycaprolactone stent a novel degradation study method. *Polym. Degrad. Stab.* **2017**, *142*, 42–49. [[CrossRef](#)]
3. Grabow, N.; Schlun, M.; Sternberg, K.; Hakansson, N.; Kramer, S.; Schmitz, K.P. Mechanical properties of laser cut poly(L-lactide) micro-specimens: Implications for stent design, manufacture, and sterilization. *J. Biomech. Eng.* **2005**, *127*, 25–31. [[CrossRef](#)] [[PubMed](#)]
4. Park, S.A.; Lee, S.J.; Lim, K.S.; Bae, I.H.; Lee, J.H.; Kim, W.D. In vivo evaluation and characterization of a bio-absorbable drug-coated stent fabricated using a 3D-printing system. *Mater. Lett.* **2015**, *141*, 355–358. [[CrossRef](#)]
5. Guerra, A.J.; Roca, A.; de Ciurana, J. A novel 3D additive manufacturing machine to biodegradable stents. *Procedia Manuf.* **2017**, *13*, 718–723. [[CrossRef](#)]
6. Guerra, A.J.; Ciurana, J. 3D-printed bioabsorbable polycaprolactone stent: The effect of process parameters on its physical features. *Mater. Des.* **2018**, *137*, 430–437. [[CrossRef](#)]
7. Guan, Y.; Wang, L.; Lin, J.; King, M.W. Compliance study of endovascular stent grafts incorporated with polyester and polyurethane graft materials in both stented and unstented zones. *Materials (Basel)* **2016**, *9*, 658. [[CrossRef](#)] [[PubMed](#)]

8. Jang, Y.; Owuor, D.; Waterman, J.T.; White, L.; Collins, B.; Sankar, J. Effect of mucin and bicarbonate ion on corrosion behavior of AZ31 magnesium alloy for airway stents. *Materials (Basel)* **2014**, *7*, 5866–5882. [[CrossRef](#)] [[PubMed](#)]
9. Tamai, H.; Igaki, K.; Kyo, E.; Kosuga, K.; Kawashima, A.; Matsui, S. Initial and 6-Month Results of Biodegradable Poly-L-Lactic Acid Coronary Stents in Humans. *Circulation* **2000**, *102*, 399–404. [[CrossRef](#)] [[PubMed](#)]
10. Shen, L.; Li, Z.; Gong, F.; Zhang, F.; Qin, Q.; Cheng, S. Characterization of tissue responses and degradation behavior of heparin-immobilized copolymer for drug-eluting stents. *Polym. Degrad. Stab.* **2013**, *98*, 1015–1021. [[CrossRef](#)]
11. Wang, G.X.; Deng, X.Y.; Tang, C.J.; Liu, L.S.; Xiao, L.; Xiang, L.H. The Adhesive Properties of Endothelial Cells on Endovascular Stent Coated by Substrates of Poly-L-Lysine and Fibronectin. *Artif Cells. Blood Substitutes Biotechnol.* **2006**, *34*, 11–25. [[CrossRef](#)]
12. Xu, H.; Nguyen, K.T.; Brilakis, E.S.; Yang, J.; Fuh, E.; Banerjee, S. Enhanced endothelialization of a new stent polymer through surface enhancement and incorporation of growth factor-delivering microparticles. *J. Cardiovasc. Transl. Res.* **2012**, *5*, 519–527. [[CrossRef](#)] [[PubMed](#)]
13. Lutter, C.; Nothhaft, M.; Rzany, A.; Garlichs, C.D.; Cicha, I. Effect of specific surface microstructures on substrate endothelialisation and thrombogenicity: Importance for stent design. *Clin. Hemorheol. Microcirc.* **2015**, *59*, 219–233. [[PubMed](#)]
14. Jiang, W.; Tian, Q.; Vuong, T.; Shashaty, M.; Gopez, C.; Sanders, T. Comparison Study on Four Biodegradable Polymer Coatings for Controlling Magnesium Degradation and Human Endothelial Cell Adhesion and Spreading. *ACS Biomater. Sci. Eng.* **2017**, *3*, 936–950. [[CrossRef](#)]
15. He, W.; Ma, Z.; Wee, E.T.; Yi, X.D.; Robless, P.A.; Thiam, C.L. Tubular nanofiber scaffolds for tissue engineered small-diameter vascular grafts. *J. Biomed. Mater. Res. Part A.* **2009**, *90*, 205–216. [[CrossRef](#)] [[PubMed](#)]
16. Rubert, M.; Dehli, J.; Li, Y.F.; Taskin, M.B.; Xu, R.; Besenbacher, F. Electrospun PCL/PEO coaxial fibers for basic fibroblast growth factor delivery. *J. Mater. Chem. B* **2014**, *2*, 8538–8546. [[CrossRef](#)]
17. Guerra, A.J.; San, J.; Ciurana, J. Fabrication of PCL/PLA Composite Tube for Stent Manufacturing. *Procedia. CIRP* **2017**, *65*, 231–235. [[CrossRef](#)]
18. Guerra, A.J.; de Ciurana, J. Fibre laser cutting of polymer tubes for stents manufacturing. *Procedia. Manuf.* **2017**, *13*, 190–196. [[CrossRef](#)]
19. Guerra, A.J.; Cano, P.; Rabionet, M.; Puig, T. Effects of different sterilization processes on the properties of a novel 3D-printed polycaprolactone stent. *Polym. Adv. Technol.* **2018**, *29*, 1–9. [[CrossRef](#)]
20. Rabionet, M.; Polonio, E.; Guerra, A.J.; Martin, J.; Puig, T.; Ciurana, J. Design of a Scaffold Parameter Selection System with Additive Manufacturing for a Biomedical Cell Culture. *Materials (Basel)* **2018**, *11*, 1427. [[CrossRef](#)] [[PubMed](#)]
21. Mclean, D.R.; Eiger, N.L. Stent design: Implications for restenosis. *Rev. Cardiovasc. Med.* **2002**, *5*, 16.
22. Lee, K.-W.; Wang, S.; Lu, L.; Jabbari, E.; Currier, B.L.; Yaszemski, M.J. Fabrication and Characterization of Poly(Propylene Fumarate) Scaffolds with Controlled Pore Structures Using 3-Dimensional Printing and Injection Molding. *Tissue Eng.* **2006**, *12*, 2801–2811. [[CrossRef](#)] [[PubMed](#)]
23. Bharadwaj, S.; Vishnubhotla, R.; Shan, S.; Chauhan, C.; Cho, M.; Glover, S.C. Higher molecular weight polyethylene glycol increases cell proliferation while improving barrier function in an in vitro colon cancer model. *J. Biomed. Biotechnol.* **2011**, *2011*, 1–7. [[CrossRef](#)] [[PubMed](#)]
24. Domingos, M.; Intranuovo, F.; Russo, T.; De Santis, R.; Gloria, A.; Ambrosio, L. The first systematic analysis of 3D rapid prototyped poly(ϵ -caprolactone) scaffolds manufactured through BioCell printing: The effect of pore size and geometry on compressive mechanical behaviour and in vitro hMSC viability. *Biofabrication* **2013**, *5*, 045004.
25. Palomerias, S.; Rabionet, M.; Ferrer, I.; Sarrats, A.; Garcia-Romeu, M.L.; Puig, T. Breast cancer stem cell culture and enrichment using poly(ϵ -caprolactone) scaffolds. *Molecules* **2016**, *21*, 537. [[CrossRef](#)] [[PubMed](#)]
26. Woodruff, M.A.; Huttmacher, D.W. The return of a forgotten polymer-Polycaprolactone in the 21st century. *Prog. Polym. Sci.* **2010**, *35*, 1217–1256. [[CrossRef](#)]



Chapter 12

Discussion and Conclusions

Abstract

Chapter 12 presents the discussion and conclusions of the present thesis work overviewing of the main results obtained. Also, a techno-economical comparison between laser cutting and 3D printing for BRS production is presented. The chapter ends with a serie of future works that could be necessary and interesting to perform.

12.1 Discussion

The inclusion of BRS concept made us to ask ourself about the applicability of current laser micro cutting process for the manufacture of this new medical device. The question basically was if this manufacturing process is able to cut the most promising materials for BRS, namely, polymers.

After the deep literature review performed in Chapter 1 and 2 the main objectives of the present thesis work were established based on the principal BRS challenges in the end of 2015. These challenges could be organized in four wide objectives: (I) Analyse the feasibility of laser cutting technology for the manufacture of BRS made of polymers, and (II) Analyse new manufacturing methods for this device that accomplish with all the strict requirements, (III) Analyse the effect the sterilization processes have on the polymeric materials properties, and (IV) Design and implement news BRS concepts made of polymer that accomplish with the BRS requirements.

At this point arised the Chapter 3. Fibre Laser Cutting of Polymer Sheets. The main objective of Chapter 3 was to analyse the feasibility of fibre laser to cut one of the most promising material for BRS, the Polycaprolactone (PCL). To feasibility study was performed by theoretical and empirical tests analysing how fiber laser process parameters affect the cutting precision and material properties.

Theoretical study revealed the feasibility of fibre laser process to achieve a complete cut of polymeric material, giving way to empirical study. To this part of the study the most important process parameters in laser cutting, namely, Peak Pulse Power, Cutting Speed, and Number of Passes, were selected and analysed by a Full Factorial Design in order to find the best parameter setup to obtain a precise cut with the less material affectation.

It was found the strong influence the Peak Pulse Power and Number of Passes have on the process to achieve a complete penetration of the material. Although the increase of these two parameters reduced the dimensional precision, also reduced the taper angle. With regards to the material properties, laser process has exhibited a lesser effect upon them [41], surely, because of the lower absorption coefficient at our laser wavelength, that reduced the thermal effect over the material structure, and thus, over their properties.

This chapter exhibited, for the first time in literature, the feasibility of fibre laser to cut polycaprolactone sheet with great precision and barely affecting the mechanical material properties. Nevertheless it was found necessary to perform further studies to analyse the effects the laser cutting process has on the main BRS property, its degradation rate, giving rise to Chapter 4.

Chapter 4. Effect of Fibre Laser on Degradation aimed to study the effect the fibre laser cutting process has upon the degradation rate of polycaprolactone. The degradation rate of biodegradable stents is one of the most important factor upon making these devices. The research for a degradable material that shows mechanical properties similar to the current permanent stents in the market and an appropriate degradation rate was and still is an open challenge.

Literature has shown the degradation rate of some biodegradable materials before the stent manufacturing process employing in-vitro degradation methods in static conditions which does not match properly with the real body conditions. Study the effects the manufacturing process has on BRS degradation properties in conditions more similar to body conditions was necessary. In the looking for these objectives, in Chapter 4 the influence the input energy density (E_{LASER}) and the degradation conditions have over the degradation rate, the geometrical changes, and the surface morphology was analysed during 8 weeks.. The degradation tests were carried out with a novel in-vitro method (dynamic) closer to body conditions and were compared with the traditional in-vitro method (static). This approach was not presented in the available literature.

Results showed that 1.08 μm wavelength Nd:YAG fibre laser affect the PCL degradation rate by accelerating it according the E_{LASER} level. This fact is mainly produced by the chains breakup that the laser irradiation produces in the material. SEM images showed a decrease in the surface imperfections in the HAZ due to the part of energy reflected towards the nozzle raises their temperature, affecting the surrounded areas of the cut-off point. All these effects make us affirm that although the laser appears to be the perfect tool for stent manufacture process because of their high precision, we must be thorough with the effect that this process cause in the material properties. Regards to the degradation method employed, results showed the strong differences between the static method and the dynamic method, which are closer to body conditions. Whereas the static method have given degradation curves according with the literature [53], the dynamics method has shown an increases in the water absorption, fact that will accelerate the degradation rate in a medium-large period of time, besides the material alteration that will reduce the resistance and the hardness of the stent, increasing it tenacity [53].

Based on the results of Chapter 3 and 4 it could be concluded that 1.08 μm fibre laser is a profitable tool to cut polymers. However for real BRS, it was necessary to study the laser process on tubes. Analyse the manufacturing process of these tubes as well as the feasibility of laser to cut them gave rise to Chapters 5 and 6.

The first step to produce real polymeric BRS is to produce the tubes for the subsequent laser cutting process. In this context emerge Chapter 5 Stents Tubes Fabrication by Dip Coating. Traditionally, tubes for stent purposes are produced by extrusion process. Nevertheless, study other technologies, such as Dip Coating became necessary due to, theoretically, presents some advances such as the possibility to produce composite tubes or a better control over the final tube thickness.

Chapter 5. Stents Tubes Fabrication by Dip Coating presented the effects the Dip Coating parameters have on the final properties of PCL, PLA, and PCL/PLA tubes for stent purposes. The effects the withdrawal speed, the number of cycles, and the solution's concentration have over the physical properties were studied. Four different tubes were fabricated with different order of layers, namely, PCL, PLA, PCL/PLA, and PLA/PCL. The tubes were analysed by Dynamic Mechanical Analysis (DMA), Surface Roughness, Dimensional Uniformity, and Degradation Study in order to find the best tube for stent purposes.

Results showed the strong influence the withdrawal speed and polymer's concentration have on the layer thickness and superficial roughness. DMA results showed some limitations of PCL and PLA as materials for the stent purpose by themselves, meanwhile the composite PCL/PLA tube showed a behaviour close to the stent requirements. The degradation study corroborated the statement that the PCL/PLA composites could be a promise material for the biodegradable stents purpose.

This chapter presented just a preliminary study that allow us to believe that a composite tubes made of PCL and PLA could be a good solution for the biodegradable stent market. Although the tests carried out were only one of many test that a stent should be go through to say that their properties are adequate, the chapter showed a good approximation of the potential of composite tubes.

The inclusion of composite tube idea for stent purposes opened a new window to solve other BRS problems such as the rapid endothelization. It is well known that PCL and PLA produce different cell proliferations, thus, a composite PCL/PLA stent could be beneficial to induce a rapid cell growth in its external wall, inducing a rapid endothelization, and on the contrary a low cell growth in its internal wall, reducing the risk of restenosis. This idea was reserved waiting to know if the 1.08 μm fibre laser is capable of cutting these tubes made of two different material with the precision required to manufacture BRS, study performed in the Chapter 6.

Chapter 6. Fibre Laser Cutting of Polymer Tubes aimed to study the effects the fiber laser cutting process has on polycaprolactone (PCL), polylactide acid (PLA), and PLA-PCL tubes for stent manufacturing. The effects the Power, Cutting Speed, and Number of Passes have over Penetration, Precision, and Dross were presented.

Results showed the difficulties to cut PLA with 1.08 μm wavelength lasers, being impossible to achieve a complete penetration both the PLA tubes, as PLA-PCL composite tubes. This is produce by the low absorption coefficient of PLA at laser wavelength 1.08 μm . To be able to penetrate the material completely, the laser power should be to high, increasing the energy reflected and thus, raising the nozzle temperature. This increase on nozzle temperature affects the surrounding cut-off zones and produces unexpected damages, making impossible the correct cutting process of the tubes made of PLA or a composite of it.

Nevertheless, in the case of PCL tubes, fibre laser was able to achieve a complete penetration of the material with dimensional precisions above than 95.75 %. Results showed an increasing trend when kerf width is compared with the number of passes raises. That increasing trend is due to the increases of the input energy density accumulated in the cut-off point. Regarding the Dross, results showed how the average dross area is reduced according to the cutting speed reduces. According to power results, a downward trend according to power increases is seen. However large amounts of Dross were found alongside to a non desirable HAZ.

Fibre laser has been shown to be a profitable tool to cut polycaprolactone tube with precision but have problem to cut other polymeric materials. Nevertheless the high cost of this technology and the pre-processing and post-processing that it required makes necessary the study of new technologies to produce BRS based on polymers that allows a better versatility and lower costs.

As mentioned in the Chapter 2, one possible solution could be the use of 3D Printing based on FFF technology. However FFF machines currently in the market/literature follow a Cartesian Coordinates a methodology that difficult the BRS manufacturing process. Because of that, a new machine design that involve a new methodology is necessary to manufacture BRS stents because of its tubular shape. This new methodology could be based on Cylindrical Coordinates. This new concept has been developed, for the first time, in this thesis work and it is present in the Chapter 7.

Chapter 7. Novel 3D Additive Manufacturing Machine presented the design, implementation, and proof of concept of Tubular 3D Printer to manufacture BRS based on polymers. The technology presented in this chapter has demonstrated the feasibility of Tubular 3D Printing to produce BRS based on polymers in just one step and in minutes. In order to perform a proof of concept, the effects the temperature, printing speed, and nozzle flow rate were studied to know if this new methodology is able to achieve the precision required for BRS production.

Results showed the strong influence the temperature and flow rate have over the printing precision. The correct selection of these two parameters becomes crucial to obtain the desired filament width and thus, the correct final dimensional accuracy. In general, the process showed a great stability, producing replicas almost 100% identical. Stability or replicability is a essential factor in stent production, to ensure the exact radial behaviour of this medical device. Also, as was expected 3D Printing process did not produce after-manufacturing problems such as dross, HAZ, or recast layer, what helps in the reduction of manufacturing steps.

Results allow us to believe that the novel technology presented in this chapter will be an interesting future research line reducing the times and costs in the manufacturing process of BRS. As have been mentioned in the chapter 2, the current stent manufacturing process by laser cutting involved at least 4 steps, meanwhile, the new manufacturing process introduced in this chapter involve only 2 steps. This could reduce the prices of this medical device.

The potential of Tubular 3D Printing for micro tubular medical devices manufacturing, such as stents, was introduced in this chapter. However, further studies about the effects the other printing parameters, materials, etc., have on the final stent properties would be interesting to perform. During the experiments, the commercial softwares available in the market to generate the G Code revealed their limitations. These softwares produced non optimal trajectories for tubular printing, producing some error in the final geometry of the stent. Create a tool to generate more optimal G Codes for this new 3D Printing methodology became necessary, as well as get in deep into the study of process parameters to know how affect to the main stents properties, namely, precision, material structure, or radial behavior among others.

These needs gave rise to the Chapter 8. Effect of Printing Process on PCL Stent in which the effects the nozzle temperature, printing speed, printing flow rate, and printing trajectories have on the dimensional precision and material structure distribution of samples were study.

To carry out the Chapter 8 experimentation, a Matlab Scrip was developed to avoid the above mentioned problems that 3D Printing commercial softwares present. With this new script we were able to study how the trayjectory affect the final precision of the stents. Trajectory A (along W axis), trajectory B (along X axis), and trajectory C (completing cells of the stent) were created. Trayjectory A showed to be the best trayjectory to produce stents by Tubular 3D Printing.

Regarding process parameters, printing temperature and printing flow rate showed again their strong influence over the dimensional precision of the printing process due to they are the parameters that control the filament width and subsequently the precision of the stent. In this study we were able to achieve precisions between 80% and 90%. Despite the gap until achieve a 100% of precision, the prediction model developed allow us to believe that mayor precision could be reached. The 3DP process precision could be improved by performing a calibration of the machine, and above all, studying the design of the extruder to achieve higher torque. The use of thinner nozzle would help to obtain better filament width and precisions.

Regards the material properties, 3D Printing process left some lesser effects over the material structure. Results showed the influence of all parameters, and their combination, over the material structure of the samples. The material's structure depend directly on the cooling rate employed to manufacture the material, thus, N_T , $F_R\%$, and P_S affect over this fact. The increase of N_T , $F_R\%$, combined with a reduction of P_S raises the material temperature, reducing the stent cooling rate. This fact allows a better placement of the polymer chains, increasing the crystallinity percentage. This effects were observed during the experiments developed in chapter 3 and 4 in which the increase of laser energy left higher crystallinity percentages.

Finally regarding of radial behaviour, all samples showed a great radial behaviour, regardless the printing process parameters. Generally, stents, exhibited an average of 320% of radial expansion with an average of 22.78% of recoil. The little differences in the material structure distribution corroborated that the differences in the radial expansion behaviour of samples were produced by the geometrical aspects of the stents.

This chapter evinced the feasibility of Tubular 3D Printing to produce stent made of polymers. However, analyse the effects the printing process has on the degradation rate of this materials becomes mandatory to validate the 3D Printing Tubular process for BRS manufacturing. Chapter 9 presented this study.

Chapter 9. 3D Printing Process on Degradation studied the effects the 3D-Printing process parameters have over the degradation rates of Polycaprolactone's (PCL) stents. The effects of nozzle temperature, printing speed, and printing flow rate were reported and related with the molecular weight, crystallinity, and degradation rate of the samples in static and dynamics conditions.

With regards to the process parameters, printing temperature, and printing flow rate have been presented as the most influence factors on the 3D-Printing process. The increase of these two parameters leaves a decrease of the molecular weight of the stents, increasing their crystallinity percentages and accelerating their degradation rates.

Regarding the degradation method employ, static conditions produced faster degradation of the samples compared with dynamics conditions. This fact could be produce by the contact between the PBS and the samples. In dynamics conditions the external wall of the stents is in contact with the pipe avoiding the contact of the PBS, while in static conditions the PBS surround the entire sample. Finally, regarding of radial behaviour of 3D-Printed stents, all the samples, showed a great radial stability after 8 week of degradation regardless the degradation conditions employ with an average of 320% of radial expansion and an average of 22.78% of recoil.

Although 3D-Printing process proved its effects over the degradation rate of the samples, these effects could be easily controlled and avoided stablishing the best printing process parameters.

In order to select the best manufacturing process for BRS it was necessary to analyse from a techno-economical point both processes. Based on the results obtained from chapter 3 to 9 it could be summarized in Table 12.1:

Table 12.1. Techno-Economical Comparison - Laser and 3D Printing (FFF)

TECHNO-ECONOMICAL COMPARISON			
Laser Cutting		Tubular 3D Printing	
✓	High Precision	✗	Medium-High Precision
✓	Low Material Affectation	✓	Low Material Affectation
✗	Long Manufacturing Process	✓	Short Manufacturing Process
✗	Expensive Implantation	✓	Cheap Implantation
✗	Low Material Versatility	✓	High Material Versatility
STENT OBTAINED COMPARISON			
✗	Sharp Struts	✓	Rounded Struts
✗	Expensive Customization	✓	Cheap Customization

It can be seen that Tubular 3D Printing based on FFF presents many advantages over the traditional laser cutting process. However, it worth to think about other possible Additive Manufacturing technologies for this purpose. With this objective, a literature review was done to find if other AM technology is more promising than Tubular FFF. It was found that only a few authors have been studying this process for BRS manufacturing, all of them in parallel of this thesis work and focused on stereolithography or sintering processes.

In 2016, Lith et al. [54] built a novel μ CLIP setup capable of speed ranging from 2.5 to 100 $\mu\text{m s}^{-1}$. Employing a Cypher BMS design they analyzed the effect of UV intensity, UV absorber, and wall thickness. Although results were promising, there are some limitations since the best performing stent had a fabrication of 70 min. Ware et al. [55] in 2017 reported the process development in manufacturing high-resolution bioresorbable stents using μ CLIP system. They employed 26.5 min to manufacture a 2 cm stent. One year later, Cabrera et al. [56] manufactured a BRS stent employing a traditional cartesian 3D printer. Although the results were promising the traditional 3D printer presents some limitations to manufacture tubular devices such as stent. In the field of BRS made of metallic material, In 2017, Demir et al. [57] produced CoCr stent through SLM as an alternative method to the conventional manufacturing cycle. Results showed that SLM can be considered as a substitute operation to laser micro cutting. Prototype stents with acceptable geometrical accuracy were achieved and surface quality could be improved through electrochemical polishing. The chemical composition remained unvaried, with a marginal increase in the oxide content.

AM processes has proved their effectiveness, and clearly they present a novel method to produce stents that could replace the current laser cutting process. Nevertheless all the processes studied present the same disadvantage, the lamination of the stents well in the radial direction or in the longitudinal direction. Depending on the AM process use manufacturer will have some advantages and disadvantages. Table 12.2 summarized some on them.

Table 12.2. AM Technologies Comparison

AM TECHNOLOGIES COMPARISON				
	Stereolithography Processes	Laser Sintering	FFF Traditional	FFF Tubular
Cost	High	High	Low	Low
Speed	Low	Low	High	High
Precision	High	High	Low	Medium
Lamination	Inevitable	Inevitable	Inevitable	Avoidable

Based on the literature review, we concluded that Tubular FFF could be the most promising technique, within the AM processes, for BRS production.

At this point, the thesis moved to the second stage showed in Figure 1.3. In this stage the main objective was to prove the biological evaluation of stents made by 3D Printing. According ISO 10993-1 when a long term implantable medical devices that is in contact with blood is produce with a new material or new manufacturing process, this device should be subjected to the a serie of tests to prove its biological safety (Table 12.3):

Table 12.3. Initial Evaluation Tests For Consideration (ISO 10993-1)

			CYTOTOXICITY	SENSITIZATION	IRRITATION	SYSTEMIC TOXICITY	SUBACUTE TOXICITY	GENOTOXICITY	IMPLANTATION	HAEMOCOMPATIBILITY	CHRONIC TOXICITY	CARCINOGENICITY	BIODEGRADATION
IMPLANT	BLOOD	C	x	x	x	x	x	x	x	x	x	x	x

Stents are categorized as implant device in contact with blood type C. To perform all these tests, stents should be sterilized. In the looking for the best sterilization process for this kind of medical device it was found that there are no studies about the effects the sterilization processes have on the material properties of stents made of polymers. For instance, Dai et al. [58] performed studies to determine the optimal sterilization method for biodegradable polyester for bone membranes using peroxide gas plasma, ethanol, and UV radiation, and determined that gas plasma showed the best results in terms of cell proliferation and differentiation. Meanwhile, Fischback et al. [59] studied the effects of UV on spin-cast films made from PLLA and PEG (polyethylene-glycol). Their results indicated that, as it did not produce alterations in cell adhesion, UV sterilization is an appropriate technique. Years later, Shearer et al. [60] analysed the effects ethanol, UV, antibiotic, and peracetic acid sterilization methods had on PLGA (poly-L-lactic-Co-Glycolic-Acid) scaffolds. Results suggested that antibiotic treatment was the method with most potential due to the low effects it exerted on the surface of the scaffolds. Despite the proven powerful effects that sterilization treatments have on the properties of polymeric materials [59]-[61], there are no studies about the effects such treatments have on a final medical device that has the high requirements that stents have. This established the need of Chapter 10 Effects of Sterilization on 3D-Printed Stent.

Chapter 10 presents the effect the most common sterilization processes, for *in-vitro* tests, have on the final properties of BRS made of polycaprolactone by Tubular 3D Printing. The effects of Ethanol, Antibiotic, and UV sterilization treatments at 0.5, 1, 2, 4, 8, and 16 hours have over the sterility, thermal stability, crystallinity structure, surface erosion, molecular weight, and degradation rates have been analysed and discussed.

UV treatment, from 2 hours, increased the surface erosion, the crystallinity, and the degradation rate. On the other hand, UV produced a reduction of the molecular weight. This fact is mainly produced by the photodegradation produced by UV irradiation. UV irradiation could be a good method to get the crystallinity, surface roughness, molecular weight, and degradation times desired. Nevertheless in the case of medical devices with such high material requirements, as is the case of stents, UV would not be the most adequate sterilization method.

Antibiotic method, from 16 hours, increased the surface erosion, barely affected the material crystallinity, and reduced the degradation rate and the molecular weight of the samples. All these facts could be produced by the degradation of the samples during the sterilisation treatment, because of the 1% Antibiotic that was employed. The increased of Antibiotic percentage not only could reduce the sterilization time, but also could reduce the effect over the material properties, mainly the surface erosion and the molecular weight changes.

Ethanol, from 8 hours and according to the experimental results, was the best method to sterilize 3D-Printed Polycaprolactone Stents. Ethanol barely affected the surface erosion and the crystallinity of the material. At higher sterilization times, Ethanol produced an increase of the degradation time. Once again, the changes produced by Ethanol in the material could be produced by the degradation of the samples during the sterilization treatment. In this case, unlike Antibiotic treatment, Ethanol only contained a 30% of PBS, reducing the degradation of the samples during the treatment and thus decreasing the changes on the material properties.

This work demonstrated the influences the sterilization treatments have over the materials properties, and thus, on the final behaviour of this device. It is important to study the sterilization of the medical devices with such high material requirements, such as stents, due to sterilization is the final manufacture process that suffer the medical devices, and it can changes the devices properties. Further works that study the effects the sterilization method in clinical practise have on the properties of stents becomes crucial.

Once the effects the manufacturing process and the sterilization treatment have been analyzed, we pushed forward to the last objective of this thesis work, design and develop a new BRS concept to solve the current problems. Based on the promising results of chapter 5, arise the idea of Chapter 11 3D-Printed Composite BRS, which with our best knowledge, it the first work about composite PCL/PLA stents using a 3D-printing process based on FFF. The effects the cell geometry (shape and area) and materials (PCL and PLA) have on 3T3 cell proliferation, degradation, dynamic mechanical properties and radial behavior were analyzed and discussed.

Results demonstrated the considerable influence the cell area and material of a stent have on 3T3 proliferation. That said, the cell shape of the stent did not show any significant influence at all. Our initial hypothesis was confirmed, i.e., the smaller the cell area of a stent, the better the cell proliferation rate. Meanwhile, PCL demonstrated better cell proliferation than PLA. Dynamics mechanical and degradation results confirmed the results obtained in Chapter 5. PLA showed its limitations due to its fast degradation and high E modulus, while PCL showed a better degradations rates for long term implantable devices but a very low E modulus. The composite PCL/PLA stents showed an almost medium degradation for all the layer configurations and a middle E modulus. The faster PLA degradation rate would eventually leave a BRS made only of PCL. Employing PCL and PLA with similar molecular weights is a must to obtain a homogenous degradation of all the layers.

Finally, the radial behavior results proved that composite PCL/PLA stents could be used to improve each material's separate limitations. For instance, PCL stents presented overly high recoil ratios but excellent expansion behavior, whereas PLA stents presented inadequate radial expansion, due to their rigidity, but excellent recoil ratio. Composite stents, either with PCL or PLA as the inner layer, demonstrated the virtues of PCL stents (i.e., their radial expansion) and PLA stents (i.e., their recoil ratio) that could be combined to provide a good solution for BRS. Their good radial behavior make composite stents a promising concept for cardiovascular problems.

Based on the thesis results it can be concluded that Tubular 3D Printing based on FFF could be a promising technique for BRS production. Regarding the stents design, polymeric composite stents have shown great properties, and they could establish a new and interesting market. The present thesis work has tried to analyze the entire manufacturing process, including the last and mandatory sterilization process. This thesis establish a starting point in the BRS manufacturing field through 3D Printing technologies. To conclude the discussion section, Figure 12.1 shows the main contribution of this thesis chronologically ordered.

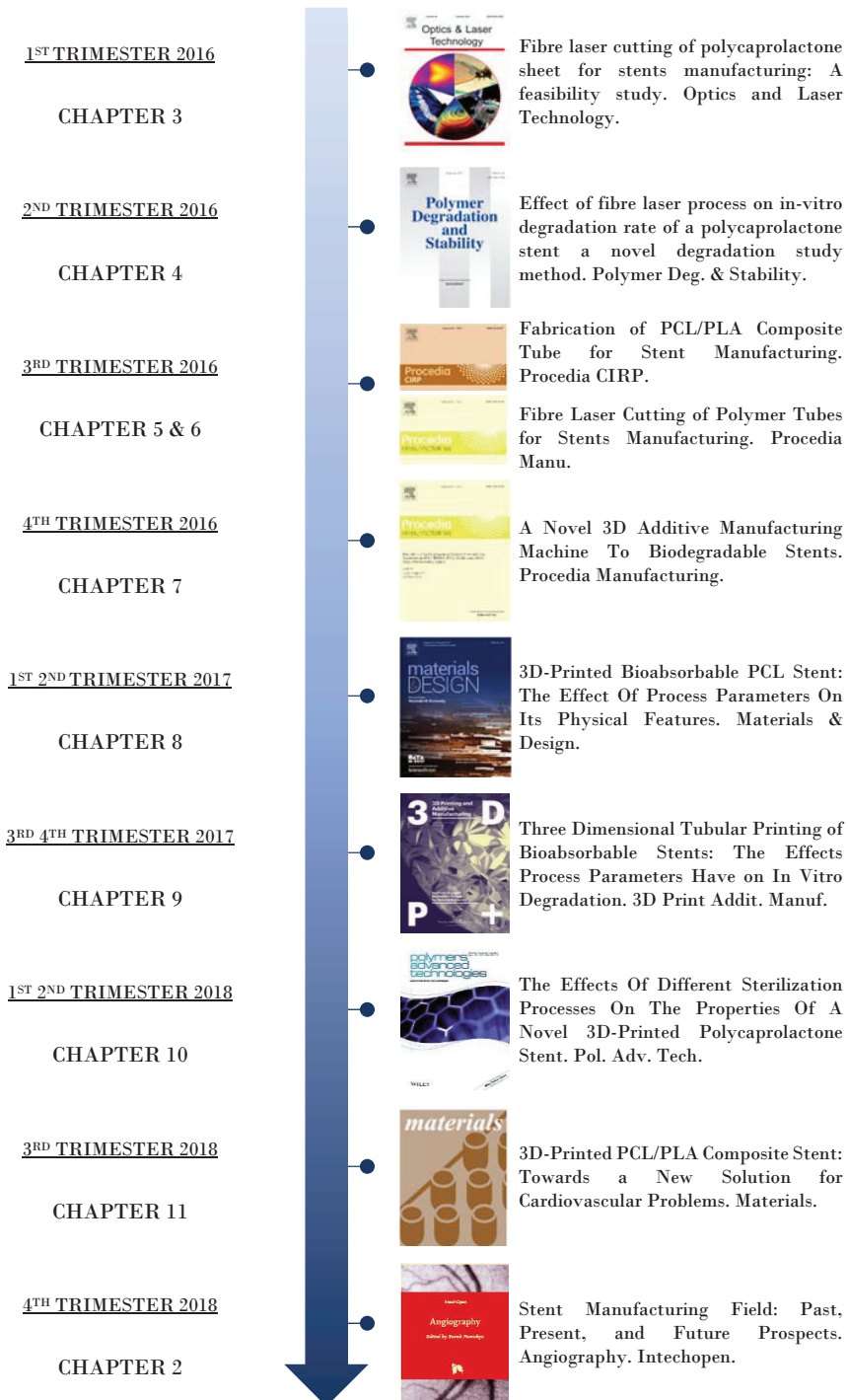


Figure 12.1. Thesis Contributions

12.2 Conclusions

Chapter 03. Peak Pulse Power and Number of Passes are the most important parameters to achieve a complete penetration of the material, while the Cutting Speed did not show any strong influence.

Chapter 03. The increase of Peak Pulse Power and Number of Passes reduced the dimensional precision, but, also reduced the taper angle. Also, the increase on these two parameters, increase the reflected energy, warming up the nozzle temperature and producing undesired defects in the nearby areas.

Chapter 03. Laser process has exhibited a lesser effect upon material properties, surely, because of the lower absorption coefficient at our laser wavelength, that reduced the thermal effect over the material structure.

Chapter 03. The feasibility of fibre laser to cut polycaprolactone sheet with great precision and barely affecting the mechanical material properties was proved.

Chapter 04. Results showed that 1.08 μm wavelength Nd:YAG fibre laser affect the PCL degradation rate by accelerating it according the E_{LASER} level. This fact is mainly produced by the chains breakup that the laser irradiation produces in the material.

Chapter 04. SEM images showed a decrease in the surface imperfections in the HAZ due to the part of energy reflected towards the nozzle raises their temperature, affecting the surrounded areas of the cut-off point.

Chapter 04. Results showed the strong differences between the static method and the dynamic method, which are closer to body conditions. Static method have given degradation curves according with the literature, but the dynamics method has shown an increases in the water absorption, fact that will accelerate the degradation rate in a medium-large period of time.

Chapter 04. Based on the results of Chapter 3 and 4 it could be concluded that 1.08 μm fibre laser is a profitable tool to cut biodegradable polymers such as polycaprolactone.

Chapter 05. Results showed the strong influence the withdrawal speed and polymer's concentration have on the layer thickness and superficial roughness of the tubes.

Chapter 05. DMA results showed some limitations of PCL and PLA as materials for the stent purpose by themselves, meanwhile the composite PCL/PLA tube showed a behaviour close to the stent requirements.

Chapter 05. The degradation study corroborated the statement that the PCL/PLA composites could be a promise idea for biodegradable stents purpose.

Chapter 05. Dip Coating has proven its validity as manufacturing method for polymeric tubes.

Chapter 06. Results showed the difficulties to cut PLA with 1.08 μm wavelength lasers, being impossible to achieve a complete penetration both the PLA tubes, as PLA-PCL composite tubes. This is produce by the low absorption coefficient of PLA at laser wavelength 1.08 μm .

Chapter 06. For PCL tubes, fibre laser was able to achieve a complete penetration of the material with dimensional precisions above than 95.75 %.

Chapter 06. Results showed an increasing trend when kerf width is compared with the number of passes raises. That increasing trend is due to the increases of the input energy density accumulated in the cut-off point.

Chapter 06. Regarding the Dross, results showed how the average dross area is reduced according to the cutting speed reduces. According to power results, a downward trend according to power increases is seen. However large amounts of Dross were found alongside to a non desirable HAZ.

Chapter 06. Fibre laser has been shown to be a profitable tool to cut polycaprolactone tube with precision but have problem to cut other polymeric materials.

Chapter 06. The high cost of laser technology and the pre-processing and post-processing required makes necessary the study of new technologies to produce BRS based on polymers that allows a better versatility and lower costs.

Chapter 07. Results have demonstrated the feasibility of Tubular 3D Printing to produce BRS based on polymers in just one step and in minutes.

Chapter 07. Results showed the strong influence the temperature and flow rate have over the printing precision. The correct selection of these two parameters becomes crucial to obtain the desired filament width and thus, the correct final dimensional accuracy.

Chapter 07. The process showed a great stability, producing replicas almost 100% identical. Stability or replicability is a essential factor in stent production, to ensure the exact radial behaviour of this medical device.

Chapter 07. Tubular 3D Printing process did not produce after-manufacturing problems such as dross, HAZ, or recast layer, what helps in the reduction of manufacturing steps.

Chapter 07. Results allow us to believe that the novel technology presented in this chapter will be an interesting future research line reducing the times and costs in the manufacturing process of BRS.

Chapter 08. Matlab Scrip was successfully developed to avoid the problems that 3D Printing commercial softwares present. Trajectory A (along W axis), trajectory B (along X axis), and trajectory C (completing cells of the stent) were created. Trajectory A showed to be the best trajectory to produce stents by Tubular 3D Printing.

Chapter 08. Printing temperature and printing flow rate showed again their strong influence over the dimensional precision of the printing process due to they are the parameters that control the filament width and subsequently the precision of the stent. The use of thinner nozzle would help to obtain better filament width and precisions.

Chapter 08. 3D Printing process left some lesser effects over the material structure. Results showed the influence of all parameters, and their combination, over the material structure of the samples. The increase of N_T , $F_R\%$, combined with a reduction of P_S raises the material temperature, reducing the stent cooling rate. This fact allows a better placement of the polymer chains, increasing the crystallinity percentage.

Chapter 08. Finally apropos of radial behaviour, all samples showed a great radial behaviour, regardless the printing process parameters. Generally, stents, exhibited an average of 320% of radial expansion with an average of 22.78% of recoil.

Chapter 08. The little differences in the material structure distribution corroborated that the differences in the radial expansion behaviour of samples were produced by the geometrical aspects of the stents.

Chapter 08. This chapter evinced the feasibility of Tubular 3D Printing to produce stent made of polymers.

Chapter 09. Printing temperature, and printing flow rate were the most influence factors on the 3D-Printing process. The increase of these two parameters leaves a decrease of the molecular weight of the stents, increasing their crystallinity percentages and accelerating their degradation rates.

Chapter 09. Regarding the degradation method employ, static conditions produced faster degradation of the samples compared with dynamics conditions. This fact could be produce by the contact between the PBS and the samples. In dynamics conditions the external wall of the stents is in contact with the pipe avoiding the contact of the PBS, while in static conditions the PBS surround the entire sample.

Chapter 09. Finally, regarding of radial behaviour of 3D-Printed stents, all the samples, showed a great radial stability after 8 week of degradation regardless the degradation conditions employ with an average of 320% of radial expansion and an average of 22.78% of recoil.

Chapter 09. Although 3D-Printing process proved its effects over the degradation rate of the samples, these effects could be easily controlled and avoided stablishing the best printing process parameters.

Chapter 10. UV treatment, from 2 hours, increased the surface erosion, the crystallinity, and the degradation rate and reduced the molecular weight.

Chapter 10. UV irradiation could be a good method to get the crystallinity, surface roughness, molecular weight, and degradation times desired. Nevertheless in the case of medical devices with such high material requirements, as is the case of stents, UV would not be the most adequate sterilization method.

Chapter 10. Antibiotic method, from 16 hours, increased the surface erosion, barely affected the material crystallinity, and reduced the degradation rate and the molecular weight of the samples. All these facts could be produced by the degradation of the samples during the sterilisation treatment, because of the 1% Antibiotic that was employed.

Chapter 10. The increased of Antibiotic percentage not only could reduce the sterilization time, but also could reduce the effect over the material properties, mainly the surface erosion and the molecular weight changes.

Chapter 10. Ethanol, from 8 hours and according to the experimental results, was the best method to sterilize 3D-Printed Polycaprolactone Stents. Ethanol barely affected the surface erosion and the crystallinity of the material. At higher sterilization times, Ethanol produced an increase of the degradation time.

Chapter 11. Results demonstrated the considerable influence the cell area and material of a stent have on 3T3 proliferation. That said, the cell shape of the stent did not show any significant influence at all.

Chapter 11. PCL demonstrated better cell proliferation than PLA. This fact could be beneficial to create a composite stent with outer layer made of PCL to make it easy the endothelial cell growth and an inner layer made of PLA to slow down the cell in charge of restenosis.

Chapter 11. Dynamics mechanical and degradation results confirmed the results obtained in Chapter 5. PLA showed its limitations due to its fast degradation and high E modulus, while PCL showed a better degradations rates for long term implantable devices but a very low E modulus.

Chapter 11. The composite PCL/PLA stents showed an almost medium degradation for all the layer configurations and a middle E modulus. The faster PLA degradation rate would eventually leave a BRS made only of PCL. Employing PCL and PLA with similar molecular weights is a must to obtain a homogenous degradation of all the layers.

Chapter 11. Radial behavior results proved that composite PCL/PLA stents could be used to improve each material's separate limitations. For instance, PCL stents presented overly high recoil ratios but excellent expansion behavior, whereas PLA stents presented inadequate radial expansion, due to their rigidity, but excellent recoil ratio.

Chapter 11. Composite stents, either with PCL or PLA as the inner layer, demonstrated the virtues of PCL stents (i.e., their radial expansion) and PLA stents (i.e., their recoil ratio) that could be combined to provide a good solution for BRS. Their good radial behavior make composite stents a promising concept for cardiovascular problems.

Chapter 12. The present thesis work has proved the feasibility of laser cutting process to cut some polymeric materials for BRS purposes. However, the difficulties to cut a wide range of material and the pre-processing and post-processing required to obtain a functional BRS made us wonder about the applicability of this technique to BRS production.

Chapter 12. The strong presence of polymers in the BRS field makes us think that other manufacturing techniques could be better for this medical devices. Between all the manufacturing techniques for polymers stand out the Additive Manufacturing processes.

Chapter 12. Based on the literature review and the research performed in the course of this thesis, it can be concluded that the novel Tubular 3D Printing process invented and developed in this work is the most promising AM technique for BRS production, due to is most versatile, fastest, and the cheapest AM process.

12.3 Future Works

This section suggests some ideas to continue with the research of BRS manufacturing. Ideas are separated into two stage, (I) Manufacturing Stage, and (II) Biological Stage.

12.3.1 Manufacturing

- Deepen in the BRS stent design to obtain a polymeric BRS stent that accomplish with the same longitudinal and radial behaviour of current permanent stents.
- Analyse the effects the Tubular 3D Printing process parameters on the final dimensional and material properties of stent made of other polymers such as PLGA or PLLA.
- Produce polymeric filament, for 3D Printing based on FFF, that include the most common drugs used in the current clinical practise to being able to print Drug Eluting Bioabsorbable Stents in just one step.
- Analyse other possible composites configuration employing other biodegradable polymers such as PLGA, PCL, PGA, or PLLA.

12.3.2 Biological

- Perform the biological tests summarized in Table 12.3 to ensured that Tubular 3D Printing is a safe manufacturing process for implantable medical devices, such as stents.
- Design a bioreactor system that allows the study of the stents in *ex-vivo* conditions, being able to simulate real *in-vivo* conditions, blood pressure, contact with real vessel, etc., in labs facilities.
- Analyse the effects the sterilization treatment, used in the clinical practice for this kind of medical devices, have on the final BRS properties.
- Analyse the crimping process of BRS made of polymers by 3D Printing to ensure the safety attachment of this medical devices to its catheter and thus the correct placement of the BRS in the body.

Chapter 13

References

- [1] Serruys PW, De Jaegere P, Kiemeneij F, Macaya C, Rutsch W, Heyndrickx G, “A Comparison Of Balloon-Expandable-Stent Implantation With Balloon Angioplasty In Patients With Coronary Artery Disease.,” *N. Engl. J. Med.*, Vol. 331, Pp. 489–95, 1994.
- [2] R. S. Schwartz, E. J. Topol, P. W. Serruys, G. Sangiorgi, And J. Holmes D.R., “Artery Size, Neointima, And Remodeling: Time For Some Standards,” *J. Am. Coll. Cardiol.*, Vol. 32, No. 7, Pp. 2087–2094, 1998.
- [3] R. Waksman, “Update On Bioabsorbable Stents: From Bench To Clinical,” *J. Interv. Cardiol.*, Vol. 19, No. 5, Pp. 414–421, 2006.
- [4] J. S. Soares And J. E. Moore, “Biomechanical Challenges To Polymeric Biodegradable Stents,” *Ann. Biomed. Eng.*, 2015.
- [5] Medipoint, “Coronary Stents – Global Analysis And Market Forecasts,” P. 34, 2014.
- [6] J. D. B. John D.Enderle, *Introduction To Biomedical Engineering*, Vol. 75. 2012.
- [7] A. Roguin, “Stent: The Man And Word Behind The Coronary Metal Prosthesis,” *Circ. Cardiovasc. Interv.*, Vol. 4, No. 2, Pp. 206–209, 2011.
- [8] S. H. Im, Y. Jung, And S. H. Kim, “Current Status And Future Direction Of Biodegradable Metallic And Polymeric Vascular Scaffolds For Next-Generation Stents,” *Acta Biomater.*, Vol. 60, Pp. 3–22, 2017.
- [9] M. I. Ther, A. Technol, D. Stoeckel, C. Bonsignore, And S. Duda, “A Survey Of Stent Designs,” *Cell*, Vol. 11, No. 4, Pp. 137–147, 2002.
- [10] Y. P. Kathuria, “The Potential Of Biocompatible Metallic Stents And Preventing Restenosis,” *Mater. Sci. Eng. A*, Vol. 417, No. 1–2, Pp. 40–48, 2006.
- [11] J. A. Nordin, A. K. Nasution, And H. Hermawan, “Can The Current Stent Manufacturing Process Be Used For Making Metallic Biodegradable Stents,” *Adv. Mater. Res.*, Vol. 746, Pp. 416–421, 2013.
- [12] D. Yuan And S. Das, “Experimental And Theoretical Analysis Of Direct-Write Laser Micromachining Of Polymethyl Methacrylate By CO[Sub 2] Laser Ablation,” *J. Appl. Phys.*, Vol. 101, No. 2007, P. 024901, 2007.
- [13] Y. T. Yung KC, Zhu HH, “Theoretical And Experimental Study On The Kerf Profile Of The Laser Micro-Cutting Niti Shape Memory Alloy Using 355 Nm Nd:YAG,” *Smart Mater. Struct.*, Vol. 14, Pp. 337–342, 2005.

- [14] C. Abeykoon, A. L. Kelly, J. Vera-Sorroche, E. C. Brown, P. D. Coates, J. Deng, K. Li, E. Harkin-Jones, And M. Price, "Process Efficiency In Polymer Extrusion: Correlation Between The Energy Demand And Melt Thermal Stability," *Appl. Energy*, Vol. 135, Pp. 560–571, 2014.
- [15] Kleine KF; Whitney B; Watkins KG, "Use Of Fiber Lasers For Micro Cutting Applications In Medical Device Industry," *21st Int. Congr. Appl. Lasers Electro-Optics*, 2002.
- [16] H. Huang, H. Y. Zheng, And G. C. Lim, "Femtosecond Laser Machining Characteristics Of Nitinol," *Appl. Surf. Sci.*, Vol. 228, No. 1–4, Pp. 201–206, 2004.
- [17] A. Raval, A. Choubey, C. Engineer, And D. Kothwala, "Development And Assessment Of 316LVM Cardiovascular Stents," *Mater. Sci. Eng. A*, Vol. 386, No. 1–2, Pp. 331–343, 2004.
- [18] Y. P. Kathuria, "Laser Microprocessing Of Metallic Stent For Medical Therapy," *J. Mater. Process. Technol.*, Vol. 170, No. 3, Pp. 545–550, 2005.
- [19] L. Shanjin And W. Yang, "An Investigation Of Pulsed Laser Cutting Of Titanium Alloy Sheet," *Opt. Lasers Eng.*, Vol. 44, No. 10, Pp. 1067–1077, 2006.
- [20] M. Baumeister, K. Dickmann, And T. Hoult, "Fiber Laser Micro-Cutting Of Stainless Steel Sheets," *Appl. Phys. A*, Vol. 85, No. 2, Pp. 121–124, 2006.
- [21] C. Lia, S. Nikumb, And F. Wong, "An Optimal Process Of Femtosecond Laser Cutting Of Niti Shape Memory Alloy For Fabrication Of Miniature Devices," *Opt. Lasers Eng.*, Vol. 44, No. 10, Pp. 1078–1087, 2006.
- [22] Y.-H. Meng, H.-Y., Liao, J.-H., Guan, B.-G., Zhang, Q.-M., Zhou, "Fiber Laser Cutting Technology On Coronary Artery Stent," *Chinese J. Lasers*, Vol. 34(5), Pp. 733–736, 2007.
- [23] H. Meng, J. Liao, Y. Zhou, And Q. Zhang, "Laser Micro-Processing Of Cardiovascular Stent With Fiber Laser Cutting System," *Opt. Laser Technol.*, Vol. 41, No. 3, Pp. 300–302, 2009.
- [24] R. Pfeifer, D. Herzog, M. Hustedt, And S. Barcikowski, "Pulsed Nd:YAG Laser Cutting Of Niti Shape Memory Alloys—Influence Of Process Parameters," *J. Mater. Process. Technol.*, Vol. 210, No. 14, Pp. 1918–1925, 2010.
- [25] T. L. Scintilla LD, Sorgente D, "Experimental Investigation On Fiber Laser Cutting Of Ti6Al4V Thin Sheet," *Adv. Mater. Res.*, Vol. 264–265, Pp. 1281–1286, 2011.

- [26] J. Powell, S. O. Al-Mashikhi, A. F. H. Kaplan, And K. T. Voisey, "Fibre Laser Cutting Of Thin Section Mild Steel: An Explanation Of The 'Striation Free' Effect," *Opt. Lasers Eng.*, Vol. 49, No. 8, Pp. 1069–1075, 2011.
- [27] N. Muhammad, D. Whitehead, A. Boor, W. Oppenlander, Z. Liu, And L. Li, "Picosecond Laser Micromachining Of Nitinol And Platinum-Iridium Alloy For Coronary Stent Applications," *Appl. Phys. A Mater. Sci. Process.*, Vol. 106, No. 3, Pp. 607–617, 2012.
- [28] L. D. Scintilla And L. Tricarico, "Experimental Investigation On Fiber And CO2 Inert Gas Fusion Cutting Of AZ31 Magnesium Alloy Sheets," *Opt. Laser Technol.*, Vol. 46, Pp. 42–52, 2013.
- [29] D. Teixidor, J. Ciurana, And C. A. Rodriguez, "Dross Formation And Process Parameters Analysis Of Fibre Laser Cutting Of Stainless Steel Thin Sheets," *Int. J. Adv. Manuf. Technol.*, Vol. 71, No. 9–12, Pp. 1611–1621, 2014.
- [30] C. H. Fu, J. F. Liu, And A. Guo, "Statistical Characteristics Of Surface Integrity By Fiber Laser Cutting Of Nitinol Vascular Stents," *Appl. Surf. Sci.*, Vol. 353, Pp. 291–299, 2015.
- [31] A. Kruusing, "Underwater And Water-Assisted Laser Processing: Part 1 - General Features, Steam Cleaning And Shock Processing," *Opt. Lasers Eng.*, Vol. 41, Pp. 307–327, 2004.
- [32] A. Kruusing, "Underwater And Water-Assisted Laser Processing: Part 2 - Etching, Cutting And Rarely Used Methods," *Opt. Lasers Eng.*, Vol. 41, No. 2, Pp. 329–352, 2004.
- [33] K. L. Choo, Y. Ogawa, G. Kanbargi, V. Otra, L. M. Raff, And R. Komanduri, "Micromachining Of Silicon By Short-Pulse Laser Ablation In Air And Under Water," *Mater. Sci. Eng. A*, Vol. 372, Pp. 145–162, 2004.
- [34] G. Daminelli, J. Krüger, And W. Kautek, "Femtosecond Laser Interaction With Silicon Under Water Confinement," *Thin Solid Films*, Vol. 467, No. 1–2, Pp. 334–341, 2004.
- [35] S. C. Authors Of Document An, R., Hoffman, M.D., Donoghue, M.A., Hunt, A.J., Jacobson, "Water-Assisted Femtosecond Laser Machining Of Electrospray Nozzles On Glass Microfluidic Devices," *Opt. Express*, Vol. 16(19), Pp. 15206–15211, 2008.
- [36] P. Kaakkunen, J.J.J., Silvennoinen, M., Paivasaari, K., Vahimaa, "Water-Assisted Femtosecond Laser Pulse Ablation Of High Aspect Ratio Holes," *Phys. Procedia*, Vol. 12 (PART2), Pp. 88–93, 2011.
- [37] N. Muhammad, D. Whitehead, A. Boor, And L. Li, "Comparison Of Dry And Wet Fibre Laser Profile Cutting Of Thin 316L Stainless Steel Tubes For

- Medical Device Applications,” *J. Mater. Process. Technol.*, Vol. 210, No. 15, Pp. 2261–2267, 2010.
- [38] J. Yang, F. Cui, And I. S. Lee, “Surface Modifications Of Magnesium Alloys For Biomedical Applications,” *Ann. Biomed. Eng.*, Vol. 39, No. 7, Pp. 1857–1871, 2011.
- [39] N. Muhammad And L. Li, “Underwater Femtosecond Laser Micromachining Of Thin Nitinol Tubes For Medical Coronary Stent Manufacture,” *Appl. Phys. A Mater. Sci. Process.*, Vol. 107, No. 4, Pp. 849–861, 2012.
- [40] D. Lootz, D. Behrend, S. Kramer, T. Freier, A. Haubold, G. Benkießer, K. P. Schmitz, And B. Becher, “Laser Cutting: Influence On Morphological And Physicochemical Properties Of Polyhydroxybutyrate,” *Biomaterials*, Vol. 22, No. 18, Pp. 2447–2452, 2001.
- [41] N. Grabow, M. Schlun, K. Sternberg, N. Hakansson, S. Kramer, And K.-P. Schmitz, “Mechanical Properties Of Laser Cut Poly(L-Lactide) Micro-Specimens: Implications For Stent Design, Manufacture, And Sterilization.,” *J. Biomech. Eng.*, Vol. 127, No. February 2005, Pp. 25–31, 2005.
- [42] F. Caiazzo, F. Curcio, G. Daurelio, And F. M. C. Minutolo, “Laser Cutting Of Different Polymeric Plastics (PE, PP And PC) By A CO₂ Laser Beam,” *J. Mater. Process. Technol.*, Vol. 159, No. 3, Pp. 279–285, 2005.
- [43] K. S. Tiaw, M. H. Hong, And S. H. Teoh, “Precision Laser Micro-Processing Of Polymers,” *J. Alloys Compd.*, Vol. 449, No. 1–2, Pp. 228–231, 2008.
- [44] N. Masmiaati And P. K. Philip, “Investigations On Laser Percussion Drilling Of Some Thermoplastic Polymers,” *J. Mater. Process. Technol.*, Vol. 185, No. 1–3, Pp. 198–203, 2007.
- [45] G. M. Baer, W. Small, T. S. Wilson, W. J. Bennett, D. L. Matthews, J. Hartman, And D. J. Maitland, “Fabrication And In Vitro Deployment Of A Laser-Activated Shape Memory Polymer Vascular Stent.,” *Biomed. Eng. Online*, Vol. 6, P. 43, 2007.
- [46] J. P. Davim, N. Barricas, M. Conceição, And C. Oliveira, “Some Experimental Studies On CO₂ Laser Cutting Quality Of Polymeric Materials,” *J. Mater. Process. Technol.*, Vol. 198, No. 1–3, Pp. 99–104, 2008.
- [47] I. A. Choudhury And S. Shirley, “Laser Cutting Of Polymeric Materials: An Experimental Investigation,” *Opt. Laser Technol.*, Vol. 42, No. 3, Pp. 503–508, 2010.
- [48] W. Y. Yeong, K. P. Lim, G. Ka Lai Ng, L. P. Tan, F. Yin Chiang Boey, And S. S. Venkatraman, “Annealing Of Biodegradable Polymer Induced By Femtosecond Laser Micromachining,” *Adv. Eng. Mater.*, Vol. 12, No. 4, Pp. 89–93, 2010.

- [49] R. Ortiz, I. Quintana, J. Etxarri, A. Lejardi, And J. R. Sarasua, “Picosecond Laser Ablation Of Poly-L-Lactide: Effect Of Crystallinity On The Material Response,” *J. Appl. Phys.*, Vol. 110, No. 9, 2011.
- [50] F. Schneider, N. Wolf, And D. Petring, “High Power Laser Cutting Of Fiber Reinforced Thermoplastic Polymers With Cw- And Pulsed Lasers,” *Phys. Procedia*, Vol. 41, Pp. 415–420, 2013.
- [51] B. D. Stepak, A. J. Antończak, K. Szustakiewicz, P. E. Koziol, And K. M. Abramski, “Degradation Of Poly(L-Lactide) Under KrF Excimer Laser Treatment,” *Polym. Degrad. Stab.*, Vol. 110, Pp. 156–164, 2014.
- [52] B. Stepak, A. J. Antończak, M. Bartkowiak-Jowska, J. Filipiak, C. Pezowicz, And K. M. Abramski, “Fabrication Of A Polymer-Based Biodegradable Stent Using A CO₂ Laser,” *Arch. Civ. Mech. Eng.*, Vol. 14, No. 2, Pp. 317–326, 2014.
- [53] M. A. Woodruff And D. W. Hutmacher, “The Return Of A Forgotten Polymer - Polycaprolactone In The 21st Century,” *Prog. Polym. Sci.*, Vol. 35, No. 10, Pp. 1217–1256, 2010.
- [54] R. Van Lith, E. Baker, H. Ware, J. Yang, A. C. Farsheed, C. Sun, And G. Ameer, “3D-Printing Strong High-Resolution Antioxidant Bioresorbable Vascular Stents,” *Adv. Mater. Technol.*, Vol. 1, No. 9, P. 1600138, 2016.
- [55] H. O. T. Ware, A. C. Farsheed, R. Van Lith, E. Baker, G. Ameer, And C. Sun, “Process Development For High-Resolution 3D-Printing Of Bioresorbable Vascular Stents,” Vol. 10115, P. 101150N, 2017.
- [56] M. S. Cabrera, B. Sanders, O. J. G. M. Goor, A. Driessen-Mol, C. W. . Oomens, And F. P. T. Baaijens, “Computationally Designed 3D Printed Self-Expandable Polymer Stents With Biodegradation Capacity For Minimally Invasive Heart Valve Implantation: A Proof-Of-Concept Study,” *3D Print. Addit. Manuf.*, Vol. 4, No. 1, Pp. 19–29, 2017.
- [57] A. G. Demir And B. Previtali, “Additive Manufacturing Of Cardiovascular Cocirc Stents By Selective Laser Melting,” *Mater. Des.*, Vol. 119, Pp. 338–350, 2017.
- [58] Y. Dai, Y. Xia, H.-B. Chen, N. Li, G. Chen, F.-M. Zhang, And N. Gu, “Optimization Of Sterilization Methods For Electrospun Poly(E-Caprolactone) To Enhance Pre-Osteoblast Cell Behaviors For Guided Bone Regeneration,” *J. Bioact. Compat. Polym.*, Vol. 31, No. 2, Pp. 152–166, 2016.
- [59] C. Fischbach, J. Tessmar, A. Lucke, E. Schnell, G. Schmeer, T. Blunk, And A. Göpferich, “Does UV Irradiation Affect Polymer Properties Relevant To Tissue Engineering?,” *Surf. Sci.*, Vol. 491, No. 3, Pp. 333–345, 2001.

- [60] P. D. Holly Shearer, M.Eng., Marianne J. Ellis, Ph.D., Semali P. Perera And P. D. And Julian B. Chaudhuri, "Effects Of Common Sterilization Methods On The Structure And Properties Of Poly(D,L Lactic-Co-Glycolic Acid) Scaffolds," Vol. 12, No. 10, 2006.
- [61] R. Ghobeira, C. Philips, V. De Naeyer, H. Declercq, P. Cools, N. De Geyter, R. Cornelissen, And R. Morent, "Comparative Study Of The Surface Properties And Cytocompatibility Of Plasma-Treated Poly- ϵ -Caprolactone Nanofibers Subjected To Different Sterilization Methods," *J. Biomed. Nanotechnol.*, Vol. 13, No. 6, Pp. 699–716, 2017.